

Université de Montréal

**Systèmes vésiculaires colloïdaux pour la vectorisation de
la 1- β -D-arabinofuranosylcytosine**

par
PIERRE SIMARD

Faculté de Pharmacie

Thèse présentée à la Faculté des études supérieures
en vue de l'obtention du grade de Philosaphae Doctor
en sciences pharmaceutiques
option technologie pharmaceutique

Août 2009

© Pierre Simard, 2009

Université de Montréal
Faculté des études supérieures

Cette thèse intitulée :

Systèmes vésiculaires colloïdaux pour la vectorisation de la 1- β -D-arabinofuranosylcytosine

présentée par :
PIERRE SIMARD

a été évaluée par un jury composé des personnes suivantes :

Dr Marc Servant, président-rapporteur
Dr Jean-Christophe Leroux, directeur de recherche
Dr Louis Cartilier, membre du jury
Dr Roxane Pouliot, examinateur externe
Dr Suzanne Bisaillon, représentante du doyen de la FES

Résumé

La 1- β -D-arabinofuranosylcytosine (ara-C) demeure l'agent anticancéreux principalement utilisé dans le traitement de la leucémie myéloblastique aiguë (LMA), malgré sa dégradation et son élimination rapide après une administration parentérale. Son encapsulation dans des vecteurs pharmaceutiques, majoritairement des liposomes, a permis de surmonter ces inconvénients. L'objectif général de ce projet de doctorat était de développer deux systèmes à libération prolongée, à base de phospholipides, de cholestérol et de poly(éthylène glycol) (PEG) afin d'encapsuler l'ara-C et ultimement, d'améliorer son efficacité dans le traitement de la LMA. Des Sphérulites[®] (vésicules multilamellaires d'un type particulier) ont d'abord été étudiées pour leur forte capacité d'encapsulation, due à leur mode de préparation. Par la suite, une formulation liposomale capable, d'une part de cibler spécifiquement les cellules leucémiques et, d'autre part, de promouvoir la libération intracellulaire de l'ara-C grâce à sa sensibilité au pH, a été mise au point. Les deux formulations se devaient d'avoir un faible diamètre, une stabilité en présence de fluides biologiques et des temps de circulation prolongés chez l'animal.

Une préparation de Sphérulites[®], composée de Phospholipon 90G, de Solutol HS15 et de cholestérol, a permis d'obtenir des vésicules de 300 nm de diamètre. Un dérivé lipidique de PEG a pu être fixé à leur surface, sans modifier la disposition concentrique des lamelles, ni changer leur stabilité. Les Sphérulites[®] PEGylées ont été chargées d'ara-C et injectées chez le rat par la voie intraveineuse. Elles ont démontré des temps de circulation significativement prolongés comparativement aux Sphérulites[®] sans PEG. Cependant, l'ara-C s'est retrouvée éliminée de la circulation sanguine très rapidement, révélant une libération précoce du principe actif à partir de ces vésicules.

Les liposomes sensibles au pH (~150 nm) ont été obtenus suite à l'insertion d'un copolymère à base de dioctadécyle, de *N*-isopropylacrylamide (NIPAM) et d'acide méthacrylique. L'anticorps anti-CD33, soit complet soit son fragment Fab', a été fixé à la surface des liposomes afin de cibler les cellules leucémiques. Les essais *in vitro* ont démontré la spécificité de la formulation pour différentes cellules leucémiques (CD33⁺), sa stabilité en présence de protéines plasmatiques et la libération intracellulaire d'un marqueur fluorescent et de l'ara-C. Enfin, des études menées chez la souris saine et immunodéprimée inoculée de cellules HL60 ont montré que la formulation exposant le fragment Fab' possédait un profil pharmacocinétique et une biodistribution semblables à ceux des liposomes contrôles non-ciblés. L'encapsulation de l'ara-C a permis d'améliorer grandement ses temps de circulation après une administration intraveineuse. Cependant, bien que les immunoliposomes ont permis de prolonger la survie des souris leucémiques comparativement à l'ara-C libre, l'addition du polymère sensible au pH n'a pas apporté de réel avantage à la formulation lorsque administrée *in vivo*.

Les résultats obtenus dans ce travail de thèse ont, dans un premier temps, mis en évidence que les Sphérulites® pourraient s'avérer utiles dans la vectorisation d'agents anticancéreux si leur capacité à retenir le principe actif *in vivo* était améliorée. Dans un second temps, les données présentées avec les immunoliposomes suggèrent qu'ils pourraient apporter un bénéfice notable dans le traitement de la LMA.

Mots-clés : leucémie myéloblastique aiguë, immunoliposomes sensibles au pH, Sphérulites®, *N*-isopropylacrylamide, libération contrôlée, anticorps monoclonal, récepteur CD33, ara-C, fragment Fab', pharmacocinétique.

Abstract

Despite its rapid degradation and fast elimination *in vivo*, 1- β -D-arabinofuranosylcytosine (ara-C) is the main anticancer agent used in the treatment of acute myeloid leukemia (AML). The encapsulation of this drug into nanocarriers such as liposomes has been shown to improve its stability, pharmacokinetic profile and, consequently, the treatment efficacy. The purpose of this doctoral work was to develop two nanocarriers employing phospholipids, cholesterol and poly(ethylene glycol) (PEG) to encapsulate ara-C, with the ultimate goal of developing more efficient treatments for AML. The first formulation relied on Spherulites[®], which are multilamellar vesicles possessing high entrapment yields due to their fabrication method. In a second part, pH-sensitive immunoliposomes were optimized to target specifically the leukemia cells and promote the release of the loaded ara-C at the desired intracellular site. Both formulations required a small diameter, stability in the presence of biological fluids and long circulation time properties when injected intravenously.

An optimized formulation of Spherulites[®] was developed. It was composed of Phospholipon 90G, Solutol HS15 and cholesterol. The vesicles (300 nm) were able to accommodate PEG-lipid derivatives at their surface without altering their concentric lamellar shape and their *in vitro* stability. The PEGylated Spherulites[®] were loaded with ara-C and injected intravenously into rats. The surface-modified vesicles exhibited longer circulation times compared to uncoated Spherulites[®]. However, most of the loaded-drug was cleared from the systemic circulation very rapidly, reflecting rapid leakage of ara-C from the vesicles.

The pH-sensitive immunoliposomes (~150 nm) were obtained by including a terminally-alkylated copolymer made of dioctadecyl, *N*-isopropylacrylamide (NIPAM) and methacrylic acid in the liposome bilayer. The whole monoclonal antibody anti-CD33 or its Fab' fragment were grafted on liposomes to target leukemic cells. *In vitro* assays revealed that this formulation was really specific for the various CD33⁺ leukemic cell lines, stable in presence of blood proteins, and able to promote the intracellular release of an encapsulated fluorescent probe as well as ara-C. *In vivo* studies in naïve Balb/c and immunodeprived (SCID) mice inoculated with HL60 cells confirmed that the anti-CD33 Fab' targeted formulation possessed pharmacokinetic and biodistribution profiles similar to those of the non-targeted liposomes. The encapsulation of ara-C in this formulation improved substantially its circulation time after intravenous injection. However, although ara-C-loaded immunoliposomes were able to prolong the survival of leukemic mice compared to the free drug, the addition of pH-sensitive polymer did not add any benefit to the formulation.

Although these formulations require some optimization, the first part of this work pointed out that Spherulites[®] could be used to deliver anticancer agents provided that leakage is reduced *in vivo*. On the other hand, the data obtained with the targeted immunoliposomes suggest that these carriers could be beneficial in the treatment of AML.

Keywords : acute myeloid leukemia, pH-sensitive immunoliposomes, Spherulites[®], *N*-isopropylacrylamide, controlled release, monoclonal antibody, CD33 receptor, ara-C, Fab' fragments, pharmacokinetic.

Table des matières

Chapitre 1. Introduction	1
1.1. Généralités sur les cancers	1
1.2. Le sang, la moelle osseuse et les leucémies.....	2
1.2.1. Le système hématopoïétique	2
1.2.2. Leucémie myéloblastique aiguë	6
1.2.3. L'antigène de surface CD33.....	10
1.3. Traitements conventionnels de la LMA.....	12
1.3.1. Le traitement à l'ara-C	13
1.3.2. Association de l'ara-C avec une anthracycline	16
1.3.3. Résistance à l'ara-C	17
1.3.4. Les limites des thérapies actuelles	18
1.4. Traitements alternatifs de la LMA	19
1.4.1. L'anticorps monoclonal M195	19
1.4.2. Le Mylotarg®	21
1.4.3. Modifications chimiques de l'ara-C.....	25
1.4.4. Systèmes à libération prolongée.....	28
1.4.4.1. Macromolécules solubles	30
1.4.4.2. Émulsion	31
1.4.4.3. Liposomes	33
Chapitre 2. Liposomes for drug delivery	37
2.1. Summary	37
2.2. General introduction.....	38
2.3. Lipids and polymorphisms.....	40
2.3.1. Material	40
2.3.1.1. Glycerolipids	40
2.3.1.1.1. General Structure	40

2.3.1.1.2. Natural phospholipids	41
2.3.1.1.3. Synthetic phospholipids and amphiphiles.....	43
2.3.1.2. Sphingolipids	44
2.3.1.2.1. Sphingomyelin	45
2.3.1.2.2. Gangliosides	46
2.3.1.3. Sterols.....	47
2.3.1.4. Polymer bearing lipids	48
2.3.1.5. Cationic lipids	50
2.3.2. Lipid selection.....	52
2.3.3. Polymorphisms.....	54
2.4. Liposome preparation methods	56
2.4.1. Nomenclature used to describe liposomes	56
2.4.2. Vesicle preparation.....	58
2.4.2.1. Lipid film hydration	59
2.4.2.2. Sonication.....	59
2.4.2.3. Shearing of lyotropic lamellar phase	60
2.4.2.4. Extrusion	60
2.4.2.5. Solvent injection method	63
2.4.2.6. Reverse phase evaporation.....	63
2.4.2.7. Microfluidisation.....	64
2.4.2.8. Dehydration-rehydration	65
2.4.2.9. Detergent removal.....	65
2.4.3. Drug Loading	66
2.4.3.1. Passive loading.....	66
2.4.3.2. Remote loading	66
2.4.4. Industrial manufacturing	68
2.5. Analytical techniques	69
2.5.1. Photon correlation spectroscopy	69

2.5.2. Gel chromatography.....	70
2.5.3. Microscopy.....	71
2.5.4. Fluorescence spectroscopy.....	72
2.5.5. Nuclear magnetic resonance spectroscopy.....	73
2.5.6. Fourier transform infrared spectroscopy	76
2.5.7. Small-angle X-ray and neutron scattering.....	77
2.5.8. Other techniques.....	78
2.6. Stability and stabilization of liposome formulations	78
2.6.1. Chemical stability of liposome formulations	79
2.6.2. Physical or colloidal stability of liposomes	81
2.6.2.1. Conventional versus sterically stabilized liposomes.....	81
2.6.2.2. Physico-chemical properties of PEG	84
2.6.2.3. Conformation of PEG at the surface of lipid membranes	85
2.6.2.4. Effect of PEG on the material properties of lipid membranes	87
2.6.2.5. Influence of PEG on the pharmacokinetic parameters of liposomes	90
2.6.2.6. Blood clearance of PEGylated liposomes on repeated injection	92
2.6.3. Drug retention properties of liposome formulations.....	93
2.7. Triggered release	95
2.7.1. Light	96
2.7.2. Temperature	98
2.7.3. pH.....	100
2.7.4. Enzymes	105
2.8. Medical applications	108
2.8.1. Cancer	111
2.8.1.1. Passive targeting.....	112
2.8.1.1.1. Anthracyclines.....	115
2.8.1.1.2. Vinca alkaloids.....	120
2.8.1.1.3. Other anticancer drugs	122

2.8.1.2. By-passing of P-glycoprotein.....	124
2.8.1.3. Tumor cells targeting	125
2.8.1.4. Tumor vasculature targeting	132
2.8.2. Infectious diseases.....	136
2.8.2.1. Parenteral antifungals.....	136
2.8.2.2. Parenteral antibiotics and antivirals	140
2.8.3. Rheumatoid arthritis.....	142
2.8.3.1. Corticosteroids	142
2.8.3.2. Folic acid antagonists.....	145
2.8.3.3. Bisphosphonates.....	145
2.8.3.4. Antioxydant enzymes.....	146
2.8.4. Pulmonary route and treatment of respiratory disorders.....	147
2.8.4.1. Anatomy and physiology of lungs	148
2.8.4.2. Treatment of asthma.....	150
2.8.4.3. Pulmonary route for systemic drug delivery	151
2.8.5. Topical and transdermal drug delivery	153
2.8.5.1. Interaction of liposomes with skin	154
2.8.5.2. Treatment of skin disease.....	158
2.8.5.3. Transdermal drug delivery	159
2.8.6. Ophtalmic disorders	161
2.8.7. Other administration routes.....	163
2.8.7.1. Oral and buccal delivery	163
2.8.7.2. Nasal delivery.....	164
2.8.7.3. Vaginal delivery	165
2.9. Other medical applications.....	166
2.9.1. Diagnostics	166
2.9.2. Vaccine.....	168
2.10. Nonmedical applications	169

2.10.1. Biomembranes and membrane proteins	170
2.10.2. Cosmetics	170
2.10.3. Food Industry	172
2.11. Concluding remarks and perspectives	174
2.12. Acknowledgments.....	175
2.13. References	176
Chapitre 3. Objectifs et hypothèses de recherche	201
3.1. Hypothèses de recherche.....	201
3.2. Objectifs généraux	202
3.2.1. Objectifs spécifiques	202
Chapitre 4. Preparation and <i>in vivo</i> evaluation of PEGylated formulations	204
4.1. Abstract	204
4.2. Introduction	205
4.3. Material and methods.....	209
4.3.1. Material	209
4.3.2. Preparation of spherulites.....	210
4.3.3. Incorporation of DSPE-PEG	211
4.3.4. Freeze-fracture electron microscopy.....	212
4.3.5. Particle size analysis	212
4.3.6. <i>In vitro</i> release of encapsulated compounds	213
4.3.6.1. Fluorescent dye (HPTS).....	213
4.3.6.2. Ara-C.....	213
4.3.7. <i>In vivo</i> pharmacokinetics and biodistribution	214
4.3.8. Statistical analysis	215
4.4. Results	216
4.4.1. Spherulite preparation characterization.....	216
4.4.2. <i>In vitro</i> release of the fluorescent dye and ara-C	217
4.4.3. Pharmacokinetic and Biodistribution.....	219

4.5. Discussion	223
4.6. Conclusion	229
4.7. Acknowledgments.....	229
4.8. References	229
Chapitre 5. pH-sensitive immunoliposomes specific to the CD33 cell surface antigen of leukemic cells.....	235
5.1. Abstract	235
5.2. Introduction.....	236
5.3. Material and Methods	243
5.3.1. Material	243
5.3.2. Preparation of copolymers	244
5.3.3. Preparation of PEGylated pH-sensitive liposomes	244
5.3.4. Modification of the antibodies	245
5.3.5. Particle Size.....	246
5.3.6. <i>In vitro</i> release of HPTS.....	247
5.3.7. Encapsulation and <i>in vitro</i> release of ara-C	247
5.3.8. Cell culture	248
5.3.9. Binding and internalization assays.....	249
5.3.10. Evaluation of the binding affinity of ILs	249
5.3.11. Intracellular release of calcein	250
5.3.12. Antiproliferative assay	251
5.4. Results and Discussion.....	252
5.4.1. Characterization of the pH-sensitive liposomes.....	252
5.4.2. Modification of the antibodies	253
5.4.3. <i>In vitro</i> cellular association of ILs	254
5.4.4. <i>In vitro</i> release of HPTS and ara-C	259
5.4.5. Intracellular release of quenched calcein	262
5.4.6. Antiproliferative assay	264

5.5. Conclusion	267
5.6. Acknowledgements	267
5.7. References	268
Chapitre 6. <i>In vivo</i> evaluation of pH-sensitive polymer-based immunoliposomes targeting the CD33 antigen.....	278
6.1. Abstract	278
6.2. Introduction	279
6.3. Material and methods	281
6.3.1. Material	281
6.3.2. Preparation of copolymers	282
6.3.3. Preparation of PEGylated pH-sensitive LP.....	283
6.3.4. Modification of the antibodies	283
6.3.5. Preparation of F(ab) ₂ and Fab' fragments.....	284
6.3.6. Coupling reaction.....	285
6.3.7. Liposomal lipid extraction procedure and ara-C assay.....	285
6.3.8. Cell culture and internalization assays.....	286
6.3.9. <i>In vivo</i> pharmacokinetics and biodistribution	287
6.3.10. <i>In vivo</i> survival experiment.....	288
6.4. Results & Discussion	288
6.4.1. Preparation and characterization of pH-sensitive immunoliposomes	288
6.4.2. Pharmacokinetics and biodistribution in Balb/c mice.....	292
6.4.3. Pharmacokinetics and biodistribution in SCID/HL60 mice.....	296
6.4.4. Preliminary <i>in vivo</i> efficacy experiment.....	300
6.5. Conclusion	302
6.6. Acknowledgements	302
6.7. References	303
6.8. Supplementary Figure	308
Chapitre 7. Discussion générale	310

7.1. Vésicules lipidiques testées.....	310
7.1.1. Sphérolites®	310
7.1.2. Liposomes sensibles au pH	311
7.2. Caractérisation <i>in vitro</i>	312
7.2.1. Caractérisation des Sphérolites®	312
7.2.2. Incorporation du PEG et propriétés <i>in vitro</i>	313
7.2.2.1. Sphérolites® PEGylées	315
7.2.2.2. Liposomes PEGylés sensibles au pH	315
7.2.3. Modification de l'anticorps	317
7.2.4. Spécificité des formulations liposomales.....	321
7.2.5. Rôle du DODA-P(NIPAM- <i>co</i> -MAA).....	322
7.2.5.1. Stabilité des immunoliposomes et libération <i>in vitro</i>	322
7.2.5.2. Libération intracellulaire du contenu des immunoliposomes	324
7.3. Caractérisation <i>in vivo</i>	325
7.3.1. Pharmacocinétique et biodistribution des Sphérolites®	325
7.3.2. Pharmacocinétique et biodistribution des immunoliposomes sensibles au pH	326
7.3.3. Le modèle murin de la leucémie myéloblastique aiguë	328
7.3.3.1. Pharmacocinétique et biodistribution des immunoliposomes sensibles au pH	328
7.3.3.2. Étude préliminaire d'efficacité thérapeutique des immunoliposomes	329
Conclusion	331
Bibliographie.....	334
Matériel et méthode – Étude de la phagocytose <i>in vitro</i>	I

Liste des tableaux

Tableau 1.1. Classification des différentes sous-classes de la LMA par le Groupe coopératif franco-américano-britannique (FAB) (Andoljsek et al. 2002, Bennett et al. 1976, Zenhausern et al. 2003).....	8
Table 2.1. Structures of the most commonly used phospholipids.....	42
Table 2.2. Properties of synthetic lipids used as liposome components. Adapted with permission from Ref. [10], E. Fattal <i>et al.</i> , in <i>Les liposomes: aspects technologiques, biologiques et pharmacologiques</i> , edited J. Delattre, P. Couvreur, F. Puisieux, J. Philipot and F. Schuber, Tec & Doc-Lavoisier, Paris (1993), p.43. Copyright @ Tec & Doc-Lavoisier.....	44
Table 2.3. Effect of molecular geometry on the phase properties of lipids. Adapted with permission from Ref. [30], D.D. Lasic <i>et al.</i> , in <i>Pharmaceutical Dosage Forms: Disperse systems</i> , edited H.A. Liberman, M.M. Rieger and G.S. Banker, Marcel Dekker, New York (1998), Vol. 3, p.43. Copyright @ Routledge/Taylor & Francis Group, LLC	55
Table 2.4. Liposome classification based on size and lamellarity.....	57
Table 2.5. Liposome classification based on method of preparation.....	58
Table 2.6. pH-sensitive peptides used to destabilize liposomal membranes.	104
Table 2.7. Liposome-based products that are on the market or in clinical development as of 2005.....	109
Table 2.8. Key characteristics of liposomal anthracyclines. Reprinted with permission from Ref. [297], T. M. Allen and F. J. Martin, Semin Oncol 31, 5 (2004). Copyright @ Elsevier.....	117
Table 2.9. Selected list of ligands (antibodies) and receptors tested as liposome-targeting agents.....	129

Table 2.10. Characteristics of therapeutic marketed amp B products administered in humans [403, 404, 417].....	138
Table 2.11. Some liposomal cosmetic formulations that are currently on the market.....	171
Table 4.1. Spherulite formulations and mean hydrodynamic diameters obtained by DLS.	225
Table 4.2. Mean pharmacokinetic parameters of spherulites and ara-C, free or encapsulated in uncoated and PEGylated spherulites (P90/Solutol HS15/Chol/DSPE-PEG, 57.4:14.8:27.2:0.6 mol%), after bolus IV administration to rats. Each data point is mean \pm S.D (n = 5 rats/group).....	228
Table 6.1. Comparison of the pharmacokinetic parameters of different pH-sensitive LP formulations and of encapsulated ara-C in naive Balb/c and SCID-HL60 mice	295

Liste des figures

Figure 1.1. Développement des différents éléments cellulaires du sang à partir des cellules de la moelle osseuse, défini comme étant l'hématopoïèse. Les cellules souches hématopoïétiques génèrent les unités de formation de colonies (CFU, «colony-forming unit»). Reproduit de (Rhoades <i>et al.</i> 2003) avec permission de Cengage Learning/Nelson.....	4
Figure 1.2. Structure de l'antigène de surface CD33. Reproduit de (Wellhausen & Peiper 2002) avec permission de Biolife s.a.s.....	11
Figure 1.3. Schéma d'activation intracellulaire de l'ara-C par diverses enzymes. Reproduit de (Mahlknecht <i>et al.</i> 2009) avec permission de Nature Publishing Group.	15
Figure 1.4. L'humanisation de l'anticorps M195, A) M195, B) M195 chimérique et C) le M195 humanisé. Un anticorps chimérique est caractérisé dans la nomenclature par le suffixe «-ximab» et est constitué de régions variables murines (fragments Fab') et de régions constantes humaines. Les anticorps humanisés ont été développés afin de réduire leur antigénicité. Ces anticorps sont caractérisés par le suffixe «-zumab» et sont composés des séquences codant les régions murines déterminant la complémentarité avec l'antigène greffées sur des séquences codant des régions charpentes des domaines variables humains. Reproduit de (Caron <i>et al.</i> 1992) avec permission de Waverly Press.....	21
Figure 1.5. La structure chimique du Mylotarg®. Reproduit de (Damle & Frost 2003) avec permission de Elsevier Limited.....	23
Figure 1.6. Modification de l'ara-C par l'ajout d'un groupement hydrophobe en position N ⁴	26
Figure 1.7. Différents types d'émulsions : une émulsion huile/eau, une émulsion eau/huile et une émulsion multiple eau/huile/eau.....	32
Figure 1.8. Vésicules lipidiques de DepoFoam®. Reproduit de (Murry & Blaney 2000) avec permission de Pacira Pharmaceuticals Inc (© 1996, 2009).	35

Figure 2.1. Structure of a phospholipid molecule.....	41
Figure 2.2. Structures of sphingosine (A) and sphingomyelin (B).	45
Figure 2.3. Structure of the ganglioside GM ₁	47
Figure 2.4. Chemical structure of <i>N</i> -palmitoyl glucosamine (<i>N</i> -PG) (A) and palmitoyl glycol chitosan (PGC) (B). Reprinted with permission from Ref. [20], C. Dufes <i>et al.</i> , Pharm Res 17, 1250 (2000). Copyright @ Springer Science & Business Media B.V.	49
Figure 2.5. Chemical structures of DOTMA (A), DOTAP (B), and DOPE (C).....	51
Figure 2.6. Schematic representation of 4 major liposome types. Conventional liposomes are either neutral or negatively charged. Sterically stabilised (stealth) liposomes carry polymer coatings to obtain prolonged circulation times. Immunoliposomes (antibody-targeted) may be either conventional or stealth. For cationic liposomes, the several different means of imposing a positive charge are shown (mono, di or multivalent interactions). Adapted with permission from Ref. [29], G. Storm and D.J.A. Crommelin, Pharm Sci Technol Today 1, 19 (1998). Copyright @ Elsevier.....	53
Figure 2.7. Characteristics of VET. Freeze-fracture electron micrographs of vesicles produced by extrusion of MLV composed of EPC (100 mg lipid/mL) through filters with pore sizes of 400 (A), 200 (B), 100 (C), 50 (D) and 30 nm (E). Each sample was extruded 10 times through 2 stacked filters (bar represents 150 nm). Reprinted with permission from Ref. [46], M.J. Hope <i>et al.</i> , Chem Phys Lipids 40, 89 (1986). Copyright @ Elsevier.....	61
Figure 2.8. The two syringe-based miniextruder for preparation of small volumes of liposomes and the pressurized large extruder. The latter device is more suitable for liposome extrusion than other similar equipment due to the wide pressure range at which it can operate, the temperature-controlled sample holder, and the quick-release sample port assembly that allows for rapid recycling.....	62
Figure 2.9. Ammonium sulfate-loading procedure for weak bases. Liposomes are first prepared in the presence of ammonium sulfate. Following removal of the exterior ammonium sulfate on a size-exclusion column, Dox is added to the extraliposomal	

medium. Ammonium sulfate can dissociate into two ammonium cations and one sulfate anion. Ammonia is free to cross the liposomal membrane, giving rise to a pH gradient across the membrane. Dox in its uncharged form can then cross the liposome membrane and upon cooling form an insoluble gel under acidic conditions with the remaining sulfate anion, effectively trapping it in the liposomal interior. The concentration of Dox in the liposomal lumen can reach concentrations in excess of the aqueous solubility of Dox. This loading procedure can be applied to a variety of weak bases, such as those comprising the anthracyclines, <i>Vinca</i> alkaloids or camptothecins. However, the stability of the complex formed with the sulfate and thus the gel in the liposomal lumen contributes to the overall stability of the formulation. Reproduced with permission from Ref. [61]. D.C. Drummond <i>et al.</i> , Pharmacol Rev 51, 691 (1999). Copyright @ American Society for Pharmacology and Experimental Therapeutics.....	67
Figure 2.10. ^2H NMR spectra of POPC-d ₃₁ /Chol (left panel) and POPC-d ₃₁ /Chol/P(NIPAM- <i>co</i> -MAA- <i>co</i> -VP- <i>co</i> -ODA) (right panel). Reprinted with permission from Ref. [81], E. Roux <i>et al.</i> , Biomacromolecules 4, 240 (2003). Copyright @ American Chemical Society.....	75
Figure 2.11. A schematic illustration of the compression (A) or interpenetration (B) of the PEG layer due to the close approach of protein to the liposome surface.....	88
Figure 2.12. Photosensitized oxidation of plasmalogen (A) and diplasmalogen (B), and the consequences of this reaction on membrane permeability (C). Legend: ROS = Reactive oxygen species. Reprinted with permission from Ref. [155], P. Shum <i>et al.</i> , Adv Drug Deliv Rev 53, 273 (2001). Copyright @ Elsevier.....	97
Figure 2.13. Thermodynamic adaptive phased array treatment in which a thermosensitive liposome encapsulating a chemotherapy agent has been infused into the patient's blood stream, and the patient's tumor is subsequently heated to a temperature that triggers release of drug into the tumor (A). Celsion Corporation prototype monopole phased array applicator for deep tumor heating (B). Reprinted with permission from	

Ref [170], A.J. Fenn, Drug Deliv Technol 2, 74 (2002). Copyright @ Drug Delivery Technology..... 99

Figure 2.14. Putative mechanisms of enzyme activated delivery. Liposomes may be activated to become fusogenic by enzymes near the surface of the cell, enzymes displayed on the surface of the cell or enzymes in the endolysosomal compartment. Charge reversal and fusogenic delivery can occur at the plasma membrane, within an endosome or *via* later cleavage in the endolysosome. Legend: stable liposome/targeting moiety complex with net negative charge (1); peptide linkers are cleaved by soluble or cell-associated proteases (2); possible direct delivery *via* fusion with plasma membrane (3); liposome becomes positively charged and fusogenic (before or after uptake) (4); uptake by endosome and fusion of liposomal membrane with endosomal membrane (5); release of cargo into cytosol (6). Adapted with permission from Ref. [151], P. Meers, Adv Drug Deliv Rev 53, 265 (2001). Copyright @ Elsevier..... 106

Figure 2.15. Distribution of radiolabeled (^{111}In -DTPA) PEGylated liposomes in patients with lung cancer (A), breast cancer (B) and cancer of the base of the tongue (C). Legend: Tu = Tumor, L = Liver, CP = cardiac blood pool, Spl = Spleen. Reprinted with permission from Ref. [277], K.J. Harrington *et al.*, Clin Cancer Res 7, 243 (2001). Copyright @ American Association for Cancer Research..... 114

Figure 2.16. Schematic diagram of the different coupling methods used. Reaction between maleimide and thiol functions (A), formation of a disulfide bond (B), reaction between carboxylic acid and primary amine group (C), reaction between hydrazide and aldehyde functions (D), crosslinking between two primary amine groups (E). Legend: EDAC = 1-ethyl-3-[3-dimethylaminopropyl]carbodiimide hydrochloride. Reprinted with permission from Ref. [351], L. Nobs *et al.*, J Pharm Sci 93, 1980 (2004). Copyright @ Wiley-Liss, Inc. a subsidiary of John Wiley & Sons, Inc. 127

Figure 2.17. Dual mechanism of action for liposomal drugs against solid tumors *via* use of peptides that are specific for targeting tumor vasculature. Reprinted with permission

- from Ref. [258], T. M. Allen and P. R. Cullis, Science 303, 1818 (2004). Copyright @ American Association for the Advancement of Science..... 134
- Figure 2.18. Therapeutic activity of a single injection of 10 mg/kg prednisolone phosphate encapsulated into PEGylated liposomes (solid circles) compared with 7 daily injections of 10 mg/kg free prednisolone phosphate (solid squares) into rats with adjuvant-induced arthritis. Control treatments were empty PEG liposomes (open circles) and saline (open squares). Bars show the mean and SEM of 5 rats. Arrows indicate times of treatment. Reprinted with permission from Ref. [455], J.M. Metselaar *et al.*, Arthritis Rheum 48, 2059 (2003). Copyright @ Wiley-Liss, Inc. a subsidiary of John Wiley & Sons, Inc. 144
- Figure 2.19. Top (upper panel) and side (lower panel) view of murine stratum corneum, visualised with the CLSM, after an epicutaneous application of a fluorescent lipophilic label in ultradeformable vesicles. The plethora of penetration pathways is seen. Less deformable colloids only penetrate into/along the widest such pathways. In this example, the SC is ~6 µm and the epidermis is approximately 15 µm wide. Reprinted with permission from Ref. [509], G. Cevc, Adv Drug Del Rev 56, 675 (2004). Copyright @ Elsevier..... 157
- Figure 2.20. (A) Early frame of a fluorescein angiogram of the retina of a patient with predominantly classic choroidal neovascularization (CNV) in AMD before PDT, as demonstrated by the strong, well-demarcated hyperfluorescent region near the center of the macula. (B) The same eye after PDT with 12mg/m² of liposomal verteporfin and 100 J/cm² of light at 689 nm, given at 600 mW/cm² approximately 15 min after the start of the slow i.v. injection. One week after PDT, the early phase of the fluorescein angiogram shows that the dark hypofluorescent spot has a diameter somewhat greater than that of the optic nerve (on the right), demonstrating that both the CNV and choriocapillaries remain closed, on this timescale. The dark spot also demonstrates that the retinal capillaries near the macula are still patent. Reprinted with

permission from Ref. [554], H. van den Bergh, Semin Ophthalmol 16, 181 (2001). Copyright @ Routledge/Taylor & Francis Group, LLC	162
Figure 4.1. Process of preparation of spherulites in suspension (A) and a schematic representation of the spherulites structure (B). Spherulites are produced by applying a moderate shear to a lamellar phase of surfactant. The lamellar phase forms a close-packed organization of MLV in which regular stacking of surfactant bilayers (n = 50-1000 layers) are separated by aqueous layers. Compacted spherulites can be dispersed by adding an excess amount of solvent. The interlamellar distance between two constitutive layers and the bilayer thickness are typically between 50 and 200 Å. Reproduced from ref. [31] with permission.....	208
Figure 4.2. Polarization (A) and freeze-fracture electron micrograph (B) of a manually sheared spherulite sample (formulation 11). These non-diluted vesicles had a typical size about 200 nm and presented the birefringent texture.....	211
Figure 4.3. Release rate of encapsulated HPTS for formulations 4 (P90/Tween 80, 76:24 mol%, dotted line), 11 (P90/Solutol HS15/Chol, 58:15:27 mol%, solid line), and 9 (P90/Solutol HS15, 66:34 mol%, dashed line) in HEPES buffer at 37°C. The leakage of HPTS for the formulation 11 in 50% (v/v) rat plasma/HEPES buffer at 37°C is also presented as a function of time (bold dotted line). The extent of content release was calculated from HPTS fluorescence intensity ($\lambda_{\text{ex}} = 413$ nm, $\lambda_{\text{em}} = 512$ nm) relative to measurement after vesicle disruption in 0.9% (v/v) Triton X-100.....	218
Figure 4.4. Elution profile of ara-C (open bars) and spherulites (P90/Solutol HS15/Chol, 58:15:27 mol%, closed bars) after passage over a Sephadex G50 column. The spherulites were labelled with 57 pCi/mg [^{14}C]-cholesterol oleate and initially loaded with 2% drug (w/w) spiked with 114 pCi/mg [^3H]-ara-C. 46 ± 1% of ara-C was entrapped in the vesicles (n = 3).	219
Figure 4.5. Blood concentration-time profiles (A) and tissue distribution 24 h post-administration (B) of uncoated (■, black bars), PEG 2000- (▲, white bars) and PEG 5000-coated spherulites (○, grey bars) (P90/Solutol HS15/Chol/DSPE-PEG,	

57.4:14.8:27.2:0.6 mol%), after IV administration to rats. Spherulites were labelled with 0.25 µCi/mg [¹⁴C]-cholesteryl oleate. Each rat received 0.33 µmol/kg lipids/surfactant. Mean ± S.D (n = 5)..... 221

Figure 4.6. Blood concentration-time profiles (**A**) and tissue distribution 24 h post-administration (**B**) of free ara-C (right dashed bars) and ara-C loaded in uncoated (■, black bars), PEG 2000- (▲, white bars) and PEG 5000-coated spherulites (○, grey bars) (P90/Solutol HS15/Chol/DSPE-PEG, 57.4:14.8:27.2:0.6 mol%) after IV administration to rats. Spherulites were initially loaded with 2% (w/w) ara-C spiked with 100 µCi/mL [³H]-ara-C. Free ara-C was removed by gel filtration over Sephadex G50. Each rat received 2.34 µg/kg ara-C. Mean ± S.D (n = 5). 223

Figure 5.1. Schematic representation of the binding and the internalization of the pH-sensitive ILs-CD33 through receptor-mediated endocytosis. Upon acidification of the endosomes, DODA-P(NIPAM-*co*-MAA) destabilizes the liposomal bilayer, thereby triggering the rapid release of encapsulated ara-C. In competitive assays free anti-CD33 binds the CD33 receptor and impedes the binding and the internalization of the ILs-CD33. Once internalized, the release of the pH-sensitive liposomal content can be slowed down by the addition of bafilomycin A1. The latter is a strong inhibitor of the vacuolar type H(+)-ATPase, which inhibits the acidification of the endosomes/lysosomes (Yoshimori *et al.* 1991). 242

Figure 5.2. (A) Fluorescent labelling of HL60 (CD33⁺) cells after 2 h incubation of pH-sensitive ILs-CD33 labelled with BODIPY FL C12 at 4°C (dotted light line) and 37°C (plain dark line) determined by flow cytometry. The x-axis represents the logarithm of green fluorescence signal, and the y-axis represents cell count. The first plain line represents basal cellular fluorescence (without any probe). (B) Confocal microscopy micrographs of an HL60 cell treated with ILs-CD33 (left panel), ILs-MOPC21 (middle panel), and pre-incubated with free anti-CD33 during 30 min before the addition of the ILs-CD33 (right panel). All the formulations contain rhodamine-labelled DODA-P(NIPAM-*co*-MAA) (red). Nuclei were stained with DAPI (blue). 255

- Figure 5.3. (A) Uptake of different liposome formulations by HL60 cells. The last bar represents competitive binding assays of pH-sensitive IL-CD33 performed in the presence of a 20-fold excess free anti-CD33 antibody. Mean \pm SD, n= 4. (B) Uptake of different pH-sensitive formulations by HL60 (black bars), KG1 (white bars), THP-1 (grey bars) and A549 (stripped bars) cells. Mean \pm SD, n = 3. 258
- Figure 5.4. *In vitro* release of encapsulated HPTS at 37°C for pH-sensitive ILs at pH 5.0 (circle), 5.8 (square), and 7.4 (triangle) after 1 h incubation in 50% (v/v) human plasma. DODA-P(NIPAM-MAA) was incorporated during liposome preparation. The extent of content release was calculated from HPTS fluorescence intensity ($\lambda_{\text{ex}} = 413$ nm, $\lambda_{\text{em}} = 512$ nm) relative to the intensity obtained upon vesicle disruption with 10% (v/v) Triton X-100. Mean \pm SD, n = 3..... 260
- Figure 5.5. Percent of ara-C released from pH-insensitive liposomes (stripped bars), pH-sensitive liposomes (black bars), ILs (white bars), and pH-sensitive ILs (grey bars) after 30 min incubation at 37°C. The formulations were previously incubated in 50% (v/v) human plasma during 1 h at 37°C. Mean \pm SD, n = 3..... 262
- Figure 5.6. Confocal microscopy micrographs of HL60 cells treated with pH-insensitive ILs-CD33 (A) or pH-sensitive ILs-CD33 (B) containing self-quenched calcein (green). Panel C shows HL60 cells treated with bafilomycin A1 30 min before addition of pH-sensitive ILs-CD33. The Nuclei were stained with DAPI (blue), and the acidic compartments were stained with Lysotracker Red® (red). 263
- Figure 5.7. Toxicity of encapsulated and free ara-C at a final concentration of 20 (open bars) and 40 μ g/mL (closed bars) on HL60 cells after an incubation time of 2 h. Mean \pm SD, n = 3. At 20 μ g/mL of ara-C, the cytotoxicity induced by pH-sensitive ILs-CD33 is statistically superior ($p<0.05$) to all the other liposomal formulations..... 265
- Figure 6.1. Schematic representation of pH-sensitive anti-CD33 Fab'-LP. 290
- Figure 6.2. Fluorescent labelling of HL60 (CD33^+) cells after 2 h incubation of different LP formulations labelled with BODIPY FL C12 at 37°C, as determined by flow cytometry. The x-axis represents the logarithm of green fluorescence signal, and the y-

- axis is the cell count. The first plain line corresponds to basal cellular fluorescence (without any probe). The striped line represents competitive binding assays of pH-sensitive LP-Fab' performed in the presence of a 20-fold excess of free anti-CD33 antibody in the medium..... 291
- Figure 6.3. Blood concentration-time profiles of pH-sensitive LP and pH-sensitive LP bearing whole anti-CD33 MAb or the Fab' fragment (**A**) and of free and encapsulated ara-C (**B**) in naive Balb/c mice. Each mouse received i.v. 3.4 mg/kg ara-C and 40 µmol/kg of lipids. Values represent the mean (\pm S.D.) obtained for n = 4 animals per group per time point..... 294
- Figure 6.4. Blood concentration-time profiles of pH-sensitive LP and pH-sensitive anti-CD33 LP bearing the Fab' fragment (**A**) and of encapsulated ara-C (**B**) in SCID-HL60 mice. Each mouse received i.v. 3.4 mg/kg ara-C and 40 µmol/kg of lipids. Values represent the mean (\pm S.D.) obtained for n = 4 animals per group per time point.... 298
- Figure 6.5. Liver distribution of different pH-sensitive LP formulations (**A**), and of free or encapsulated ara-C (**B**) in Balb/c and SCID/HL60 mice. Each mouse received i.v. 3.4 mg/kg ara-C and 40 µmol/kg of lipids. Values represent the mean (\pm S.D.) obtained for n = 4 animals per group per time point. 300
- Figure 6.6. Kaplan-Meier plot for HL60-bearing SCID mice treated with various ara-C formulations. SCID mice (n = 8 mice/group) were injected with 1.2×10^7 HL60 cells (day 0) and were treated 24 h later with either saline (○), free ara-C (), ara-C-loaded Fab'-LP (□), and ara-C-loaded, pH-sensitive Fab'-LP loaded with ara-C (▲), at a dose of 8 mg ara-C/kg. A second injection of saline or ara-C formulations (8 mg ara-C/kg) was repeated at day 3. Mice were monitored daily and were euthanized when tumor size exceeded 1,500 mm³ or when hind-leg paralysis appeared. 301
- Supplementary Figure 6.7. Spleen distribution of different pH-sensitive LP formulations (**A**) and of free or encapsulated ara-C (**B**) in Balb/c and SCID/HL60 mice. Each mouse received i.v. 3.4 mg/kg ara-C and 40 µmol/kg of lipids. Values represent the mean (\pm S.D.) obtained for n = 4 animals per group per time point. 309

Figure 7.1. Effet du PEG sur la diminution de l'opsonisation et la reconnaissance des liposomes par les macrophages.....	315
Figure 7.2. Internalisation des liposomes par les macrophages RAW264.7 en fonction du temps. La capacité phagocytaire normalisée (% cellules fluorescentes multipliée par l'intensité moyenne de fluorescence) a été obtenue par cytométrie de flux. Les liposomes ont été préparés tel que décrit par Roux <i>et al.</i> (Roux <i>et al.</i> 2002b). Moyenne ± écart-type (n=3).....	317
Figure 7.3. Principales étapes de modifications de l'anticorps effectuées avant leur couplage aux liposomes : 1) Oxydation de la partie sucre des IgGs par le periodate de sodium (40 min, 4°C). 2) Fixation du PDPH (5 h, 25°C). 3) Clivage des ponts disulfure par le DTT (20 min, 25°C). 4) Purification de l'anticorps modifié par chromatographie d'exclusion de taille (Sephadex® G50).	320
Figure 7.4. Pourcentage de HPTS libéré des liposomes sensibles au pH en présence ou non de l'anticorps anti-CD33 à leur surface. La libération du marqueur fluorescent à pH acide indique que la capacité du copolymère à déstabiliser la bicoche lipidique est retenue malgré la présence d'un anticorps.....	323

Liste des sigles et abréviations

<i>p/p</i>	poids/poids
[³ H]	tritium
5-FU	5-fluorouacil
5NT	5'-nucléotidases
6-CF	6-carboxyfluorescein
^{99m} Tc-DTPA	^{99m} Tc-diethylenetriamine-pentaacetate
A549	human lung carcinoma cells
ABC	accelerated blood clearance
AcBut	4-(4-acétylphenoxy)acide butanoïque
ADCC	cytotoxicité cellulaire dépendante des anticorps
AIDS	acquired immune deficiency syndrome
ALL	leucémie lymphocytique aiguë
AMD	macular degeneration
AML	acute myeloid leukemia
amp B	amphotericin B
ANOVA	analysis of variance
ANTS	8-aminonaphthalene-1,2,3-trisulfonic acid
Ap5A	P ¹ ,P ⁵ -di(adenosine-5)pentaphosphate
APRPG	(Asn-Gly-Arg) peptide
ara-C	1-β-D-arabinofuranosylcytosine, cytarabine, cytosine arabinoside
ara-CTP	cytarabine triphosphate
ara-U	1-β-D-arabinofuranosyluracil, uracil arabinoside
ASC	aire sous la courbe
AUC	mean area under the blood concentrations <i>vs</i> time curve
BD	biodistribution
BH-AC	N ⁴ -behenoyl-1-β-D-arabinofuranosylcytosine
BPD-MA	benzoporphyrin derivative monoacid ring A
C _{Ab}	molar concentration of the antibody
CCL	leucémie lymphoïde chronique
CFU	unités de formation de colonies, «colony-forming unit»
CHEMS	cholesteryl hemisuccinate
Chol	cholesterol

cholesteryl-	4,4-difluoro-5,7-dimethyl-4-bora-3a,4a-diaza- <i>s</i> -
BODIPY FL C12	indacene-3-dodecanoate
CL	clearance
CLSM	confocal laser scanning microscopy
CML	leucémie myéloïde chronique
CNV	choroidal neovascularization
CP	capacité phagocytaire
CT	computed tomography
DCP	dicethylphosphate
ddI	2',3'-dideoxyinosine
DLPC	1,2-dilauroyl- <i>sn</i> -glycero-3-phosphocholine
DLS	dynamic light scattering
DMEM	Dulbecco's modified Eagle's medium
DMPA	1,2-dimyristoyl- <i>sn</i> -glycero-3-phosphate
DMPC	1,2-dimyristoyl- <i>sn</i> -glycero-3-phosphocholine
DMPE	1,2-dimyristoyl- <i>sn</i> -glycero-3-phosphoethanolamine
DMPG	1,2-dimyristoyl- <i>sn</i> -glycero-3-[phospho- <i>rac</i> -(1-glycerol)]
DMSO	dimethylsulphoxide
DODA-501	4,4'-azobis(4-cyano- <i>N,N</i> -dioctadecyl)pentanamide
DOPC	1,2-dioleoyl- <i>sn</i> -glycero-3-phosphocholine
DOPE	1,2-dioleoyl- <i>sn</i> -glycero-3-phosphoethanolamine
DOPG	1,2-dioleoyl- <i>sn</i> -glycero-3-[phospho- <i>rac</i> -(1-glycerol)]
DOTAP	1,2-dioleyloxy-3-[trimethylammonio]-propane
DOTMA	<i>N</i> -(1-(2,3-dioleyloxy)propyl)- <i>N,N,N</i> -trimethyl ammonium
Dox	doxorubicin
DPPA	1,2-dipalmitoyl- <i>sn</i> -glycero-3-phosphate
DPPC	1,2-dipalmitoyl- <i>sn</i> -glycero-3-phosphocholine
DPPE	1,2-dipalmitoyl- <i>sn</i> -glycero-3-phosphoethanolamine
DPPG	1,2-dipalmitoyl- <i>sn</i> -glycero-3-[phospho- <i>rac</i> -(1-glycerol)]
DPPS	1,2-dipalmitoyl- <i>sn</i> -glycero-3-[phospho-L-serine]
DPSG	dipalmitoylsuccinylglycerol
DPX	<i>p</i> -xylene- <i>bis</i> -pyrimidium
DPX	<i>p</i> -xylene- <i>bis</i> -pyridinium bromide
DRV	dehydration-rehydration vesicles
DSPC	1,2-distearoyl- <i>sn</i> -glycero-3-phosphocholine
DSPE	1,2-distearoyl- <i>sn</i> -glycero-3-phosphoethanolamine

DSPE-PEG	1,2-distearoyl- <i>sn</i> -glycero-3-phosphatidylethanolamine- <i>N</i> -[methoxy poly(ethylene glycol)]
DSPG	1,2-distearoyl- <i>sn</i> -glycero-3-[phospho- <i>rac</i> -(1-glycerol)]
DTT	dithiotreitol
e/h	émulsion eau-dans-huile
e/h/e	émulsion eau-dans-huile-dans-eau
EDAC	1-ethyl-3-[3-dimethylaminopropyl]carbodiimide hydrochloride
EDC	1-éthyl-3-(3-diméthylaminopropyl)carbodiimide
EE	entrapment efficiency
EGF	epidermal growth factor
EPC	egg phosphatidylcholine
EPR	enhanced permeation and retention
ESR	electron spin resonance
FAB	Groupe Coopératif Franco-Américano-Britannique
FATMLV	MLVs prepared by repeated freezing-thawing
FBS	fetal bovine serum
FDA	US food and drug administration
FFEM	freeze fracture electron microscopy
FR	folate receptor
FSC	forward scatter
FTIR	fourier transform infrared
GALA	(glutamic acid-alanine-leucine-alanine) peptide
G-CSF	facteur de croissance granulocytaire
Gd-DTPA-BMA	gadolinium-diethylene-triamine-pentaacetic-acid-bis-methylamide
GI	gastrointestinal
GM ₁	monosialoganglioside
GUV	giant unilamellar vesicles
h/e	émulsion huile-dans-eau
h/e/h	émulsion huile-dans-eau-dans-huile
HAV	hepatitis A virions
HBS	HEPES buffered saline
HBs	hepatitis B antigens
hENT1	human equilibrative nucleoside transporter 1
HEPES	<i>N</i> -[2-hydroxyethyl]piperazine- <i>N'</i> -[2-ethanesulfonic acid]
HER-2	human EGF receptor 2

H _{II}	inverted hexagonal phase
HIV	human immunodeficiency virus
HL60	human promyelocytic leukemia cells
HLA-DR	histo-compatibility antigen D region
HPTS	trisodium 8-hydroxypyrene trisulfonate
HSPC	hydrogenated soy phosphatidylcholine
HuM195	anticorps monoclonal M195 humanisé
ILs	immunoliposomes
IND	Investigational New Drug
IR	infrared spectroscopy
ITIMs	motifs inhibiteurs dépendants de la tyrosine des immunorécepteurs
IV / i.v.	intravenous
J774	macrophages de souris
K _{Dapp}	apparent dissociation constant
KG-1	human myeloid cells
KS	Kaposi's sarcoma
L1210	cellules lymphocytaires murines
L _a	fluid liquid crystalline phase (or liquid-crystal phase)
L _b	rigid crystalline liquid phase (or gel phase).
LCST	lower critical solution temperature
LLO	listeriolysin O
LMA	leucémie myéloblastique aiguë
LP	PEGylated liposomes
LPS	lipopolysaccharide
LUV	large unilamellar vesicles
LUVET	large unilamellar vesicles prepared by extrusion
MAA	methacrylic acid
mAb / MAb	monoclonal antibody
MDR	multidrug resistance
MEA	mercaptoethylamine
MES	2-N-(morpholino)ethanesulfonic acid
MFI	mean fluorescence intensity
MHC	major histocompatibility complex
MLV	multilamellar vesicles
MLV-REV	multilamellar vesicles formed by the reverse-phase evaporation method

MMC	4-(<i>N</i> -maleimidomethyl)cyclohexane-1-carboxylate
MOPC21	mouse isotype control IgG1b
MPPC	1-myristoyl-2-palmitoyl- <i>sn</i> -glycero-3-phosphocholine
MPS	mononuclear phagocytic system
MTT	3-(4,5-dimethylthiazol-2-yl)-2,5-diphenyl tetrazolium bromide
MTX	methotrexate
MUV	medium sized unilamellar vesicles
MVV	multi vesicular vesicles
M_w	weight-average molecular weights
NBD	<i>N</i> -4-nitrobenzo-2-oxa-1,3-diazole
NGR	Asn-Gly-Arg motif peptide
NHAC	<i>N</i> ⁴ -hexadecyl-1- β -D-arabinofuranosylcytosine
NIPAM	<i>N</i> -isopropylacrylamide
NMR	nuclear magnetic resonance
NOAC	<i>N</i> ⁴ -octadecyl-1- β -D-arabinofuranosylcytosine
OA	oleic acid
ODA	octadecylacrylate
OLV	oligolamellar vesicles
PA	phosphatidic acid
PBS	phosphates buffered saline
PC	phosphatidylcholin
PDPH	3-(2-pyridyldithio)propionyl hydrazide
PDT	photodynamic therapy
PE	phosphatidylethanolamine
PEG	poly(éthylène glycol)
PG	phosphatidylglycerol
PGA	l'acide poly-l-glutamique
PGC	palmitoyl glycol chitosan
PGP / Pgp-1	P-glycoprotein
PHEG	poly- <i>N</i> ⁵ -(2-hydroxyéthyle)-l-glutamine
PI	polydispersity index
PK	pharmacokinetic
PL-AC	<i>N</i> ⁴ -palmitoyl-1- β -D-arabinofuranosylcytosine
PMPC	1-palmitoyl-2-myristoyl- <i>sn</i> -glycero-3-phosphocholine
POPC	palmitoyl-oleoyl-phosphocholine
PS	phosphatidylserine

PSC 833	Valspodar® (Novartis Pharmaceuticals Corp)
PSPC	1-palmitoyl-2-stearoyl- <i>sn</i> -glycero-3-phosphocholine
PTH	parathyroid hormone related peptide
PVP	poly <i>N</i> -(vinyl pyrrolidone)
RA	rheumatoid arthritis
RET	resonance energy transfer
REV	single or oligolamellar vesicles formed by the reverse-phase evaporation method
ROS	reactive oxygen species
SA	stearylamine
SANS	small-angle neutron scattering
SAXS	small-angle X-ray scattering
SC	stratum corneum
SCID	severe combined immunodeficiency
SDS	sodium dodecyl sulphate
SEC	size exclusion chromatography
Siglec	« <i>Sialic Acid Binding Immunoglobulin-like Lectins</i> »
SiRNA	short interfering RNA
SM	sphingomyelin
SMPB	4-(<i>p</i> -maléimidophényl)butyrate de <i>N</i> -succinimidyle
SOD	superoxide dismutase
SPDP	3-(2-pyridyldithio)propionate de <i>N</i> -succinimidyle
sPLA ₂	secretory phospholipase A ₂
SPLV	stable plurilamellar vesicles
SPM	système des phagocytes mononucléés
SPPC	1-stearoyl-2-palmitoyl- <i>sn</i> -glycero-3-phosphocholine
SPR	surface plasmon resonance
SSC	side scatter
SUV	small (or sonicated) unilamellar vesicle
T _c	transition temperature
TEM	transmission electron microscopy
TNBS	2,4,6-trinitrobenzenesulfonic acid solution
TRITC-DHPE	<i>N</i> -(6-tetramethylrhodaminethiocarbamoyl)-1,2-dihexadecanoyl- <i>sn</i> -glycero-3-phosphoethanolamine, triethylammonium salt
Tween® 80	polyoxyethylene 80 sorbitan monooleate
UV	unilamellar vesicles

VEGF	vascular endothelial growth factor
VET	vesicles prepared by extrusion
VP	<i>N</i> -vinyl-2-pyrrolidone
XPS	X-ray photoelectron spectroscopy

À mes parents, Arché & Louise, pour leur soutien, leurs encouragements et leur amour

Remerciements

Je tiens à exprimer toute ma reconnaissance envers mon directeur de recherche, Jean-Christophe Leroux, pour m'avoir ouvert les portes de son laboratoire, initié à la recherche dans le domaine de la galénique et aidé à développer mon sens critique. Merci pour ton efficacité, ta rapidité, ton savoir immense et ton dévouement pour la recherche. Ces qualités font de toi un excellent professeur qui ne cessera jamais de progresser.

Je voudrais également remercier tous mes collègues de travail du laboratoire de Jean-Christophe, tant les anciens que les derniers arrivés après moi. J'ai eu la chance de côtoyer plusieurs personnes super accueillantes que j'ai eu un grand plaisir à voir chaque jour. Merci à toi Didier de m'avoir supervisé lors de mon entrée au sein de laboratoire. Merci à Emmanuelle de m'avoir introduit à ton ancien projet de recherche, à la chimie, aux études animales, aux liposomes... Mes plus sincères remerciements à Marie-Christine, Marie-Hélène, Marie-Andrée, et bien sûr Marc pour m'avoir tant appris sur la science, l'anglais, la musique, l'alcool, la bouffe, etc. Je garde de très bons souvenirs avec vous tous, que ce soit au laboratoire en train de travailler, de discuter en remplissant mon cahier de labo, ou lors de nos sorties amicales. Le temps a avancé, je suis super fier et heureux pour votre «nouvelle vie» et content d'être toujours parmi vous. «Ah ouais, MC, j'ai une question !!!» Pour sûr, je dois te dire un énorme merci personnel, Marie-Christine, pour m'avoir encouragé et soutenu malgré les petites difficultés rencontrées, pour tes bras, pour tes connaissances sans fin dans tous les domaines de la vie, pour toutes les heures que tu as passées à corriger mes articles et, tout dernièrement, ma thèse... Merci d'avoir été là pendant toutes ces années.

Je me dois également de remercier François pour toute ton aide, tant par tes tâches administratives que par les multiples études animales faites ensemble. Merci à Geneviève, Jeanne, Nicolas, Esra, Sukkhy, Maud et tous ceux du labo que je ne nomme pas (la liste est

longue) pour avoir partagé mes dernières années de doctorat, corrigé mes articles et ma thèse, et pour les nombreuses soirées passées ensemble. Et finalement, un grand merci à mes parents, mes frères et ma sœur pour m'avoir continuellement encouragé à continuer mes études, aidé quand j'en avais de besoin, et pour votre présence sur laquelle je peux toujours compter.

Chapitre 1. Introduction

1.1. Généralités sur les cancers

Le cancer est un terme général utilisé afin de définir une maladie caractérisée par une prolifération de cellules anormales. Chez tous les individus sains, il existe un équilibre entre le renouvellement cellulaire et la mort cellulaire, de sorte que la production de nouvelles cellules est régulée afin de conserver un nombre constant des différents types cellulaires de l'organisme (Waugh & Grant 2007). Cependant, il arrive que des cellules ne répondent pas aux mécanismes normaux de contrôle de la croissance suite à une mutation ou une activation anormale des gènes régulant la mitose. Ces dernières donnent naissance à des clones de cellules qui prolifèrent indéfiniment, en devenant insensibles aux mécanismes de l'apoptose et en déjouant les processus normaux de réparation de l'ADN. Cette multiplication cellulaire incontrôlée peut résulter en un nombre considérable de clones et ainsi former une tumeur ou un néoplasme dans les organes atteints. Les tumeurs qui continuent à croître avec le temps et deviennent invasives sont dites malignes et portent le terme de cancer. Les cancers sont classés selon l'origine du tissu dont ils dérivent. Plus de 80% des carcinomes proviennent de tissus endodermiques ou ectodermiques ; ceux-ci comprennent entre autres les cancers de la peau, du colon, du sein, du poumon, etc. (Canada 2009).

Aujourd'hui, le cancer est devenu la seconde cause de mortalité dans le monde occidental, devancé seulement par les maladies cardiaques. Au Canada, on prévoit qu'une personne sur trois développera un cancer et les estimations actuelles prédisent qu'une personne sur cinq en mourra (Canada 2009). De plus, le nombre de nouveaux cas de cancer au Canada en 2009 est estimé à 171 000, dont environ 75 300 décès seront dus à cette maladie. Parmi tous les cancers, celui du poumon demeure la principale cause de décès par cancer tant chez les hommes (28%) que chez la femme (26%), suivie du cancer du sein chez la femme et celui du colon et du rectum chez l'homme.

Il existe également les tumeurs du système immunitaire, les leucémies et les lymphomes, qui sont des tumeurs malignes des cellules hématopoïétiques de la moelle osseuse. Ces derniers représentent environ 9% de la totalité des cancers diagnostiqués. En 2008, environ 14 000 personnes apprenaient qu'elles étaient atteintes par ce type de cancer au Canada (Canada 2009). Les lymphomes se développent sous forme de masse tumorale au sein de tissus lymphoïdes, tels que la moelle osseuse, les ganglions lymphatiques ou le thymus, tandis que les leucémies prolifèrent en tant que cellules isolées. Dans les deux cas, on parle de cancer du sang.

1.2. Le sang, la moelle osseuse et les leucémies

1.2.1. Le système hématopoïétique

Le volume total du sang circulant équivaut à environ 7% du poids corporel (5,6 L chez un homme de 70 kg) et 45% de ce volume est représenté par les éléments figurés: les leucocytes (*i.e.* globules blancs), les érythrocytes (*i.e.* globules rouges ou hématies) et les plaquettes (Waugh & Grant 2007). Ces cellules se forment dans la moelle osseuse chez l'adulte et se retrouvent en suspension dans le plasma lorsqu'elles circulent dans tout l'organisme. Quant à la moelle osseuse, malgré le fait qu'elle soit dispersée anatomiquement, elle constitue l'un des plus gros organes du corps (Ganong 2001); son poids et sa taille sont à peine inférieurs à ceux du foie, correspondant environ à 4% du poids total du corps d'un adulte, soit environ 2,6 kg. Sa fonction principale est de produire et de libérer dans la circulation les cellules sanguines, soit approximativement entre 100 à 200 milliards de globules rouges, 50 milliards de neutrophiles et de 75 à 150 milliards de plaquettes par jour, afin de maintenir ces cellules en nombre constant dans le sang (Goldsby *et al.* 2003, Royer & Arock 1998).

La moelle osseuse rouge contient des cellules souches non spécialisées, dites multipotentes, qui sont capables de s'autorenouveler, de se multiplier, de se différencier en divers types de cellules souches unipotentes, appelés progéniteurs (Figure 1.1). Des réserves distinctes de cellules souches unipotentes existent pour les mégacaryocytes, les lymphocytes, les érythrocytes, les éosinophiles et les basophiles, mais les neutrophiles et les monocytes proviennent d'un précurseur commun (Ganong 2001). Il existe également d'autres lignées cellulaires qui proviennent des cellules souches médullaires, telles que les ostéoclastes, les cellules de Kupffer, les mastocytes et les cellules dendritiques. Chez un individu sain, environ 25% des cellules de la moelle osseuse sont des érythrocytes en voie de maturation et 75% des autres cellules médullaires appartiennent à la lignée myéloïde afin de produire les leucocytes, c'est-à-dire les monocytes, les lymphocytes et les granulocytes (Ganong 2001).

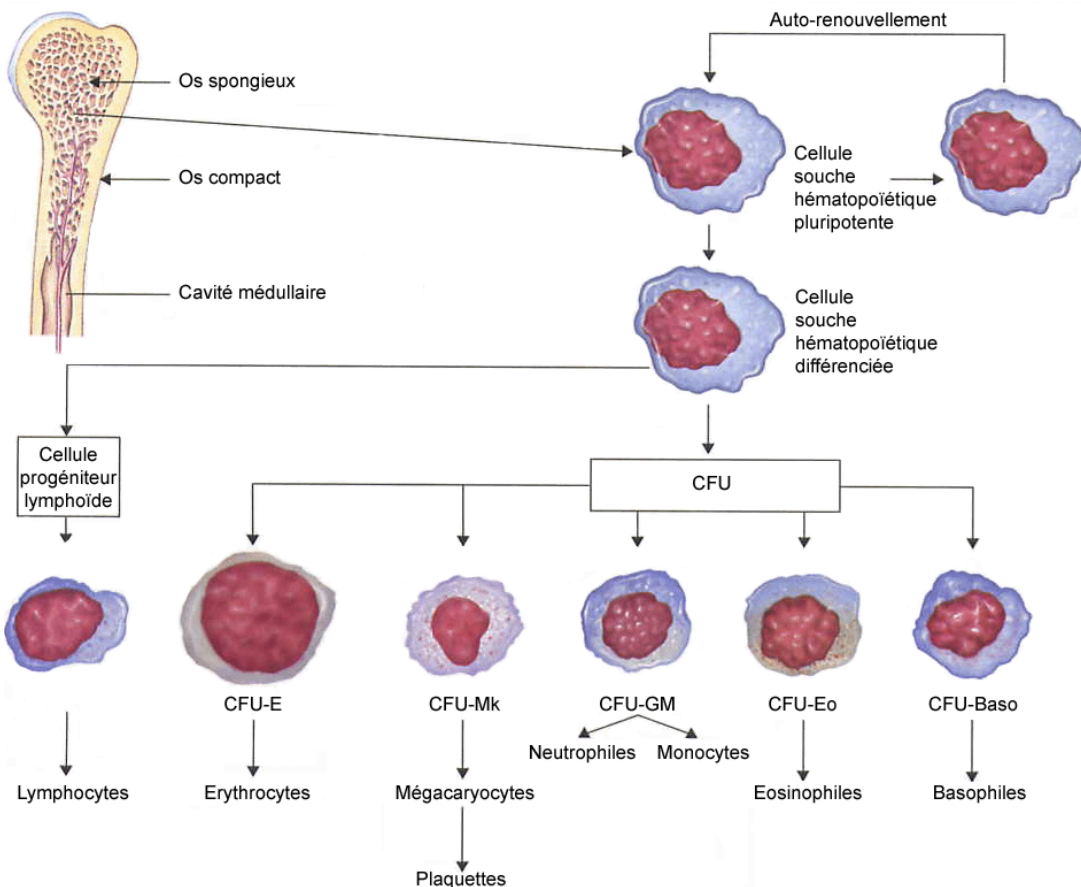


Figure 1.1. Développement des différents éléments cellulaires du sang à partir des cellules de la moelle osseuse, défini comme étant l'hématopoïèse. Les cellules souches hématopoïétiques génèrent les unités de formation de colonies (CFU, «colony-forming unit»). Reproduit de (Rhoades et Pflanzer 2003) avec permission de Cengage Learning/Nelson.

Les cellules souches myéloïdes se développeront en trois différents types de cellules sanguines matures : (i) les érythrocytes qui transportent l'oxygène vers tous les tissus de l'organisme, (ii) les plaquettes qui jouent un rôle dans la prévention des hémorragies en

formant des caillots dans les vaisseaux sanguins endommagés et (iii) les leucocytes de types granulocytes et monocytes qui détruisent les bactéries et luttent contre les infections. Une fois produits, les monocytes quittent la moelle osseuse afin de circuler dans le sang pendant une période moyenne de 72 heures (Ganong 2001). Si aucune substance exogène n'est détectée par les monocytes, ceux-ci migrent alors dans les tissus où ils se différencient en macrophages tissulaires pour y demeurer environ 3 mois. Les macrophages tissulaires comprennent les cellules de Kupffer du foie, les macrophages des alvéoles des poumons et la microglie du cerveau (Ganong 2001). Autrefois appelé le système réticulo-endothélial, le système des phagocytes mononucléés (MPS) est formé ainsi de l'ensemble des monocytes, des macrophages mobiles et tissulaires et de quelques cellules endothéliales spécialisées dans la moelle osseuse, la rate et dans les ganglions lymphatiques. Ce système constitue une barrière efficace contre toutes particules exogènes (ex. bactéries, micro-organismes, vecteurs colloïdaux transportant des principes actifs) pénétrant dans l'organisme.

Un dysfonctionnement des lignées lymphoïdes ou myéloïdes peut être occasionné par divers facteurs physiques et chimiques et ainsi entraîner le développement d'un cancer au niveau des cellules médullaires. En effet, plusieurs facteurs peuvent favoriser le développement d'une leucémie : l'âge avancé de la personne, une radiothérapie ou une chimiothérapie antérieure pour traiter un cancer ou une autre maladie, l'exposition à des doses élevées de radiation ou de substances chimiques (ex. benzène), le tabagisme, certains troubles ou anomalies génétiques (ex. syndrome de Down, chromosome Philadelphie), la présence d'un gène défectueux héréditaire, une affection du système sanguin (ex. syndrome myélodysplasique) ou une infection virale antérieure (ex. virus T-lymphotrope humain I) (Waugh & Grant 2007). Cependant, comme tout cancer, la leucémie peut parfois se développer en l'absence de tous ces facteurs de risque.

Il existe deux stades de leucémies, aiguë ou chronique, dont la distinction est fondée principalement sur la maturité de la cellule impliquée. En règle générale, plus les cellules impliquées sont immatures et indifférenciées, plus la leucémie est dite aiguë et entraîne une survie de quelques mois en l'absence de traitement (Waugh & Grant 2007). Les leucémies aiguës incluent la leucémie lymphocytique aiguë (ALL) et la leucémie myéloblastique aiguë (LMA) possédant la caractéristique commune de se développer à n'importe quel âge. Au contraire, lorsque les cellules matures et différenciées sont atteintes, la maladie peut être quasi chronique et évoluer parfois très lentement, pendant 10 à 20 ans. Ces dernières incluent la leucémie lymphoïde chronique (CCL) et la leucémie myéloïde chronique (CML). Elles sont surtout rencontrées chez l'adulte.

1.2.2. Leucémie myéloblastique aiguë

La LMA est le sous-type de leucémie le plus commun, environ 13 000 nouveaux cas sont diagnostiqués par année aux Etats-Unis. L'incidence annuelle est de l'ordre de 2,5/100 000 et augmente en fonction de l'âge jusqu'à 12-13/100 000 chez les personnes âgées de plus de 65 ans. L'âge moyen au moment du diagnostic de la LMA est de 62 ans (Zenhausern *et al.* 2003). À travers le monde, l'incidence de la LMA est en croissance chez les personnes âgées. Elle est principalement due aux conséquences d'un traitement antérieur envers les tumeurs solides par chimiothérapie et/ou radiothérapie ou fait suite à l'exposition néfaste et chronique de certains facteurs environnementaux.

Contrairement aux leucémies lymphoïdes qui se caractérisent à la fois par un taux élevé de globules blancs et l'absence de cellules immatures dans le sang, la LMA implique une série de changements génétiques chez les cellules hématopoïétiques précurseurs. Il y a alors modification de la croissance et de la différenciation des cellules normales hématopoïétiques, suivie d'une expansion du clone malin dans la moelle osseuse et dans le

sang. Ces cellules précurseurs hématopoïétiques malignes peu différenciées, appelées blastes, peuvent proliférer de façon illimitée, mais ne sont pas capables de devenir des cellules sanguines normales. Comme les autres types de cancers, les altérations génétiques rencontrées dans la LMA résultent à la fois d'une activation des oncogènes et du dysfonctionnement des gènes suppresseurs de tumeur (Gilliland *et al.* 2004). Quel que soit le tissu d'origine (*i.e.* moelle osseuse ou ganglion lymphatique), presque toutes les leucémies s'étendent aux organes fortement vascularisés, tels que la rate, les ganglions lymphatiques ou le foie. On retrouve fréquemment une destruction de ces tissus au fil du temps, puisqu'en envahissant ces organes, les cellules cancéreuses se reproduisent en utilisant les éléments du métabolisme tissulaire normal. Plusieurs manifestations cliniques sont alors observées, comme par exemple des manifestations neurologiques, des lésions cutanées ainsi qu'une hépato-spléno-adénomégalie (Ball *et al.* 1991, Zenhausern *et al.* 2003). Dès le début de la maladie, des anomalies quantitatives et qualitatives du sang périphérique sont constatées dû à l'occupation de la moelle osseuse par les cellules leucémiques non fonctionnelles (Zenhausern *et al.* 2003). L'anémie est constante, souvent sévère, le taux de plaquettes est inférieur à $50 \times 10^3 / \mu\text{L}$, le nombre de leucocytes est le plus souvent élevé (entre 10×10^3 et $100 \times 10^3 / \mu\text{L}$) mais peut être diminué ($< 5 \times 10^3 / \mu\text{L}$) (Ball *et al.* 1991).

Le processus cancéreux conduit parfois à la production de cellules partiellement différenciées, provoquant ainsi des leucémies spécifiques à la lignée des neutrophiles, des éosinophiles, des basophiles ou les monocytes. Il existe également différentes sous-classes de la LMA, allant de M0 à M7, tel que proposé par le Groupe Coopératif Franco-Américano-Britannique (FAB) (Bennett *et al.* 1976) (Tableau 1.1). Ces sous-classes sont déterminées par la morphologie cellulaire observée au microscope et par le degré de maturation des cellules leucémiques. En classifiant les différents types de la LMA de cette façon, les traitements développés sont devenus plus ciblés et plus efficaces afin d'éradiquer les cellules anormales.

Tableau 1.1. Classification des différentes sous-classes de la LMA par le Groupe coopératif franco-américano-britannique (FAB) (Andoljsek et al. 2002, Bennett et al. 1976, Zenhausern et al. 2003).

Sous-Classe FAB	Nom	Marqueurs cellulaires exprimés (+) ou absents (-)	Fréquence relative des différentes formes de la LMA
M0	Leucémie myéloblastique aiguë indifférenciée	CD13+, CD33+, CD34+ CD14-, MPO-, HLA-DR+	2-5 %
M1	Leucémie myéloblastique aiguë sans différenciation	CD13+, CD33+, CD34+, CD14-, MPO+, HLA-DR-, CD11a +/-	15-20%
M2	Leucémie myéloblastique aiguë avec différenciation	(CD11a), CD13+, CD33+, CD34+/-, CD14-, MPO+, HLA-DR+, CD15+/-, CD11a +/-	10-30%
M3	Leucémie promyélocyttaire aiguë	CD13+, CD33+, CD34-, CD14-, CD15+/-, MPO+, HLA-DR-, CD11a +/-	10-11%
M4	Leucémie myélomonocytaire aiguë	CD11a+, CD13+, CD33+, MPO+, CD14+, HLA-DR+	25-37%
M5	Leucémie monocyttaire aiguë	CD11a+, CD13+, CD33+, MPO-, CD14+, HLA-DR+	9-10%
M6	Érythroleucémie aiguë	CD13+, CD33+, MPO+, glikoforine A+	3-5%
M7	Leucémie mégacaryoblastique aiguë	CD41+, CD33+, CD34+, HLA-DR+	1-5%

Les critères diagnostiques reposent sur la morphologie des cellules observées au microscope, la cytochimie par coloration d'enzymes spécifiques présentes dans le cytoplasme des cellules leucémiques, la cytogénétique, l'étude du phénotype des blastes à l'aide de marqueurs cellulaires spécifiques analysés par cytométrie en flux et la recherche de certains marqueurs moléculaires intracellulaires (Griffin *et al.* 1981, Zenhausern *et al.* 2003). Le diagnostic d'une LMA est alors posé si l'on trouve plus de 20-30% de blastes myéloïdes dans la moelle ou le sang périphérique ou si une tumeur extramédullaire se compose de blastes myéloïdes (Zenhausern *et al.* 2003).

Afin de définir et confirmer le phénotype particulier des blastes leucémiques, plusieurs études immunologiques des antigènes de surface ont été menées ces dernières années. Elles ont consisté à produire un grand nombre d'anticorps monoclonaux contre des structures antigéniques de surface des cellules myéloïdes normales et leucémiques. Puisqu'ils sont hautement spécifiques, ces anticorps monoclonaux s'avèrent maintenant essentiels dans le diagnostic des différents sous-types de leucémie et sont utilisés seuls ou en association avec d'autres marqueurs cellulaires afin de corroborer la nature de la pathologie (Tableau 1.1). Par exemple, 80% des leucémies monoblastiques aiguës et myélomonocytaires (M4 et M5 de la classification FAB) et 40% des leucémies myéloblastiques et promyélocytaires (M1, M2, M3) peuvent être identifiées par l'anticorps monoclonal Mo1 (CD11a). Ce dernier reconnaît une glycoprotéine de surface composée de 2 sous-unités de 94 et 144 kDa et est associé au récepteur C3bi sur les monocytes et les granulocytes (Arnaout *et al.* 1983). L'anticorps monoclonal Mo2 (CD14) présente un fort intérêt diagnostique en reconnaissant une glycoprotéine de 55 kDa. Il sert à identifier les cellules de la lignée monocytaire et est positif dans 50% des cas de leucémie aiguë monoblastique et myélomonocytaire (M4 et M5). Les anticorps monoclonaux de la série My1-My9 sont également importants. Par exemple, My7 (CD13) et My9 (CD33) reconnaissent 80% des leucémies myéloblastiques (M1 et M2), 100% des leucémies aiguës promyélocytaires (M3) et plus de 80% des leucémies monoblastiques et myélomonocytaires (M4 et M5) (Griffin *et al.* 1984, Griffin *et al.*

al. 1981). Certains anticorps peuvent infirmer certaines classes de leucémies, comme c'est le cas pour le My9 qui est toujours négatif dans les leucémies lymphoïdes (Griffin *et al.* 1984). Quant à l'anti-My-10 (CD34) produit par Civin *et al.* (Civin *et al.* 1984), il se lie à un antigène qui s'exprime uniquement aux premiers stades de la différenciation hématopoïétique. Le CD34 est utile dans l'identification de blastes médullaires chez les patients en rémission complète, puisqu'il n'est pas spécifique pour la lignée myéloïde. Il réagit avec 32% de leucémies aiguës lymphoblastiques et 28% des leucémies myéloïdes.

1.2.3. L'antigène de surface CD33

Le CD33 est un marqueur phénotypique spécifique et fiable pour la LMA, étant donné son expression sur plus de 70-90% des blastes. La densité relative de l'expression du CD33 varie parmi les différents types de leucémies mais on retrouve environ entre 10 000 et 20 000 sites de liaisons sur chaque cellule leucémique (Scheinberg *et al.* 1991). L'expression du CD33 est restreinte à la lignée myéloïde des cellules hématopoïétiques, incluant une densité élevée sur les monocytes circulants, les macrophages tissulaires, les cellules de Langerhans, les mastocytes et un faible niveau d'expression sur les granulocytes. L'antigène de surface CD33 est une glycoprotéine transmembranaire de 67 kDa, désignée également gp67, pouvant se lier spécifiquement à l'acide sialique. Cet antigène de surface fait partie de la famille des lectines de type 1 et de la superfamille des immunoglobulines (Ig) par son homologie de séquence (comme les domaines variables et C2) avec les Ig (Wellhausen & Peiper 2002) (Figure 1.2). Il possède donc une structure semblable aux autres Siglec («*Sialic Acid Binding Immunoglobulin-like Lectins*»), comprenant le CD22, la sialoadhésine (SN) et la glycoprotéine associée à la myéline spécifique aux neurones (MAG).

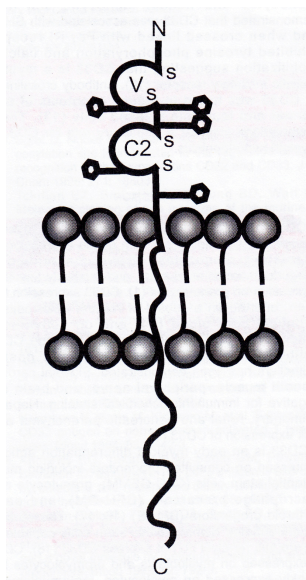


Figure 1.2. Structure de l'antigène de surface CD33. Reproduit de (Wellhausen & Peiper 2002) avec permission de Biolife s.a.s.

Le CD33, localisé sur le chromosome 19q 13.1-3, est un polypeptide composé de 364 acides aminés qui possède 2 motifs inhibiteurs dépendants de la tyrosine des immunorécepteurs (ITIMs). De façon générale, lorsque ces motifs ITIMs sont phosphorylés par une enzyme, ils ont comme rôle de bloquer l'activation cellulaire en inhibant le signal de transduction. Bien que le rôle précis du CD33 ne soit pas encore élucidé, la présence du site de phosphorylation de la tyrosine dans le domaine cytoplasmique du CD33 met en évidence une implication de ce dernier dans la signalisation intracellulaire. Effectivement, la phosphorylation de la tyrosine par les kinases de la famille des Src (*i.e.* lyn, fyn et lck) s'est démontrée essentielle dans le mécanisme d'internalisation du récepteur *via* les ITIMs (Taylor *et al.* 1999, Paul *et al.* 2000, Balaian *et al.* 2005, Walter *et al.* 2008). De récentes études sur des lignées monocytaires humaines ont démontré une association entre le CD33, les protéine tyrosine phosphatase SHP-1, l'adapteur CrkL, la phospholipase PLC- γ 1

(phosphorylée par la kinase Syk), le récepteur Fc- γ RI et une mobilisation du calcium (Ulyanova *et al.* 1999, Walter *et al.* 2008). La protéine kinase Syk, une enzyme de protéine de gène «suppresseur de tumeur» connue pour jouer un rôle dans l'adhésion, la phagocytose, la prolifération et la différentiation des cellules myéloïdes est également phosphorylée suite à l'activation du récepteur CD33 (Balaian *et al.* 2003). Ceci confirme que le CD33 pourrait jouer un rôle de récepteur inhibiteur spécifique à la lignée myéloïde. En conclusion, le CD33 serait impliqué dans les interactions entre les cellules, aurait un rôle dans la voie de signalisation du système hématopoïétique et pourrait posséder également des fonctions de régulation au niveau du système immunitaire ainsi que dans la prolifération cellulaire (Lajaunias *et al.* 2005, Pagano *et al.* 2007).

Ce récepteur s'est avéré une cible de choix pour le diagnostic et le traitement de la LMA puisqu'il est typiquement exprimé par les blastes leucémiques et non par les cellules pluripotentes hématopoïétiques progénitrices. Il y a quelques années, un anticorps monoclonal murin anti-CD33 (M195) a été isolé et «humanisé» en greffant des régions complémentaires à l'anticorps, dans le but d'augmenter la reconnaissance et l'affinité pour le récepteur CD33 humain (Caron *et al.* 1992) (Figure 1.4). Cet anticorps, lorsqu'associé à un agent anticancéreux (Figure 1.5), a permis d'augmenter la survie des patients réfractaires à la chimiothérapie conventionnelle de la LMA (Larson *et al.* 2005) (voir Section 1.4.2).

1.3. Traitements conventionnels de la LMA

La chimiothérapie intensive d'induction demeure le traitement quasi obligatoire pour les patients atteints de la LMA. Elle a pour unique but l'élimination des blastes leucémiques et la restauration rapide de la fonction médullaire normale. On parle alors de rémission lorsque les paramètres cliniques et biologiques sont normaux pendant une

période d'au moins un mois : cela inclut une moelle osseuse contenant moins de 5% de blastes leucémiques et assurant en périphérie, entre autres, une concentration en hémoglobine supérieure à 9 mg/dL, plus de 1500 polynucléaires neutrophiles/ μ L et plus de 100 000 plaquettes/ μ L (Larson *et al.* 2005). Afin d'y parvenir, l'anticancéreux cytosine arabinoside, appelée aussi cytarabine, 1- β -D-arabinofuranosylcytosine, ara-C, ou Cytosar-U[®] est l'agent thérapeutique le plus utilisé. L'ara-C fait partie de la famille des analogues nucléosides et diffère de la cytidine au niveau du ribose. Celui-ci est remplacé par un arabinose. Cette molécule est utilisée seule ou en combinaison avec d'autres agents cytostatiques de la classe des anthracyclines, comme par exemple la daunorubicine, l'idarubicine, la mitoxantrone. Le fluorouracil, le méthotrexate, le dexaméthasone font également partie des molécules actives régulièrement administrées en association avec l'ara-C pour le traitement d'induction de la LMA (Shipley & Butera 2009, Zenhausern *et al.* 2003).

1.3.1. Le traitement à l'ara-C

De façon générale, les analogues de nucléosides constituent une famille largement utilisée dans le traitement des leucémies et de quelques tumeurs solides. Ce sont des molécules de très faible poids moléculaire dont le métabolisme est similaire à celui des nucléotides physiologiques. En effet, comme pour leur analogue respectif, ces molécules inactives traversent la membrane cellulaire *via* un transporteur spécifique et subissent plusieurs étapes de phosphorylations intracellulaires par les enzymes présentes dans les cellules, permettant ainsi la production et l'accumulation des métabolites actifs, les dérivés di- et tri-phosphates (Powis 1994). Ces derniers exercent principalement leur activité cytotoxique par interaction avec les enzymes du métabolisme des nucléotides physiologiques et par leur incorporation dans l'ADN et/ou l'ARN provoquant la mort

cellulaire par apoptose. Toutes ces caractéristiques sont applicables pour l'antipyrimidine ara-C. En effet, après internalisation cellulaire de l'ara-C par les transporteurs transmembranaires hENT1/hCNT1, celle-ci est convertie en cytarabine monophosphate, puis en cytarabine triphosphate (ara-CTP) suite à sa phosphorylation par l'enzyme déoxycytidine kinase présente dans le cytoplasme cellulaire (Powis 1994) (Figure 1.3). Il y a alors compétition entre l'ara-CTP et son analogue naturel, la déoxycytidine triphosphate, pour son incorporation dans l'ADN. Cette molécule est efficace seulement chez les cellules dont le cycle cellulaire est en phase de synthèse (phase S) et son efficacité dépend alors du taux de synthèse de l'ADN. Une concentration intracellulaire et un temps d'exposition minimaux sont également importants afin que l'ara-CTP puisse avoir un effet cytotoxique (Muus *et al.* 1987). Les mécanismes d'action de l'ara-C sont nombreux : (i) elle induit la différenciation des cellules leucémiques en diminuant l'expression de l'oncogène CmyC (Mitchell *et al.* 1986); (ii) elle inhibe l'ADN polymérase ; (iii) elle empêche la transformation de la cytidine en déoxycytidine ; (iv) elle s'incorpore dans l'ADN et ralentit l'elongation de la chaîne d'ADN en créant un défaut de liaison des fragments d'ADN nouvellement synthétisés ; (v) elle interfère avec la réparation de l'ADN en inhibant les polymérasées α et β , entraînant ainsi un arrêt de l'elongation et un blocage du cycle cellulaire en phase S, suivi de la mort de la cellule (Powis 1994). Contrairement à l'antipyrimidine 5-Fluorouracile et l'anticancéreux Fludarabine (9- β -D-arabinofuranosyl-2-fluoroadenine, F-ara-A) qui s'incorpore à la fois dans l'ADN et l'ARN, l'ara-CTP se limite à l'ADN (Major *et al.* 1981).

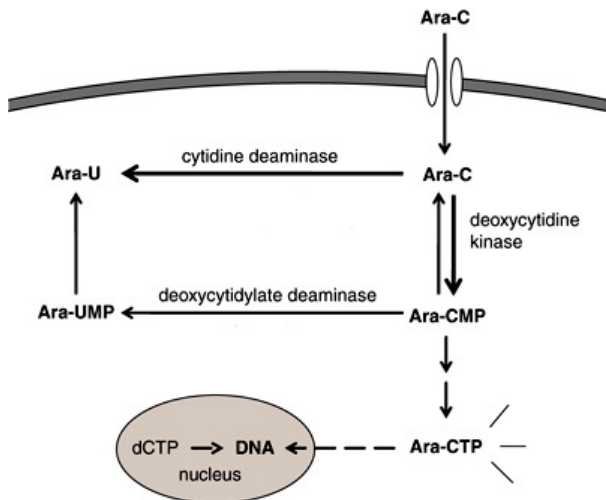


Figure 1.3. Schéma d'activation intracellulaire de l'ara-C par diverses enzymes. Reproduit de (Mahlknecht *et al.* 2009) avec permission de Nature Publishing Group.

L'ara-C a été approuvée aux États-Unis et au Canada pour le traitement de la leucémie il y a environ 40 ans. Cette dernière est devenue un composé essentiel pour le traitement initial de la LMA. Elle permet une rémission complète chez 30% des patients lorsqu'elle est administrée par la voie intraveineuse en monothérapie aux doses conventionnelles de 100-200 mg/m² par jour. Une administration répétée pendant 7 jours consécutifs et une infusion continue sur une période de 5 heures demeurent, par contre, indispensables afin d'observer une réponse au traitement. En effet, lorsque l'ara-C est administrée de façon systémique, son activité est grandement diminuée à cause de sa rapide déamination par l'enzyme cytidine déaminase (Powis 1994). Le principe actif est alors transformé en métabolite dépourvu d'activité biologique, le 1-β-D-arabinofuranosyluracil (uracil arabinoside, ara-U). Ce dernier se retrouve rapidement éliminé dans l'urine. L'élimination de l'ara-C est biphasique, avec un temps de demi-vie initial variant de 7 à 20

minutes et un temps de demi-vie terminal de 2 à 3 heures (Plunkett *et al.* 1987). Dépendamment de l'âge des patients et des facteurs de risque, un meilleur taux de rémission peut être obtenu, soit de 60 à 80%, suite à une administration d'ara-C à fortes doses, c'est-à-dire 2-3 g/m² par la voie intraveineuse (12 doses) (Bolwell *et al.* 1988), ou lorsqu'elle est associée à d'autres médicaments, principalement ceux de la classe des anthracyclines (Bishop 1997, Estey 2001, Stone 2002).

1.3.2. Association de l'ara-C avec une anthracycline

De meilleurs taux de rémission sont obtenus suite à la co-administration de l'ara-C à une anthracycline, puisque les propriétés et les mécanismes d'action de ces deux principes actifs sont différents. En effet, les anthracyclines diffusent passivement dans les cellules et, une fois dans le noyau, elles s'intercalent dans l'ADN et inhibent l'activité de la topoisomérase II. Cette dernière joue un rôle essentiel dans de nombreuses étapes de la vie cellulaire (*e.g.* réPLICATION, transcription, séparation des chromosomes, etc) en clivant et recollant les 2 brins d'ADN afin de permettre son élongation (Capranico *et al.* 1995). La daunorobucine est l'anthracycline la plus utilisée dans le traitement de la LMA, elle est infusée par la voie intraveineuse sur une période de 15 minutes et son administration est répétée pendant 3 jours. Son analogue, l'idarubicine, est lipophile et peut, quant à lui, être administré par la voie orale. Bien que les anthracyclines fassent partie du traitement conventionnel pour la LMA, leur toxicité n'est pas négligeable. En effet, la cardiotoxicité est très élevée, empêchant leur usage lors d'un second traitement chez les patients leucémiques réfractaires ou chez les personnes âgées possédant des problèmes cardiaques. Afin de remédier à ce problème, des chercheurs ont encapsulé les anthracyclines dans des liposomes (voir Chapitre 2). Leurs applications dans le traitement de la LMA sont résumées par Fassas et Anagnostopoulos (Fassas & Anagnostopoulos 2005). Comme attendu,

l'encapsulation de la daunorubicine à l'intérieur des vésicules lipidiques a permis de protéger le principe actif contre sa conversion en métabolite toxique ainsi que de diminuer les effets secondaires, tels que la cardiototoxicité, l'alopécie, les nausées et la myélosuppression. La daunorubicine liposomale, combinée ou non à l'ara-C, permet un taux de rémission complet variant entre 30-45% chez les patients LMA réfractaires (Cortes *et al.* 2001, Fassas & Anagnostopoulos 2005, Fassas *et al.* 2002).

1.3.3. Résistance à l'ara-C

Malgré une rémission complète chez environ 80% des patients nouvellement diagnostiqués, il persiste cependant des cellules tumorales, non décelables par microscopie conventionnelle, qui peuvent entraîner une rechute dans les mois suivants si le traitement n'est pas poursuivi. En effet, la majorité des patients atteints de LMA développent une résistance au traitement due principalement aux faibles concentrations intracellulaires de l'ara-CTP et à certaines modifications d'expression des gènes. Il a été démontré que les lignées cellulaires leucémiques exposées à des concentrations croissantes d'ara-C sur une longue période deviennent résistantes par le biais de (i) modifications de l'affinité de l'ara-CTP pour l'ADN polymérase; (ii) d'une réduction de la quantité des transporteurs membranaires hENT1 et hCNT1 (Gourdeau *et al.* 2001); (iii) d'une délétion de la déoxycytidine kinase (Tattersall *et al.* 1974); (iv) d'une perte des gènes impliqués dans la dégradation des analogues des nucléosides, tels que les 5'-nucléotidases (5NT), provoquant ainsi une augmentation du pool intracellulaire de dCTP qui entre en compétition avec l'ara-CTP; (v) des modifications de l'expression membranaire des pompes d'efflux ou des transporteurs bidirectionnels. Finalement, un taux élevé d'enzyme cytidine déaminase, intervenant dans les processus de dégradation de l'ara-CTP (Chabner *et al.* 1979), a

également été corrélé avec une baisse d'efficacité du traitement par l'ara-C chez les patients leucémiques (Schroder *et al.* 1998).

Dus à ces différents mécanismes de résistance, une maladie résiduelle s'installe, nécessitant une seconde chimiothérapie. La phase de traitement suivante se nomme traitement de consolidation, consiste principalement en une dose très élevée d'ara-C et requiert une hospitalisation des patients pendant quelques semaines (Shipley & Butera 2009). Comme les traitements intensifs de chimiothérapie détruisent la moelle osseuse en même temps que les cellules leucémiques, la greffe de cellules souches hématopoïétiques est nécessaire afin de régénérer la moelle osseuse des patients souffrant d'aplasie définitive (Zenhausern *et al.* 2003). Habituellement, avant le début de la chimiothérapie intensive, des cellules souches de la moelle osseuse du patient sont prélevées (Shipley & Butera 2009). Quelques temps après la thérapie, les cellules souches sont réinjectées dans le sang du patient et, en quelques semaines, ces nouvelles cellules souches produisent des cellules sanguines normales, il s'agit alors d'une autogreffe. La greffe allogénique est effectuée lorsque des cellules souches provenant de donneur HLA identique familial ou non apparenté sont disponibles pour le patient. Bien que l'efficacité anti-tumorale des greffes des cellules souches de la moelle osseuse soit supérieure aux autres traitements, avec un taux de rechute plus faible, il existe quelques complications (*e.g.* douleur, infection, hémorragie, rejet du greffon de l'hôte, etc.), limitant cette application à des patients pour lesquels le risque de rechute ou de mortalité liée à la maladie est nettement supérieur au risque du traitement lui-même.

1.3.4. Les limites des thérapies actuelles

La majorité des patients souffrant de la LMA ne survit pas plus de cinq ans. La mortalité dépend (i) de l'âge de la personne atteinte, (ii) de l'étendue de la maladie au

moment du diagnostic, (iii) des facteurs de risques, (iv) de la toxicité du traitement d'induction, (v) de la résistance face au traitement et (vi) de la rechute de la leucémie. Depuis plusieurs années, de nouveaux protocoles de recherche tentent d'améliorer la survie à long terme des patients, soit en intensifiant la posologie, soit en ajoutant d'autres classes de médicaments mais aucune différence significative n'a été obtenue jusqu'à maintenant (Shipley & Butera 2009). De nouvelles stratégies thérapeutiques plus spécifiques sont alors nécessaires afin de cibler préférentiellement les cellules cancéreuses, d'éliminer complètement ces dernières au niveau de la moelle osseuse, et de diminuer la toxicité intensive associée à la chimiothérapie actuelle.

1.4. Traitements alternatifs de la LMA

1.4.1. L'anticorps monoclonal M195

Cibler directement les molécules à la surface des cellules pour le traitement du cancer est un progrès thérapeutique majeur et très prometteur. En effet, par l'usage d'un ligand spécifique, il est possible de diriger les composés actifs directement envers les cellules anormales ou les tissus d'intérêt après une administration systémique. Certains récepteurs provoquent, à la suite d'une reconnaissance et d'une association avec leur ligand, une internalisation du principe actif dans les cellules cibles et permettent par conséquent d'augmenter les concentrations intracellulaires de médicament (Prokop & Davidson 2008). Parmi les molécules de reconnaissance utilisées pour la LMA, on peut citer les antigènes de surface CD33, CD45, et CD66 (Burke *et al.* 2002). L'emploi d'un anticorps monoclonal possédant un pouvoir délétère sur la survie des cellules cancéreuses, utilisé seul, en association avec d'autres molécules endogènes du système immunitaire ou conjugué à un principe actif est maintenant envisageable. Plusieurs anticorps monoclonaux

sont présentement en étude clinique ou même déjà commercialisés (Burke *et al.* 2002, Chames *et al.* 2009).

Parmi ceux-ci, il y a le M195, un anticorps monoclonal de souris qui se lie à l'antigène de surface CD33. Le M195 marqué à l'iode 131 a démontré un ciblage rapide et efficace chez les patients atteints de la LMA lorsque administré à une dose inférieure à 5 mg/m². Cependant, l'anticorps seul ne démontre aucune efficacité thérapeutique chez les patients leucémiques et la formation d'anticorps humain anti-souris s'est manifestée lors d'administrations répétées (Schwartz *et al.* 1993). Ainsi, l'anticorps humanisé M195, appelé HuM195 ou lintuzumab, a été développé principalement par les Drs Jurcic et Scheinberg au centre Memorial Sloan-Kettering Cancer à New York (Figure 1.4). Le HuM195 a été obtenu en greffant des régions complémentaires déterminantes de l'anticorps de souris M195 au squelette d'un IgG1 humain. En plus d'acquérir une avidité 8 fois plus élevée pour le site de liaison, ce nouvel anticorps humanisé possède une activité *in vitro* envers les cellules cancéreuses en initiant le mécanisme de cytotoxicité cellulaire dépendante des anticorps (connu sous l'abréviation de ADCC) (Caron *et al.* 1992). Des études cliniques sont présentement en cours afin de déterminer la dose minimale efficace pour détruire les blastes leucémiques présents dans la moelle osseuse. Malgré une augmentation de la cytotoxicité *in vitro* des agents chimiothérapeutiques suite à une co-incubation du HuM195 avec les principes actifs couramment employés dans le traitement de la LMA (*i.e.* ara-C, idarubicin), une étude clinique randomisée de phase III effectuée chez 191 patients réfractaires atteints de la LMA n'a apporté aucune justification de l'emploi du HuM195. En effet, cette étude n'a pas démontré une amélioration du traitement lorsque le lintuzumab était co-administré avec la mitoxantrone, l'étoposide ou l'ara-C (Feldman *et al.* 2005).

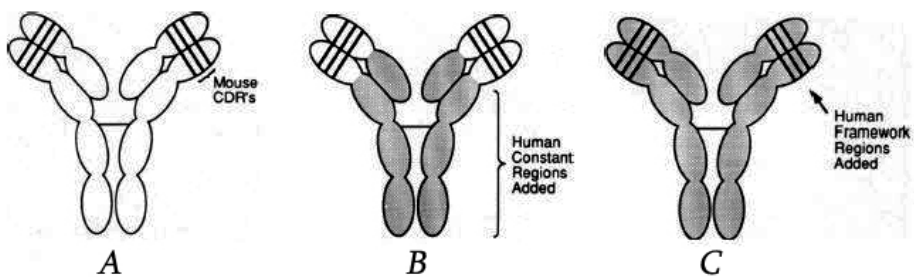


Figure 1.4. L’humanisation de l’anticorps M195, A) M195, B) M195 chimérique et C) le M195 humanisé. Un anticorps chimérique est caractérisé dans la nomenclature par le suffixe «-ximab» et est constitué de régions variables murines (fragments Fab') et de régions constantes humaines. Les anticorps humanisés ont été développés afin de réduire leur antigénicité. Ces anticorps sont caractérisés par le suffixe «-zumab» et sont composés des séquences codant les régions murines déterminant la complémentarité avec l’antigène greffées sur des séquences codant des régions charpentes des domaines variables humains. Reproduit de (Caron *et al.* 1992) avec permission de Waverly Press.

1.4.2. Le Mylotarg®

Une manière d’accroître l’activité antitumorale d’un anticorps monoclonal consiste à le conjuguer à un principe actif ou à une toxine dérivée de bactéries (*ex.* toxine de la diphtérie, l’exotoxine A de *Pseudomonas*), ou de plantes (*ex.* ricine, gélonine). Cette association covalente entre l’anticorps anti-CD33 et un principe actif a vu le jour en 1987. Le Mylotarg®, connu également sous le nom de gemtuzumab ozogamicin et CMA-676, est le premier traitement ciblé par un conjugué anticorps-principe actif destiné au traitement de la LMA (Damle & Frost 2003). Il a été approuvé aux États-Unis par la Food and Drug

Administration (FDA) en mai 2000 et au Japon en 2005, dans le but de traiter uniquement les patients qui ont récidivé suite au traitement par les principes actifs conventionnels et qui ne pouvaient pas recevoir d'autres types de chimiothérapie intensive. Le Mylotarg® est distribué aux États-Unis par la compagnie Wyeth Pharmaceuticals® sous forme de poudre à une dose de 5 mg, prête à être diluée et administrée par perfusion. La dose clinique recommandée est 9 mg/m², administrée par voie intraveineuse pendant 2 heures, pour un total de 2 infusions sur 2 semaines séparées (Larson *et al.* 2005). Par contre, cette nouvelle forme thérapeutique n'est toujours pas disponible au Canada.

Le Mylotarg® est constitué de l'anticorps monoclonal anti-CD33 humanisé, le hP67.6, qui est attaché de façon covalente à la *N*-acétyl- γ calichéamicine diméthyle hydrazide à l'aide du bras espaceur 4-(4-acétylphenoxy)acide butanoïque (AcBut) sensible au pH (Figure 1.5). De façon simplifiée, le Mylotarg® se lie avec une forte avidité au récepteur CD33 et est rapidement internalisé dans les endosomes/lysosomes. Le lien hydrazone est hydrolysé au cours de l'acidification de ces organelles, libérant ainsi la calichéamicine, qui est un principe actif puissant synthétisé naturellement par *Micromonospora echinospora*. Suite à sa réduction par les thiols intracellulaires (*i.e.* glutathion), la partie enediyne (*i.e.* structure cyclique très réactive) se réorganise sous forme de radicaux 1,4-benzenoïdes (Damle & Frost 2003). Cette espèce radicalaire exerce sa toxicité en captant les hydrogènes du squelette de l'ADN. Elle initie alors une scission irréversible de la double hélice de l'ADN et provoque ainsi la mort cellulaire par apoptose (Lee *et al.* 1991).

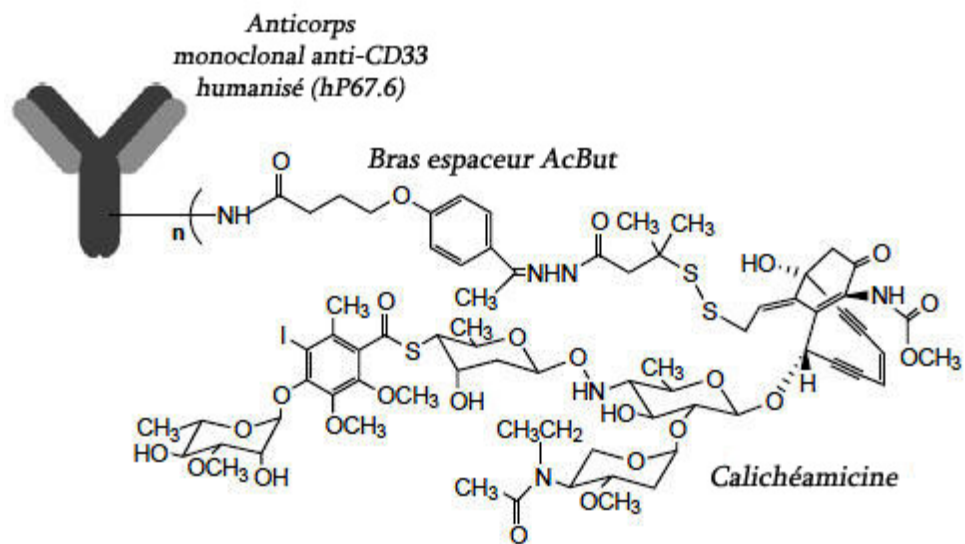


Figure 1.5. La structure chimique du Mylotarg®. Reproduit de (Damle & Frost 2003) avec permission de Elsevier Limited.

Quelques études cliniques ont été réalisées afin de vérifier l'effet thérapeutique du Mylotarg® chez les patients souffrant de la LMA qui ont récidivé après leur phase de traitement d'induction. Ces études ont démontré une rémission complète, c'est-à-dire que les cellules leucémiques n'ont pas été détectées dans le sang et étaient présentes à des taux très faibles dans la moelle osseuse (< 5%) chez environ 30% des 277 patients traités (Larson *et al.* 2005, Sievers *et al.* 2001, Tallman *et al.* 2005). Malgré cette efficacité de traitement, plus de 190 des patients traités ont démontré des réponses variables au Mylotarg®. L'incapacité de ce dernier à éliminer complètement les blastes dans la moelle osseuse et à induire une rémission chez ces patients a été corrélée à des modifications d'expression du récepteur CD33 à la surface des cellules et de l'expression transmembranaire de la Pgp-1 (Damle & Frost 2003, Walter *et al.* 2007). La Pgp-1 est en

effet une glycoprotéine responsable de la résistance de plusieurs médicaments en provoquant un efflux rapide du principe actif à l'extérieur des cellules. Peu après, il a été démontré que l'efficacité du Mylotarg® pouvait être améliorée par la stimulation *in vivo* de l'expression du CD33 sur les blastes leucémiques à l'aide du facteur de croissance granulocytaire (G-CSF) (Leone *et al.* 2004) ou en diminuant l'efflux de la calichéamicine des cellules cancéreuses par des inhibiteurs de la Pgp (Naito *et al.* 2000).

Le Mylotarg® est bien toléré chez les patients et les effets secondaires correspondent davantage aux symptômes dus à l'administration par infusion, c'est-à-dire fièvre, hypotension et frissons. Cependant, un effet indésirable important suite à l'administration du Mylotarg® est la myélosuppression. Une hépatotoxicité a également été identifiée chez certains patients (Larson *et al.* 2005, Pagano *et al.* 2007). Il a été démontré lors d'une étude clinique qu'une baisse de la toxicité hépatique et hématopoïétique pouvait être obtenue par l'administration combinée du Mylotarg® avec l'ara-C et la daunorubicine chez des patients qui n'avaient pas reçu d'autres traitements auparavant. De plus, cette association a permis d'élever le taux de rémission à 80% (Bishop 1997, Estey 2001).

Une étude clinique de phase II conduite sur 142 patients a permis de démontrer qu'aucun sujet n'avait développé de réponse immunitaire contre l'anticorp humanisé ou le complexe calichéamicine-bras espaceur (Sievers *et al.* 2001). Cependant, il existe quelques inconvénients liés à ce nouveau traitement. Par exemple, la liaison entre le principe actif et le bras espaceur sensible au pH possède une faible stabilité à la température corporelle, ce qui pourrait provoquer un relargage prématûré de la calichéamicine dans la circulation et engendrer une toxicité au niveau des cellules et organes sains. De plus, les cellules leucémiques subissant une diminution ou une perte de l'expression du CD33 ne sont pas éliminées par le Mylotarg® chez les patients réfractaires. Ces paramètres sont suivis de près pour permettre d'évaluer le rapport bénéfice/risque apporté par ce médicament.

La production, la commercialisation et les résultats prometteurs du Mylotarg® ont par la suite servi de modèle pour le traitement d'autres cancers tels les lymphomes. En effet, l'anticorps CD22 a également été fixé sur le complexe calichéamicine-AcBut afin de cibler spécifiquement les lymphocytes B et de favoriser l'internalisation du principe actif (Dijoseph *et al.* 2007). Cette nouvelle entité thérapeutique est présentement en phase pré-clinique. Une variété de stratégies ont été testées dans le but d'améliorer l'utilité thérapeutique d'un anticorps monoclonal, telle que la production d'un anticorps chimérique ou son humanisation qui permettraient d'augmenter l'activité immunologique et de limiter son antigénicité. Néanmoins, les résultats escomptés demeurent insuffisants pour éradiquer totalement la maladie. Il demeure nécessaire de combiner différents traitements, de développer de nouvelles molécules et d'améliorer les principes actifs déjà commercialisés, en les modifiant chimiquement ou en les formulant différemment afin de les rendre plus stables et d'améliorer leur biodisponibilité.

1.4.3. Modifications chimiques de l'ara-C

Afin d'améliorer le traitement de la LMA à l'aide de l'ara-C, certaines molécules pouvant jouer un rôle synergique avec cette dernière ont été co-administrées, comme par exemple, la thymidine (Fram *et al.* 1983) ou l'inhibiteur de l'enzyme déaminase, la tetrahydrouridine (Marsh *et al.* 1993). Ces combinaisons se sont avérées efficaces pour améliorer l'effet antitumoral de l'ara-C chez quelques modèles animaux et chez l'humain, mais les doses et la toxicité doivent être évaluées plus en détail afin de diminuer la variabilité inter-individuelle.

En raison de sa fonction amine et de ses multiples groupements hydroxyles, l'ara-C est une molécule très hydrophile. Une biodisponibilité accrue peut être obtenue en la

rendant plus lipophile. C'est pourquoi, quelques essais ont été effectués afin de contrôler la déamination de l'ara-C en modifiant directement la molécule par l'ajout de groupements hydrophobes sur la partie amine en position N⁴ (Figure 1.6). Il s'agit, par exemple, de l'insertion de groupements palmitiques et stéaryles en position N⁴ ou d'esters 5'-(alkyl phosphate) ou 3'-O-acyl-2,2'-anhydre sur la molécule (Aoshima *et al.* 1976, Rosowsky *et al.* 1982). Ces modifications altèrent les propriétés pharmacodynamiques et pharmacocinétiques intrinsèques de la molécule et la transforment ainsi en pro-droge.

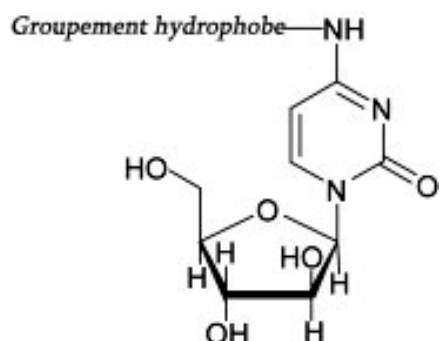


Figure 1.6. Modification de l'ara-C par l'ajout d'un groupement hydrophobe en position N⁴.

De façon générale, une pro-droge est un composé à usage thérapeutique, qui, lorsqu'il est administré, doit subir une biotransformation pour exercer son activité biologique. De ce fait, la partie fragile de l'ara-C, son amine, peut être protégée suite à l'ajout d'un groupement protecteur afin d'être indisponible pour les enzymes déaminases et de demeurer active *in vivo* sur une période prolongée. Un changement structurel de l'ara-C

peut également servir à modifier sa voie d'administration. En effet, pour contrer l'administration d'une infusion systémique prolongée, Kodama *et al.* (1989) ont synthétisé et administré par voie orale l'ara-C modifiée par l'ajout d'un groupement stéaryle en position 5' sur l'ara-C, appelée ainsi cytarabine ocfosfate (1- β -D-arabinofuranosylcytosine-5'-stearylphosphate). Cette nouvelle forme d'ara-C a permis de conserver sa forme active sur une période prolongée (*i.e.* 0,4-0,8 nmol/mL d'ara-C est toujours présent dans le plasma 24 heures après son administration) et s'est démontrée efficace dans le traitement de la leucémie chez le modèle murin de leucémie L1210 (Kodama *et al.* 1989). Des résultats similaires ont été obtenus par Hori *et al.* (1984) à l'aide du N⁴-palmitoyl-1- β -D-arabinofuranosylcytosine (PL-AC) également administré par la voie orale (Hori *et al.* 1984). Ces deux composés sont des dérivés d'acide gras auxquels une biotransformation doit être nécessaire afin de rendre la molécule active dans l'organisme. L'ancitabine (2,2'-anhydro-1- β -D-arabinofuranosylcytosine, cyclotide, cyclo-C) et l'enocitabine (N⁴-behenoyl-1- β -D-arabinofuranosylcytosine, BH-AC) sont d'ailleurs approuvés au Japon depuis 1992 pour le traitement de la LMA.

Les dérivés renfermant de longues chaînes d'acides gras sur le groupe amine de l'ara-C ont démontré une plus grande amélioration de l'activité antitumorale chez la souris leucémique comparativement à l'ajout de courtes chaînes de carbone (Aoshima *et al.* 1976). C'est pourquoi, plusieurs autres dérivés très lipophiles de l'ara-C ont été synthétisés plus récemment, tels que le N⁴-octadecyl-1- β -D-arabinofuranosylcytosine (NOAC) et le N⁴-hexadecyl-1- β -D-arabinofuranosylcytosine (NHAC) (Koller-Lucae *et al.* 1997, Schwendener *et al.* 1996, Schwendener & Schott 1992). Par contre, à cause de la faible solubilité aqueuse des longues chaînes alkyles ajoutées, l'ara-C modifiée ne peut plus être administrée convenablement par la voie intraveineuse. En effet, afin d'obtenir une réponse anti-tumorale adéquate, ces dérivés hydrophobes ont dû être incorporés à l'intérieur de membranes de liposomes unilamellaires composés de phosphatidylcholine de soya et de cholestérol pour être administrés de façon parentérale. Ces liposomes ont démontré une

cytotoxicité supérieure à l'ara-C seule chez la souris inoculée avec des cellules cancéreuses L1210 (Schwendener & Schott 1992). L'incorporation de ces composés NOAC et NHAC dans ces liposomes a également permis de conserver l'activité cytostatique de l'ara-C envers les tumeurs L1210 suite à une administration *per os* chez la souris. D'autres études sont présentement en cours afin d'améliorer la stabilité des ces composés et d'identifier les dérivés hydrophobes de l'ara-C les plus efficaces dans le traitement de la leucémie (Liu *et al.* 2009).

1.4.4. Systèmes à libération prolongée

Les propriétés pharmacologiques des principes actifs peuvent également être améliorées par l'utilisation d'un système à libération prolongée plutôt qu'une modification chimique de la molécule. Ces systèmes de vectorisation sont principalement constitués de lipides, de tensioactifs et/ou de polymères. Ils sont destinés à : (i) modifier les paramètres pharmacocinétiques du principe actif et sa distribution à l'intérieur de l'organisme (*i.e.* biodistribution) ; (ii) servir de réservoir pour le principe actif afin de le protéger contre une agression environnementale/enzymatique ou d'une excrétion prématuée ; (iii) amener le principe actif à son site d'action intra- ou extracellulaire ; (iv) promouvoir une libération soutenue et contrôlée du médicament à travers le temps ; et (v) finalement minimiser sa distribution dans les tissus sains afin de diminuer la toxicité et les effets secondaires (Prokop & Davidson 2008). Pour être considéré comme un système de vectorisation utilisable chez l'humain et devenir efficace dans le traitement d'une pathologie telle que la leucémie, plusieurs caractéristiques sont essentielles: (i) l'incorporation adéquate du principe actif et le contrôle de sa libération, (ii) la stabilité de la formulation dans le temps, (iii) la biocompatibilité des excipients utilisés, (iv) des pharmacocinétiques et

biodistributions optimales et notamment, (v) la capacité à cibler les cellules tumorales ou les organes désirés.

La force particulière des systèmes à libération prolongée consiste à altérer la pharmacocinétique et la biodistribution des principes actifs encapsulés ou associés. Ainsi, le couplage d'un polymère inerte et flexible (*ex.* le poly(éthylène glycol, PEG) à une molécule active, permet d'obtenir un composé de poids moléculaire supérieur qui est excrété plus lentement (Harris & Chess 2003). Il s'agit de macromolécules solubles couramment utilisées comme système de vectorisation de molécules de petites tailles ou toxiques à l'état naturel. L'encapsulation de principe actif à l'intérieur de vecteurs colloïdaux est également une technologie très répandue et permet essentiellement de transformer les propriétés intrinsèques du médicament à celui du vecteur utilisé. En général, lorsqu'un principe actif est encapsulé ou associé à un vecteur : (i) sa clairance diminue ; (ii) son temps de demi-vie augmente ; (iii) son volume de distribution diminue ; et (iv) la surface sous la courbe du temps *vs* la concentration plasmatique augmente (Prokop & Davidson 2008). Les vecteurs tels que les liposomes, les conjugués polymère-principe actif et les nanoparticules peuvent être conçus de manière à demeurer confinés un certain temps dans le compartiment sanguin. Le volume de distribution du médicament vectorisé se rapproche ainsi du volume plasmatique lorsque la libération du principe actif est lente. Ces nouveaux paramètres de pharmacocinétique permettent, dans de nombreux cas, d'améliorer l'efficacité du principe actif et de diminuer les effets toxiques associés au médicament. Le taux de libération du principe actif des vecteurs représente néanmoins un paramètre important puisqu'il a une influence majeure sur l'effet thérapeutique du système employé. Dans de nombreux cas, le principe actif doit être libéré de son vecteur à une vitesse adéquate ou provoqué à l'aide d'un stimulus, pour démontrer une activité supérieure à celle du composé libre (Allen *et al.* 1992a). Ces différents paramètres sont discutés en détail au Chapitre 2.

Afin d'augmenter l'efficacité de l'ara-C, diverses stratégies de vectorisation ont été investiguées, telles que la complexation à des macromolécules (Kato *et al.* 1984), l'encapsulation dans des émulsions (Benoy *et al.* 1974) ou des liposomes (Allen 1992, Kobayashi *et al.* 1977).

1.4.4.1. Macromolécules solubles

Les polymères naturels ou synthétiques hydrosolubles sont couramment utilisés pour le transport de médicaments. Les macromolécules hydrophiles incluent par exemple les anticorps ainsi que plusieurs polymères, tels que le PEG, le poly(hydroxypropyl methacrylamide), la poly(L-lysine), le poly(acide aspartique), la poly(vinylpyrrolidone), le poly(*N*-vinyl-2-pyrrolidone-*co*-vinylamide) et le poly(acide glutamique). Le principe actif peut être conjugué directement au polymère ou à l'aide d'un bras espaceur. Ce dernier permet une meilleure exposition de la molécule au milieu biologique. Cependant, sa dégradabilité est une caractéristique essentielle afin de libérer le médicament pour qu'il retrouve son activité biologique (Prokop & Davidson 2008). La conjugaison de la molécule active à un polymère permet de restreindre sa biodistribution, diminuant ainsi les effets secondaires et permettant également d'augmenter la concentration au site d'action notamment grâce à l'effet EPR (voir Chapitre 2). Le rayon hydrodynamique moyen de ces vecteurs est d'environ 1 à 10 nm. À titre d'exemple, les interférons PEGylés, PEG-Intron® et Pegasys®, utilisés pour le traitement de l'hépatite C, sont présentement sur le marché. Leur PEGylation a permis de diminuer le nombre d'injections à une administration hebdomadaire (Harris & Chess 2003). Cependant, le principal inconvénient associé à ces macromolécules solubles dans l'eau est le faible taux de chargement en principe actif.

Quelques pro-drogues macromoléculaires d'ara-C ont été étudiées afin d'améliorer le profil pharmacocinétique de cette dernière. Par exemple, l'acide poly-L-glutamique (PGA) et le poly-N⁵-(2-hydroxyéthyle)-L-glutamine (PHEG) ont été conjugués en position

N^4 via un lien amide (Kato *et al.* 1984), de même que le chitosan a été couplé à l'ara-C via un bras d'anhydride glutarique, abrégé chi-glu-ara-C (chitosan- N^4 -(4-carboxybutyryl)-1- β -D-arabinofuranosylcytosine) (Ichikawa *et al.* 1993). L'effet antitumoral de ces nouveaux composés a été évalué chez la souris porteuse de tumeurs. Par exemple, Ichikawa *et al.* (1993) ont démontré que le composé chu-glu-ara-C augmentait le taux de survie des souris porteuses de leucémie P338 à 61% suite à une dose de 88 mg ara-C/kg. A contrario, 100 mg ara-C/kg n'ont pu prolonger la survie des animaux. Cependant, que ce soit les PGA/PHEG ou la chi-glu-ara-C, ces nouvelles formes pharmaceutiques comportent certains inconvénients. En effet, le degré de chargement et l'emplacement de la molécule d'ara-C sur les copolymères est aléatoire affectant ainsi l'hydrolyse de l'ara-C. De plus, une libération hâtive du principe actif a été observée *in vitro* pour certains conjugués dans des conditions physiologiques (37°C, pH 7.0) (Kato *et al.* 1984). Bien que les conjugués PGA/PHEG ont eux aussi apporté une activité anti-leucémique améliorée chez le modèle murin L1210 par rapport à l'ara-C seule, leur commercialisation demeure improbable en raison des nombreux problèmes devant être encore résolus. Afin d'éviter ces incertitudes, la majorité des chercheurs a opté pour des nanosystèmes émulsifiés afin d'encapsuler l'ara-C, plutôt que de la conjuguer à un polymère.

1.4.4.2. Émulsion

Une émulsion consiste d'au moins deux phases liquides non-miscibles, dont l'une est une dispersion de globules (phase interne) dans une phase continue (phase externe), stabilisée par des agents émulsifiants. Les globules dispersées présentent un diamètre entre 0.1 et 10 μm mais leur taille dépend des excipients utilisés et du procédé d'émulsification choisi (Le Hir 2006). Cette forme pharmaceutique peut être employée pour: (i) permettre la solubilisation d'un principe actif hydrophobe, (ii) augmenter sa stabilité et (iii) accroître sa biodisponibilité.

En fonction de la nature de la phase interne ou externe, différents types d'émulsions peuvent être préparées. Lorsque la phase huileuse est dispersée dans une phase aqueuse continue, on parle d'émulsion huile-dans-eau (h/e) ; tandis qu'une émulsion eau-dans-huile (e/h) se définit comme une phase aqueuse dispersée dans une phase huileuse (Le Hir 2006) (Figure 1.7). Il y a également le terme «émulsion multiple» qui est employé afin de définir les émulsions dont la phase dispersée contient des gouttelettes d'une autre émulsion. Il s'agit alors d'émulsions eau-dans-huile-dans-eau (e/h/e) ou huile-dans-eau-dans-huile (h/e/h) (Pal 1996). Les émulsions multiples sont davantage utilisées comme système à libération prolongée pour l'encapsulation de protéines, de peptides, et de principes actifs hydrophiles comme l'ara-C.

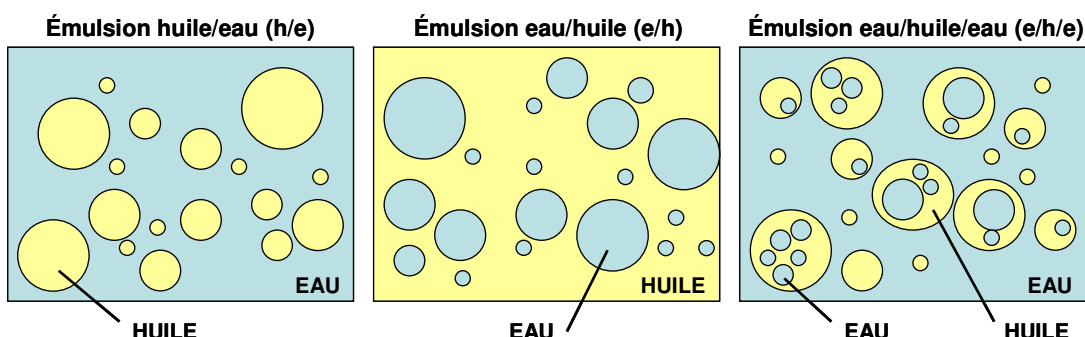


Figure 1.7. Différents types d'émulsions : une émulsion huile/eau, une émulsion eau/huile et une émulsion multiple eau/huile/eau.

Une double émulsion e/h/e a été développée par Fukushima *et al.* (1983) afin d'encapsuler l'ara-C, la protéger contre une dégradation enzymatique et favoriser sa libération soutenue. Cependant, l'inconvénient majeur des émulsions est la fuite prématurée (*i.e.* libération rapide) du principe actif des gouttelettes. D'après différents paramètres testés

lors de la préparation d’émulsions multiples contenant de l’ara-C, les auteurs ont rapporté que la libération du principe actif peut être ralentie suite à une augmentation du volume interne des gouttelettes formant l’émulsion, mais également en utilisant de fortes concentrations de principe actif ou d’émulsifiant, tel que l’huile de ricin hydrogénée (Fukushima *et al.* 1983, Okochi & Nakano 1997). D’ailleurs, Benoy *et al.* ont démontré que la formulation de l’ara-C sous forme d’émulsion e/h/e pourrait être efficace sur des souris porteuses de tumeurs R1. Une seule injection de cette double émulsion contenant l’ara-C a permis d’obtenir des résultats sur la survie des animaux atteints de la leucémie similaires à l’ara-C seule injectée pendant 5 jours consécutifs (Benoy *et al.* 1972, Benoy *et al.* 1974). Cependant, cette émulsion ne peut être conservée plus de 3 jours et aucune étude clinique n’a été menée afin d’investiguer les bienfaits d’une telle formulation chez l’humain.

1.4.4.3. Liposomes

Les liposomes, définis de manière simplifiée, sont des vésicules unilamellaires ou multilamellaires (0.02 à 5 µm) constituées de bicouches de phospholipides. Ces vecteurs lipidiques sont très versatiles, puisqu’ils peuvent incorporer dans leur structure aussi bien des molécules hydrophiles que des composés ayant une affinité pour la phase lipidique (Lasic 1995). Parmi les formulations liposomales disponibles sur le marché on peut citer l’Ambisome® (amphotéricine B) utilisé dans le traitement des mycoses systémiques, le Doxil®/Caelix® (doxorubicine) et le Daunoxome® (daunorubicine) employés comme traitement de première ligne pour le sarcome de Kaposi (Cattel *et al.* 2003) (Chapitre 2).

Les liposomes constituent le principal système à libération contrôlée pour l’encapsulation de l’ara-C. En effet, plusieurs investigateurs ont démontré l’efficacité *in vivo* de l’ara-C encapsulée à l’intérieur des liposomes. Par exemple, Kobayashi *et al.* ont encapsulé l’ara-C dans quatre différentes formulations de liposomes afin de comparer l’effet thérapeutique des vecteurs avec le principe actif seul chez les souris CD2F

leucémiques porteuses des tumeurs L1210 (Kobayashi *et al.* 1977, Kobayashi *et al.* 1975). L'activité antitumorale s'est avérée significativement améliorée, augmentant le taux de survie des animaux de 60% par rapport à l'administration de l'ara-C libre à une dose de 50 mg/kg. Parmi les quatre types de liposomes préparés, la formulation composée de sphingomyéline, de stéarylamine et de cholestérol (20:2:15 ratio molaire) s'est révélée la plus efficace, probablement à cause de sa stabilité physique, à la protection de l'ara-C contre sa rapide dégradation dans le sang et à sa libération soutenue. Quelques années plus tard, l'équipe de Richardson a démontré que l'utilisation de liposomes permettait non seulement de protéger le principe actif mais également de surmonter le problème de la résistance à l'ara-C *in vitro* associée à la glycoprotéine transmembranaire Pgp-1 (Richardson *et al.* 1982).

En 1987, Kim *et al.* ont rapporté l'utilisation de liposomes multilamellaires pour une libération prolongée de l'ara-C suite à une administration dans le liquide céphalorachidien (administration intrathécale) chez le rat (Kim *et al.* 1987). Le temps de demi-vie intrathécale de l'ara-C a ainsi atteint 148 heures, comparativement à 2,7 heures pour le principe actif non-encapsulé. Son encapsulation dans les liposomes a permis de diminuer les doses d'ara-C et de réduire sa toxicité. Suite à plusieurs optimisations de la formulation, une préparation liposomale d'ara-C a été commercialisée sous le nom de Dépocyt® pour le traitement de la leucémie lymphoblastique aiguë avec envahissement du système nerveux central (Glantz *et al.* 1999). Il s'agit d'une suspension injectable stérile de vésicules lipidiques multilamellaires, appelée DepoFoam® (Figure 1.8). Ce système consiste en des particules sphériques de 3 à 30 µm composées de nombreux compartiments aqueux internes non-concentriques contenant le principe actif. Le DepoFoam® est constitué approximativement de 4% de lipides et de 96% d'eau ce qui est idéal pour l'encapsulation de principe actif hautement hydrophile comme l'ara-C. Après une simple injection intrathécale de Depocyt® de 50 ou 75 mg, des concentrations cytotoxiques efficaces d'ara-

C dans le liquide céphalorachidien sont maintenues pendant 2 semaines (Glantz *et al.* 1999).

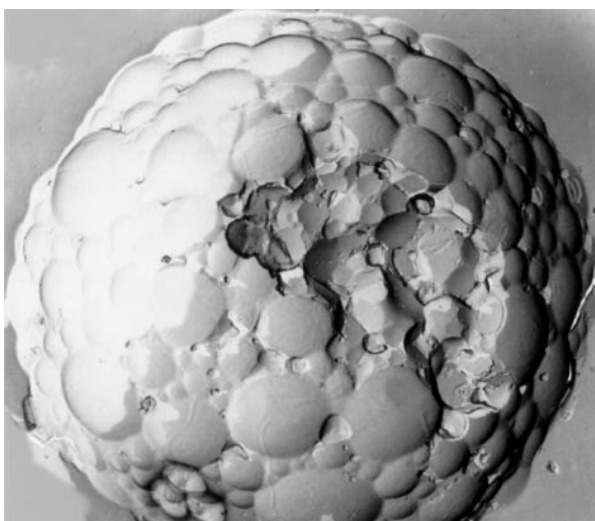


Figure 1.8. Vésicules lipidiques de DepoFoam[®]. Reproduit de (Murry & Blaney 2000) avec permission de Pacira Pharmaceuticals Inc (© 1996, 2009).

Un autre vecteur pharmaceutique à base de surfactants et de phospholipides a été développé afin d'encapsuler l'ara-C et de tenter d'améliorer le devenir de cette molécule active. En effet, l'ara-C a également été utilisée dans la préparation de Sphérulites[®] (Simard *et al.* 2005). Ces derniers sont des vésicules de structures similaires aux liposomes, c'est-à-dire, qu'elles sont composées de bicouches de phospholipides multilamellaires possédant un centre hydrophile et permettant l'encapsulation de principes actifs (Chapitre 4; Figure 4.1). Contrairement aux liposomes, les Sphérulites[®] possèdent la caractéristique de disposer des lamelles concentriques de bicouches de molécules amphiphiles qui la composent de

distances uniformes entre chacune d'elles. Cette distinction provient du fait que la préparation des Sphérolites® repose sur une force de cisaillement précise et contrôlée (Diat & Roux 1993, Diat *et al.* 1993) et non sur une extrusion au travers de membranes poreuses. Grâce à leur grand volume aqueux et à leur rendement élevé d'encapsulation (Freund *et al.* 2000), l'ara-C fut incorporée dans ces vésicules lipidiques. Les résultats obtenus sont présentés au Chapitre 4.

En somme, les liposomes représentent un vecteur colloïdal de choix pour l'encapsulation de cette molécule fragile qu'est l'ara-C. Plusieurs chercheurs ont démontré les avantages qu'offraient les liposomes pour l'ara-C, tels que (i) l'amélioration de sa pharmacocinétique (Allen *et al.* 1992a), (ii) le ciblage du principe actif vers les cellules cancéreuses (Connor & Huang 1986), (iii) la libération soutenue et prolongée de la molécule (Allen *et al.* 1992a) et conséquemment, (iv) l'amélioration du taux de survie des modèles animaux porteurs de leucémies (Allen *et al.* 1992a, Kobayashi *et al.* 1977, Kobayashi *et al.* 1975). Le prochain chapitre de ce manuscrit porte essentiellement sur les liposomes en tant que formes pharmaceutiques prometteuses pour la libération de divers principes actifs. Les méthodes de fabrication, les techniques de caractérisation ainsi que différentes utilisations thérapeutiques sont abordées.

Chapitre 2. Liposomes for drug delivery

Pierre Simard¹, Jean-Christophe Leroux^{1*}, Christine Allen² and Olivier Meyer³

¹Canada Research Chair in Drug Delivery, Faculty of Pharmacy, University of Montreal, P.O. Box 6128 Downtown Station, Montreal (Qc), Canada, H3C 3J7

²Faculty of Pharmacy, University of Toronto, Toronto (Ontario), Canada

³AstraZeneca R&D Montreal, 7171 Frederick-Banting, Ville Saint-Laurent (Qc), Canada, H4S 1Z9

Published in: A.J. Domb, Y. Tabata, M.N.V. Kumar (Eds.), Nanoparticles for Pharmaceuticals Applications, American Scientific Publishers, Valencia, 2007, pp. 1-62.

2.1. Summary

Since their introduction by A. Bangham in the 1960s, liposomes have been successfully used in various areas. Their applications range from cosmetics to medical technologies such as delivery systems for anticancer and antifungal drugs. The significant advances for these colloidal particles resulted in the publication of more than 20,000 scientific articles and the commercialisation of several liposomal formulations. Indeed, liposomes represent the most studied particulate drug carriers and are now considered to be a mainstream drug delivery technology. This book chapter reviews the theoretical and development aspects of liposomes. More specifically, their molecular constituents are

discussed in terms of the structural, physical, and functional properties that they impart to the carrier system. Nomenclature of the different liposome classes is presented in association with the diverse preparation methods. Drug loading processes including passive and remote loading methods, as well as industrial manufacturing considerations are discussed. The characterization of these vesicles by conventional and more recent analytical techniques is presented. This chapter also covers physical and chemical stability aspects, sustained and triggered release properties, surface modification, as well as pharmacokinetics and biodistribution in animal models and humans. In addition, the biological processes and mechanisms through which liposomes exert their pharmacological benefits are reviewed. Finally, the applications of liposomes as drug carriers for the treatment of various pathologies are discussed.

2.2. General introduction

Phospholipids are naturally occurring molecules that tend to self-assemble in aqueous media into spherical vesicles that are referred to as liposomes. The latter thus obtained consist of one or more concentric lipid bilayers separated by water compartments. Their diameters generally range from 50 nm to a few micrometers, while the thickness of the membrane is around 4 nm. Although, at first, liposomes were developed by A. Bangham as analytical tools to study biomembrane dynamics (*e.g.* phase transition, fluidity and diffusion characteristics) [1-4], their potential as drug delivery agents rapidly emerged with the first *in vivo* experiments performed in the early 1970s [5-7]. Less than a decade later, the pharmaceutical industry witnessed the emergence of several independent liposome-oriented companies and of speciality groups within larger companies. However, the enthusiasm for medical application faded rather quickly, mainly because of unforeseen difficulties in large-scale preparation, reproducibility, and long-term stability of the formulations, problems that were almost irrelevant in the academic environment.

Nevertheless, over time, these problems were essentially worked out allowing liposomes to cross over from the laboratory to the clinic. The pioneered efforts of G. Gregoriadis, D. Papahadjopoulos and others, as well as the work of those inspired by them, finally led to the development of liposomal formulations of doxorubicin (Dox), daunorubicin and amphotericin B (amp B) now available in the clinic, and opened the door to the commercialization of several other formulations.

The interest towards this colloidal system extended past drug delivery with liposomes finding applications as adjuvants in vaccination, signal carriers in medical diagnostics and analytical biochemistry, protective carriers for various food ingredients and penetration enhancers in dermatology/cosmetics. Liposomes now represent the most studied particulate drug carriers and are considered to be a mainstream drug delivery technology. Over 20,000 scientific articles on liposomes have been published since the early 1960s and this number is still growing at a frantic rate.

This book chapter reviews the background and development of liposomes. More specifically, the different components entering in the design of liposomes are discussed in terms of the structural, physical, and functional properties that they impart to the carrier system. The preparation procedures, characterization methods and applications in the diagnostic, pharmaceutical and cosmetic fields are discussed in depth with particular emphasis on the latest technical developments and liposomal products that are used or currently being investigated in the clinic.

2.3. Lipids and polymorphisms

2.3.1. Material

The rationale for using liposomes as drug delivery systems to cells was originally based on the possibility of fusion between the liposome and the target cell membranes. Therefore, liposomes had to be prepared from lipids that are present in cell plasma membranes or from synthetic lipids with structures and physico-chemical properties that resemble those of natural lipids. Biological membranes are composed of a wide range of lipids. The most abundant lipids found in natural membranes are glycerolipids, sphingolipids, and sterols.

2.3.1.1. Glycerolipids

2.3.1.1.1. General Structure

The majority of natural glycerolipids are members of the phospholipid family. All phospholipids are composed of a polar and a hydrophobic moiety. They are derived from a glycerol entity from which two alcoholic groups are esterified by fatty acids (aliphatic chains) forming the hydrophobic part of the molecule. The third hydroxyl group bears the polar group and constitutes the polar head of the lipid. The general structure of a phospholipid is shown in Figure 2.1. Phospholipids may differ by length and number of unsaturations in their aliphatic chains, their shape, their polarity, and the net charge of their hydrophilic groups.

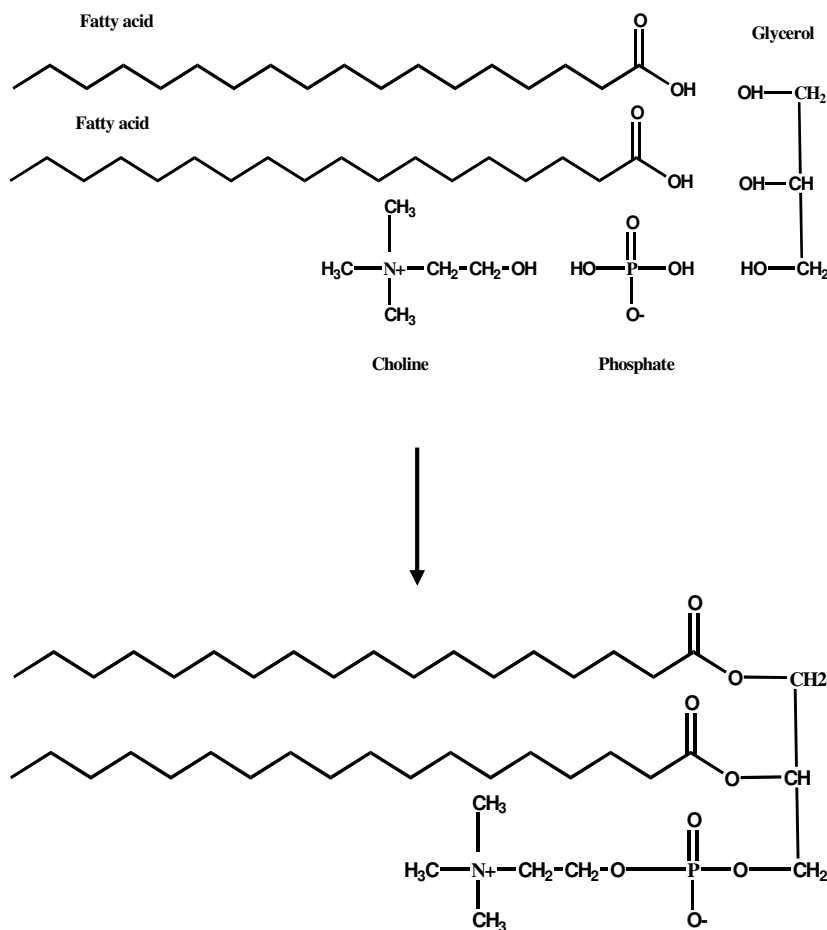


Figure 2.1. Structure of a phospholipid molecule.

2.3.1.1.2. Natural phospholipids

The most abundant phospholipids found in biological membranes are phosphatidylcholine (PC) (lecithin) and phosphatidylethanolamine (PE) (cephalin) that are neutral (zwitterionic) lipids. Phosphatidylserine (PS), phosphatidylinositol (PI), phosphatidic acid (PA) and phosphatidylglycerol (PG) are negatively charged

phospholipids (Table 2.1). Natural phospholipids contain two aliphatic chains and are often named bicanary lipids. However, some of those such as lysolecithins in which a chemical bound at the glycerol site has been hydrolyzed, have a single carbon chain. Aliphatic chains differ by their length, the most common are composed of 16 (palmitic) or 18 (stearic) carbons. One of the two chains can be unsaturated (generally the chain linked to the C-2 of glycerol), with a *cis* double bound on position 9 and 12 (octadienoic or linoleic). Finally, certain minor lipids have polar head linked carbohydrates and form the glycolipid family. Glycerolipids are predominantly found in eukaryotes, however, sphingolipids also represent a major lipid fraction of their membranes. Glycolipids are known to play an essential role in cellular recognition.

Table 2.1. Structures of the most commonly used phospholipids.

Phosphatidyl	Polar Head	Name	Abbre-viation	Charge
	OH	Phosphatidic acid	PA	Negative
		Phosphatidylcholine	PC	Neutral
		Phosphatidylethanolamine	PE	Neutral
		Phosphatidylserine	PS	Negative
		Phosphatidylglycerol	PG	Negative
		Phosphatidylinositol	PI	Negative

2.3.1.1.3. Synthetic phospholipids and amphiphiles

Purified natural lipids are often mixtures of phospholipids having the same polar head (*e.g.* choline) with different aliphatic chain lengths and/or degrees of unsaturation. Because of this, they are generally not suited to studying the influence of the structure of lipids on their supramolecular organization and dynamic properties in membranes. Advances in lipid chemistry have allowed this problem to be circumvented by providing well-defined synthetic lipids with a high degree of purity. A wide variety of synthetic lipids are now commercially available from different suppliers (www.avantilipids.com, www.lipoid.com, www.nof.co.jp, www.genzymepharmaceuticals.com).

Besides their utility in preparing liposomes as model biological membranes, synthetic lipids may be used as alternate materials for preparation of pharmaceutical formulations with improved properties. For example, fully saturated phospholipids provide a stabilization effect by preventing oxidation and conferring rigidity to the membrane. The semi-synthetic lipid hydrogenated soy phosphatidylcholine (HSPC) is the component of the marketed liposomal Dox, Doxil® (or Caelyx™). Moreover, synthetic lipids having a cationic polar head group have revolutionized the field of non viral gene delivery [8].

Non-ionic surfactants such as polyglyceryl alkyl ether, polyethylene glycol (PEG) alkyl ether, PEG fatty acid ester, or sucrose diester can be used to prepare non-ionic liposomes also called “niosomes”. The potential application of niosomes includes transdermal drug delivery, passive tumor targeting, vaccine adjuvants, and sustained release depot at point of injection [9]. Examples of synthetic lipids used as components of liposomes and their properties are given in Table 2.2.

Table 2.2. Properties of synthetic lipids used as liposome components. Adapted with permission from Ref. [10], E. Fattal *et al.*, in *Les liposomes: aspects technologiques, biologiques et pharmacologiques*, edited J. Delattre, P. Couvreur, F. Puisieux, J. Philipot and F. Schuber, Tec & Doc-Lavoisier, Paris (1993), p.43. Copyright @ Tec & Doc-Lavoisier.

Lipid	Abbreviation	Charge	T _c (°C)	Mw	Carbon : Insaturation
1,2-Dilauroyl-sn-Glycero-3-Phosphocholine	DLPC	0	-1.8	640	12:0
1,2-Dimyristoyl-sn-Glycero-3-Phosphocholine	DMPC	0	23	696	14:0
1,2-Dipalmitoyl-sn-Glycero-3-Phosphocholine	DPPC	0	41	752	16:0
1,2-Distearoyl-sn-Glycero-3-Phosphocholine	DSPC	0	58	808	18:0
1,2-Dioleoyl-sn-Glycero-3-Phosphocholine	DOPC	0	-22	804	18:1
1,2-Dimyristoyl-sn-Glycero-3-Phosphoethanolamine	DMPE	0	40	635	14:0
1,2-Dipalmitoyl-sn-Glycero-3-Phosphoethanolamine	DPPE	0	60	692	16:0
1,2-Distearoyl-sn-Glycero-3-Phosphoethanolamine	DSPE	0	74	748	18:0
1,2-Dioleoyl-sn-Glycero-3-Phosphoethanolamine	DOPE	0	-16	744	18:1
1-Myristoyl-2-Palmitoyl-sn-Glycero-3-Phosphocholine	MPPC	0	27	724	14:0-16:0
1-Palmitoyl-2-Myristoyl-sn-Glycero-3-Phosphocholine	PMPC	0	35	724	16:0-14:0
1-Stearoyl-2-Palmitoyl-sn-Glycero-3-Phosphocholine	SPPC	0	45	780	18:0-16:0
1-Palmitoyl-2-Stearoyl-sn-Glycero-3-Phosphocholine	PSPC	0	44	780	16:0-18:0
1,2-Dimyristoyl-sn-Glycero-3-[Phospho-rac-(1-glycerol)]	DMPG	-1	23	666	14:0
1,2-Dipalmitoyl-sn-Glycero-3-[Phospho-rac-(1-glycerol)]	DPPG	-1	41	722	16:0
1,2-Distearoyl-sn-Glycero-3-[Phospho-rac-(1-glycerol)]	DSPG	-1	55	779	18:0
1,2-Dioleoyl-sn-Glycero-3-[Phospho-rac-(1-glycerol)]	DOPG	-1	-18	775	18:1
1,2-Dimyristoyl-sn-Glycero-3-Phosphate	DMPA	-1	51	592	14:0
1,2-Dipalmitoyl-sn-Glycero-3-Phosphate	DPPA	-1	67	648	16:0
1,2-Dipalmitoyl-sn-Glycero-3-[Phospho-L-Serine]	DPPS	-1	51	735	16:0
Dicethylphosphate	DCP	-1	-	546	-
Stearylamine	SA	+1	-	269	-

2.3.1.2. Sphingolipids

Sphingolipids contain sphingosine as their structure backbone (Figure 2.2). They are composed of three building blocks, namely, a fatty acid, a molecule of sphingosine (or a related derivative) and a head group that can vary from simple alcohols such as choline to very complex carbohydrates. The main classes of sphingolipids are sphingomyelins (SM) and gangliosides.

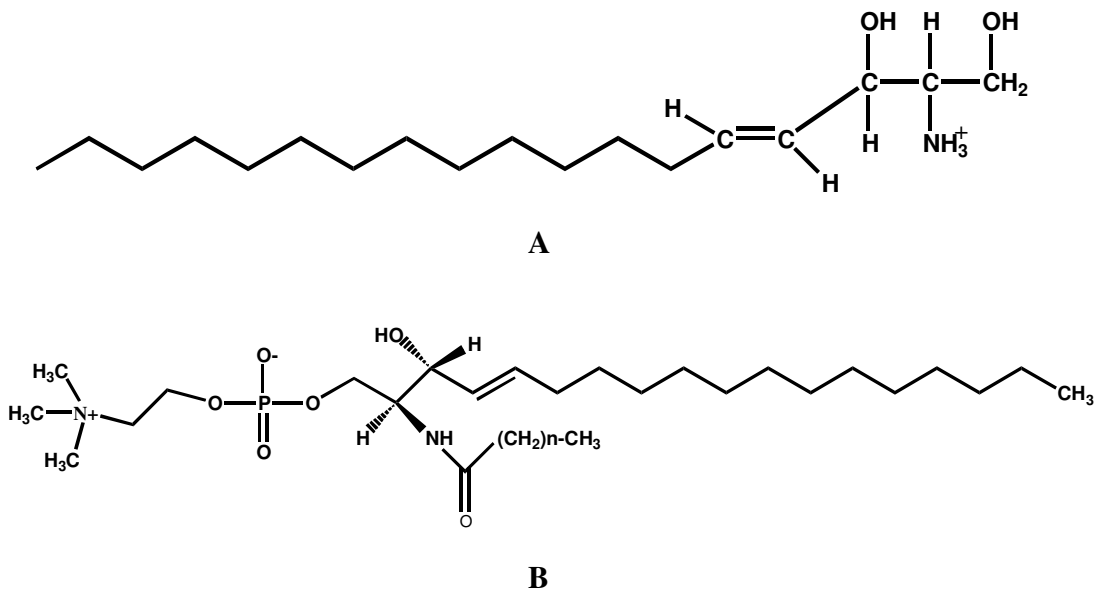


Figure 2.2. Structures of sphingosine (A) and sphingomyelin (B).

2.3.1.2.1. Sphingomyelin

SM or ceramide phosphorylcholine (Figure 2.2) consists of a ceramide unit with a phosphorylcholine moiety attached to position 1. It is thus the sphingolipid analogue of PC.

It is a ubiquitous component of animal cell membranes, where it is by far the most abundant sphingolipid. Indeed, it can comprise as much as 50% of the lipids in certain tissues, though it is usually less abundant than PC. For example, it makes up about 10% of the lipids of brain. It is the single most abundant lipid in erythrocytes of most ruminant animals, where it replaces PC entirely.

SM has aliphatic chains differing by their length and number of unsaturations giving rise to a phase transition temperature (T_c) that ranges from 20 and 40°C. SM provides a tight membrane packing due to the hydrogen bonding that is present between adjacent SM molecules and SM with cholesterol (Chol). SM/Chol liposomes have been developed as potential drug delivery systems for *vinca* alkaloids [11, 12] (see Section 2.8).

2.3.1.2.2. Gangliosides

Gangliosides, a second class of sphingolipids, are mainly found in the brain tissue and red blood cells. They are often used as a minor component of some liposome formulations. These molecules contain complex oligosaccharides with one or more sialic acid residues in their polar head group and thus have a net negative charge at neutral pH.

The first liposomes that were described as having the long circulation half-lives in mice contained monosialogangliosides, GM₁, in their bilayer (Figure 2.3). They indeed had compositions that mimicked the outer leaflet of red blood cell membranes (Egg PC (EPC)/SM/Chol/ganglioside GM₁, 1:1:1:0.14 molar ratio). Several other gangliosides and glycolipids were examined, but none could substitute for GM₁ in their ability to prolong circulation time [13, 14].

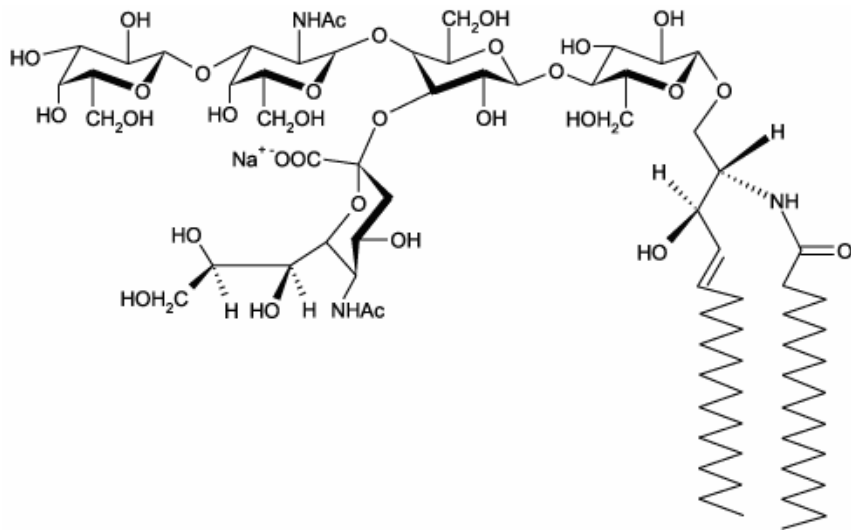


Figure 2.3. Structure of the ganglioside GM₁.

2.3.1.3. Sterols

Sterols are steroid-based alcohols having a hydrocarbon (aliphatic) side-chain of 8-10 carbons at the 17- β position and a hydroxyl group (-OH) at the 3- β position. Chol is one type of sterol that is quite often included as a component of liposomal membranes as a stabilizing agent. The latter is also a major component of eukaryotic membranes, particularly in plasma membranes of mammalian cells, where it can be found in the same proportion as phospholipids (*i.e.* 50 mol%). Chol is exclusively found in mammary cell membranes. Ergosterol, a Chol analog, is present in plant membranes.

Considerable differences can be observed regarding the amount of Chol found in the membranes of different cell types. Plasma membranes such as those of myelin or erythrocyte have an equimolar proportion of Chol and phospholipids, whereas membranes

of intracellular organelles contain only a small amount or no Chol at all. It is of interest to point out that the distribution of Chol correlates well with that of SM. More generally, Chol is known to be a “modulator” of membrane fluidity. It will increase the fluidity of rigid membranes and rigidify or reduce the fluidity of fluid membranes. Increasing the amount of Chol leads to the abolition of the liquid-crystal (L_α) to gel phase (L_β) transition. Chol has also been reported to stabilize the lipid bilayer in the presence of biological fluids such as plasma. In this way, the inclusion of Chol has proven useful in the formulation of liposomes for drug delivery applications that are administered *via* the i.v. route. Liposomes without Chol are known to interact rapidly with plasma proteins such as albumin, transferrin, and macroglobulins. These proteins tend to extract bulk phospholids from liposomes, thereby depleting the outer monolayer of the vesicles leading to physical instability. Chol appears to substantially reduce this type of interaction between proteins and liposomes.

2.3.1.4. Polymer bearing lipids

The fast and efficient elimination of conventional liposomes from the body by the mononuclear phagocyte system (MPS, also called reticulo-endothelial system) has seriously compromised their application in the treatment of a wide range of diseases. The emergence of novel liposome formulations that could persist for prolonged periods in the blood stream renewed interest in liposomal drug delivery in the late 80s. Soon after ganglioside GM₁-coated liposomes had been shown to circulate for longer periods in the blood, when compared to conventional liposomes, attachment of poly(ethylene) glycol (PEG) chains at the liposome surface was tried and found to have similar if not a greater effect on circulation lifetime [15-17] (see Section 2.6).

PEGylated phospholipids are negatively charged lipids, neutral alternative molecules such as PEGylated ceramides, and PEGylated Chol have also been introduced. In an

attempt to create alternative polymers to PEG that would provide the same “stealth” characteristics to liposomes, the properties of several other hydrophilic polymers have been investigated including polyvinyl alcohol, hydroxypropylmethylcellulose [18] and poly *N*-(vinyl pyrrolidone) (PVP) [19].

Another example of the use of polymeric liposome components is in the active targeting of drugs. Polymeric vesicles bearing glucose or transferrin ligands have been described [20]. A glucose-PGC (Figure 2.4) conjugate was synthesized and vesicles were prepared by sonication of a glucose-PGC/Chol dispersion.

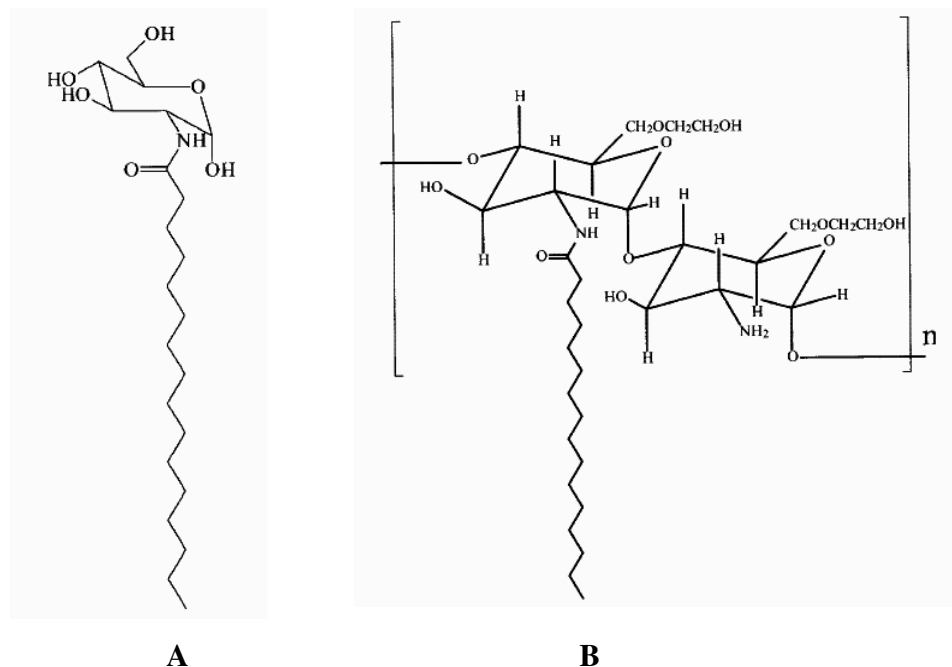


Figure 2.4. Chemical structure of *N*-palmitoyl glucosamine (*N*-PG) (A) and palmitoyl glycol chitosan (PGC) (B). Reprinted with permission from Ref. [20], C. Dufes *et al.*, Pharm Res 17, 1250 (2000). Copyright @ Springer Science & Business Media B.V.

Recently, polymeric vesicles using the new polymer-palmitoyl glycol chitosan (PGC) and Chol (2:1 w/w) have been described [21]. These polymeric vesicles have also been encapsulated within EPC/Chol liposomes yielding a vesicle in vesicle system.

Finally, a synthetic lipidic cationic lysine-based dendron (partial dendrimer) has lately been reported as a potential drug carrier [22]. The dendron was prepared by solid-phase peptide synthesis. Dendrisomes of all compositions have higher encapsulation efficiencies and slower release rates compared to neutral DSPC/Chol liposomes.

2.3.1.5. Cationic lipids

Due to the relatively large molecular weight of macromolecules such as nucleic acids, their encapsulation into small liposomes has remained a difficult challenge. Although some attempts to develop specific encapsulation methods have been described [23], none of them can compete with the revolutionary new idea of forming nucleic acid-cationic lipid complexes via electrostatic interactions.

The synthesis and use of cationic lipids was pioneered by a number of different laboratories in the late 80's [8]. However, these systems were recognized as potentially powerful tools for delivery of nucleic acids to cells due to the work of P. Felgner in 1987 [24]. Felgner *et al.* not only demonstrated that such complexes could form but also showed that depending on several physicochemical parameters, they could efficiently transfect numerous types of cells [25].

Among others the most relevant parameter affecting the formation of lipoplex particles as well as their transfection efficiency to cells in culture is the nucleic acid-lipid charge ratio. The physical chemistry of mixtures of polyelectrolytes is not straightforward and the preparation of stable, small nucleic acid-cationic lipid particles has been a challenge for

quite some time. Within the first “euphoric period” in the field of non-viral gene delivery many groups attempted to synthesize the most efficient transfecting agent. Some of the earliest cationic lipids described in the literature are dioctadecyldimethyl ammonium bromide/chloride (DODAB/C), 1,2-dioleoyloxy-3-[trimethylammonio]-propane (DOTAP) and *N*-[1-(2,3-dioleyloxy)propyl]-*N,N,N*-trimethyl ammonium (DOTMA). The chemical structures of DOTAP and DOTMA are shown in Figure 2.5. The growing knowledge of the characteristics and functionality of nucleic acid-cationic lipid complexes has led to the realization that the structure or type of cationic lipids used is far from being the sole and most important parameter involved in the design of a successful gene delivery system. Indeed, the addition of a co-lipid such as 1,2-dioleoyl-*s*n-glycero-3-phosphoethanolamine (DOPE) (Figure 2.5) or Chol and (+)/(−) charge ratio were found to be crucial parameters in the optimization of cationic lipid-based gene delivery systems.

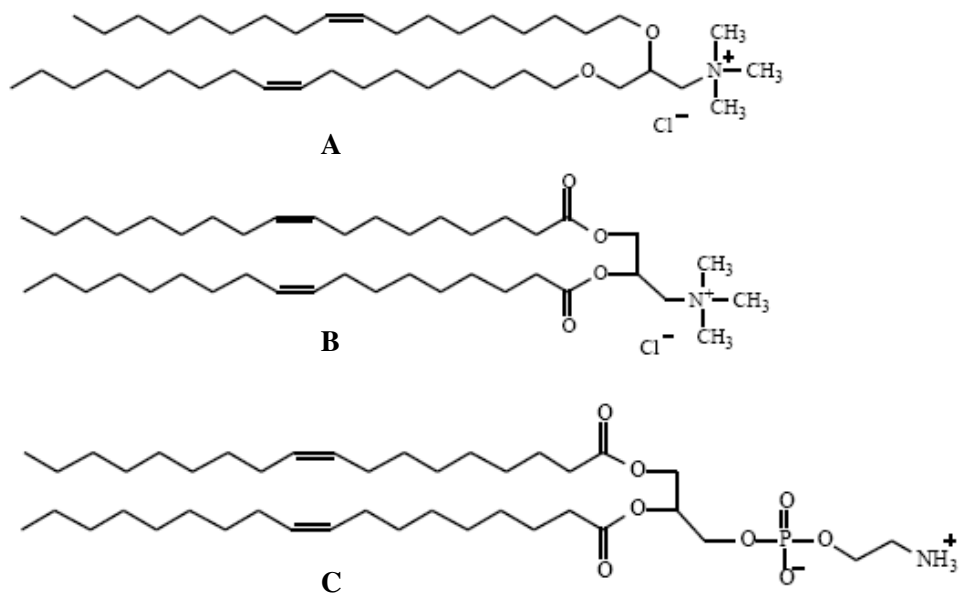


Figure 2.5. Chemical structures of DOTMA (A), DOTAP (B), and DOPE (C).

2.3.2. Lipid selection

The choice of lipids as liposome components is based on the principle that the bulk of the liposomal membrane is composed of a single neutral phospholipid acting as the structural “backbone” of the bilayer. Other lipids can be incorporated as minor components into the membrane in order to confer specific properties that may modulate the behaviour in a desired fashion [26].

Negatively-charged phospholipids can be added to prevent liposomes from aggregation/fusion, or to favour these events in the presence of calcium. A few mol% of negatively charged lipids such as PA, PG or PI may be used to increase the internal aqueous volume between adjacent bilayers of MLVs. Some negatively charged lipids such as cholesteryl hemisuccinate (CHEMS) [27] or oleic acid (OA) [28] have been used to prepare pH-sensitive liposomes (see Section 2.8). At pH values where CHEMS or OA become protonated (neutral), *i.e.* below pH 8-9, the surface area of their polar head groups decreases resulting in a change in their molecular shape (from cone-shape to cylinder-shape, see Section 2.3.3 about polymorphism). The inverted cone-shaped DOPE is not able to organize into lipid bilayers when mixed with cylindrical lipids, rather it tends to rearrange in a hexagonal phase, resulting in the destabilization/rupture of the liposomal membrane.

Inclusion of Chol is an important issue in liposomal formulations of drugs since it reduces the fluidity of membranes above the phase transition temperature, with a corresponding reduction in permeability to aqueous solutes. Therefore, the presence of Chol will have a significant impact on liposome stability. It can be incorporated up to 50 mol% in PC-based vesicles. Increase in liposome stability may also be achieved by the incorporation of PEG-derivatized lipids that confers steric stabilization to the particles and

a shielding effect which in turn results in prolonged circulation properties in the bloodstream (see Section 2.6). Also, the use of highly saturated phospholipids with elevated phase transition temperatures as the major lipid component of liposomes, such as DSPC or HSPC, may improve the *in vitro* and *in vivo* stability of the liposomes.

Finally, some natural or synthetic lipids can be used to impart specific properties to liposomes including triggered drug release or targeting to specific tissues. These issues will be addressed in detail in Section 2.8. A schematic representation of the different types of liposomes is included in Figure 2.6.

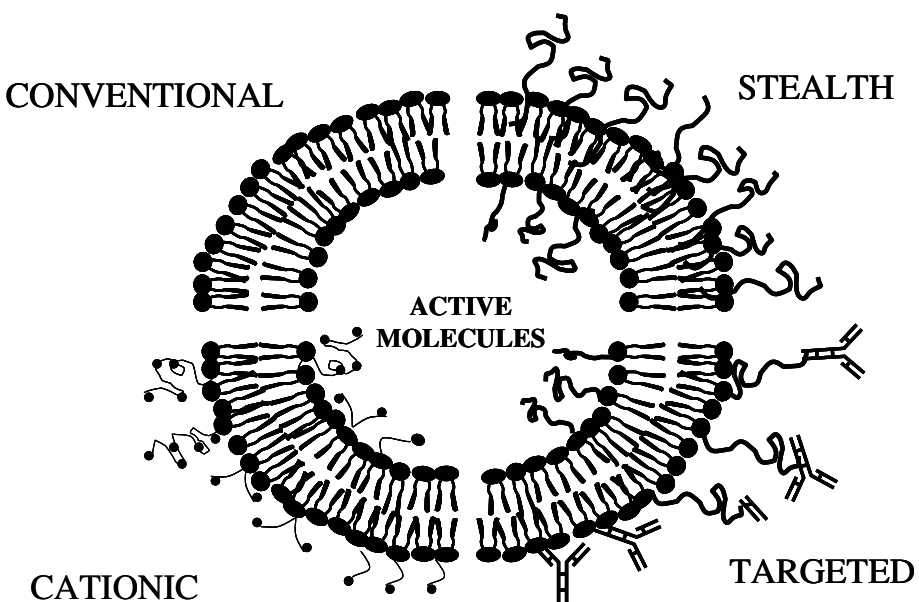


Figure 2.6. Schematic representation of 4 major liposome types. Conventional liposomes are either neutral or negatively charged. Sterically stabilised (stealth) liposomes carry polymer coatings to obtain prolonged circulation times. Immunoliposomes (antibody-targeted) may be either conventional or stealth. For cationic liposomes, the several different means of imposing a positive charge are shown (mono, di or multivalent interactions).

Adapted with permission from Ref. [29], G. Storm and D.J.A. Crommelin, Pharm Sci Technol Today 1, 19 (1998). Copyright @ Elsevier.

2.3.3. Polymorphisms

Due to their amphiphilic nature, lipids in excess of water spontaneously self-associate above a concentration called the critical aggregation concentration which is in the order of 10^{-10} M. This phenomenon is spontaneous and cooperative and results in a variety of structures of variable size and geometry depending on several parameters including temperature and ionic strength. Phospholipid-water systems can therefore exist in different states or phases. The aggregation process results from both the hydrophobic effect of the aliphatic chains and polar type interactions between the hydrophilic heads of the phospholipids. The structure and stability of these phases depend on the molecular geometry of lipids, water content and temperature. Phospholipids present two mesomorphisms, lyotropic and thermotropic, respectively.

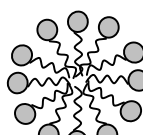
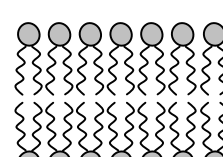
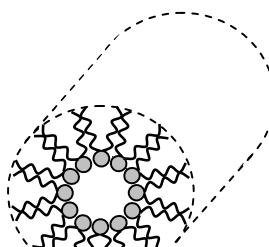
The spontaneous radius of curvature (R_0) for the aggregates is defined by the geometric structure of the amphiphilic molecule. This parameter is quantitatively characterized by Eq. 1:

$$1 / R_0 = v / (a_0 \cdot l_c) \quad (\text{Eq. 1})$$

where a_0 is the surface area of the polar head of the amphiphile, v is the volume occupied by aliphatic chains, and l_c is the critical aliphatic chain length for the average section of the aggregate. R_0 is dependent on the chemical structure of the amphiphile through the values of l_c and v , and dependent on the repulsive forces at the interface through the values of a_0 .

Examples of the impact of the molecular geometry of amphiphiles on the supramolecular phases that they can form are illustrated in Table 2.3.

Table 2.3. Effect of molecular geometry on the phase properties of lipids. Adapted with permission from Ref. [30], D.D. Lasic *et al.*, in Pharmaceutical Dosage Forms: Disperse systems, edited H.A. Liberman, M.M. Rieger and G.S. Bunker, Marcel Dekker, New York (1998), Vol. 3, p.43. Copyright @ Routledge/Taylor & Francis Group, LLC.

Lipid	Phase	Molecular Shape
Lysophospholipids Detergents	MICELLAR 	 
Phosphatidylcholine Sphingomyelin Phosphatidylserine Phosphatidylglycerol Phosphatidic acid Cardiolipin Digalactosyldiglyceride	BILAYER 	 
Phosphatidylethanolamine (unsaturated) Cardiolipin-Ca ²⁺ Phosphatidic acid-Ca ²⁺ (pH < 6) Phosphatidic acid (pH < 3) Phosphatidylserine (pH < 4) Monogalactosyldiglyceride	HEXAGONAL (H _{II}) 	 

Other environmental factors such as modifications in ionic strength or pH can lead to isothermal transitions. For example by varying the temperature as a function of water content for a given phospholipid, a phospholipid-water binary phase diagram can be established. Such a diagram will define the conditions under which the phospholipids are organized into one or several phases [31].

Under physiologic conditions, lipid components of natural biomembranes are in a highly hydrated state and therefore prone to self-associate to form lamellar structures, even though some other phases may be present locally. At least two lamellar structures have been identified: the L_α phase corresponding to a fluid liquid crystalline phase (or liquid-crystal phase) and the L_β phase corresponding to a rigid crystalline liquid phase (or gel phase). The gel phase takes place at temperatures below the critical phase T_c and corresponds to the fusion of aliphatic chains. Above the T_c the lipids are assembled in a liquid-crystal phase.

2.4. Liposome preparation methods

2.4.1. Nomenclature used to describe liposomes

Liposomes may be classified according to their size, the number of bilayers they contain or the method employed for preparation. Some abbreviations that are typically used may be confusing as they can be “translated” in different manners. One example is the term SUV which can both mean small unilamellar vesicle or sonicated unilamellar vesicle. By chance, liposomes formed by sonication are generally small. It is admitted that the average diameter for SUV usually ranges between 40 and 80 nm. The term LUV is used for large unilamellar vesicles, meaning vesicles having a mean particle diameter superior to SUV,

i.e. ranging from 80 nm to 400 nm. LUV prepared by the reverse phase evaporation method may also be referred to as REV. Multilamellar vesicles (MLV) are sometimes named GOV for giant oligolamellar vesicles. The diameter of the latter typically varies from 400 nm to 1 μm or more. The types of classification for liposomes based on structural parameters and methods of preparation are summarized in Table 2.4 and 2.5, respectively [29, 32].

Table 2.4. Liposome classification based on size and lamellarity.

Abbreviation	Complete Name / Lamellarity	Size
MLV	Multilamellar vesicles	> 0.5 μm
OLV	Oligolamellar vesicles	0.1-1 μm
UV	Unilamellar vesicles	All size range
SUV	Small (or sonicated) unilamellar vesicle	40-100 nm
MUV	Medium sized unilamellar vesicles	-
LUV	Large unilamellar vesicles	Up to 400 nm
GUV	Giant unilamellar vesicles	> 1 μm
MVV	Multi vesicular vesicles	> 1 μm

Table 2.5. Liposome classification based on method of preparation.

Abbreviation	Complete Name / Method of preparation
REV	Single or oligolamellar vesicles formed by the reverse-phase evaporation method
MLV-REV	Multilamellar vesicles formed by the reverse-phase evaporation method
SPLV	Stable plurilamellar vesicles
FATMLV	Multilamellar vesicles prepared by repeated freezing-thawing
VET	Vesicles prepared by extrusion
LUVET	Large unilamellar vesicles prepared by extrusion
DRV	Dehydration-rehydration vesicles

2.4.2. Vesicle preparation

As described in detail in the following section, a wide variety of methods have been developed for preparation of liposomes. However, the basic step involved in all methods relies on the hydration of a solid lipid film. Once a lipid film is formed, liposomes can assemble by the addition of an aqueous solution that is at a temperature superior to the gel to crystalline T_c of the lipid. In the case of lipid mixtures, liposomes having a homogeneous composition can only be prepared at a temperature that is above that of the lipid having the highest T_c within the mixture.

2.4.2.1. Lipid film hydration

The preparation of MLV by hydration of a lipid film was first described by Bangham *et al.* in 1965 [3]. The first step of the procedure involves the evaporation of solvent from an organic solution of lipids and should result in a lipid film that is thin and homogeneous. Spontaneous formation of MLV in aqueous solution will then occur upon hydration of the lipid film. Dispersion of the lipid may be facilitated with the aid of mechanical energy supplied by vortexing or the presence of small glass beads in the round flask. As such, hydration of a lipid film does not allow one to control the size or size population distribution of the vesicles. MLV formed by hydration are large vesicles and generally have poor encapsulation efficiencies (2-15%) for drugs. However, a prolonged hydration time can favour the formation of vesicles having a lower number of concentric bilayers resulting in a higher encapsulation efficiency (up to 50% for small solutes) [33].

2.4.2.2. Sonication

MLV can be transformed into SUV by the use of ultrasound. The sonication method of preparation for SUV was first introduced by Saunders *et al.* [34]. Sonication provides enough energy to break the large oligolamellar vesicles and allow for the formation of unilamellar vesicles. It can be performed by the use of an ultrasound bath or an ultrasound probe. Sonication methods using an ultrasound probe is more powerful when compared to sonication bath yet they can damage the chemical structure of certain lipids and metal particles may be released from the probe. Therefore a centrifugation step is often necessary for the removal of these particles as well as the potential presence of remaining MLV in the liposome suspension [35].

2.4.2.3. Shearing of lyotropic lamellar phase

A new solvent-free process to prepare well defined MLV has been described by Diat *et al.* [36, 37]. They discovered that moderate shearing of a lyotropic lamellar phase of PC and surfactants in the presence of a minimal amount of water could lead to the formation of MLV. These so formed vesicles have been referred to as Spherulites®. Their size (200-1000 nm) can be controlled precisely by varying the shear rate [36, 37] and the components in the preparation [38, 39]. The Spherulite® system is unique in that it is made of uniformly spaced concentric bilayers of amphiphiles alternating with layers of aqueous medium. The interlamellar distances between two constitutive layers and the bilayer thickness are always constant. This structure remains stable in the dispersion medium [38, 40, 41] and is characterized by high encapsulation efficiencies (*i.e.* 40-85%) for a variety of compounds, such as copper salts [41], fluorescent dye [39, 42], anticancer drug [39] and macromolecules like proteins [43] and DNA [38, 44].

2.4.2.4. Extrusion

Controlling particle diameter, lamellarity and homogeneity in the size of MLV prepared by lipid film hydration can be achieved by extrusion. Extrusion involves passing the liposome suspensions through polycarbonate membranes of well-defined pore diameter. The number of passages through the polycarbonate membranes affects both the lamellarity and the polydispersity in the size of the liposome preparation. Depending on the lipid mixture, about 5 to 10 passages are necessary to obtain a homogeneous population of unilamellar or oligolamellar liposomes with diameters that are close to the mean diameter of the pores in the membrane employed [45]. Figure 2.7 shows electron micrographs of LUVET prepared using membranes with pores of different diameters. Sequential extrusion through membranes having pore diameters of decreasing size can also be used. The mean

diameter of the final particle is in this case close to the pore size of the final membrane employed (*i.e.* having the smaller pore diameter). Different types of membranes are commercially available, each of them having pore diameters ranging from 30 nm to 800 nm.

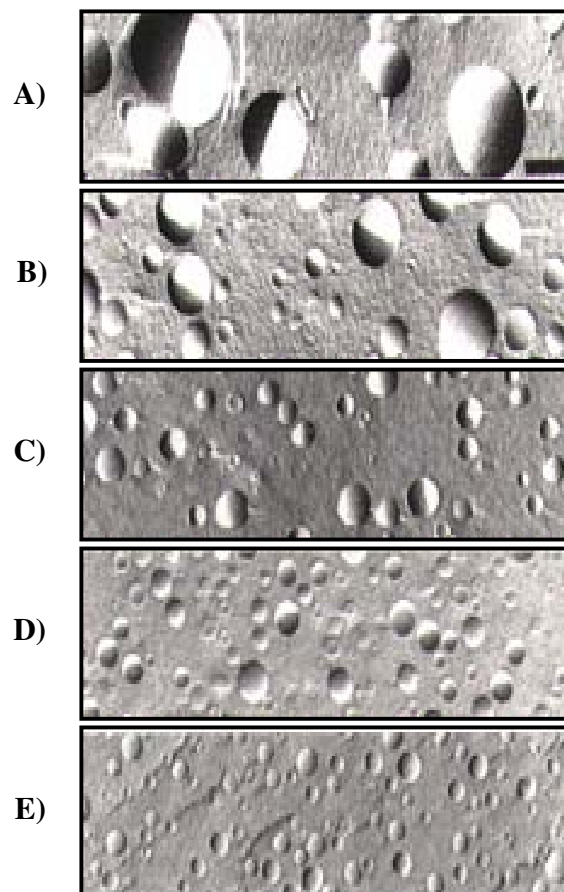


Figure 2.7. Characteristics of VET. Freeze-fracture electron micrographs of vesicles produced by extrusion of MLV composed of EPC (100 mg lipid/mL) through filters with pore sizes of 400 (A), 200 (B), 100 (C), 50 (D) and 30 nm (E). Each sample was extruded

10 times through 2 stacked filters (bar represents 150 nm). Reprinted with permission from Ref. [46], M.J. Hope *et al.*, Chem Phys Lipids 40, 89 (1986). Copyright © Elsevier.

Steel cell type thermobarrel extruders of volume capacities ranging between 1.5 mL to 800 mL are commercially available from Northern Lipids, Inc. (Canada) and/or Lipex Biomembranes (Canada). Larger extruders can also be made for preparation of clinical and commercial batch sizes (up to 50 L). Small syringe-based extruders are commercially available for preparation of small volume samples (0.25 mL, 1 mL) from Avanti Lipids Inc (USA) and/or Northern Lipids Inc. (Canada) (Figure 2.8).



Figure 2.8. The two syringe-based miniextruder for preparation of small volumes of liposomes and the pressurized large extruder. The latter device is more suitable for liposome extrusion than other similar equipment due to the wide pressure range at which it

can operate, the temperature-controlled sample holder, and the quick-release sample port assembly that allows for rapid recycling.

2.4.2.5. Solvent injection method

The hydration of a lipid film is the most commonly used method for preparation of liposomes. However, it is not appropriate as a pharmaceutical manufacturing process due to the large quantity of organic solvents that are required for this method. Therefore, other methods that avoid relatively toxic organic solvents have been considered. Among the few examples given in this chapter, injection of an ethanol based solution of lipids into a large aqueous volume results in the spontaneous formation of liposomes. In this method the ethanol-to-water ratio, rate of injection, initial lipid concentration, size and lamellarity of liposomes can be controlled to some extent [47]. Ethanol can be easily eliminated by dialysis [48] or exclusion chromatography [49]. This method may be scaled-up and is particularly adequate for industrial manufacturing. However, a limitation of this preparation procedure is the possible inactivation of biologically active macromolecules by ethanol.

2.4.2.6. Reverse phase evaporation

In the late 70's, Szoka and Papahadjopoulos developed the so-called reverse phase evaporation method to prepare liposomes with a large internal aqueous space [50]. In this method, phospholipids are solubilized in diethyl ether and the aqueous phase is then added in a 1:3 volume ratio (aqueous solution / organic solvent). An emulsion of the mixture is obtained by sonication resulting in the formation of inverted micelles. The ether is removed by rotary evaporation under reduced pressure (around 300 mmHg) during which the inverted micelles aggregate to form a gel-like structure. The rupture of the gel is achieved

by further increase in pressure (around 700 mmHg) that favors the evaporation of the organic solvent. During this step the lipid monolayers become close enough to form liposome bilayers. Evaporation is continued in order to completely remove the ether.

Depending on the ionic strength of the solution used the maximum drug encapsulation efficiency can range from 20 to 65%. Generally, the lower the ionic strength the higher the encapsulation efficiency. Liposomes prepared by this method are unilamellar or oligolamellar vesicles with mean diameters of about 500 nm. The resulting liposome suspensions have a rather high polydispersity in terms of size. Szoka *et al.* [51] reported that sequential extrusion of REV through decreasing pore size polycarbonate membranes to 100 nm pore diameter membranes may be used as a means to reduce the polydispersity and to control the size of REV. This results in homogeneous unilamellar liposome suspensions of about 150 nm in particle mean diameter with reduced encapsulation capacity when compared to non-extruded REV. Several modifications to the initial method of REV preparation have been reported to form REV-MLV or SPLV [52, 53].

2.4.2.7. Microfluidisation

Microfluidisation is another technique to form SUV from MLV. The method is based on the collision of liposomes caused by a pump-mediated fast passage (superior to 500 m/s) of liposomes through a 5- μm diameter pore filter followed by separation of the suspension via 2 channels which are both connected to an interaction chamber. The collision between MLV particles causes a membrane rupture of large particles resulting in the formation of smaller vesicles. After 10 passages, MLV become SUV of less than 100 nm in mean diameter that are homogeneous in size [54]. This method is adequate for large scale manufacturing of liposomes with high initial lipid concentrations.

2.4.2.8. Dehydration-rehydration

Lyophilization of SUV followed by liposome rehydration has been described as a simple method for high yield drug entrapment in liposomes [55] and used for the preparation of liposomal immunoadjuvants [56]. This method has recently been modified to prepare sterile and pyrogen-free submicron sized liposomes of narrow size distribution. The method is based on the formation of a homogenous dispersion of lipids in water-soluble carrier materials. To obtain the lipid-containing solid dispersion, liposome-forming lipids and water-soluble carrier materials are dissolved in *tert*-butyl alcohol/water co-solvent systems to form an isotropic monophase solution, and then the resulting solution is lyophilized after sterilization by filtration through 0.2 µm pores. Upon addition of water, the lyophilized product spontaneously forms a homogenous liposome preparation [57].

2.4.2.9. Detergent removal

Removal of detergent from phospholipid/detergent mixed micelles results in the formation of liposomes. Several detergent removal methods can be used including dialysis [58], gel exclusion chromatography [59] or detergent adsorption on hydrophobic resin beads [60]. Different types of detergents can be utilized; however, the most appropriate are those having a high critical micelle concentration and a low aggregation number. The most commonly used detergents include sodium cholate or deoxycholate, Triton X-100, and octylglucoside. The final size of the vesicles is strongly dependent on the rate of detergent removal.

2.4.3. Drug Loading

2.4.3.1. Passive loading

Depending on their molecular weight, solubility, and polarity, drugs can interact with liposomes in different ways. Water-soluble drugs can be encapsulated into the aqueous internal volume of lipid vesicles and between adjacent lipid bilayers, whereas hydrophobic drugs may be solubilized in the hydrophobic core domains of the liposomal membranes. Hydrophilic drugs are spontaneously encapsulated into liposomes upon lipid hydration. Non-entrapped material is then removed by methods including gel exclusion chromatography or dialysis. This so-called passive loading generally provides only moderate encapsulation efficiencies (*e.g.* < 20%).

2.4.3.2. Remote loading

Weakly acidic or alkaline drug molecules can be efficiently encapsulated by the so-called remote loading method. This method is based on the principle that neutral molecules can be shuttled into liposomes, due to a difference in the ion concentration and/or pH between the inside and the outside of the lipid membrane. Once inside liposomes, drug molecules become charged which prevents their rapid release from the lipid vesicles. Most anthracyclines (*e.g.* Dox, daunorubicin) and *Vinca* alkaloids (*e.g.* vincristine, vinblastine) can be encapsulated with high efficiency (> 90%) using an ammonium sulphate gradient method. The principle of this loading method is outlined in Figure 2.9.

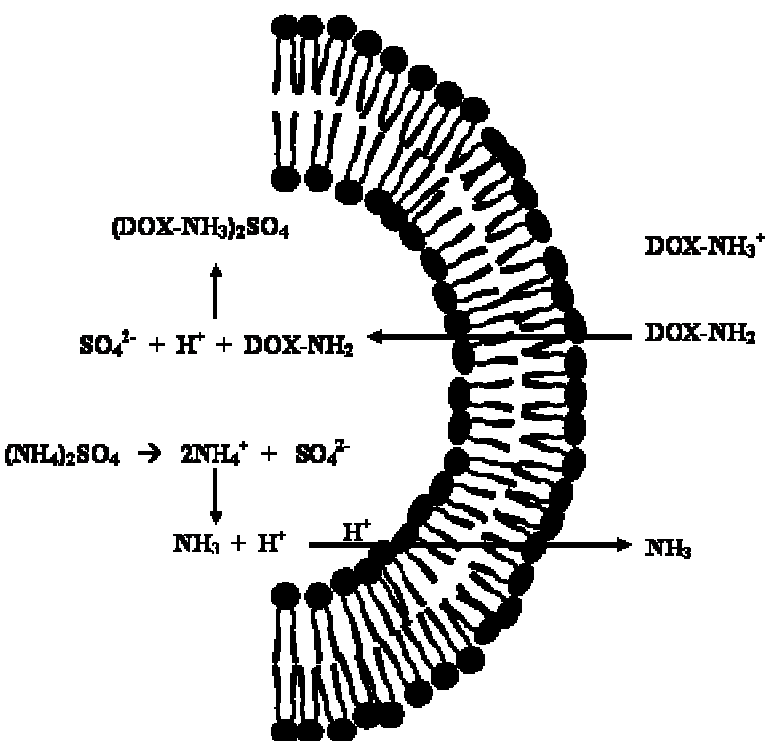


Figure 2.9. Ammonium sulfate-loading procedure for weak bases. Liposomes are first prepared in the presence of ammonium sulfate. Following removal of the exterior ammonium sulfate on a size-exclusion column, Dox is added to the extraliposomal medium. Ammonium sulfate can dissociate into two ammonium cations and one sulfate anion. Ammonia is free to cross the liposomal membrane, giving rise to a pH gradient across the membrane. Dox in its uncharged form can then cross the liposome membrane and upon cooling form an insoluble gel under acidic conditions with the remaining sulfate anion, effectively trapping it in the liposomal interior. The concentration of Dox in the liposomal lumen can reach concentrations in excess of the aqueous solubility of Dox. This loading procedure can be applied to a variety of weak bases, such as those comprising the anthracyclines, *Vinca* alkaloids or camptothecins. However, the stability of the complex formed with the sulfate and thus the gel in the liposomal lumen contributes to the overall

stability of the formulation. Reproduced with permission from Ref. [61]. D.C. Drummond *et al.*, Pharmacol Rev 51, 691 (1999). Copyright © American Society for Pharmacology and Experimental Therapeutics.

2.4.4. Industrial manufacturing

In the manufacturing of pharmaceutical liposomal products a number of problems may be encountered including poor quality of lipids available as raw material, low drug payload, short shelf-life, or complex scale-up processes. In the early 1980s the quality of lipids could still vary considerably reducing the possibility of forming well-defined, reproducible and homogeneous batches of liposomal drugs. Nowadays, quality is ensured by improved and validated analytical techniques and purification methodologies. Physicochemical properties of liposomal products must also be determined accurately in order to determine whether liposome batches display the defined final product specifications in terms of size, shape, lamellarity, payload together with prolonged stability over time under given storage conditions. For a pharmaceutical product, a minimum shelf-life of about a year preferably without the need for storing it in a freezer are important requirements [29]. Contrary to sterically stabilized liposomal products that display adequate shelf-life in liquid form when kept at 4-8°C, storage of conventional liposomes as suspensions might be problematic. However, this drawback can be quite easily solved knowing that liposomal drugs can be lyophilized and reconstituted upon rehydration displaying the same characteristics as those of the initial suspension [62, 63]. As the use of a large quantity of organic solvents including chloroform or diethyl-ether is to be avoided, methods of preparation such as homogenization, detergent removal method, ethanol injection method will be preferred as manufacturing processes. Specific analytical methods must be developed for a given product. For example, a targeted liposomal drug having a specific ligand at the liposome

surface must be tested for its functionality in terms of recognition and binding capacity to the target cell receptor.

2.5. Analytical techniques

2.5.1. Photon correlation spectroscopy

Photon correlation spectroscopy (dynamic light scattering or quasi-elastic light scattering) is a quick and easy method to determine the size of lipid aggregates. Light scattering is particularly sensitive to dust; therefore, one main requirement to the use of such a technique is the removal of dust by filtration prior to particle size determination. Lipid dispersions must be diluted to a lipid concentration of around 1 mg/mL in order to avoid multiple scattering effects. Modern equipment for size determination based on photon correlation spectroscopy is commercially available from a number of manufacturers. This method is based on analysis of the time dependence of fluctuations in the intensity of scattered light that results due to the Brownian motion of particles in solution/suspension. Since small particles diffuse more rapidly than large ones, the rate of fluctuation of the scattered light intensity varies accordingly [64]. The hydrodynamic radius (R_h) is determined from the analysis of the light scattered by the particles. It is related to the particle diffusion constant (D) by the Stokes-Einstein equation:

$$D = k_B \cdot T / (6\pi \cdot \eta \cdot R_h) \quad (\text{Eq. 2})$$

where k_B is Boltzmann constant, T the temperature in Kelvin and η the viscosity of the medium. D depends on the fluctuations of the diffused light detected by a photomultiplier and analyzed. Measurement validation requires that the analyzed objects are spherical and homogeneous, which is the case for extruded liposomes.

The electrophoretic mobility and thus the zeta potential can be derived from the Doppler shift in frequency of light that is scattered from the liposomes moving in an electric field [64]. Knowing the value of zeta potential is important as it may impact on the fate of liposomes *in vivo* [65], as well as their interactions with cells [66] and drugs [67].

2.5.2. Gel chromatography

High performance liquid gel exclusion chromatography can also be used to determine the particle size and homogeneity of lipid vesicles. Gels of various exclusion diameters can be used and the columns can be calibrated using polystyrene beads of known diameter. An exclusion chromatography method has been described by Ollivon *et al.* in 1986 [68] and refined by Lesieur *et al.* [69]. This method is based on the determination of the distribution coefficient of the column using the following equation :

$$K_d = (V_e - V_0) / (V_t - V_0) \quad (\text{Eq. 3})$$

where V_e is the elution volume of the sample, V_0 the exclusion volume of the column and V_t the total elution volume of the column.

The K_d values are then related to the mean diameter (MD) of vesicles by the following equation:

$$\text{Log}(MD) = 3.03 - 4.43 (K_d) + 9.63 (K_d)^2 - 8.85 (K_d)^3 \quad (\text{Eq. 4})$$

The precision of this method is lower than dynamic light scattering and microscopy, but is simple, fast and can be recommended as a preliminary approach to characterize the mean particle size of liposomal preparations.

2.5.3. Microscopy

Microscopy techniques are often used to determine the size, size distribution and morphology of liposomes, although this requires the observation of a large number of liposome sample micrographs. The microscopy methods that are most commonly used are transmission electron microscopy (TEM) and cryofracture [70]. Yet recently, new techniques such as atomic force microscopy [71] and environmental scanning electron microscopy [72] are becoming more popular.

Negative staining is often employed in TEM and involves the deposition of an electron opaque metal film (usually molybdate and phosphotungstate) on a liposome sample that has been placed on a grid covered by a colloidal film that is stabilized by a thin layer of carbon [26]. The vesicles then appear as bright structures on a shaded background when observed by TEM. This technique is not appropriate for large vesicles where distortions and membrane folding may be a source of multiple artefacts.

Cryofracture is usually a preferred technique as it is associated with fewer artefacts. This is mainly due to the fact that chemical fixation of samples is not required. The principle of this technique is based on a rapid freezing of the samples which are then fractured to form replicas of the exposed surfaces. The replicas are then rigidified by deposition of a thin carbonic layer.

Electron microscopy is not always available in laboratories and easier and more rapid techniques, like gel exclusion chromatography, dynamic and static light scattering are often preferred as methods for particle size determination.

2.5.4. Fluorescence spectroscopy

Among all probing techniques, labelling of liposomes with fluorescent markers is the most widely used. Principles of fluorescent techniques are described in detail by J.R. Lakowicz [73]. The main parameter that is determined in static fluorimetry is the fluorescence intensity which is proportional to the concentration of the fluorescent probe and to the wavelength displacement of its emission spectrum. The wavelength displacement occurs as a result of a change in the polarity of the microenvironment of the marker. Fluorescent probes can be either chemically linked to the polar head or to the acyl chains of phospholipids. Liposome properties/phenomena such as membrane rigidity, membrane destabilization, membrane fusion, and leakage of soluble liposomal content can be monitored using fluorescent probes or fluorescently-labelled lipids.

It is for example possible to study the resonance energy transfer (RET) between two probes that are sufficiently close to each other. The vesicle-to-micelle transition of lipid-surfactant mixtures has been studied using the RET between rhodamine-labelled and *N*-4-nitrobenzo-2-oxa-1,3-diazole (NBD)-labelled phospholipids [74]. When the two lipid markers are close enough to each other in a lipid membrane, the donor (NBD) can transfer a large part of its energy to the acceptor (rhodamine). Therefore, upon addition of increased concentration of a detergent to the liposome, lipids including the lipid probes will be progressively solubilized in micellar structures separating the donor from the acceptor. This results in an increase in the fluorescence intensity of the donor and a decrease in the fluorescence intensity of the acceptor. Other membrane probes such as pyrene can, depending on their local concentration, be inserted in a lipid bilayer as monomers or complexes called excimers. Since the fluorescent properties of these two forms are different it has been used to study the flip-flop of a pyrene-labelled lipid from one monolayer to the other in a lipid bilayer [75].

Soluble fluorescent probes that self-quenches its fluorescence at high concentrations such as 6-carboxyfluorescein (6-CF) can be used to monitor the leakage of liposomal content from their aqueous internal volume [76]. This method can be useful to study the membrane stability of liposomes under various conditions. Upon destabilization of the membrane, 6-CF is released in the exterior medium where the probe is diluted leading to an increase in its fluorescence intensity. As the spectroscopic properties of 6-CF are sensitive to pH other non-pH sensitive probes are preferred for certain studies.

Time-resolved fluorescence spectroscopy can determine the life times of fluorescent probes which enables molecular rotation correlation time measurements. Another technique utilizing impulses of a laser called photobleaching recovery can provide diffusion coefficient values of membrane components.

2.5.5. Nuclear magnetic resonance spectroscopy

Nuclear magnetic resonance (NMR) spectroscopy is a powerful tool for the evaluation of liposomal formulations. One of the major advantages of this technique is that it exploits intrinsic reporter moieties, such as ^{13}C , ^{31}P , ^1H , ^2H , ^{15}N , ^{195}Pt nuclei, contrary to most other approaches (*e.g.* spectrofluorimetry) that require the use of bulky external probes.

As discussed above, electron microscopy and light scattering methods are often used to measure the liposome size. Interestingly, ^{31}P NMR spectroscopy can also fulfill this task. The fragmentation of lipid vesicles modifies the NMR lineshapes because of the change in averaging of the anisotropic chemical shift and relaxation parameters of the phosphorus nucleus [77]. By considering both the rotational diffusion of the vesicles and the lateral diffusion of phospholipids along the curved surfaces [78], ^{31}P NMR spectra provide information on the state of phospholipids in vesicle membranes and homogeneity of

liposomal preparations with respect to size distribution and number of lamellae [79]. Indeed, due to its sensitivity to the time scale of reorientation, ^{31}P broad band NMR allows one to assess the size distribution for vesicles with a diameter below 1 μm [78]. For lamellarity determination, ^{31}P -NMR signals are recorded before and after the addition of a nonpermeable broadening agent such as manganese (Mn^{2+}). Mn^{2+} interacts with the outer leaflet of the outermost bilayer and reduces the intensity of the original NMR signal by 50 or 25% for uni- and bilamellar liposomes, respectively [45]. Barenholz and co-workers employed NMR spectroscopy to characterize PEGylated liposomes loaded with the anticancer drug cisplatin [80]. They obtained information both on the phospholipids (physical state, rate of motion) and on the platinum complex (oxidation state and coordination sphere, interaction with the lipids). Moreover, combining NMR and atomic absorption data permitted quantification of the amount of soluble platinum in the formulations. [80].

^2H NMR spectroscopy has recently been used to characterize the membrane destabilization mechanisms of *N*-isopropylacrylamide (NIPAM) copolymers in stimuli-responsive liposomes [81]. Spectra of perdeuterated (d_{31}) POPC in MLVs (POPC- d_{31} /Chol) both in the presence and absence of NIPAM/methacrylic acid (MAA)/*N*-vinyl-2-pyrrolidone (VP)/octadecylacrylate (ODA) copolymer were collected as a function of temperature (Figure 2.10). The bare liposomes displayed the typical spectra of phospholipids in the liquid-crystalline phase, showing a superposition of powder patterns of systems with axial symmetry, attributed to the deuterated methylene groups along the chain [82, 83]. The acyl chain order was not affected by the polymer below its coil-to-globule phase transition temperature. However, upon heating above the lower critical solution temperature (LCST), the polymer introduced a local curvature in the bilayer plane, which led to significant averaging of the quadrupolar interactions on the NMR time scale. It was concluded that the introduction of highly curved local lipid planes is a consequence of the

increased amplitude of motion of the acyl chains, which can be ascribed to defects resulting in the release of entrapped materials [81].

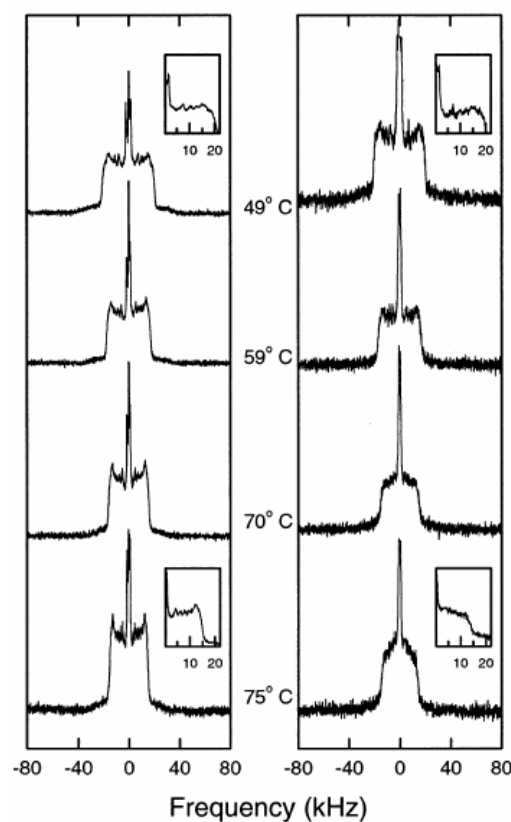


Figure 2.10. ^2H NMR spectra of POPC- d_{31} /Chol (left panel) and POPC- d_{31} /Chol/P(NIPAM-*co*-MAA-*co*-VP-*co*-ODA) (right panel). Reprinted with permission from Ref. [81], E. Roux *et al.*, Biomacromolecules 4, 240 (2003). Copyright @ American Chemical Society.

2.5.6. Fourier transform infrared spectroscopy

Fourier transform infrared (FTIR) spectroscopy is a skillful yet relatively inexpensive technique for studying the structure and organization of phospholipid bilayers. The application of infrared spectroscopy (IR) to this particular aspect of lipid research is largely based upon the fact that IR-active groups are often present in the headgroup, interfacial, and hydrophobic regions of most lipid molecules. IR has played an important role in the detection, assignment and characterization of phospholipid phase transitions, as well as in the structural analysis of the various polymorphic forms that lipids adopt [84, 85]. Simultaneous and nonperturbed monitoring of all regions of a lipid bilayer is usually possible without the added expense of introducing specific isotopic replacements or reporter groups.

Subtle variations in the frequencies, bandwidths and band shapes of the IR bands can be exploited to monitor the interactions between liposomes and biological molecules [86]. Severcan *et al.* [87, 88] employed this technique to study oil, vitamin or hormone interactions with phospholipids. They reported that fish oil changed the physical properties of the DPPC multilamellar liposomes by broadening the phase transition profile as indicated by the increase in the bandwidth of the CH₂ stretching bands. In MLV containing melatonin, the same authors [85] revealed that the encapsulated drug changed the physical properties of the bilayer by decreasing the main phase transition temperature, abolishing the pre-transition, ordering the system in the gel phase, and increasing the dynamics of the system both in the gel and liquid crystalline phases.

Thermal FTIR spectroscopy was shown to provide information on the bonding state of chemical groups involved in the physical phase transition of polymers [89-91] used to prepare stimuli-responsive liposomes. For example, the amide I' band of NIPAM

copolymer which corresponds to the carbonyl stretching mode of the amide group experiences a shift to higher frequencies upon heating. Moreover, the spectral deconvolution of this band provides additional insight on the evolution of hydrogen bonding with temperature [81].

2.5.7. Small-angle X-ray and neutron scattering

Small-angle X-ray (SAXS) and neutron scattering (SANS) are reliable analytical tools for the determination, with reasonable accuracy, of vesicle size, polydispersity, membrane hydration state, and internal membrane structure [92]. These methods can be used to characterize the structure of unilamellar vesicles in a highly diluted system [92-94]. For instance, when interacting with X-ray or neutron beams, unilamellar vesicle dispersions yield scattering intensities characterized by continuous high values at low scattering angles instead of sharp reflexes as in the case of multilamellar systems [95]. The combination of SANS and SAXS provides information on the thickness of the polar and hydrophobic regions of the bilayer, and the distance between the phosphate group and the boundary between the polar and hydrocarbon region of the bilayer.

SANS analysis of unilamellar PC liposomes (50-300 nm) dispersed in water allowed calculation of the steric bilayer thickness, the lipid surface area at the bilayer-aqueous phase interface, and the number of water molecules intercalated in the polar region of the bilayer [94]. Furthermore, Gallova *et al.* [96] employed SANS to study the bilayer thickness when Chol was added at 44.4 mol% to DMPC bilayers (ca. 50 nm). Using the $^1\text{H}_2\text{O}/^2\text{H}_2\text{O}$ contrast variation and the small-angle form of Kratky-Porod approximation, they demonstrated that Chol significantly increased the bilayer thickness from 3.7 to 4.3 nm.

2.5.8. Other techniques

As liposomal systems are constantly evolving, additional techniques are needed to better characterize these drug carriers. X-ray photoelectron spectroscopy (XPS) has been used to detect lectins grafted on the liposome surface [97]. Electron spin resonance (ESR) spectroscopy can be applied to investigate the integrity of multilamellar liposomes formed from hydrogenated phospholipids following subcutaneous injection [98]. Surface plasmon resonance (SPR) has proven effective to characterize drug absorption on immobilised liposomes that serve to mimic physiological membranes [99]. Finally, Leroux and co-workers examined the molecular interactions between pH-sensitive polymers and phospholipid bilayers with the Langmuir balance technique [100] and the surface force apparatus [101].

2.6. Stability and stabilization of liposome formulations

Stability is a critical factor that must be considered for the successful design and development of liposome-based formulations of drugs. The three major components that may be considered to contribute to the overall stability of a liposomal formulation are: (1) the chemical stability of the lipid and drug, (2) the physical or colloidal stability of the liposomes and (3) the drug release properties of the liposomes. The chemical stability of the formulation under relevant storage conditions is of particular significance if it is to be pursued for clinical use. Phospholipids, as well as various drugs, are sensitive to acidic or basic hydrolysis and unsaturated phospholipids are susceptible to oxidative degradation. The physical or colloidal stability of liposomes refers to their ability to remain as distinct colloids. In general, colloidal stability may be defined as the inhibition or prevention of processes, such as aggregation, that lead to formation of a macrophase [102]. For a

liposomal formulation it is desired that the size and size distribution of the vesicles remain unaltered or relatively constant over time. The physical stability of the formulation under storage conditions as well as in biologically relevant media must be considered. In addition, the *in vitro* and *in vivo* drug release properties of a specific formulation must be evaluated. It is necessary that the liposomes retain the drug, under the relevant storage conditions, prior to administration. Following administration, the required release properties of the formulation *in vivo* will depend on whether the liposomes are to serve primarily as solubilizers or as true drug delivery vehicles. If the liposomes are to function as excipients or solubilizers, a rapid release profile of the drug from the liposomes *in vivo* is acceptable. However, if the liposomes are to act as drug delivery vehicles and carry drug to a specific site then a delayed release profile is necessary. The passive or active targeting of drugs using liposomes requires that the drug be retained within the vesicle prior to reaching the desired site.

In the remainder of this section the three major components that contribute to the overall stability of liposome formulations are considered in detail. Specific attention is given to the extent to which the stability may be optimized by altering the composition of the lipid membrane.

2.6.1. Chemical stability of liposome formulations

The chemical stability of aqueous solutions of phospholipids may be compromised by hydrolytic and oxidative degradation. The actual organization of phospholipids into lipid membrane assemblies has been shown to reduce the susceptibility of the lipids to both hydrolytic and oxidative damage [103]. The oxidative degradation of liposomes is propagated by a free radical chain mechanism and may result in formation of oxidative products that have membrane destabilizing effects [61, 103]. Phospholipids that are

vulnerable to oxidative degradation are those that contain unsaturated hydrocarbon or fatty acyl chains [61]. Specifically, lipids containing diunsaturated fatty acyl chains are more sensitive to oxidation than those that include only monounsaturated chains [61]. Studies have found that the oxidation of liposomal formulations may be limited by use of purified starting materials (*i.e.* transition metals removed) as well as protection from exposure to light and storage at low temperatures. It has been found that the addition of components such as anti-oxidants (*e.g.* vitamin E) and chelating agents to the formulation can serve to protect against oxidative damage [103]. The inclusion of Chol in the liposome has also been shown to reduce the degree of oxidative degradation for polyunsaturated phospholipids [103, 104]. Chol's protective effect has been attributed to the increase in order and rigidity that it provides for bilayers formed from unsaturated lipids as well as its ability to decrease the hydration of the lipid bilayer [105].

Phospholipids are also susceptible to acidic and basic hydrolytic degradation owing to the ester groups within their chemical structure [61, 103]. The hydrolysis of one of the acyl ester groups in diacyl phospholipids results in the production of lysophospholipids and free fatty acids that can act to destabilize lipid membranes. The further hydrolysis of the lysophospholipids produces glycerophospho compounds and free fatty acids [103]. In general, hydrolytic degradation of liposomes results in an increase in the permeability of the lipid bilayer as well as a change in the particle size. Zuidam *et al.* demonstrated that lysophospholipid and fatty acid content can promote the disruption of the vesicles lamellar morphology and result in the formation of micellar systems if the formulation is cooled or heated through the gel to liquid crystalline phase transition of the lipids [105]. Specifically, in their study, liposomes formed from DPPC/DPPG (10:1) were shown to undergo a slight increase in particle size when the lipids had been at least 40 % hydrolyzed. The heating of the DPPC/DPPG samples, with greater than 9 % hydrolysis, to temperatures above the T_c of the lipids was found to result in micelle formation. Indeed, the ability of lysophospholipids to promote the formation of lipid micelles has been well documented

[106]. Interestingly, the inclusion of Chol in liposome formulations reduces the extent of hydrolytic degradation and prevents the increase in particle size and/or formation of micelles that may result under hydrolytic conditions [61, 103, 105].

Due to the susceptibility of phospholipids to acidic and basic hydrolysis the effects of the conditions employed for drug loading on the stability of liposomes must be considered. Use of many of the active strategies to load drugs can result in the exposure of liposomes to relatively low or high pH media. For example, use of the remote loading technique that relies on a calcium-acetate gradient results in a high pH within the internal aqueous volume (*i.e.* liposomes encapsulating diclofenac); while, use of the ammonium-sulfate gradient technique results in a low pH for the intravesicular medium (*i.e.* liposomes encapsulating Dox) [61, 107-109]. In addition, exposure to basic or acidic media may result in the hydrolytic degradation of some drugs. By contrast, in some cases the drugs stability and activity may be preserved owing to storage in low or high pH media [107]. The physical state of the drug within a liposome formulation has also been shown to influence its chemical stability [110]. Therefore, the various factors that influence the chemical stability of both the drug and phospholipid components should be carefully considered in the design and development of a liposomal formulation. Stability is one of the critical factors that influences the potential for a formulation to be moved forward into clinical development and use.

2.6.2. Physical or colloidal stability of liposomes

2.6.2.1. Conventional versus sterically stabilized liposomes

The physical or colloidal stability of a liposome formulation refers to the ability of the particles to retain their size, size distribution and morphology under certain conditions. Liposomes are most often concerned with changes in particle size due to aggregation and/or

fusion. The composition of most of the original liposome formulations included a neutral phospholipid (*e.g.* PC) with Chol and in some cases a small amount of a negatively charged phospholipid such as PG [106]. Liposomes having this composition are referred to as “conventional” and the negatively charged lipid serves as a means to prevent aggregation [106]. Conventional liposomes have limited circulation lifetimes since they are removed from the bloodstream by cells of the MPS. Typically, within minutes to hours following i.v. administration these liposomes are cleared from the circulation and mostly accumulate in the liver and spleen. *In vivo* study of the conventional formulations demonstrated that liposomes having diameters of 100 nm or less and neutral, rigid bilayers had the longest circulation lifetimes. Specifically, these are liposomes formed from neutral phospholipids with high melting temperatures (*e.g.* DSPC, $T_c = 56^\circ\text{C}$) and Chol. Due to the limited biological performance of the conventional formulations the laboratories of both T.M. and D. Papahadjopoulos modified the surface of the liposomes as a strategy to improve their circulation lifetime [106, 111, 112]. The surface modification involved the addition of a hydrophilic layer that is analogous to the hydrophilic polymer coating termed the glycocalyx that is found on the surface of most cells *in vivo* [106]. The glycocalyx consists of glycolipids and glycoproteins and is largely responsible for the prolonged circulation lifetime of red blood cells [106, 111]. Initially, the surface of the vesicles was modified by incorporating a small amount of the glycolipid, monosialoganglioside (GM₁). Indeed the incorporation of GM₁ was found to provide a pronounced increase in the circulation lifetime of vesicles and a significant decrease rate of their accumulation in the liver [111, 112]. Studies also revealed that inclusion of PI provided an increase in the circulation lifetime of the vesicles yet to a lesser extent than GM₁. The incorporation of GM₁ and PI introduces hydrophilic carbohydrate residues, as somewhat bulky groups, and “shielded” negative charge at the surface of the vesicles. In this way, the glycolipid-containing formulations included a steric barrier at the surface and were referred to as “stealth” or “sterically stabilized” systems. In later years alternatives for GM₁ were sought largely due to its expense and the difficulties associated with its purification [111]. The incorporation

of phospholipids terminated with the hydrophilic polymer, PEG, later emerged as another approach to extend the circulation lifetime of liposomes [111].

Over the years considerable research has been devoted to uncovering the mechanism by which GM₁, PEG and other hydrophilic polymers lead to an increase in the circulation lifetime of liposomes. Overall there is general agreement that the presence of these moieties at the surface of the liposomes results in a reduction in their rate of uptake by the phagocytic cells of the MPS [106, 111, 112]. The ability of GM₁ and/or PEG to lead to this reduction in MPS uptake rate has been attributed to a wide range of factors including, but not limited to: increase in surface hydrophilicity, reduction in tendency to aggregate, reduction in binding of opsonins (*e.g.* C3b), reduction in destabilization by lipoproteins, increase in binding of dysopsonins and reduction in specific interactions with cells of the MPS [106, 113]. As reviewed in detail elsewhere, there is direct experimental evidence to support the role of each of these factors in extending the circulation lifetime of liposomes [111]. However, in some cases the evidence is somewhat controversial and to this point there is still question surrounding the exact mechanism by which GM₁ or PEG exert their effect. Additional research in this area will allow for improved engineering of the liposome surface as a means to further extend their circulation lifetime and optimize their biological performance. At present, surface modification with PEG remains the “gold standard” in terms of strategies for extending the circulation lifetime of liposomes as well as other nano-sized carriers. Yet other hydrophilic polymers, such as poly [N-(2-hydroxypropyl)methacrylamide], PVP, hydroxypropylmethylcellulose and poly(vinyl alcohol), have also been employed for the surface modification of liposomes [18, 19, 114, 115].

2.6.2.2. Physico-chemical properties of PEG

PEG (*i.e.* -CH₂-CH₂-O-) is a semi-crystalline, hydrophilic polyether with a high solubility in water and other aqueous media [116]. In comparison to other structurally similar polyethers the virtually “unlimited” water solubility of PEG has been found to be unique and is largely attributed to its high degree of hydrogen bonding with water [116]. If we consider the parameters that are commonly used to describe polymers in solution such as the Flory Huggins interaction parameter (χ) and the second virial coefficient (A_2) it becomes clear that water is a “good” solvent for PEG [116, 117]. χ describes the energy of interaction between a segment of a polymer and solvent molecules. A value of χ that is less than 0.5 signifies that the polymer is in a “good” solvent and interactions between the polymer and solvent are stronger than solvent-solvent and polymer-polymer interactions. For polymer-solvent systems where $\chi < 0.5$ the polymer is said to exist as an expanded coil. When the value of $\chi = 0.5$ the polymer is said to be present as a Gaussian or random coil. For values of $\chi > 0.5$ the interactions between the polymer and solvent are weak and the polymer is in a collapsed state. For PEG in water, under various conditions, the χ parameter has been reported to range between 0.4 and 0.5 [116]. In this way, from consideration of the χ value for PEG in water the polymer molecules are predicted to exist as either Gaussian or expanded coils. In addition, the value for A_2 for PEG in water also provides an indication that the polymer exists as an expanded coil in water. Specifically, the value of A_2 has been measured experimentally and found in most cases to have a high positive value [117]. A high positive value for A_2 signifies the presence of favorable interactions between polymer and solvent and/or repulsive interactions between the individual segments within the polymer chain (*i.e.* polymer-polymer interactions). Finally, the steric factor (σ) for PEG in water has been reported to have a value that is close to one which means that PEG is a flexible, freely rotating chain in water [117]. Therefore, from consideration of the values of

χ , A_2 and σ for the PEG-water system it is clear that the PEG molecules interact favourably with water and are present in an expanded conformation as freely rotating chains [118].

2.6.2.3. Conformation of PEG at the surface of lipid membranes

When the PEG-modified lipid is incorporated during the preparation process it results in the presence of the hydrophilic polymer at the outer and inner surfaces of the lipid membrane. By contrast, if the PEG-lipid is exchanged in following liposome preparation then the hydrophilic polymer is only present at the outer surface. In an aqueous medium, the surface grafted PEG extends away from the bilayer since water is a “good” solvent for the polymer and it is not attracted to the lipid surface [119]. Theories based on polymer physics and put forth by deGennes predict that there are two conformational regimes for polymers grafted to a surface [120, 121]. At a low graft density the polymer is said to be in the “mushroom regime” wherein the polymers adopt a random coil conformation. In this regime the polymer chains are non-interacting and present at the membrane surface in a mushroom or “half-sphere” configuration. Each mushroom or half-sphere is said to have a Flory radius (R_f) that may be described by the following equation:

$$R_f \approx a N^{3/5} \quad (\text{Eq. 5})$$

where a is the size of the monomer, N is the degree of polymerization of the polymer. For PEG, the value of a for the oxyethylene monomeric unit has been reported to be approximately 0.35 nm [106, 122]. Therefore, for PEG chains having molecular weights of 550 (*i.e.* $N = 13$), 2000 ($N = 45$), 5000 ($N = 114$) the R_f values would be 1.6, 3.4 and 6 nm. In this way, at a low density the PEG molecules would be expected to be in a mushroom configuration and extend away from the surface at a distance (*i.e.* $2 \times R_f$) of 3.2, 6.8 and 12 nm for molecular weights of 550, 2000 and 5000, respectively.

At a high graft density the polymer is said to be in the “brush regime”, the chains are densely packed and may interact laterally. In this regime the polymers extend away from the surface to form a brush of thickness, L [121]. The transition from the mushroom to the brush regime will occur at the concentration that results in an initial lateral overlap of the individual polymer chains or mushrooms. Thus, the two key parameters that determine the conformation of the polymer are the molecular weight of the polymer and the graft density [106, 121]. For PEG grafted to the surface of a liposome the specific conformation of the PEG chains will be determined by the molecular weight of the PEG moiety as well as the mole fraction of PEG in the formulation. The following equation may be used to predict the mole fraction at which the mushroom to brush transition may occur for PEG of a specific molecular weight:

$$X_{\text{PEG-lipid}}^{\text{m} \rightarrow \text{b}} > [A/(\pi a^2)] N^{-6/5} \quad (\text{Eq. 6})$$

where A is the membrane surface area per lipid headgroup [121]. The value for A in fluid-phase bilayers is reported to range from $0.6 - 0.7 \text{ nm}^2$; while, for lipids in the gel phase $A = 0.4 - 0.48 \text{ nm}^2$ [121]. Using this equation, it is calculated that in a typical fluid-phase liposome the transition from the mushroom to the brush regime would be predicted to occur when the mole fraction of PEG-lipid is $X = 0.08, 0.02$ and 0.005 for PEG having molecular weights of 550, 2000 and 5000, respectively (with $A = 0.7 \text{ nm}^2$ and $a = 0.35 \text{ nm}$). In a gel-phase liposome the transition from the mushroom to the brush regime would be expected when the mole-fraction of PEG-lipid is $X = 0.06, 0.01$ and 0.004 for PEG having molecular weights of 550, 2000 and 5000, respectively (with $A = 0.48 \text{ nm}^2$ and $a = 0.35 \text{ nm}$). Therefore, an increase in the molecular weight of the PEG chain results in a decrease in the mole fraction required to initiate the mushroom to brush transition. As reviewed by Marsh *et al.* the values obtained for $X_{\text{PEG-lipid}}^{\text{m} \rightarrow \text{b}}$ using equation 6 correlate fairly well with the experimentally determined values [121]. The limitations of this equation in terms of

providing an accurate prediction of $X_{\text{PEG-lipid}}^{m \rightarrow b}$ for a specific liposome system are also further discussed in the review by Marsh *et al.* [121].

For PEG in the brush regime the thickness or height (L) of the polymer “brush” may be described by the following equation [121]:

$$L \approx N a^{5/3} (X_{\text{PEG-lipid}}/A)^{1/3} \quad (\text{Eq. 7})$$

From this equation it is shown that in the brush regime the layer thickness increases with an increase in the degree of polymerization of the polymer, when the mole fraction of PEG-lipid is held constant. It should be noted that an increase in the mole fraction of PEG-lipid beyond a certain point induces a morphological change from vesicles to micelles [121]. There has also been found to be a range of mole fractions of PEG-lipid for which the vesicle and micelle morphologies co-exist. The mole fraction at which the PEG-lipid will begin to induce micelle formation depends on both the composition of the lipid bilayer and the length of the PEG chain. For example, Marsh *et al.* reported that for PEG of molecular weight 2000 the mole fraction of PEG-lipid required for the onset of micellization is 0.07 (*i.e.* 7 mol %) for a DPPC/DPPE-PEG formulation [121]. They also found that there was a region of co-existence for the lamellar and micellar morphologies when the mole fraction of PEG-lipid ranged from 0.07 to 0.45; while, beyond a mole-fraction of approximately 0.45 for the PEG-lipid the lipid is only arranged in the micellar morphology.

2.6.2.4. Effect of PEG on the material properties of lipid membranes

The presence of PEG at the surface of the liposome alters the material properties of the lipid membrane. The inclusion of the PEG-lipid in the formulation may alter the zeta potential of the vesicles and the PEG chains act to increase the surface hydrophilicity [118,

121, 123]. In addition, the surface grafted PEG layer provides what is termed “steric stabilization” of the liposomes as it acts as a barrier preventing the close approach of some macromolecules, other liposomes and cells [106]. The steric barrier afforded by the PEG layer is largely attributed to repulsive forces generated due to a change in the conformational entropy of the polymer chains and/or a change in the osmotic pressure at the PEG-modified surface of the liposomes [106, 121]. As illustrated in Figure 2.11, when an entity such as a protein approaches a PEG-grafted surface the polymer chains may be compressed which results in a reduction in the volume available per polymer chain. In this way, a repulsive force develops owing to the unfavourable decrease in the conformational entropy of the polymer coils [123]. In addition, if a protein penetrates the PEG layer, this will result in an osmotic repulsive force due to the presence of the protein within the PEG layer. The steric protection provided by the PEG layer is said to be kinetic rather than thermodynamic; therefore, the polymer acts to retard or decrease the rate of adsorption or association of species with the lipid membrane rather than preventing these interactions entirely [119].

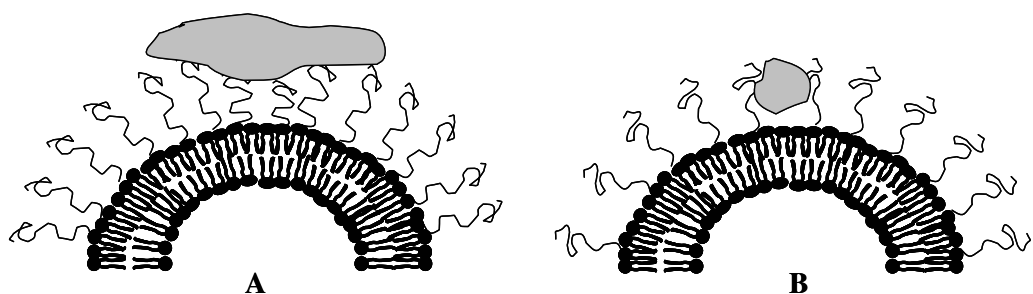


Figure 2.11. A schematic illustration of the compression (A) or interpenetration (B) of the PEG layer due to the close approach of protein to the liposome surface.

Several theoretical and experimental approaches have been used to assess the size or height of the steric barrier provided by PEG grafted to a lipid membrane. X-ray diffraction analysis of MLV subjected to osmotic pressure has been employed to determine the distance between apposing lipid bilayers as a function of pressure [106, 124]. The pressure-distance relationships provide a measure of the repulsive pressure that exists between the bilayers [106]. For example, Kenworthy *et al.* evaluated the pressure-distance relationships for MLV formed from DSPC and 1,2-distearoyl-sn-glycero-3-phosphoethanolamine (DSPE)-PEG for PEG having molecular weights of 350, 750, 2000 and 5000, where the mol % of PEG-lipid was increased from 0 to 20-40 [124]. Overall, the distance between the apposing bilayers and hence the steric repulsive pressure provided by the PEG layer was found to depend on both the molecular weight of the PEG and the graft density of PEG-lipid.

The X-ray diffraction analysis of MLV and studies using other techniques that examine the close approach of apposing lipid membranes provide a good indication of the extent to which the presence of PEG can prevent the self-aggregation of liposomes. The prevention of liposome self-aggregation is one of the means by which the presence of surface grafted PEG is said to increase the circulation lifetime of the vesicles [118]. In a study by Ahl *et al.* a direct correlation was observed between the extent of aggregation of liposomes *in vitro* and their circulation lifetime *in vivo* [125]. Specifically, formulations that were shown to remain in a disaggregated state *in vitro* had an extended circulation lifetime *in vivo*, when compared to formulations that aggregated *in vitro*. The influence of PEG-lipid on liposome-liposome interactions has also been studied by other groups as described elsewhere [126, 127].

To this point much attention has been given to examining the ability of a PEG layer to exclude or prevent the adsorption of proteins or other macromolecules of varying sizes [106]. Needham's group has reported on several studies that examine the surface

association or adsorption of a wide range of molecules (*e.g.* peptides, proteins, polymers) and particles (*e.g.* micelles) to lipid bilayers using the micropipet technique [106]. Their studies have enabled the development of a model to predict the decrease or retardation in the “on rate” of adsorbing species provided by a layer of surface grafted PEG. From their analyses it has been found that PEG chains of higher molecular weights such as 2000 or 5000 are more effective at preventing the close approach of large macromolecules or colloidal particles. While a high density of lower molecular weight PEG, such as PEG 550 or 750, is more effective at excluding smaller sized macromolecules. Furthermore, their studies revealed that the ability for PEG to exclude certain species depends on the strength of the interaction between the species and the surface of the lipid membrane as well as the concentration of the species present [106].

Therefore, the kinetic protection provided by a PEG layer may be modified by adjusting the molecular weight of PEG employed as well as the amount or graft density. However, the extent of the protective effect is influenced by the concentration of the adsorbing species as well as the nature of the species in terms of its size and affinity for the lipid membrane.

2.6.2.5. Influence of PEG on the pharmacokinetic parameters of liposomes

The incorporation of PEG-modified lipids into liposomes has been shown to have profound effects on the pharmacokinetic parameters of the vesicles *in vivo* [61, 106, 111]. The specific differences between the pharmacokinetic parameters of conventional and sterically stabilized liposomes have been reviewed in detail by T.M. Allen [106]. Most importantly, the sterically stabilized vesicles have a prolonged circulation lifetime *in vivo*, in comparison to conventional liposomes. The extent to which the incorporation of PEG-lipid alters the pharmacokinetics of the liposomes depends not only on the molecular weight of PEG as well as the amount of PEG-lipid present but also on the composition of

the remaining lipid. To this point, in terms of improving the circulation lifetime of the vesicles *in vivo*, the incorporation of 5 mol % PEG-lipid with PEG of molecular weight 2000 has been found to be optimal [106].

Conventional liposomes formed from high transition lipids (*e.g.* DSPC) are known to have longer circulation lifetimes than vesicles formed from low transition lipids (*e.g.* EPC). However, the steric stabilization of liposomes has been shown to enable the rate of clearance of liposomes from the circulation to become “relatively independent of the remaining lipid composition” [61]. In this way, as reviewed by Drummond *et al.*, the addition of PEG-lipid has been found to increase the levels of lipid in plasma (in mice) by approximately two fold for liposomes formed from high T_c lipids (*e.g.* DSPC/Chol) and up to ten fold for liposomes formed from low T_c lipids (*e.g.* EPC/Chol) [61]. Thus, the presence of PEG-lipid has a more significant influence on the pharmacokinetic parameters of liposomes formed from low T_c lipids.

In addition, the clearance of sterically stabilized liposomes has been found to be non-saturable; while, that of the conventional liposomes is saturable [106]. The non-saturable clearance of the liposomes from the circulation has important implications in terms of the calculation of doses required clinically as discussed elsewhere [106, 128]. The rate of clearance of the sterically stabilized liposomes is also much less sensitive to the size of the vesicles for diameters of less than 300 nm. The primary sites of accumulation of both conventional and sterically stabilized liposomes is the liver and spleen. In this way, the presence of surface grafted PEG on liposomes does not act to prevent MPS uptake rather it causes a reduction in the rate of uptake by the MPS [61].

The longer circulation lifetimes of the sterically stabilized liposomes affords the opportunity for accumulation in “leaky” tissues (*e.g.* tumors or sites of infection) via the enhanced permeation and retention (EPR) effect [106]. The passive accumulation of

sterically stabilized liposomes at tumor sites has been exploited as a mean to enhance the therapeutic efficacy of various anticancer agents (see Section 2.8). The extent to which the PEG layer enhances the efficacy of the drug depends on the pharmacokinetics of the liposomes as well as the release kinetics of the drug from the vesicles *in vivo*.

2.6.2.6. Blood clearance of PEGylated liposomes on repeated injection

Although PEGylation is known to change the pharmacokinetic of liposomes following a single injection, this property may be lost upon multiple dosing. This effect, referred to as the “accelerated blood clearance (ABC) phenomenon” [129-133], is likely to reduce the expected therapeutic efficacy of subsequent administrations of PEGylated liposomes. The actual mechanism remains unclear, even if several hypotheses have been proposed. Dams *et al.* [130] suggested that the accelerated particle removal is mediated by a soluble heat labile serum factor, probably secreted by the liver and spleen macrophages in response to the first dose. This is in line with other results showing that the complement system pathway and anti-PEG IgM may be involved [131, 134].

However, the presence of PEG on the liposomes does not seem to be a prerequisite for the induction of the ABC phenomenon. Indeed, similar observations were reported for conventional liposomes such as DPPC LUV (100 nm) [129]. In this case, the liposomes contained a synthetic DSPE-hydrazinonicotinamide conjugate on their surface that might have stimulated the primary defence system and subsequently affected the liposome clearance in rats. For conventional liposomes, factors such as the lipid dose [131, 132], vesicle size and surface charge [131] were identified as possible inducers of the ABC phenomenon. Understanding the underlying mechanism for this accelerated clearance is important in order to further improve liposome-based therapies by preventing undesired alterations in the pharmacokinetics and biodistribution patterns which could occur upon multiple dosing.

2.6.3. Drug retention properties of liposome formulations

The drug release properties of a liposomal formulation depend largely on the properties of the drug, properties of the liposomes and drug loading method employed [106]. The physico-chemical properties of the drug will determine the methods that may be employed effectively for loading as well as the localization of the drug within the vesicles and physical state following incorporation. Passive and active loading techniques have been developed for loading drugs into liposomes. The passive loading technique is commonly employed for incorporation of highly hydrophilic drugs and leads to entrapment of the drug within the internal aqueous volume of the vesicles [61]. Liposomal formulations for hydrophilic drugs such as cytosine arabinoside (ara-C) and 5-fluorouracil (5-FU) have been reported [61, 135]. The hydrophilic drugs are easily retained within the liposomes due to their inability to permeate lipid membranes [61]. In fact, for hydrophilic drugs formulated in liposomes the drug may be retained until the carrier reaches the target site; yet, this will only translate into improvements in therapeutic efficacy if the drug is released. Thus, liposomal formulations of hydrophilic drugs may benefit from the use of a triggered drug release strategy. As outlined in Section 2.8, in recent years, several different strategies have been put forth for achieving triggered drug release from liposomes [61, 106, 136].

In liposomal formulations of hydrophobic drugs the drug is localized or entrapped within the hydrophobic region of the lipid membrane. Since the drug is incorporated within the lipid bilayer there is a limit in terms of the maximum amount of drug that can be solubilized without compromising the stability of the formulation [61]. For example, various liposome formulations of the hydrophobic anticancer agent paclitaxel have been prepared. The encapsulation efficiency for the lipid formulations of this drug have been quite high ranging from 50 – 100 %; yet, the maximum drug to lipid ratio for a stable formulation was only 1:33 mol:mol and the highest concentration of paclitaxel achieved

was 2 mg/mL [137, 138]. In addition, in some cases it has been found that liposome formulated hydrophobic drugs quickly dissociate from the vesicles following administration owing to their affinity for plasma components. Nonetheless, liposomes may serve as effective solubilizers of hydrophobic drugs and do not have the toxicity issues that are associated with some of the common excipients such as Cremophor EL.

To this point, liposomes have been most effective as delivery vehicles for amphiphilic drugs that are weak acids or weak bases [61]. As discussed in Section 2.4.3, these drugs may be incorporated efficiently into the internal aqueous volume of the liposomes using active loading techniques that rely on pH or ion gradients [107-109, 139, 140]. Amphiphilic drugs such as Dox, daunorubicin and vincristine have been successfully formulated in liposomes at a high drug to lipid ratio [61, 106]. In addition, the composition of the lipid membrane may be selected such that the drug is retained within the liposome until reaching the target site.

For drugs that are incorporated within the internal aqueous volume of the liposome the release of the drug from the vesicles will depend on both the properties of the drug and the composition of the lipid membrane. Inclusion of significant amounts of Chol results in an increase in the conformational ordering of the lipids which in turn reduces the permeability of the membrane [141]. Also in general, membranes formed from saturated lipids and lipids with longer acyl chain lengths are less permeable to small molecules. In a systematic study by T.M. Allen's group they compared the *in vitro* and *in vivo* drug release properties of liposome formulations of Dox; wherein the lipid composition was varied in terms of degree of unsaturation and acyl chain lengths of the lipids [142]. In their study it was clearly shown that an increase in the rigidity of the bilayer resulted in a decrease in the release rate of drug *in vitro*. Specifically, the *in vitro* "leakage half-lives" were reported to be 14.9, 14.6, 23.0 and 91.8 h for Dox formulated in DOPC/Chol/DSPE-PEG-2000 2:1:0.1 molar ratio (T_c of PC lipid = -20°C), POPC/Chol/DSPE-PEG-2000 2:1:0.1 molar ratio (T_c of PC

lipid = -2°C), DMPC/Chol/DSPE-PEG-2000 2:1:0.1 molar ratio (T_c of PC lipid = 23°C), and HSPC/Chol/DSPE-PEG-2000 2:1:0.1 molar ratio (T_c of PC lipid = 55°C), respectively. Also, in their *in vivo* evaluation of the pharmacokinetics of Dox administered in the liposomal formulations, it was found that the vesicles having the more rigid bilayers gave rise to higher plasma concentrations of drug over prolonged periods (*i.e.* up to 72 h). In this way, the drug release profile of the liposomes may be tailored by selection of the appropriate lipid composition.

Finally, the incorporation of PEG-modified lipid has also been found to alter the permeability of the lipid membrane and drug retention properties of liposomes [61, 143]. There have been reports that the incorporation of PEG-modified lipid may reduce the permeability of the lipid membrane and decrease the leakage rate of small molecules from the liposomes [143]. In other cases the inclusion of the PEG-modified lipid has been found to reduce the stability of the formulation in terms of drug retention. In such cases a balance must be achieved such that the amount of PEG-lipid added is sufficient to enhance the physical stability of the formulation without compromising the retention of the drug.

2.7. Triggered release

Liposomes that include a triggered release mechanism have been designed for several different applications, but have been mainly investigated in the field of cancer chemotherapy. The mechanism of drug release generally exploits a physical/chemical change in the environmental conditions that can be either physiological or extrinsic. Stimuli such as temperature [144, 145], light [146, 147], pH [101, 148, 149], enzymatic degradation [150, 151], electricity [152, 153] and ultrasound [154] have been successfully used to initiate a breakdown or change in the membrane carrier, which induces the release of the

encapsulated cargo. In this section, only the four most studied strategies of triggered release, *i.e.* light, temperature, pH and enzymatic degradation, will be discussed.

2.7.1. Light

Light activation is a versatile method for provoking liposome destabilization since it provides a broad range of adjustable parameters (*i.e.* pulse duration, intensity, pulse cycle, and wavelength) that can be optimized to suit a given application [155]. Liposomes can be made photosensitive with lipids that either isomerize, fragment or polymerize upon photoexcitation [147, 156, 157]. A strategy that has been proposed by Thompson and co-workers [156] exploits the effect of plasmalogen photooxidation on membrane permeability upon cleavage of plasmenylcholine to single chain surfactants. Singlet oxygen, formed by irradiation of a suitable sensitizer in the presence of oxygen, cleaves the vinyl ether linkage of plasmenylcholine-type lipids to create lamellar defects within the liposome (Figure 2.12). Other approaches currently investigated to prepare temperature-responsive liposomes include photodeprotection of fusogenic lipids [158] and acid catalysis of vinyl ether containing lipids upon irradiation of photoacid generators [155, 159]. Although the principle of light-triggered activation seems relatively straightforward, it is somewhat limited to applications where the target site is accessible to a light beam, such as during a surgical intervention or for localized pathologies (*e.g.* solid tumor). However, this approach may not be adequate for disseminated diseases like metastatic cancer [160].

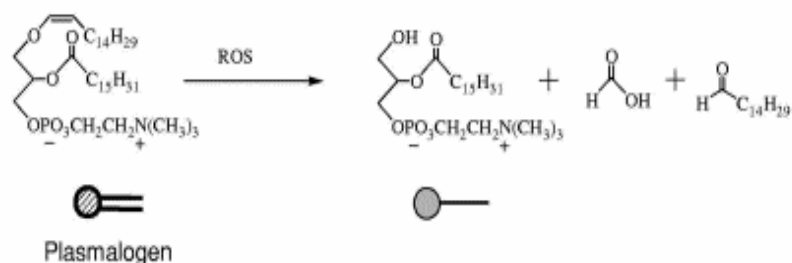
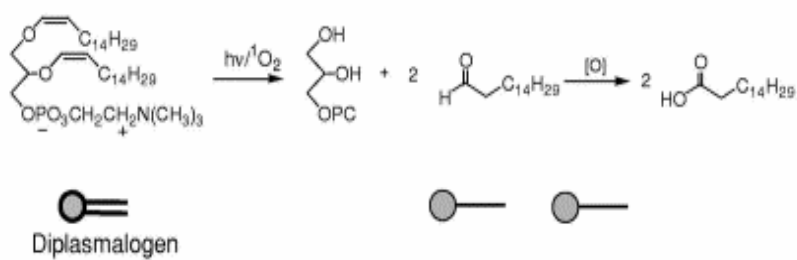
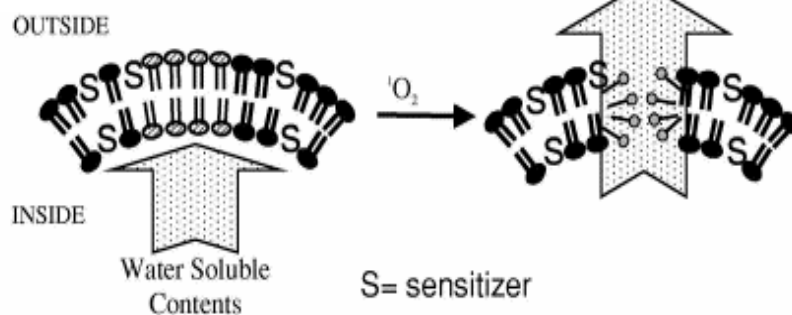
A)**B)****C)**

Figure 2.12. Photosensitized oxidation of plasmalogen (A) and diphasmalogen (B), and the consequences of this reaction on membrane permeability (C). Legend: ROS = Reactive oxygen species. Reprinted with permission from Ref. [155], P. Shum *et al.*, Adv Drug Deliv Rev 53, 273 (2001). Copyright @ Elsevier.

2.7.2. Temperature

The most common mechanism underlying temperature-triggered release is based on an increase in the membrane disorder and permeability when the target tissue is warmed above the lipid T_c . Lipids with a T_c slightly exceeding the physiological temperature (37°C), such as DPPC and DPPG [161, 162], are ideal candidates to construct thermally-responsive liposomes. When DPPC ($T_c = 41^\circ\text{C}$) is the sole phospholipid in the vesicle, the rate of release and the amount of content released are relatively low but they can be increased by supplementing the bilayer with other lipids, such as HSPC and DSPC [145]. These mixtures possess a slightly higher T_c and the width of the transition is broad ranging from 43-45°C [145]. When applied at the tumoral site, heat can not only trigger the release of encapsulated drug but also improve the extravasation of the liposomes [163]. The increase in extravasation after heating has been attributed to morphological changes in the vessel wall affecting interendothelial junctions [164], which increase the permeability of the vessels [165, 166]. Early studies with thermosensitive liposomes were often carried out at relatively high temperatures that were not necessarily relevant in the clinic [160]. In this respect, Needham and co-workers developed a liposome formulation that was optimized for drug release at 39–40°C [167-169]. The liposomes contain a lyso-phospholipid (MPPC) (DPPC/MPPC/DSPE-PEG-2000, 90:10:4 molar ratio, 140 nm) that is kinetically trapped in the membrane gel phase. When the liposomes are heated above the main phase transition, the lyso-phospholipid leaves the bilayer, making the membrane highly permeable to the encapsulated solute [169]. At 42°C, these liposomes released approximately 45% of their contents (Dox) within the first 20 s, compared with only 20% over 1 h for pure DPPC vesicles. This temperature-responsive Dox formulation, in combination with mild hyperthermia, was found to be significantly more effective than free drug or control PEGylated HSPC or DPPC liposomes at reducing the tumor growth in a human squamous cell carcinoma xenograft model (FaDu). In addition to conferring temperature-sensitivity to

liposomes, the lysolipid may further increase the antitumor effect due to its own cytotoxic activity [169]. Celsion Corporation has recently obtained FDA Investigational New Drug (IND) approval for a thermosensitive liposomal Dox formulation used with focused heating. These liposomes, which contain the lysolipid MPPC, are currently under clinical evaluation for patients with deep prostate tumors. Figure 2.13 presents a prototype monopole phased array applicator for human deep tumor heating.

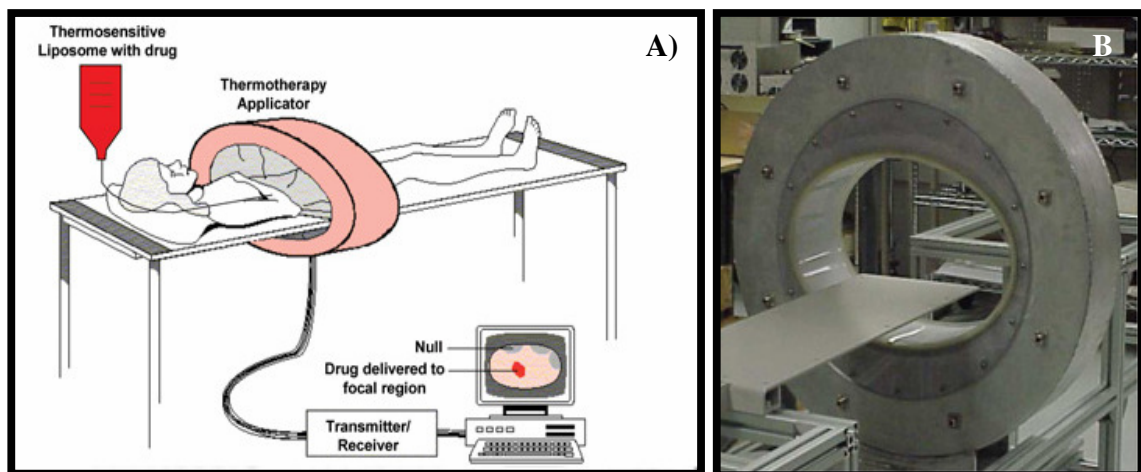


Figure 2.13. Thermodynamic adaptive phased array treatment in which a thermosensitive liposome encapsulating a chemotherapy agent has been infused into the patient's blood stream, and the patient's tumor is subsequently heated to a temperature that triggers release of drug into the tumor (A). Celsion Corporation prototype monopole phased array applicator for deep tumor heating (B). Reprinted with permission from Ref [170], A.J. Fenn, Drug Deliv Technol 2, 74 (2002). Copyright @ Drug Delivery Technology.

Another strategy to obtaining thermosensitive vesicles involves decorating conventional liposomes with a polymer that possesses an LCST [171]. The coil-to-globule phase

transition at the LCST can be exploited as a trigger for liposomal drug delivery. Among thermosensitive polymers, those prepared with NIPAM have been studied most extensively. P(NIPAM) phase separates near 32°C but the LCST can be tailored by incorporating hydrophilic/hydrophobic comonomers [172]. Several reports have shown that liposomes coated with NIPAM copolymers bearing long alkyl anchor chains acquire temperature-responsive properties [173-175]. Kono and coworkers [144] further demonstrated that L_a-DOPE can be stabilized in the lamellar phase with a copolymer of NIPAM and octadecylacrylate (ODA). However, a recent study [176] revealed that EPC may be better suited than DOPE for preparing thermosensitive liposomes as in the latter case, an appreciable amount of drug leakage occurred below the phase transition of the copolymer. To this point, temperature-sensitive liposomes prepared with NIPAM copolymers have not been evaluated in animal models.

2.7.3. pH

Conceptually, pH-sensitive liposomes are stable vehicles at neutral pH and become leaky and/or fusion competent under acidic conditions [177-179]. Vesicles of this type were first proposed as a means of enhancing the release of liposomal cargo in regions of the body where the local pH is reduced below normal due to pathological conditions such as inflammation, infection or malignant transformation [177, 180, 181]. However, the pH of the tumor interstitium rarely declines below pH 6.5 [178], and this makes it technically difficult to engineer liposomes that become disrupted in response to such a minor change in pH. pH-sensitive liposomes have been proposed for the delivery of fragile membrane-impermeable compounds (*i.e.* oligonucleotides, DNA), to the cytoplasmic compartment following uptake by endocytosis [182-184]. Indeed, endocytosed liposomes are eventually delivered to lysosomes where both the carrier and the drug may be degraded by metabolic enzymes (*i.e.* various hydrolases and peptidases), resulting in diminished biological activity.

of the drug [185, 186]. pH-sensitive liposomes have been designed to circumvent drug degradation problems by releasing their contents in the endosomes ($\text{pH} < 6.5$), and at least partly, into the cytosol prior to reaching the lysosomes [187].

Unsaturated PE has been widely employed to confer intrinsic pH-sensitivity to liposomes. At physiological pH in isotonic buffer, the equilibrium phase of unsaturated PE is the inverted hexagonal (H_{II}) phase. Under these conditions, PE is protonated and unable to form bilayer (L_{α}) vesicles [188]. However, the bilayer phase of unsaturated PE can be stabilized by weakly acidic amphiphiles, such as oleic acid (OA) [179, 189], cholesterylhemisuccinate (CHEMS) [149, 190], *N*-succinyl-DOPE [191] or DPSG [192], which confer a negative charge to the headgroup at pH 7.4. This charge provides electrostatic repulsion to block PE intermolecular interaction/interbilayer contact, thus preventing H_{II} phase formation under physiological conditions [193]. Protonation of the amphiphile headgroup, caused by a reduction in pH, neutralizes the negative charge, and the vesicles become destabilized as the PE component reverts to the H_{II} phase. This is generally accompanied by the release of the liposomal contents [194]. Liposomes of this type have been successfully used for the *in vitro* cytoplasmic delivery of antitumor drugs [195], antibiotics [196, 197], protein toxins [198], antigens [199], plasmid DNA [200], antisense oligonucleotides [197] and SiRNA [201]. Some success has also been achieved *in vivo* with pH-sensitive immunoliposomes administered to mice by i.v. injection [202] or the intraperitoneal route [203]. Nevertheless, the moderate plasma stability of PE liposomes, particularly LUV [204], has hampered their clinical use. As for other liposome formulations [111], the inclusion of ganglioside GM₁ [205] or PEG-derivatized lipids [190, 206] in DOPE vesicles was shown to increase the stability and blood residence time of liposomes but significantly decreased the pH-dependent release of their contents.

pH-sensitive vesicles can also be prepared from “caged” lipid derivatives. Acid-induced hydrolysis of specifically engineered chemical bonds results in an increased presence of membrane-destabilizing lipid components in the liposome membrane, and thus enhanced permeability to encapsulated solutes. Thompson and co-workers [188, 207, 208] have used acid-labile PEG conjugated vinyl ether lipids to stabilize DOPE liposomes. Acid-catalyzed hydrolysis of the vinyl ether bond at pH values lower than 5 resulted in removal of the PEG moiety after which the liposomes became fusogenic. Szoka and co-workers [209, 210] have recently shown that long-circulating pH-sensitive liposomes can be produced by combining DOPE with a PEG-diorthoester lipid conjugate, which is cleaved under acidic conditions. The diorthoester attached polymers are completely degraded within 1 h at pH 5, and are reasonably stable at physiological pH.

Another approach utilizes proteins or peptides that exhibit membrane lytic or fusion properties under acidic conditions. Such peptides/proteins are synthesized *de novo* or purified from viruses [178, 211] and bacterial pathogens [199, 212] (Table 2.6). They can be used to render conventional liposomes sensitive to pH or be incorporated into conventional pH-sensitive liposomes to serve as endosomolytic agents. For example, listeriolysin O (LLO) is a pore-forming protein derived from the Gram-positive facultative intracellular bacteria, *Listeria monocytogenes* [213], that has been widely investigated for this purpose. In combination with CHEMS/PE liposomes, LLO has been shown to deliver dyes [212], toxins [214], antigenic proteins [199], antisense oligonucleotides [215] and plasmid DNA [216] to the cytosol. Synthetic and relatively simple peptides such as GALA also display membrane lytic properties at acidic pH. GALA is a 30 amino acid peptide that undergoes a pH-dependent conformational change and induces leakage of contents from liposomes when in a helical conformation [217]. At neutral pH the formation of an α -helix is disfavored due to the electrostatic repulsions between the carboxylic acid moieties of the glutamic acid residues, whereas at pH 5.0 the neutralization of these groups promotes the formation of an amphipathic α -helix and the binding to the lipid bilayer [218, 219]. In the

optimal pH range of 5.0 and below, GALA was shown to induce the leakage of the liposomal contents at very low ratios of membrane-bound peptide per vesicle (from 1/30000 to 1/500) and to induce rapid flip-flop of membrane phospholipids [218-220]. Leakage occurred when a critical number of peptides assembled into a supramolecular aggregate in the bilayer. It was suggested that GALA forms a transbilayer channel composed of 8-12 monomers with a diameter that ranges from 5 to 10 Å [219]. GALA has been grafted to liposomes *via* a Chol anchor and used to increase the cytosolic release of the liposomal content [221]. It has also been complexed to lipoplexes by electrostatic interactions and found to enhance their transfection efficiency [222, 223]. Since the size of the pores caused by GALA is too small to allow the direct passage of DNA, GALA was suggested to not only induce the membrane disruption at low pH but also to promote the unpacking of DNA [223].

Table 2.6. pH-sensitive peptides used to destabilize liposomal membranes.

Peptides	Number of amino acid	Content	References
GALA	30	Plasmid DNA, oligonucleotide, ANTS/DPX, acid blue 9, Ap5A, inulin	[211, 218-220, 224]
EALA	29	Propidium iodide, Texas red dextran, calcein, ara-C	[225, 226]
INF5, INF6, INFA EGLA- I, INF10	19-34	Calcein, plasmid DNA	[227, 228]
JTS1, INF7	20-23	Plasmid DNA, calcein, trypsin inhibitor	[229-231]
HA, E5, K5, E5NN	20	Plasmid DNA	[211, 232-234]
AcE4K	21	ANTS/DPX	[235]

Finally, acid-triggered liposome destabilization/fusion has been achieved extrinsically by employing non-peptidic titratable synthetic polymers, such as poly(alkyl acrylic acid) derivatives [236, 237], succinylated PEG [238, 239], and NIPAM copolymers [240, 241]. The advantage of this approach is that it affords the possibility to render different lipid-based formulations sensitive to pH, without the limitations associated with PE-based liposomes (*i.e.* moderate plasma stability, rapid removal by the MPS) and endosomolytic peptides/proteins (potential immunogenicity [242], high production cost). Complexation of

hydrophobically-modified copolymers of NIPAM and MAA with EPC/Chol liposomes resulted in an enhancement of *in vitro* release of both highly-water soluble markers and amphipathic drugs upon acidification [240, 243, 244]. Such formulations were found to be stable in serum and have preserved pH-sensitivity following contact with serum proteins [245]. Moreover owing to their hydrophilicity under non-destabilizing conditions, NIPAM copolymers were also shown to slightly increase the circulation times of liposomes *in vivo* [81, 101]. Recently, a mixed liposomal formulation containing DSPE-PEG-5000 and the pH-responsive polymer dioctadecylamine(DODA)-P(NIPAM-*co*-MAA) was shown to exhibit both pH-sensitivity and long circulation time [245]. Investigations are currently ongoing to evaluate the efficiency of such formulations in various tumor models.

2.7.4. Enzymes

The exploitation of enzymes that are up-regulated in diseased tissues (*e.g.* tumors) or simply found in endosomes/lysosomes is another interesting strategy for achieving triggered release [246]. Two approaches for the design of lipid conjugates that are activated by enzymes have been investigated [136, 151, 246]. One is based on the cleavage of the lipid conjugate resulting in the generation of fusogenic lipids that will destabilize the liposome. The other involves lipid conjugates acting as masking components that protect other fusogenic lipids within the liposome membrane until enzymatic cleavage removes the conjugate. Putative mechanisms of enzyme activated delivery are presented in Figure 2.14.

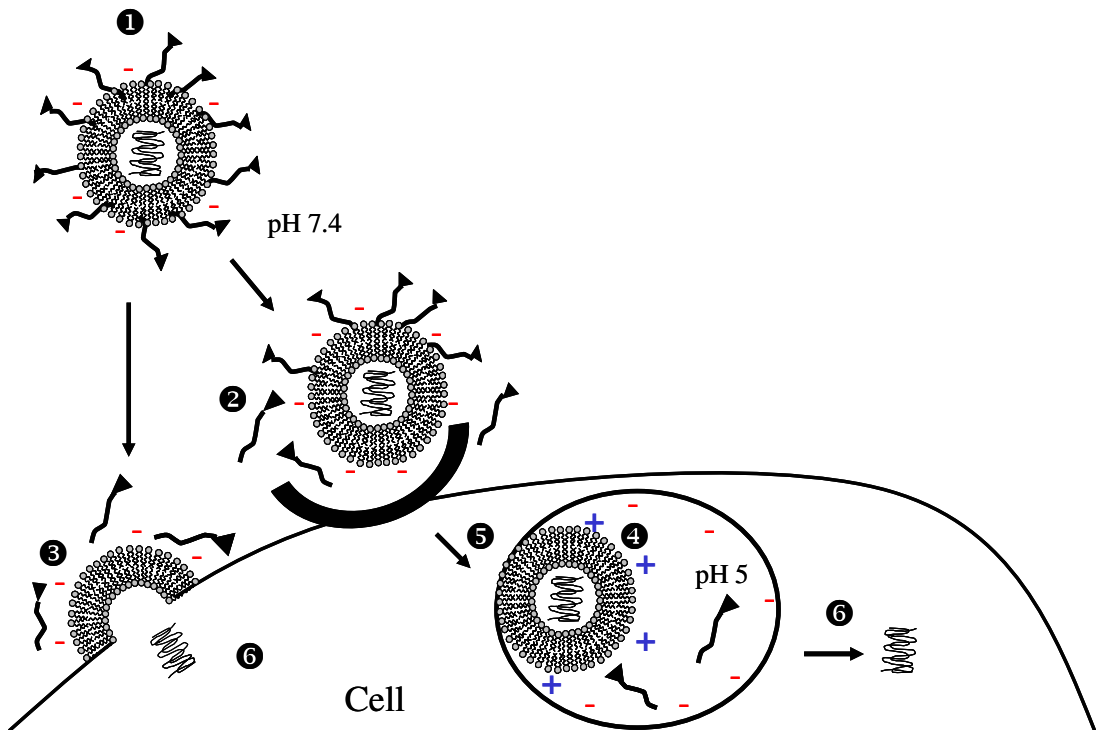


Figure 2.14. Putative mechanisms of enzyme activated delivery. Liposomes may be activated to become fusogenic by enzymes near the surface of the cell, enzymes displayed on the surface of the cell or enzymes in the endolysosomal compartment. Charge reversal and fusogenic delivery can occur at the plasma membrane, within an endosome or *via* later cleavage in the endolysosome. Legend: stable liposome/targeting moiety complex with net negative charge (1); peptide linkers are cleaved by soluble or cell-associated proteases (2); possible direct delivery *via* fusion with plasma membrane (3); liposome becomes positively charged and fusogenic (before or after uptake) (4); uptake by endosome and fusion of liposomal membrane with endosomal membrane (5); release of cargo into cytosol (6). Adapted with permission from Ref. [151], P. Meers, Adv Drug Deliv Rev 53, 265 (2001). Copyright @ Elsevier.

Liposomes that are rapidly degraded by a variety of enzymes, such as elastase [151, 247], sphingomyelinase and phospholipase C [248], PI-specific phospholipase C [249], secretory phospholipase A₂ (sPLA₂) [250, 251] and alkaline phosphatase [150] have been designed. For example, sPLA₂ is an interfacially active enzyme that catalyzes the hydrolysis of the ester-linkage in the *sn*-2 position of glycerophospholipids, producing free fatty acids and lysophospholipids. It is overexpressed in inflammatory and tumor tissue [252, 253] and thus can act as a site-specific trigger for liposomes [250, 251]. A high level of Chol in the membrane was found to inhibit lipid catalysis by sPLA₂ [254], whereas the addition of negatively charged PEG-lipids had an opposite effect [255]. This was attributed to the high activity of sPLA₂ towards negatively-charged surfaces [256]. Alkaline phosphatase is another example that has been used as a trigger for liposomes composed of different Chol phosphate derivatives, and DOPE. This enzyme is found in endosomes and lysosomes, and catalyzes the hydrolysis of phosphate monoesters. By removing the phosphate and its corresponding charge from the bilayer surface, it provokes collapse to the hexagonal phase and release of the liposome content [150].

These examples provide a background of recent developments in the design of triggered-release vesicles. Although such systems can be efficiently tailored to rapidly release their contents once a stimulus is applied, they have, in general, not yet proven highly effective under *in vivo* conditions. A number of issues such as stability upon storage conditions and in plasma, and circulation lifetime remain to be improved for several systems. Furthermore, in the case of physiological triggers, the intersubject variability may lead to unreplicable release patterns which may ultimately affect the efficiency of the liposomes. More fundamental work is therefore required to determine the pathological/physiological conditions where stimuli-responsive liposomes would be most beneficial.

2.8. Medical applications

Liposomes have attracted considerable interest in the medical field as therapeutic and diagnostic tools [257]. Their physiochemical properties, such as composition, size, and stability of the carrier, can easily be tailored depending on the intended application. Liposomes have been used to protect sensitive molecules (*i.e.* cytosine arabinoside, DNA, RNA, antisense oligonucleotides), improve intracellular uptake, and change the pharmacokinetics and biodistribution (temporal and spatial) of the encapsulated drug [258]. The latter accounts for the decreased toxicity of liposomal formulations as the exposure of entrapped drug molecules to healthy organs is reduced.

Liposomes can be formulated as injectable liquid suspensions, aerosols, creams or gels and can thus be administered by several routes, although they are usually given by i.v. injection. Table 2.7 lists liposomal products on the market and in advanced clinical phase development. So far, most of the liposomal formulations that have reached the clinical stage have been developed for cancer chemotherapy [259]. In this section, we will show how drug-loaded liposomes can be used in the treatment of cancer, infections, arthritis, asthma, psoriasis and ophthalmic disorders. In addition, their role as absorption enhancers for poorly bioavailable therapeutics will be discussed.

Table 2.7. Liposome-based products that are on the market or in clinical development as of 2005.

Product (Administration route)	Drug	Target disease	Status in 2005
Gilead Sciences			
Ambisome® (i.v.)	Amp B	Systemic fungal infections; visceral leishmaniasis	On the market since 1990 (Europe), 1997 (USA) 2000 (Canada)
DaunoXome® (i.v.)	Daunorubicin citrate	Advanced Kaposi's sarcoma	On the market since 1996 (USA and Europe)
MiKosome (i.v.)	Amikacin	Serious bacterial infections	Phase I / II
Lohmann Animal Health			
Newcastle disease vaccine® (i.m.) (Novasome®)	Newcastle disease virus (killed)	Newcastle disease (chicken)	On the market (USA)
Avian Rheovirus vaccine® (i.m.) (Novasome®)	Avian Rheovirus (killed)	Vaccination of breeder chickens; Passive protection of chicks against rheovirus infection	On the market (USA)
Novavax Inc.			
<i>E.Coli</i> 0157:H7 vaccine (oral) (Novasome®)	<i>E.Coli</i> 0157 (killed)	<i>E.Coli</i> infection	Phase I
<i>Shigella Flexneri</i> 2A vaccine (oral)	<i>S. Flexneri</i> 2A (killed)	<i>S. Flexneri</i> 2A infection	Phase I
Johnson and Johnson Inc. (Ortho Biotech Products)			
Doxil® / Caelix™ (i.v.)	Dox sulfate	Kaposi's sarcoma (AIDS). Refractory ovarian cancer	On the market since 1995 (USA), 1996 (Europe) and 2003 (Canada)
SPI-077 (i.v.)	Cisplatin	Head and neck squamous cell carcinoma	Phase I / II
Elan Pharmaceuticals Inc.			
Myocet® / Evacet® / TLC-D99 (i.v.)	Dox citrate	Metastatic breast cancer in combination with cyclophosphamide	On the market since 2000 (Europe), NDA filed (USA)
Ventus® / C53 (i.v.)	Prostaglandin E1	Acute respiratory distress syndrome	Phase III
OSI Pharmaceuticals			
OSI-211 (NX211, i.v.)	Lurtotecan	Refractory myeloid leukemias, ovarian cancer, small cell lung cancer	Phase II
OSI-7904L (GS7904L, i.v.)	OSI-7904 (Thymidylate synthase inhibitor)	Gastroesophageal adenocarcinoma, gastric adenocarcinoma	Phase II

Berna Biotech AG			
Epaxal® vaccine (i.m.)	HAV	Hepatitis A	On the market since 1994 (Europe)
Inflexal® V (i.m.)	Haemagglutinin and neuraminidase from H1N1, H3N2 and B strains	Influenza	On the market since 1997 (Switzerland) and 2002 (Europe)
Pevion Biotech Ltd			
PeviPRO™ PEV3A (i.m.)	Synthetic peptide epitopes of <i>Plasmodium falciparum</i>	Malaria	Phase I
Ferndale Laboratories Inc.			
L-M-X4 / ELA-Max® (local)	Lidocaine	Temporary relief of pain and itching	On the market since 1998 (USA)
Inex Pharmaceuticals Inc.			
Marqibo (i.v.)	Vincristine	Non-Hodgkin's lymphoma	Phase III
Aronex Pharmaceuticals Inc.			
Nyotran® (i.v.)	Nystatin	Candidemia	Phase II / III
Liposomal annamycin (i.v.)	Annamycin	Breast cancer	Phase I / II
Antigenics Inc.			
Aroplatin / Platar (i.v.)	Platinum compounds (e.g. cisplatin)	Mesothelioma; colorectal cancer; solid tumors	Phase II
ATRA-IV / Antragen® (i.v.)	All-trans retinoic acid	Acute premyelocytic leukemia; Kaposi's sarcoma	Phase II Phase II / III
SkyePharma Inc.			
DepoCyt® (intrathecal injection.)	Ara-C	Lymphomatous meningitis, neoplastic meningitis	On the market since 1999
Novartis AG			
Visudyne® (i.v.)	Verteporfin	Wet macular degeneration in conjunction with laser treatment	On the market since 2000 (USA) and 2003 (Japan)
AGI Dermatics			
Dimericine® (topical)	Bacterial endonuclease T4N5	Renal transplant Xeroderma pigmentosum	Phase II Phase III
Janssen-Cilag Ltd			
Pevaryl creme® (topical)	Econazole	Fungal infections	On the market since 1988 (Switzerland)
MIKA Pharma GmbH / GiEnne Pharm			
Dolaut® (topical)	Diclofenac	Painful, inflammatory, rheumatic or traumatic complaints in the muscles, joints or tendons	On the market since 1999 (Italy)
Vical Inc.			
Allovectin-7 (intralesional)	HLA-B7 plasmid	Gene therapy of metastatic cancers	Phase II

2.8.1. Cancer

Cancer is a general term used to define any disease characterized by uncontrolled proliferation of abnormal cells. In healthy tissues, cellular growth is a closely regulated process with each cell having a pre-determined life span and with proliferation occurring only to replace cells that have undergone apoptotic death or died as a result of injury. The growth of normal cells is impaired in an environment deprived of nutrients and oxygen. In contrast, cancerous cells will grow indefinitely even under hostile conditions. However, as tumors require the normal building blocks (*i.e.* oxygen, glucose, amino acids) they recruit the formation of blood vessels to provide the nutrients necessary to fuel their continuous expansion [260, 261]. This process is called angiogenesis and often leads to a defective vascular architecture [262]. The leaky tumor vasculature combined with impaired lymphatic drainage is central to what is known as the EPR effect [263].

The treatment of cancer rests mainly on three strategies: surgery, radiation and chemotherapy. The use of the first two is limited to localized solid tumors while for circulating or disseminated tumors, chemotherapy is the only option. Most of the chemotherapeutic agents induce cell death by interfering with the synthesis/reparation of DNA or with cellular mitosis. The anticancer drugs that are commonly used in the clinic include anthracyclines (Dox), *Vinca* alkaloids (vincristine), nucleoside analogues (ara-C), topoisomerase inhibitor (camptothecin-analogs), alkylating agent (cisplatin), and taxanes (paclitaxel, docetaxel). Despite their high potency, the efficacy of chemotherapeutic drugs is often limited by their inability to accumulate in sufficient quantity at their site of action [264]. In most cases, only a small fraction of the administered dose reaches the tumor, while the remaining drug is distributed throughout the body. This unavoidable distribution into healthy organs and tissues combined with a depression in immune function generally limits the total dose that can be given.

Liposomal formulations take advantage of the EPR effect to favour the accumulation of the drug in the tumor, while minimizing its deposition in other tissues. Furthermore, intrinsic properties of cancerous cells, such as the overexpression of surface antigens or receptors can be exploited to improve targeting and/or uptake, as long as the targets are not expressed in significant amounts on healthy cells. Finally, the use of liposomes may also offer suitable pharmacological advantages in the treatment of leukemia by providing sustained drug levels in the blood compartment. In this case, liposomes are not dependent on leaky blood vessels to access the neoplastic cells.

2.8.1.1. Passive targeting

Passive targeting of tumors rests on the ability of a carrier to take advantage of the EPR effect. It is generally assumed that prolonged circulation times leads to enhanced accumulation of liposomes in the extravascular diseased sites where blood vessels exhibit pore sizes varying between 100 to 800 nm [257, 265, 266]. As mentioned above, several factors can influence the biological half-life, such as the size, surface charge, and the lipid composition of the vehicle.

The first liposomes investigated for *in vivo* applications were simple mixtures of Chol and phospholipids. These “conventional” liposomes were rapidly removed from the bloodstream in a dose-dependent manner by the MPS. Indeed, long circulation times achieved at high lipid doses ($>4 \mu\text{mol lipids/kg}$) with these liposomes were attributed to saturation of the MPS [267-270] and/or depletion of plasma opsonins [271, 272]. At such high doses, tumor accumulation was observed in a number of studies [269]. Moreover, the circulation time was also found to depend on the transported cytostatics as their toxic effect on the MPS impairs the liposome clearance [273]. On the other hand, as it was recognized early on that conventional liposomes could naturally target the MPS organs, formulations

for which MPS delivery was desirable (*e.g.* hepatocarcinoma) were among the first to be investigated [274, 275]. However, for most anticancer agents, uptake by the MPS is not desirable because it may compromise its function and thus adversely affect patient outcome [276].

To reduce uptake by the MPS and enhance drug accumulation in cancerous tissues, particles should be ~100 nm or less in diameter and have a hydrophilic surface. It was reported that liposomes coated with PEG display terminal half-lives of 12 to 30 h in animal models and 21 to 54 h in humans and accumulate selectively in a variety of solid tumors (Figure 2.15) [277, 278]. Although steric stabilization clearly increases the circulation lifetimes, its effect on extravasation *per se* is an area of controversy. Wu *et al.* [279] have investigated the influence of PEGylation (2 mol%) on the extravasation of EPC/Chol/TRITC-DHPE liposomes (60:33:5 molar ratio; 100 nm). They showed that the tumor vasculature was twice as permeable to PEGylated liposomes (3.42×10^{-7} cm/s) in comparison to the conventional formulation (1.75×10^{-7} cm/s). It was hypothesized that the stealth liposomes extravasated to a higher degree due to their lower propensity to aggregate and adsorb on the glycocalyx present on the endothelial cell surface. In contrast, several studies [280-282] have demonstrated that PEGylated liposomes extravasate to the same extent as conventional liposomal formulations in solid tumors.

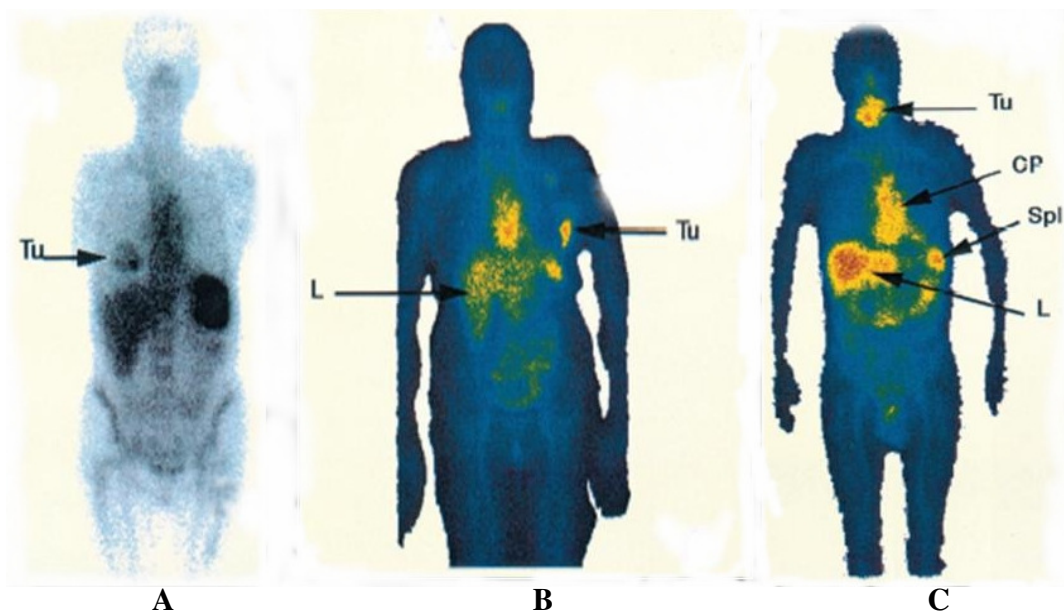


Figure 2.15. Distribution of radiolabeled (^{111}In -DTPA) PEGylated liposomes in patients with lung cancer (A), breast cancer (B) and cancer of the base of the tongue (C). Legend: Tu = Tumor, L = Liver, CP = cardiac blood pool, Spl = Spleen. Reprinted with permission from Ref. [277], K.J. Harrington *et al.*, Clin Cancer Res 7, 243 (2001). Copyright © American Association for Cancer Research.

Following extravasation, non-targeted liposomes remain in the tumoral interstitium [283, 284] where the drug is thought to be released slowly by diffusion or following enzymatic degradation (*i.e.* phospholipases) [278]. Higher interstitial pressure, compared to healthy tissue, limits the distribution of liposomes to the interstitium [285, 286]. Moreover, the formation of clusters after extravasation further impairs the ability of liposomes to circulate freely in the extracellular fluid [284]. Large tumors are more difficult to treat than small ones, in part because of the resulting increase in interstitial pressure, which prevents access of drugs to the necrotic core [285, 287]. Recently, advancements (*i.e.* active

targeting, triggered release) were made in order to reach specific tumor tissues and allow for uniform penetration in cancerous cells [145, 288, 289].

2.8.1.1.1. Anthracyclines

Anthracyclines are natural antibiotics that have been used in the treatment of breast, lung and superficial bladder cancer, and Kaposi's sarcoma (KS). Dox and daunorubicin both belong to this class, with the former being one of the most commonly used anticancer agents. The antineoplastic effect of anthracyclines stems from their ability to damage DNA by intercalating between strands, and generating free radicals. Anthracyclines also prevent DNA reparation by inhibiting topoisomerase II which is critical to DNA function. Several side effects have been associated with anthracyclines including myelosuppression, gastrotoxicity and dose-limiting cardiotoxicity, all of which were shown to be minimized by encapsulation in liposomes [290].

Liposomal Dox has been examined extensively in a variety of tumor models, including human lung [291], human ovarian [292], rat brain [293], mouse colon [17, 283], mouse breast tumor [294, 295], and mouse lymphoma [296]. In many of these models liposomes have shown enhanced antitumor efficacy compared to the free drug, independent of the location of the tumor. Huang *et al.* [283] reported a 48.3% increase in life span when Dox was administered in small (88 nm) PEGylated liposomes (DSPC/Chol/DL- α -tocopherol/DSPE-PEG-2000, 56.1:38.2:0.2:5.5 molar ratio) vs only a 5.1% increase for animals receiving treatment with conventional liposomes and a 4.2% decrease for treatment with free drug given as a single dose at 10 mg/kg to BALB/C mice bearing C26 colon tumor. After 48 h, the stealth liposomes accumulated 2.5-times more in the tumor while the levels detected in the liver and spleen were half of those obtained for the non-PEGylated liposomes [283]. Similar success was achieved in mammary carcinoma-bearing

mice [294]. The PEGylated formulations were also substantially more effective in reducing the incidence of metastases.

Liposome encapsulated anthracyclines have had the greatest clinical impact to date. Three liposomal formulations are now commercially available (Table 2.7). They differ in their primary target, size, lipid composition, the presence or absence of PEG and the active drug encapsulated (Table 2.8). Two of the liposomal formulations are commercially available in the USA, Europe, Canada and Japan for the treatment of AIDS-related KS.

Table 2.8. Key characteristics of liposomal anthracyclines. Reprinted with permission from Ref. [297], T. M. Allen and F. J. Martin, Semin Oncol 31, 5 (2004). Copyright @ Elsevier.

Characteristic	Doxil®	DaunoXome®	Myocet®
MPS Relationship	Avoiding	Avoiding	Targeting
Diameter	80 to 100 nm	45 nm	150 to 180 nm
Lipid composition (molar ratio)	HSPC, Chol, DSPE-PEG-2000 (56.2: 38.3: 5.3)	DSPC, Chol (2 :1)	EPC, Chol (55:45)
PEGylated	Yes	No	No
Active drug	Dox HCl	Daunorubicin citrate	Dox citrate
Administration	Liquid suspension to be diluted in 250 mL of 5% dextrose before administration	Liquid suspension to be diluted 1:1 with 5% dextrose before administration	3-vial kit. Drug loaded into liposomes (requires 30 to 40 min) in pharmacy just before administration
Half-life	50 to 80 h	2 to 4 h	10 to 15 min
Safety vs conventional anthracycline	Reduced GI toxicity, cardiotoxicity, and alopecia. Slight reduction in bone marrow toxicity. Hand-foot syndrome and stomatitis are dose-limiting.	Reduced cardiotoxicity, alopecia. Myelosuppression is dose limiting.	Reduced GI toxicity and cardiotoxicity. Slight reduction in alopecia. Myelosuppression is dose limiting.
Approved indications	USA and Canada: second-line treatment of advanced HIV-associated KS, advanced ovarian carcinoma refractory to paclitaxel and platinum. Europe and Canada: also approved as monotherapy for metastatic breast cancer	First-line therapy for advanced HIV-associated KS	Not approved in USA. Approved in Europe for metastatic breast cancer in combination with cyclophosphamide.

Myocet[®] (formerly known as TLCD-99 and Evacet[®]) is an MPS-targeting liposomal formulation of Dox citrate in moderately sized liposomes (150-180 nm) composed of EPC/Chol (molar ratio of 55:45). In 2000, it was approved in Europe for the treatment of metastatic breast cancer in combination with cyclophosphamide. Entrapment of Dox in such liposomes significantly alters its pharmacokinetics. The encapsulated drug has a higher AUC (20-fold), a lower clearance (9-fold) and lower volume of distribution (25-fold) [298]. It has been estimated that at least 85% of the circulating Dox in patients is encapsulated in liposomes. Myocet[®] liposomes are rapidly removed from the circulation by the MPS. In this case, it is the slow release of Dox from the liposomes that is exploited to reduce cardiotoxicity and improves the drug's therapeutic index [290]. Myocet[®] was, however, found to be equally effective as the free drug in terms of antitumoral activity in humans (*i.e.* metastatic breast cancer) [299].

Doxil[®] was the first liposomal anticancer drug formulation approved by the FDA and has been on the market since 1995. It has been shown to be effective against a number of solid tumor types, such as KS [300], ovarian cancer [301] and metastatic breast cancer [302]. To date, Doxil[®] is approved as a second-line treatment for advanced HIV-associated KS and is also indicated for paclitaxel and platinum refractory advanced ovarian carcinoma. It is composed of Dox entrapped in HSPC/Chol/DSPE-PEG-2000 SUV (80-100 nm). The drug is encapsulated into preformed liposomes as an insoluble salt using the ammonium-sulphate-gradient technique (Figure 2.9) [303]. Most of the drug is present as a crystalline-like precipitate, lacking osmotic effects and thus contributing to the stability of the entrapment. This loading technology provides great stability with negligible drug leakage in the circulation, while still enabling satisfactory rates of drug release in tissues and malignant effusions.

The Doxil[®] liposomes were shown to circulate for prolonged periods of time in the bloodstream (up to several days). Their stability is due to both their PEG-coated surface

(5.3 mol%) and their mechanically stable bilayer [304-306]. At doses between 10 and 80 mg/m² injected in humans and animals, the pharmacokinetic profile showed two distribution phases: an initial phase with a half-life of 1-3 h and a second phase with a half-life of 30–90 h. After a dose of 50 mg/m², the AUC was approximately 300-fold greater than that for the free drug. Clearance and volume of distribution were drastically reduced by at least 250- and 60-fold, respectively [261, 278, 307]. Tumor concentrations were also reported to be significantly higher for the liposomal formulation than free Dox (between 5- and 11-fold), which translated into increased antitumoral activity in AIDS patients with KS [300]. Due to its long circulation time, Doxil® is generally administered i.v. once every 4 weeks for patients with ovarian cancer, and once every 3 weeks for patients with AIDS-related KS. These altered pharmacokinetic and biodistribution patterns result in reduced cardiotoxicity and myelotoxicity [278, 307]. However, the Doxil® formulation also displayed “new” toxicities, the most noticeable being the palmar-plantar erythrodysesthesia known as hand-foot syndrome. This syndrome is due to the fact that the liposomes get stuck in the small capillaries of the palms and soles, giving rise to high local Dox concentrations [308]. In patients with KS, practically all subjects displayed a considerable decrease in modularity of skin lesions while total flattening was observed in 25% of the cases. At a dose of 20 mg/m² injected i.v. every 14 days for 6 cycles, the liposomal Dox was shown to be more effective and less toxic than the standard combination chemotherapy regimen Dox (20 mg/m²), bleomycin (10 mg/m²), and vincristine (1 mg)) for treatment of AIDS-KS. The high efficacy was due to the approximately 10-fold higher drug concentration in lesions as compared to the free drug [300]. Another randomized study in patients with metastatic breast cancer showed comparable efficacy yet reduced risk of cumulative-dose cardiotoxicity for Doxil® 50 mg/m² every 4 weeks compared with conventional Dox 60 mg/m² every 3 weeks [309].

DaunoXome[®] was approved in 1996 by the FDA for treatment of HIV-related KS. It consists of daunorubicin-loaded SUV (45 nm) composed of DSPC/Chol (2:1 molar ratio). Although they are not PEGylated, these liposomes are relatively stable in the circulation (half-life between 2 and 4 h). This may be attributed to several factors including their small size, neutral surface charge and rigid membrane, all of which limit interactions with plasma components [306]. A comparison of the plasma levels in patients who were administered similar doses of daunorubicin either as free drug or in liposomes demonstrated that the peak concentration and mean AUC were respectively 100- and 36-fold higher for DaunoXome[®] [310]. DaunoXome[®] was shown to be as effective as conventional therapies, with reduced drug toxicity and improved quality-of-life scores for the patients with KS [311]. For patients with AIDS-related KS, the recommended doses are 40 mg/m² every 2 weeks compared with Doxil[®] 20 mg/m² every 3 weeks. Because it is administered more frequently, the cost to achieve a clinical response is more than that for Doxil[®] (26,483\$ and 11,976\$, respectively) [312].

2.8.1.1.2. *Vinca alkaloids*

Vincristine is a dimeric Catharanthus alkaloid with indications for lymphomas, lung cancer, leukemia, and breast cancer [313]. It acts by binding to tubulin and blocking metaphase in actively dividing cells. As for other chemotherapeutic agents, its use is also associated with dose-limiting toxicity, mainly peripheral neuropathy. Liposomes have been shown to enhance the efficacy of vincristine while slightly decreasing its toxicity [314, 315]. Vincristine has been encapsulated into liposomes by several techniques, including passive loading, pH gradient loading, and ionophore-assisted loading (for review see reference [316]). Boman *et al.* [314] reported that for drugs such as vincristine, optimizing the payout rate is crucial to achieving maximum efficacy. If the drug leaks out of the vesicles too rapidly, high tumoral drug levels may not be reached. On the other hand, if the

drug is released very slowly, it will get to the tumor but the levels of free drug may not reach therapeutic concentrations. For liposomes loaded by the pH gradient technique, the internal pH was shown to control the vincristine efflux rate and ultimately the drug's efficacy. For instance, decreasing the internal pH of LUV (DSPC/Chol, 55:45 molar ratio) from 4 to 2, prevented the leakage of vincristine in serum for 24 h (*vs* ~55% at internal pH 4) and increased the life-span of mice inoculated with P388 lymphocytic leukemia from 36 to more than 60 days [314].

The stability of liposomal vincristine was also found to depend strongly on the composition of the bilayer. The substitution of DSPC for SM [315] resulted in a significant reduction in leakage rates both *in vitro* and *in vivo*. This was explained by a decrease in susceptibility to hydrolysis caused by the acidic interior of the liposomes. Indeed, the aliphatic chain of SM is amide-linked and therefore more resistant to degradation than the ester-linked fatty acids that are typical constituents of PCs. Moreover, SM is able to form strong intermolecular hydrogen bonds with neighbouring Chol molecules to provide a very rigid membrane that is relatively impermeable compared with other lipid compositions [317]. An *in vivo* study reported that 72 h following i.v. injection into mice, 25% of the loaded vincristine remained entrapped in circulating SM/Chol liposomes compared with only 5% for the DSPC/Chol liposomes [315]. The improved retention properties of this formulation resulted in 7-fold higher plasma vincristine levels, and increased deposition in peritoneal ascitic murine P388 and subcutaneous A431 human tumors. The SM liposomes achieved more than 50% cures in the P388 model, a result that could not be achieved with the DSPC formulation [315]. Similarly, in the A431 xenograft model, these liposomes delayed the time required for 100% increase in tumor mass to more than 40 days, compared with 5, 7 and 14 days for mice receiving no treatment, free vincristine or DSPC/Chol formulations, respectively [315]. The addition of DSPE-PEG-2000 further increased liposome circulation longevity but at the same time caused a significant increase in the vincristine leakage rate, which resulted in no improvement in terms of vincristine

accumulation at the tumoral site and no therapeutic benefit. Liposomal vincristine, Marqibo® (Inex Pharmaceuticals Inc.), has recently completed human clinical trials for the treatment of relapsed lymphoma [318]. These results prompted Inex Pharmaceutical Corporation to file for accelerated New Drug Application (NDA) approbation. However, as the clinical benefits remain unclear, further studies are required before this formulation can reach the market. Besides relapsed non-Hodgkin's lymphoma, Marqibo® has also shown promising anti-tumor activity in phases IIa/IIb clinical trials involving patients with Hodgkin's disease and pediatric malignancies.

2.8.1.1.3. Other anticancer drugs

Ara-C is an effective chemotherapeutic agent for the treatment of acute myelogenous and lymphocytic leukaemias. This S-phase-specific drug is a nucleoside analogue of deoxycytidine in which the ribose sugar has been replaced with an arabinose sugar [319]. It has a half-life of about 20 min in mice and humans due to rapid inactivation by cytidine deaminases [320, 321]. Ara-C has been encapsulated into liposomes to protect it from premature degradation and to provide sustained drug levels in the blood compartment [322-324]. While conventional liposomes generally displayed better efficacy than the free drug in several models [322, 324, 325], the optimal results have been obtained with stealth formulations [323]. Apart from providing increased efficiency, long-circulating liposomes can also simplify the dosage regimen. Indeed, treatment of L1210/C2 leukemia mice with bolus i.v. injection of 50 mg/kg ara-C loaded into HSPC/Chol/DSPE-PEG (2:1:0.1 molar ratio, 190-220 nm) REV was shown to be equivalent to a 24 h infusion of 100 mg/kg free drug in terms of prolonging the mean survival time. As discussed previously for vincristine, the release rate was identified as an important parameter for therapeutic efficacy of liposomal ara-C [323].

Lurtotecan, a semi-synthetic water-soluble analog of camptothecin, represents another anticancer agent for which liposomal delivery is a rational response to address the inherent pharmacological limitations (*i.e.* rapid hydrolysis in biological fluids, high toxicity and adverse gastrointestinal (GI) effects) associated with this agent. It has been formulated in small HSPC/Chol liposomes (2:1 molar ratio, 100 nm, OSI-211, OSI Pharmaceuticals) and is currently being evaluated in humans for the treatment of refractory myeloid leukemia [326] and ovarian cancer [327]. Relative to free lurtotecan (1 mg/kg), OSI-211 exhibits a prolonged plasma half-life, a 1,500-fold increase in the plasma AUC, a 40-fold increase in tumoral distribution in nude mice and, in single-dose efficacy studies a 3-fold or greater increase in therapeutic index [328]. Similar pharmacokinetic patterns have been observed in rats [328]. In humans, the disposition half-life of liposomal lurtotecan is approximately 5 to 6 h and the volume of distribution of lurtotecan averages 3.92 to 4.43 L/m², suggesting that distribution takes place mainly within the central compartment [329]. OSI-211 administered on days 1 and 8 of a 3-week schedule showed modest activity in resistant ovarian cancer (phase II) [327].

Since the first studies evaluating liposomal cytostatics in the early 80's [330, 331], knowledge on their optimal use and limitations has increased dramatically. Despite the fact that liposomes do not necessarily improve the therapeutic efficacy of anticancer drugs in the clinic, they have definitely found a niche in chemotherapy. Their unique physico-chemical and pharmacokinetic properties have been shown to impact the drug's stability, the mode of administration and, most evidently, the toxicity profile. Clinical trials conducted to date have not identified a clear survival advantage for liposomal Dox over the use of free Dox. However, the lower incidence of side-effects greatly improves the quality of life of the cancer patients [311]. Within the next decade, liposome formulations are likely to evolve and improve by providing better control of drug release at the tumoral sites, optimized combination approaches, delivery of more efficient cytostatics and enhanced target selectivity.

2.8.1.2. By-passing of P-glycoprotein

Multidrug resistance (MDR) is a significant obstacle to the successful treatment of many human malignancies by chemotherapy, affecting as many as 50% of all cancer patients [332]. It is characterized by the resistance of tumor cells to a broad range of structurally and functionally unrelated drugs. One very common and well-characterized mediator of MDR is the plasma membrane protein P-glycoprotein (PGP) that acts by pumping anticancer drugs out of tumor cells in an ATP-dependent process [332]. Numerous methods relying on liposomal technology have attempted to block or by-pass PGP in order to circumvent MDR and improve the antitumor activity of cytostatics. This has first been done by using liposomes prepared with lipids capable of modulating PGP. A second approach consists of incorporating PGP drugs in the lipid bilayer of liposomes that are administered separately from the cytostatics. An additional strategy involves entrapment of the PGP inhibitor with the anticancer agent in the vesicle. Finally, another way to bypass the MDR is to use immunoliposomes for which the receptor of the antibody is internalized upon ligand-receptor interaction [333].

Liposomes composed of certain acidic phospholipid-based systems, such as PS [334] or cardiolipin [335] have been shown to increase the cytotoxicity of encapsulated or complexed anticancer drugs against resistant cells. MDR reversal by these phospholipids has been related to increased intracellular drug accumulation as well as to a direct PGP blocking effect. Liposomes can either compete with free drugs for binding to PGP, or modify its structure, resulting in inhibition of drug efflux [336, 337]. Unfortunately, these PGP modulating lipids are readily recognized by phagocytic cells of the MPS. Indeed, liposomes containing these lipids are cleared within minutes from the circulation [338].

Several hydrophobic compounds already approved for human use, such as verapamil [339] and cyclosporine A [340], have been shown to effectively block PGP in tumor cells

in vitro and restore their sensitivity to anticancer agents. However, when administered in the free form, they display significant toxicities at doses required to achieve PGP blocking. To reduce their toxicities, these MDR reversing agents have been entrapped within liposomes. However, after i.v. administration, it was found that they migrated to the lipoproteins and, to a lesser extent, the erythrocytes thereby compromising their efficacy [340].

Second-generation agents, such as the cyclosporin derivative PSC 833 (Valspodar®, Novartis Pharmaceuticals Corp), have alleviated many of the problems (*i.e.* high doses required, inherent toxicity, lipoprotein exchange) experienced with first-generation MDR modulators. Despite their better tolerability, when co-administered they were found to cause significant alterations in the pharmacokinetics and biodistribution of anticancer drugs and narrow their safety margin [341]. Also, drug interaction with PSC 833 may create the need for a dose reduction which in return can decrease the tumor exposure to the cytostatic. For example, Krishna *et al.* reported that MDR human breast carcinoma was unaffected by combinations of PSC 833 and free Dox. In contrast, the MDR tumors regressed and were kept in remission for weeks when PSC 833 was co-encapsulated with Dox in DSPC/Chol/DSPE-PEG liposomes [342]. Confocal fluorescence microscopy of fresh solid tumor specimens revealed an accumulation of the liposomal cytostatic in the MDR tumor. The accumulation was significantly greater for PEGylated formulations compared to non-PEGylated liposomes. These findings indicate that the combination of liposomal Dox with PSC 833 allows for elevated tumor exposure to the anticancer drug in conjunction with PGP inhibition.

2.8.1.3. Tumor cells targeting

The newest generation of liposomes under development feature direct molecular targeting of cancer cells via antibody or other ligand-mediated interactions. These systems

are dependent on interactions with targets found specifically on the surface of cancerous cells, and not on the surface of healthy cells. One type of ligand includes monoclonal antibodies (MAb), which were first shown to bind to specific tumor antigens in 1975 [343]. A number of cancer treatments using MAb have since been approved by the FDA [344]. While antibodies have proven to be therapeutic agents in their own right, they can serve as pilot molecules for drug delivery systems.

Tumor targeting agents can be attached to the liposome phospholipid headgroup or to the distal end of a PEG derivative that is anchored in the bilayer (Figure 2.6). The latter approach has proven to be most successful due to better accessibility of the antibody to its target [345, 346]. Five main conjugation procedures are generally used to couple ligands to liposomes (Figure 2.16) [347-352]: (A) reaction between maleimide derivatives and thiols, yielding thioether bonds; (B) conjugation between pyridyldithiols and thiols, producing disulphide bridges; (C) reaction between activated carboxyl groups and amines, yielding an amide bond; (D) reaction between the carbohydrate moiety of the antibody and hydrazide groups to form a hydrazide bond (D); and (E) crosslinking between 2 primary amine groups.

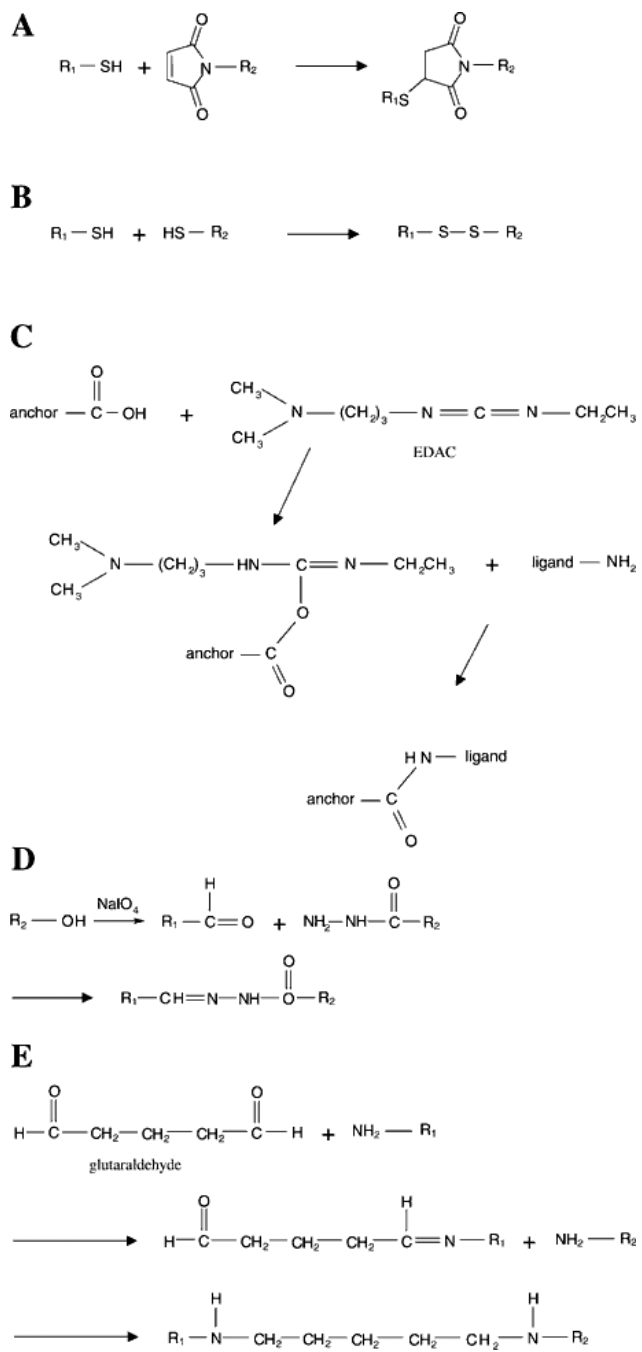


Figure 2.16. Schematic diagram of the different coupling methods used. Reaction between maleimide and thiol functions (A), formation of a disulfide bond (B), reaction between

carboxylic acid and primary amine group (C), reaction between hydrazide and aldehyde functions (D), crosslinking between two primary amine groups (E). Legend: EDAC = 1-ethyl-3-[3-dimethylaminopropyl]carbodiimide hydrochloride. Reprinted with permission from Ref. [351], L. Nobs *et al.*, J Pharm Sci 93, 1980 (2004). Copyright © Wiley-Liss, Inc. a subsidiary of John Wiley & Sons, Inc.

In active targeting, the amount of antibody at the vesicle surface should be sufficient to achieve adequate binding but not too high as enhanced recognition by the MPS must be avoided [346, 353, 354]. An optimal coating ratio of 10-30 antibody molecules per liposome was shown to provide optimal delivery of drugs to tumors, with limited increase in MPS uptake [346, 354]. Liposomes can be targeted to surface molecules expressed either in the vascular or extravascular systems on tumor cell membranes, as well as on circulating abnormal cells. Numerous studies, both *in vitro* and *in vivo*, have been performed using targeted liposomes. The tumoral antigens for MAb that have mostly been investigated include the CD19, CD33, CD34 receptors, and the human EGF receptor 2 (HER-2) (Table 2.9).

Table 2.9. Selected list of ligands (antibodies) and receptors tested as liposome-targeting agents.

Ligand/receptor	Targeting moiety	Target cell / tissue	References
CD19	Complete MAb	Non-Hodgkin's lymphoma and other B-cell lymphoproliferative diseases	[355, 356, 357, 358, 359]
HER-2	Complete MAb, Fab' and scFv	Breast carcinoma cells	[353, 360-363]
CD34	Complete MAb	Hematopoietic progenitors	[364, 365]
CD33	Complete MAb	Myeloid leukemia cells	[366, 367]
CD25	Complete MAb	T-cell lymphoma, Hodgkin's lymphoma	[368]
CD20	Complete MAb	Non-Hodgkin's lymphoma and other B-cell lymphoproliferative diseases	[359]
CD105	scFv	Solid tumors (prostate, breast cancer and melanoma)	[369]
Human carinoembryonic antigen	Complete MAb and Fab'	Colorectal, small-cell lung and ovarian cancers	[370, 371]
Human β_1 -integrin	Fab'	Non-small cell lung carcinoma	[372, 373]
GD ₂	Complete MAb and Fab'	Neuroblastoma	[374, 375]
Anti-MUC1	Complete MAb	Breast and bladder cancers	[376]

The surface of circulating cells such as lymphocytes represents a readily accessible target site for immunoliposomes [346]. For example, the CD19 receptor is a potentially interesting antigen for treating multiple myeloma as it is overexpressed on malignant B cells. When bound by specific MAbs this receptor has been implicated in a number of signaling functions such as control of cell differentiation, and cell cycle arrest or apoptosis [377]. Lopes de Menezes *et al.* [355, 356] have used PEGylated immunoliposomes to target CD19 on B lymphoma (Namalwa) cells both *in vitro* and *in vivo*. It was shown that the targeted liposomes were internalized by endocytosis and could deliver Dox to the nucleus. The binding specificity was also confirmed with CD19⁺ B-cells originating from the blood of a multiple myeloma patient. Interestingly, SCID mice inoculated with CD19⁺ human B-lymphoma cells treated with Dox encapsulated in pH-sensitive immunoliposomes (DOPE/CHEMS/DSPE-S-S-mPEG-2000 [anti-CD19], 6:4:0.24:0.06 molar ratio, 120 nm) had a significantly increased life span when compared to control mice treated with non-pH-sensitive immunoliposomes and non-targeted pH-sensitive liposomes (mean survival times of 53.8, 43.2 and 25.8 days, respectively) [357]. The efficacy of the targeted pH-sensitive formulation was superior to that of non-pH sensitive vesicles despite faster drug leakage and increased clearance. These findings could be explained by the rapid release in endosomal or lysosomal compartments following receptor-mediated internalization of the pH-sensitive immunoliposomes.

Among various antigens found on malignant cells, glycoprotein p185^{HER-2}, a member of the EGFR family of receptor tyrosine kinases encoded by the HER-2/neu (c-erbB-2) proto-oncogene, is another attractive target for chemotherapy. This protein is overexpressed in various cancers, including breast, lung, and ovarian carcinomas [378, 379]. The humanized monoclonal antibody HER-2 (Trastuzumab, Herceptin®, Genentech Inc.), which can induce antitumor responses as a single agent, has demonstrated clinical benefit in the treatment of advanced breast cancer [380]. However, this antibody is more efficacious when combined with chemotherapy [381]. Anti-HER-2 liposomes have been mainly constructed by

covalent conjugation of recombinant MAb fragments (Fab' and scFv) either to the vesicle bilayer [360] or to the termini of PEG chains anchored to the liposome [361]. The use of antibody fragments was reported to reduce immunogenicity and liposome clearance [382, 383]. Immunoliposomes bearing Fab'-fragments targeting HER-2 were shown to be effectively endocytosed into SKBR-3 cells *in vitro* [361]. The number of Fab' molecules per liposome (POPC/Chol, 3:2 with 0.6-5.7 mol% of DSPE-PEG-2000, 70-100 nm) that was found to be optimal for cell binding was 40 while for internalization, a plateau was reached at 10-15 Fab' molecules per liposome [361]. The uptake of such immunoliposomes by HER-2-overexpressing SKBR-3 cells in culture reached a concentration of 7.21 ± 0.45 nmol phospholipid/mg cell protein, which is equivalent to 23,000 immunoliposomes per cell [361]. Since each immunoliposome can accommodate 10^4 drug molecules, extremely efficient delivery can be achieved using this approach.

The efficacy of anti-HER-2 liposomes loaded with Dox was evaluated in a series of HER-2-overexpressing xenografts, including one lung and four breast cancer models. Park and co-workers [353, 362] have compared liposomes with both Fab'-fragments and single chain fragments, ScFv, against the p185^{HER-2} epitope, and found that both conjugates had a similar effect. This approach is also highly specific, with total uptake being more than 700-fold greater in HER-2-overexpressing cells than in non-overexpressing cells. A Doxil®-based formulation bearing a recombinant fully human scFv F5 anti HER-2 is presently in clinical trials (NSC 701315). In animal studies, Dox-loaded anti-HER-2 liposomes have been shown to be more efficient than free Dox, non targeted liposomal Dox or the HER-2 antibody treatment, Trastuzumab [363].

While MAb are frequently used for site-specific delivery, they display a number of shortcomings such as high production costs, potential immunogenicity, and low long-term stability. Accordingly, several low molecular weight ligands including vitamins [384], hormones [385] and peptides [386-388] are receiving increased interest as homing devices

for liposomes. Folic acid is a vitamin that is essential for the biosynthesis of nucleotides. It is consumed in elevated quantities by proliferating cells and it is transported across the plasma membrane using either the membrane-associated reduced folate carrier or the folate receptor (FR). The family of human FR consists of 3 well-characterized isoforms (α , β , and γ) that are quasi identical in amino acid sequence, but distinct in their expression patterns. While FR- β and FR- γ are expressed only at very low levels, FR- α is often overexpressed in malignant tissues of epithelial origin (*e.g.* ovary, uterus, endometrium, brain, kidney, head and neck, mesothelium) [389]. Folate is non-allergenic, inexpensive, stable, intrinsically non-toxic to cells, and internalized following its binding to the FR, making it a suitable molecule for drug targeting applications. There is currently no evidence that FR-targeted macromolecular therapeutics damage normal tissues with elevated levels of FR expression (*i.e.* kidneys, brain) [389]. However, it has been suggested that *in vivo* the binding of folate-coated carriers may compete with intrinsic free folate, thereby impairing the targeting efficiency [390]. The therapeutic potential of folate-targeted liposomes was initially demonstrated by encapsulating Dox in PEGylated liposomes (DSPC/Chol/folate-DSPE-PEG, 58.3:41.6:0.1 molar ratio) [384]. Uptake of folate-liposomal Dox by KB cells was found to be 45- and 1.6-times higher than that of the non-targeted liposomal formulation and free Dox, respectively, while the cytotoxicity was 86- and 2.7-times higher, respectively [384]. Targeting liposomes to the FR has also been investigated for a number of other liposome encapsulated compounds, such as antisense oligonucleotides [391], photodynamic drugs [392], and boronated agents (*e.g.* polyamines) [393, 394]. In the latter case, the folate-coated vesicles did not significantly enhance overall tumor localization in mice but improved boron delivery at the cellular and subcellular levels.

2.8.1.4. Tumor vasculature targeting

Novel strategies to target tumor-vasculature have recently emerged with great interest as a means to improve cancer treatment. The best illustration that can be given to date is

the recent approval by the FDA of the anti-VEGF monoclonal antibody AvastinTM (Bevacizumab) as the first-line treatment for metastatic colorectal cancer.

A liposomal system that targets tumor vasculature has recently been described by Pastorino *et al.* [388]. This system consists of an NGR (Asn-Gly-Arg) peptide-coated PEGylated liposome containing Dox (NGR-SL[Dox]). Contrary to the vast majority of targeted liposomal systems developed as anticancer products bearing ligand recognizing tumor cell receptors, the antitumor activity of NGR-SL[Dox] is based on the specific destruction of the tumor vasculature leading to the starvation, apoptosis, and necrosis of the tumor. Its mechanism of action involves the specific binding of its NGR motif containing ligand to a CD13 (or aminopeptidase N) isoform overexpressed in the tumor endothelium [395].

There are several existing isoforms of CD13 having differences in glycosylation [396]. Although the CD13 antigen is widely distributed in the body, only one isoform is the receptor for the specific NGR peptide that has been found exclusively in angiogenic vessels. This peptide motif has been identified by phage display [397]. Therefore, NGR-SL[Dox] can potentially be employed in all adult cancer patients having no other angiogenesis related disorders. In an orthotopic human neuroblastoma model in mice, solid tumor and associated metastasis regression in kidney and liver has been associated with a drastic destruction of the tumor vasculature upon treatment with NGR-SL[Dox]. These observations were concomitant with long-term survival.

Biodistribution studies revealed the significant accumulation of NGR-SL[Dox] only in tumor tissue and the organs of the MPS. Importantly, the presence of the CD13 isoform in surgical specimens of cancer patients has been evidenced so far in renal carcinoma, primary breast cancer and associated metastases, malignant glioma, prostate metastases in bone, and lymph node metastases from multiple tumor types [398]. This suggests that a wide variety

of cancers may be successfully treated with NGR-SL[Dox]. A dual mechanism for the mode of action of this system has been proposed that combines indirect tumor cell kill via the destruction of tumor endothelium (active targeting) with direct tumor cell kill via localization of liposomal Dox to the interstitial space (passive targeting). The rationale for this dual mechanism of action is illustrated in Figure 2.17.

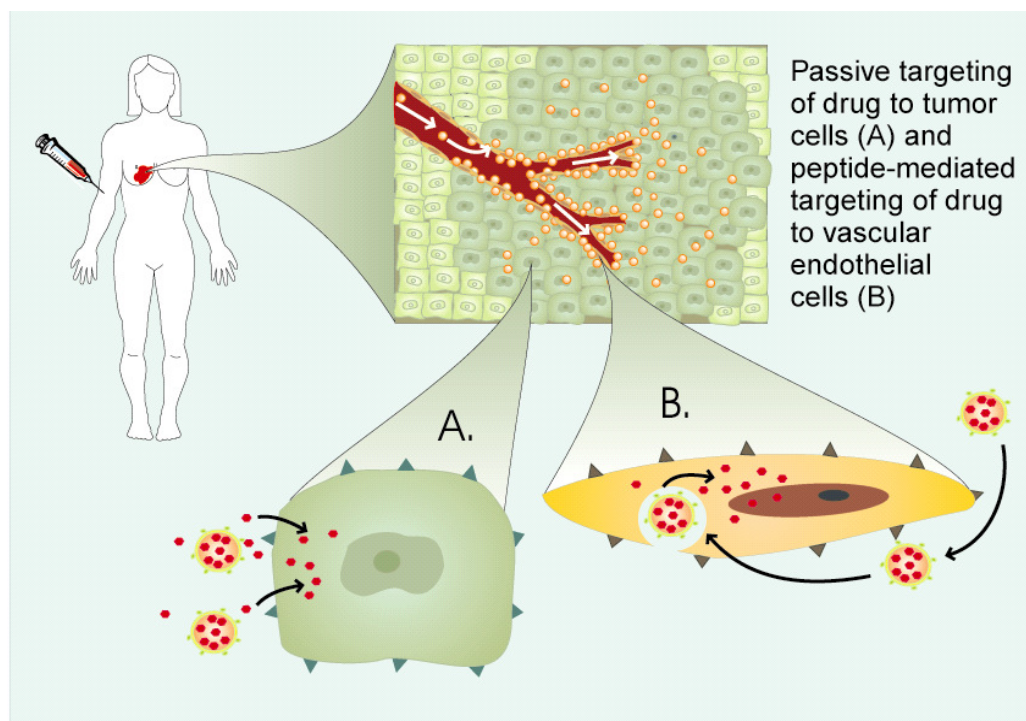


Figure 2.17. Dual mechanism of action for liposomal drugs against solid tumors *via* use of peptides that are specific for targeting tumor vasculature. Reprinted with permission from Ref. [258], T. M. Allen and P. R. Cullis, Science 303, 1818 (2004). Copyright @ American Association for the Advancement of Science.

A similar system having a novel angiogenesis-targeted peptide APRPG (Ala-Pro-Arg-Pro-Gly) attached to the surface of PEGylated liposomes has been reported by Maeda *et al.* [399]. Although this targeted liposomal system accumulated more significantly in subcutaneous colon 26 NL-17 carcinoma, than the corresponding PEGylated liposomes lacking the 5-mer peptide, the difference in the extent of accumulation was only modest. Treatment in mice bearing these tumors with APRPG-modified liposomal Dox was found to be superior to treatment with PEGylated liposomes lacking the ligand [400].

The same liposomal system has been used to deliver the photosensitizer benzoporphyrin derivative monoacid ring A (BPD-MA) to achieve successful Meth-A sarcoma growth suppression after photodynamic therapy (PDT) [401]. Despite the lack of differential accumulation between targeted and non-targeted liposomes 3 h post-injection, laser irradiation at this time resulted in a significant suppression in tumor growth. Also, the prolonged animal survival observed for treatment with the targeted liposomal formulation correlated well with vascular damage, whereas the combination of non-targeted liposomal BPD-MA and laser irradiation had little or no antitumor effect.

Antitumor efficacy with tumor vascular-targeted liposomal Dox has also been achieved using a cyclic RGD (Arg-Gly-Asp) peptide in a murine C26 colon carcinoma model which is a Dox-insensitive tumor [387]. RGD motif containing peptides bind to $\alpha v\beta 3$ integrins present at the surface of endothelial cells. In this case, the accumulation of the targeted and non-targeted liposomes in tumors was identical. Specific *in vivo* binding of RGD-liposomes with the endothelium was evidenced by intravital microscopy.

2.8.2. Infectious diseases

Conventional liposomes are largely taken up by phagocytic cells after i.v. administration, and thus represent ideal vehicles for passive drug targeting to macrophages as these cells are often hosts for parasites, fungi, virus and bacteria. For example, leishmaniasis is a parasitic infection of macrophages caused by the hemoflagellate protozoan causing a spectrum of clinical syndromes ranging from cutaneous ulcerations to systemic infections [300, 402]. Moreover, encapsulation of antimicrobial agents into long-circulating liposomes can alter their pharmacokinetic and biodistribution profiles and hence increase their therapeutic index. This section will provide a brief overview of the recent developments in liposomal antimicrobial therapy but will be restricted to the parenteral route.

2.8.2.1. Parenteral antifungals

Many antifungals including, amp B [403-405], nystatin [405, 406], hamycin [407, 408], ketoconazole and miconazole [408, 409] have been encapsulated into liposomal vehicles. Amp B was one of the first drugs considered for formulation in liposomes due to its unique physiochemical properties, and high affinity for biological membranes [410]. It interacts with ergosterol in the plasma membrane, causing membrane disruption, increased permeability, leakage of vital intracellular constituents, and eventual cell death. Amp B is highly hydrophobic and is commonly administered i.v. in a deoxycholate micelle formulation. This commercial preparation (Fungizone[®]) is associated with severe neuro- and nephrotoxicity, limiting the dose that can be injected [411]. In some cases, the severity of its side-effects (*i.e.* headache, chills, fever, severe hemolytic anemia and acute nephritis) necessitates interruption of treatment. The anticipated benefits of a liposomal carrier for

Amp B were confirmed by early studies with DMPC/DMPG MLV (0.5-6.0 μm). In animal models and pilot clinical trials, this formulation appeared to increase the safety of Amp B, while being active against systemic fungal infections [412, 413]. Another liposomal SUV formulation of Amp B (EPC/Chol/stearylamine) was subsequently shown to be well tolerated in cancer patients with fungal infections [414]. While neither of these formulations progressed to commercial development, they served as a basis for formulation optimization and led to the development of effective lipid antifungal products that are currently available on the market.

Three different lipid-based Amp B products, Abelcet[®], Amphotec[®], and AmBisome[®] have been introduced on the market over the past 2 decades (Table 2.10) [415]. Abelcet[®] is comprised of DMPC, DMPG and Amp B in the form of ribbon-like structures with a diameter of about 2-11 μm . Amphotec[®] is a Chol sulfate complex that forms disk-like structures of about 75-170 nm in diameter whereas Ambisome[®] is a true liposomal system (HSPC/DSPG/Chol) with a particle size of 45-80 nm [416]. HSPC and DSPG were chosen to enhance the stability and rigidity of the Ambisome[®] formulation. The direct interaction of Amp B with Chol *via* its sterol binding region and charge interaction between the amino group of the Amp B and phosphate groups of DSPG further stabilizes the formulation. In order to maintain a “true” liposomal structure, the content of Amp B is kept at about 12% by weight, which is substantially lower than the other Amp B lipid systems (Table 2.10). AmBisome[®] is sold as a lyophilized preparation with a shelf-life of more than one year [416].

Table 2.10. Characteristics of therapeutic marketed amp B products administered in humans [403, 404, 417].

Description	Fungizone®	Abelcet®	Amphotec®	Ambisome®
Company	Bristol-Myers Squibb Company	Enzon Inc.	Johnson and Johnson Inc.	Gilead Pharmaceuticals Inc.
Type	Detergent micelle complex	Ribbon-like complex	Disc-shaped complex	Unilamellar liposome
Size (nm)	<25	200-11 000	120	45-80
Composition	Deoxycholic acid	DMPC/DMPG	Chol sulfate	HSPC/Chol/DSPG
Amp B (weight %)	36	50	65	12.5
Dose (mg/kg/day)	1	5	5	5
Maximum concentration (µg/mL)	2.9	1.7	3.1	83
AUC (mg x h/L)	36	14	43	555
Volume of distribution (L/kg)	1.1	131	4.3	0.11
Clearance (mL/h/kg)	28	436	121	11

In the early 1990s, three studies [418-420] demonstrated the safety and efficacy of AmBisome®. These trials showed that Amp B could be administered over 1 h compared to 4–6 h with control formulations. Liposomal Amp B resulted in fewer infusion-related reactions (*e.g.* chills, rigors, bone pain) and pre-medication with corticosteroids or analgesics was also reduced. Similar results from early phase studies were obtained with

the other lipid-associated, non-liposomal products, Abelcet® [421] and Amphotec® [422]. However, AmBisome® has a plasma pharmacokinetic profile that is different from the lipid complex formulations [417, 423-425]. While Abelcet® and Amphotec® are rapidly cleared, AmBisome® remains in the plasma compartment for an extended period ($t_{1/2} = 6-10$ h in humans and animals). Although it is cleared more slowly, AmBisome®, still accumulates primarily in MPS-associated tissues [424]. The results obtained from pre-clinical and clinical trials of AmBisome® have recently been thoroughly reviewed elsewhere [403, 404].

AmBisome® is an effective alternative to conventional Amp B in the management of immunocompromised patients with proven or suspected fungal infections. Because of its improved tolerability profile compared with Fungizone®, it should be preferred for patients with pre-existing renal dysfunction. AmBisome® may also be considered for first- or second-line treatment of immunocompetent patients with visceral leishmaniasis [403]. It is approved in the USA and Canada for treatment of visceral leishmaniasis and also for the treatment of systemic or disseminated infections due to *Candida*, *Aspergillus*, or *Cryptococcus* in patients who are refractory or intolerant to conventional Amp B therapy, or suffer from renal impairment.

The main disadvantage of AmBisome® is its high cost compared to the micellar formulation. A cost-effectiveness analysis [426] suggested that savings associated with the reduced toxicity and improved efficacy of the liposomal formulation in immunocompromised adults were not enough to offset its high acquisition cost. This study was confirmed by another analysis [427] that revealed that conventional Amp B (*i.e.* Fungizone®) as a first-line strategy in adults with invasive fungal infection has the lowest expected cost per-complete-cure after 15 days (\$13,674) compared with \$15,509 and \$20,024 for doses of 1 and 3 mg/kg/day of AmBisome®, respectively. This is mainly a result of the much lower acquisition cost of Fungizone® (\$8.03/day) vs. AmBisome® at 1 (\$314/day) and 3 mg/kg/day (\$944/day).

2.8.2.2. Parenteral antibiotics and antivirals

Several antibiotics have been encapsulated into liposomes [428] in order to improve their pharmacokinetic pattern [429], interactions with pathogens [430] and/or reduce their toxicity [431]. Moreover, by accumulating in macrophage-rich tissues liposomes can improve the intracellular delivery of drugs to cells that are hosts for pathogens such as *Mycobacterium tuberculosis* [428]. Gilead Sciences Inc. have developed MiKasome®, a SUV formulation (HSPC/Chol/DSPG) of the aminoglycoside, amikacin. The lipid:drug ratio is 5:1 (*w/w*), with more than 85% of the amikacin encapsulated in the liposomes. After i.v. injection, this formulation substantially increased the amikacin plasmatic AUC and half-life compared with the free drug in rats [429], mice [432], rhesus monkeys [433], and humans [434]. MiKasome® has been found to exhibit increased antibacterial activity in several models, including intracellular and extracellular infections [435, 436]. In a case report, liposomal amikacin was shown to be well tolerated in a patient treated for advanced pulmonary-multidrug resistant tuberculosis and accumulated significantly in the sputum [434]. This formulation is currently in clinical phase (I/II) for the treatment of acute bacterial infections in patients with cystic fibrosis.

As discussed in Section 2.6, liposomes that have a gel-phase bilayer and/or that are sterically shielded are those demonstrating the highest stability *in vivo*. However, high stability may not always be required especially when the drug has to be delivered in high concentrations inside the bacterial cell (*e.g.* drug resistant bacteria). Indeed, sterically stabilized liposomes with gel-state bilayers have generally low bactericidal activity against extracellular bacteria *in vitro* [437]. To eradicate extracellular bacteria that do not reside in macrophages, Lagacé and co-workers [438, 439] developed liposomes that are claimed to increase the penetration of antibiotics in the pathogen by a fusion mechanism [430]. The

liposomes are negatively-charged (DPPC/DMPG, 400 nm) and present a low T_c ($<37^{\circ}\text{C}$). These liposomes can deliver antibiotics efficiently against a variety of extracellular bacteria, both *in vitro* [440] and *in vivo* [439]. They were shown to enter inside *Pseudomonas aeruginosa* [440], a bacteria which possesses one of the most efficient permeability barriers to antibiotics. The main limitation of these vesicles is that they need to be administered directly to the infected site as the relatively large liposome size and absence of steric shielding makes them prone to rapid removal following systemic administration.

Besides antibiotics, liposomes have also been investigated for delivery of a variety of antivirals such as indinavir [441, 442], ribavirin [443], and antisense oligonucleotides [444, 445]. Encapsulation of the anti-HIV agent 2',3'-dideoxyinosine (ddI) into liposomes greatly reduced its systemic clearance and side effects in mice [446] and rats [447, 448], while allowing efficient targeting of macrophage-rich tissue following i.v. administration. However, the plasma half-life of the entrapped drug (3.5 h) was much lower than that of the PEGylated liposomes (14.5 h), indicating a release of the antiviral agent in the blood compartment [448]. A key factor to reduce viral burden in HIV reservoirs resides in the use of more selective systems. Immunoliposomes targeting specific epitopes such as the HLA-DR determinant of the major histocompatibility complex class II (MHC-II) could represent a strategic approach to achieve higher levels of drugs within HIV-1 infected cells present in lymphoid tissues. Anti-HLA-DR immunoliposomes were shown to be very efficient in delivering the antiviral indinavir to lymphoid tissues for at least 15 days post-injection, increasing by up to 126 times the drug accumulation in lymph nodes of mice, as compared to the free drug. *In vitro*, immunoliposomal indinavir was as efficient as the free drug at inhibiting HIV-1 replication in cultured cells. In the same study, the authors demonstrated that liposomes bearing Fab' fragments were 2.3-fold less immunogenic than liposomes bearing the entire IgG [441]. To the best of our knowledge, so far no *in vivo* study has been conducted to assess the efficacy of these liposomes in animal models.

2.8.3. Rheumatoid arthritis

Rheumatoid arthritis (RA) is one of the most common chronic autoimmune diseases along with multiple sclerosis, type I diabetes and Crohn's disease. It is characterized by an infiltration of the affected articulations by blood-derived cells, mainly neutrophils, macrophages and dendritic cells. In response to activation, these cells are responsible for the generation of cytokine and reactive oxygen species (ROS) [449], which are released in vast amounts into the surrounding tissue. The resulting oxidative stress can induce destruction of the affected joint constituents, such as synovial fluid, articular cartilage, lipids and subchondral bone if the endogenous antioxidant defense system is overcome [450, 451].

Although the number of drugs used in the treatment of RA has increased over the past 10–20 years, there is still need for more effective drugs with reduced side-effects [450]. This arthritic disease is characterized by increased vascular permeability to circulating colloids, making liposomal therapy potentially useful. Moreover, since the phagocytes involved in the inflammatory response can take up colloidal particles, they represent selective targets for liposomal drugs. Basically, four main classes of anti-arthritic compounds (*i.e.* glucocorticoids, folic acid antagonists, bisphosphonates, and antioxoydant enzymes) have been encapsulated in liposomes and tested *in vivo*.

2.8.3.1. Corticosteroids

Corticosteroids are among the most effective anti-inflammatory drugs, and are frequently used in the treatment of RA. They strongly reduce the production and release of pro-inflammatory cytokines and cartilage degrading enzymes by macrophages in arthritic joints [452]. High and frequent dosing is necessary to achieve sufficient activity in the

joints, due to poor drug localization at the target site as a result of efficient clearance [453]. As early as 1978, Dingle *et al.* [454] reported in *Nature* that the intra-articular injection of 35.5 µg liposomal cortisol palmitate (DPPC/egg yolk phosphatidic acid) to arthritic rabbits resulted in a significant reduction in joint temperature and diameter, whereas an equivalent amount of cortisol acetate particles in suspension or empty liposomes had no effect. The anti-inflammatory activity of the suspended free drug was seen at much higher doses (equivalent to 0.2-2.0 mg of cortisol) and was restricted to a 24 h period, while the liposome formulation provided a sustained (3-5 days) reduction in inflammation. Although these preliminary findings were promising, the fact that the drug was injected intra-articularly limited the clinical value of the system. Indeed, only systemic administration ensures simultaneous access to all diseased joints. Long-circulating PEGylated liposomes (90-100 nm) were indeed found to be efficient in delivering the corticosteroid, prednisolone phosphate, to inflamed joints and in improving its therapeutic activity compared with the free drug in arthritic rat [455] (Figure 2.18) and mouse models [456]. Histochemical evaluation revealed that the liposomes accumulated in the synovial lining of diseased joints [456]. This study suggests that PEGylated liposomes administered i.v. can effectively target joints, and exert an anti-inflammatory effect.

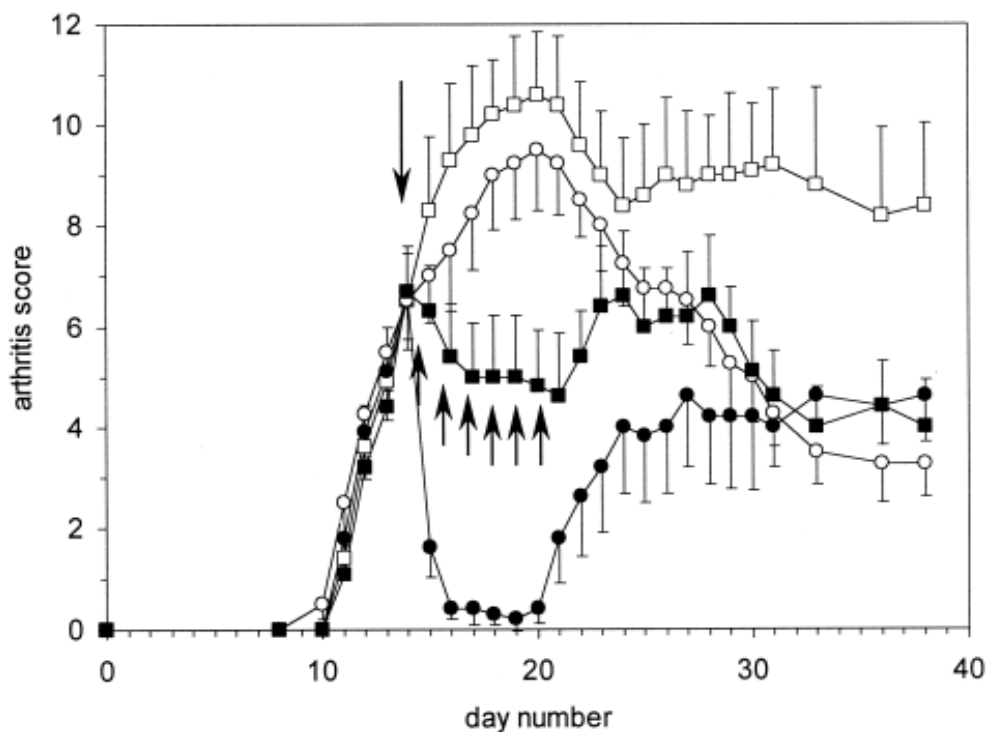


Figure 2.18. Therapeutic activity of a single injection of 10 mg/kg prednisolone phosphate encapsulated into PEGylated liposomes (solid circles) compared with 7 daily injections of 10 mg/kg free prednisolone phosphate (solid squares) into rats with adjuvant-induced arthritis. Control treatments were empty PEG liposomes (open circles) and saline (open squares). Bars show the mean and SEM of 5 rats. Arrows indicate times of treatment. Reprinted with permission from Ref. [455], J.M. Metselaar *et al.*, Arthritis Rheum 48, 2059 (2003). Copyright @ Wiley-Liss, Inc. a subsidiary of John Wiley & Sons, Inc.

2.8.3.2. Folic acid antagonists

Methotrexate (MTX) is a folic acid antagonist with antineoplastic and anti-inflammatory activity. MTX acts by suppressing T cell activation, decreasing adhesion molecule expression, inducing apoptosis, and reducing cytokine production in the joints of patients with RA [457]. As a cytotoxic drug, it may slowdown the rapid growth of cells in the synovial membrane that lines the joints. MTX is increasingly regarded as the first-line agent in the treatment of RA because of its early onset of action and superior efficacy and tolerability [458]. However, the systemic use of this drug is associated with a number of side effects, notably hepatotoxicity and hemocytopenia [458] that could be alleviated by the incorporation of MTX in liposomes [459]. It has been reported, however, that considerable MTX leakage from liposomes occurs upon *in vivo* administration [460]. To achieve maximum drug loading and joint retention Williams *et al.* [460, 461] synthesised a phospholipid conjugate of methotrexate (MTX- γ -DMPE) which was incorporated into POPC/Chol MLVs (1.2 μ m) or SUVs (100 nm). After intra-articular injection into rats, this formulation generated significantly less haematopoietic toxicity than free MTX [460, 462], while providing an enhanced and sustained therapeutic effect [461]. Indeed, a greater reduction in knee swelling (26.5%) was obtained in arthritic rats 1 day after dosing with MTX-MLV compared with MTX-SUV (14.4%) and free MTX (3.5%). The anti-inflammatory activity of the MLV *vs* SUV was attributed to a better drug retention within the joint space [461].

2.8.3.3. Bisphosphonates

Bisphosphonates are another class of drugs that have been encapsulated in liposomes for the treatment of RA. They are commonly used to manage skeletal diseases because of their capacity to prevent bone resorption [463]. Bisphosphonates also have anti-

inflammatory properties in experimental arthritis and reduce the production of several pro-inflammatory mediators *in vitro* [464, 465]. Liposomes have proven to be effective carriers of bisphosphonates to macrophages *in vitro* [466, 467]. Van Lent *et al.* [468] demonstrated in experimental arthritic mice that intra-articular administration of clodronate (dichloromethylene bisphosphonate) entrapped in MLV selectively depleted the synovial lining macrophages, which resulted in a marked decrease in joint inflammation. Before the onset of the disease, this intervention prevented arthritis, arthritic flares, cartilage destruction and moderated ongoing chronic arthritis [468, 469]. The immunohistological and potential toxic effects of the liposome encapsulated clodronate were examined in an open study involving 6 arthritic patients [470]. After a single intra-articular administration, it was shown that liposomal clodronate produced macrophage depletion, and decreased expression of adhesion molecules in the synovial lining. The system was well tolerated, and its therapeutic potential is currently under investigation.

2.8.3.4. Antioxydant enzymes

Recently, there has been growing interest in the antioxidant enzyme superoxide dismutase (SOD) for RA therapy. SOD is a cytoplasmic enzyme with anti-inflammatory properties that dismutases the superoxide radical in molecular oxygen and hydrogen peroxide, which helps protect cells against the toxic byproducts of aerobic metabolism. Controlled delivery of SOD is highly desired, since following its bolus i.v. injection into humans, the enzyme is rapidly eliminated from the circulation *via* the kidneys, with a plasma half-life of 6 min [471]. In addition, the cellular penetration of SOD is slow due to its high molecular weight. Early work by Michelson and Puget [472, 473] evaluated cationic MLV as a means to promote cellular uptake of SOD and increase its biological half-life *in vivo*. However, such liposomes were found to be ineffective in patients showing mild symptoms of RA, probably due to an inadequate deposition in the affected joints [471, 474]. More recently, SOD encapsulated in small (110 nm) sterically-stabilized liposomes

was compared to a cationic liposomal formulation in rats [475]. This study established the superiority of the long-circulating liposomes over the cationic ones for targeting of SOD to inflamed sites and for the anti-inflammatory effect [476, 477]. However, as the encapsulation efficiency of SOD in liposomes is poor (c.a. 7%) and enzyme activity is difficult to preserve over time, optimization of the dosage form is still required to make such a system clinically viable [476].

The encapsulation of anti-inflammatory agents in liposomes has been shown in several animal models to increase their activity in rheumatic disease when administered either parenterally or intra-articularly. Liposomes can provide sustained drug levels in the joint and/or improve the targeting efficiency provided that their systemic circulation time is sufficient. However, retention of colloidal drugs in the synovial space may be more difficult to achieve than in tumoral tissues because the lymphatic drainage is not impaired by the arthritic disease [478]. While large vesicles exhibit better retention and depot properties, their use is limited to direct injection in the joint. Indeed, their systemic administration generally results in rapid clearance from the bloodstream by the MPS. Recent success with small PEGylated liposomes seems to indicate that the systemic administration of these vehicles for treatment of arthritis is a feasible approach that is worthy of further investigation.

2.8.4. Pulmonary route and treatment of respiratory disorders

Compared to conventional aerosol formulations, liposomes exhibit several features that make them attractive for the delivery of drugs through the tracheobronchial pathway [479]. They can act as pulmonary sustained release reservoirs, facilitate intracellular delivery of drugs especially to alveolar macrophages and reduce local toxicity. However, administering liposomes *via* the pulmonary route can be a relatively complex approach due to the

characteristic anatomy and physiology of the respiratory tract. Some of these aspects are briefly discussed below.

2.8.4.1. Anatomy and physiology of lungs

The pulmonary route is particularly well suited for systemic delivery of therapeutic agents due to the fact that the lungs exhibit a large absorptive surface area (up to 100 m^2) with an extremely thin air-blood barrier ($0.1\text{-}0.2\text{ }\mu\text{m}$), a good blood supply, relatively low metabolic activity (vs. oral route) and no hepatic first-pass metabolism [479, 480]. The delivery of drugs directly to the lungs for a local effect is also associated with a number of advantages, such as a lower dose to produce a pharmacological effect, less systemic side-effects and a rapid onset of action. Moreover, this route of administration may avoid the stability problem associated with i.v. injection, where liposomes may release their cargo in the blood before reaching the target site. There are, however, some shortcomings associated with this route such as access to the alveolar region, difficulties with proper use of the delivery devices, potential oropharyngeal deposition that may result in local side-effects and leakage of the encapsulated drug upon nebulization [480, 481].

Size is a critical property influencing the deposition site for inhaled particles in the lungs. Generally the liposome size is very small, it is the aerosol droplet size that determines the pulmonary deposition [482, 483]. Three mechanisms of aerosol kinetics govern the majority of particle deposition within the respiratory tract [484]. Inertial impaction is the principal mechanism for large particles from a few microns to greater than $100\text{ }\mu\text{m}$. Sedimentation is another important mechanism of deposition. Every particle allowed to fall in air will accelerate to a terminal settling velocity where the force of gravity is balanced by the resistance of the air through which the particle is falling. Factors that may increase particle deposition by sedimentation are particle density, size and airflow.

Particle deposition by diffusion or Brownian motion predominates for smaller particles (<5 µm) and occurs predominantly in the periphery of the lung (respiratory bronchiole and alveolus). This mechanism is responsible for deposition of only a tiny percentage of particles. For a therapeutic aerosol, it should generally not exceed 5 µm in order to penetrate into the tracheobronchial tree and smaller airways. Some other pharmaceutical factors affecting aerosol deposition are the charge, density, aerodynamic diameter and shape of particles, as well as the surface chemistry and elastic properties of both the particles and lung surface [480]. In general, 14-20% of the inhaled aerosol mass containing liposomes reaches the alveolated areas of the lung in healthy humans [485, 486].

Once deposited, particles are retained in the respiratory tract for varying times depending on their chemical properties, their location within the lung, and the clearance mechanism involved. The structures with which the particle interacts at the site of deposition include the surfactant film at the air-liquid interface and different kinds of cells (*i.e.* macrophages, lymphocytes, granulocytes, epithelial and dendritic cells) [487, 488]. Pulmonary surfactant, the major component being DPPC, stabilizes the gas exchange region of the lung by reducing the surface tension at the air-liquid interface of the alveoli [489]. Inhaled liposomes are probably eliminated by the same pathways as that for pulmonary surfactants, including bidirectional flux across the alveolar epithelium, ingestion by macrophages, associations with mucus and propulsion up to the airways *via* mucociliary pathway, and lymphatic clearance from the interstitial spaces [488, 490]. Barker *et al.* [491] evaluated the pulmonary deposition and clearance of nebulized liposomes (DPPC/Chol, aerosol droplets < 5 µm) containing ^{99m}Tc-diethylenetriamine-pentaacetate (^{99m}Tc-DTPA) in humans. At 5 h post-inhalation, 58.5% of the liposome entrapped radioactivity remained in the lungs compared to 16.8% for the control solution of free ^{99m}Tc-DTPA. Interestingly, as much as 44.7% of liposomal ^{99m}Tc was still residing in the lung after 24 h.

2.8.4.2. Treatment of asthma

One of the major advantages of liposomes over other colloidal drug carriers for lung delivery is that they can be prepared entirely from endogenous materials (*e.g.* DPPC). A number of lung pathologies including cancer [492], infections [493], cystic fibrosis [494], and asthma [495, 496] have been shown to respond to aerosolized liposomal drugs. Asthma is the most common chronic illness in childhood. The diseased airway is characterized by vascular leakage, mucus hypersecretion, epithelial shedding, and extensive narrowing of the airway [497]. Corticosteroids are among the most commonly used drugs to manage asthma [498]. However, the need for daily administration of inhaled steroids may lead to poor compliance and treatment failure. In addition, corticosteroids have a short half-life and are relatively toxic at high doses [499]. Doses above 1.5 mg/day have been associated with marked adrenalin suppression, a significant reduction in bone density, and an increase in the risk of posterior subcapsular cataracts [499, 500].

Liposomal corticosteroids have been shown to exhibit fewer adverse events and to prolong the effect of drugs by preventing rapid clearance in the lungs [501]. It was reported that the encapsulation of beclomethasone provided prolonged release and limited redistribution to other tissues [485, 486, 491]. The tolerability and safety of liposomal aerosols have been tested in animals as well as in humans without any reported side-effects [485, 502]. A clinical trial was conducted in healthy volunteers using ^{99m}Tc-labelled-beclomethasone-DLPC liposome aerosols (droplets of 1-3 µm) [486]. Inhaled liposomes were cleared slowly; 56-70% of inhaled radioactivity was still present in the lung after 6 h, whereas free ^{99m}Tc was eliminated from the lungs within minutes. However, when administered to mild and severe asthmatic patients [503], the deposition and clearance of the liposomal formulation changed. DLPC aerosol particles were deposited more centrally in the lungs of patients with severe asthma than those with the mild form of the disease. Due to the more peripheral penetration of inhaled liposomes in patients with mild asthma,

the clearance of the DLPC liposomes proved to be slower in the mild than in the severe asthmatic group. Indeed, in patients with mild asthma, a greater portion of the inhaled liposomal aerosol penetrated into the alveolar region, where removal of the particles by absorption and phagocytosis of the macrophages is markedly slower [503]. Finally, it was recently demonstrated in asthmatic patients that over a 4 month treatment period, the deposition and clearance pattern of beclomethasone-DLPC liposomes did not change as observed by lung scintigraphy [496]. The efficacy of this liposomal formulation in the treatment of asthma now remains to be established.

The efficiency of another aerosolized liposomal corticosteroid, budesonide, was assessed recently in mice [495]. A weekly administration of budesonide in PEGylated MLV resulted in a significant reduction in the total lung inflammation score, peripheral blood eosinophil counts, total serum IgE level, and airway hyperreactivity in a mouse model of asthma. In this specific study, PEGylated liposomes were preferred since conventional vesicles were shown to elicit a non-specific inflammatory reaction. Moreover, liposomal budesonide given once a week reduced inflammation as effectively as once-a-day dosing of the free drug. From these findings, it is clear that liposomal anti-asthmatic drugs display a clear advantage in terms of retention and sustained effect at the disease site, while apparently not increasing their side-effects [486, 501, 503].

2.8.4.3. Pulmonary route for systemic drug delivery

The respiratory tract represents a convenient non-invasive route of administration for therapeutics not only in the treatment of local pulmonary diseases, but also for systemic drug delivery. The pulmonary route has been shown to be efficient for the absorption of fragile macromolecules such as proteins and peptides [487, 504].

Insulin (5.7 g/mol) has been the most studied peptide for pulmonary delivery with liposomes. The addition of exogenous phospholipids such as DPPC, may accelerate the surfactant turnover process (*i.e.* clearance and recycling) in the alveolar cells, leading to enhanced absorption of insulin that is incorporated in liposomes [488, 505]. Entrapment of insulin into DPPC/Chol liposomes has been shown to induce hypoglycemia in rats, following intratracheal administration [505]. The effect was size independent (0.1-1.98 μm) [506] but was influenced by liposome composition (acyl chain length and charge) and concentration. The overall hypoglycemic response could be linearly correlated with the lipid concentration for both the neutral and charged liposome-insulin preparations tested. The strongest response was observed with the positively charged liposomes followed by negatively charged and neutral liposomes. Toxicological studies indicated that the charged vesicles caused a disruption of pulmonary epithelial cells, precluding the use of such formulations in humans [506]. The cumulative hypoglycemic response was inversely correlated with the acyl chain length of the phospholipid with an optimal effect obtained with medium acyl-chain lipid (C10). An effective absorption of insulin was achieved for liposomes in the liquid-crystalline state.

In conclusion, the administration of liposomes by inhalation has emerged in recent years as a feasible and promising approach for the treatment of pulmonary diseases and systemic delivery of drugs. Due to their natural compositions, liposomes are favoured over other drug carriers. While the safety of a few liposomal components is well established, it is unknown for many others. Cationic lipids have been found to induce oxygen radical-mediated pulmonary toxicity [507]. It is important to point out that PC is the only excipient currently approved by the FDA for lung delivery, so there is a long regulatory road ahead before some of the more sophisticated polymeric and targeted carriers are used in clinical practice. As most applications are presently aimed at treating chronic diseases, there is a

need to conduct more extensive toxicological studies to assess the impact of liposomal components on the pulmonary tissue during chronic use.

2.8.5. Topical and transdermal drug delivery

Administration of drugs to or through the skin offers several advantages compared to the oral or parenteral routes. When a localized treatment is sought, it allows application of high and sustained levels of drug to the skin. In case of systemic delivery, hepatic first-pass metabolism is avoided while typical peak-trough plasma-profiles associated with frequent dosage regimens can be eliminated [508]. To date, relatively few drugs are commercially available as transdermal formulations. The major limitation lies in the barrier function of the skin, which is relatively impermeable to most exogenous substances. Human skin is, on average, 0.5 mm thick (ranging from 0.05 to 2 mm) and is composed of four main layers: the stratum corneum (SC), viable epidermis, dermis and hypodermis. The fact that the skin is a very efficient biological barrier is mainly due to the outermost part of the epidermis, the SC. More than 90% of all cells in the SC are corneocytes which are tightly packed [509]. Individual corneocytes are merged together with desmosomes and sealed tightly with inter-cellular lipids [509, 510]. In addition, the skin contains hydrophilic pathways having pores with diameters that are estimated to range from 0.3 nm to approximately 40 nm [511, 512]. In general, polar molecules have particular difficulty overcoming the skin barrier, whose resistance decreases quasi-exponentially with the octanol-water partition coefficient of the molecule. Even lipophilic molecules, only diffuse through the skin if they are relatively small in size (< 400 g/mol).

Topical formulations should, in principle, provide a sufficient increase in drug penetration into the skin, without inducing significant irreversible alterations to the function of the skin barrier. To increase drug transport across the skin, penetration enhancers and

different physical methods (*e.g.* electrophoresis, iontophoresis, and sonophoresis) have been used. Penetration enhancers such as ethanol, dimethylsulphoxide, and propylene glycol, act by fluidizing cutaneous lipids [513, 514]. However, these products often have toxic or irritant effects (*i.e.* skin dryness and lipid loss), and can eventually increase drug absorption to an extent where systemic side effects occur. As phospholipids contain polar headgroups, they can enhance transepidermal water loss by disrupting interlipid hydrogen bonding [515]. Thus, their use may represent a safer alternative to promoting the transport of molecules across the skin. Mezei and Gulasekharam pioneered research in cutaneous delivery of drugs with liposomal formulations in the 1980s [516-518]. In their early publications, they reported that liposomes applied to rabbit skin favoured the deposition of drugs in the epidermis and dermis, while reducing the amount of drug found in peripheral organs. As topical delivery systems, liposomes offer a number of potential advantages [519]. These include (1) enhanced penetration through the SC, especially for vesicles with compositions similar to that of the epidermis; (2) decreased systemic absorption; and (3) depot effect. Although it is generally accepted that liposomes can increase drug transport across the skin, many questions arise about their mechanism of action.

2.8.5.1. Interaction of liposomes with skin

The mechanism of SC-liposome interaction is not entirely clear yet, although many investigations have been performed using several techniques such as TEM [520], freeze fracture electron microscopy (FFEM) [520, 521], fluoromicrography [522, 523], confocal laser scanning microscopy (CLSM) [524, 525] and X-ray diffraction and ESR [98, 521, 526]. The data reported in the literature on the depth of penetration of liposomes into the skin is somewhat contradictory and the observed differences may arise from the experimental methods used to track the vesicles or to prepare the skin samples. Possible artefacts may be alleviated by using CLSM [512, 525, 527] since the diffusion of a fluorescent probe in the skin can be monitored, without cryofixing or embedding the tissue.

However, CLSM does not provide much information about the integrity of the liposomes in the skin, unless a quencher or a high amount of drug is encapsulated. Then, indirect information on the stability can be obtained by following leakage from liposomes [528]. Zellmer *et al.* [525] examined the penetration of fluorescently labelled DMPC liposomes applied non-occlusively on fresh human skin using CLSM. After 18 h, the fluorescent label could only be detected on the surface of the skin. However, differential scanning calorimetry of the skin samples revealed that individual DMPC molecules penetrated into the SC and disturbed the well-organized structure of the intercellular lipids. Similar results were obtained for DSPC/CHEMS liposomes (82:18 molar ratio, 228 nm) [527].

Vesicle–skin interactions are strongly dependent on the condition of the skin [510, 529], animal species [527], liposomal formulation (*i.e.* size, composition, thermodynamic state of the bilayer), and use of penetration enhancers [530]. Obviously, a partly damaged skin is more permeable than normal intact skin [510]. The effect of vesicle size on liposome penetration across the intact skin remains to be completely established. Yet, for the delivery of the hydrophobic drug cyclosporin-A through hairless mouse, hamster and pig skin [531] the effect of the size of REVs composed of EPC/Chol/cholesteryl sulphate (1:0.5:0.1 molar ratio, 60 and 600 nm) was reported to be minimal. In contrast, Foldvari *et al.* [532] found by electron microscopic autoradiography that intact liposomes (DPPC/Chol, 2:1 molar ratio, 250-700 nm), labelled with colloidal iron, could reach the dermis. They reported that the majority of liposomes found in the skin were unilamellar, although some MLV (< 700 nm) could also be observed.

It appears that physical parameters such as vesicle size and lamellarity are less important than the thermodynamic state of the bilayers for achieving drug transport across skin. Liposomes in the gel-state (DSPC/CHEMS) were shown not to penetrate as deep into the skin compared to liquid-state liposomes (DLPC/CHEMS) [527, 533]. Liquid-state

vesicles might act not only in superficial SC layers, but may also induce lipid perturbations in deeper layers of the SC, while vesicles in the gel-state interact only with the outermost layers of the SC. In addition, gel-state vesicles deposited on the surface of the SC may act as an additional barrier for drug diffusion and therefore inhibit drug penetration. Interestingly, the incorporation of ethanol (20–50% v/v) in liposomal formulations was reported to promote their interaction with the SC by lowering the phase T_c of the lipids and increasing the fluidity of the liposomal membrane. Most probably, ethanol decreases the interfacial tension of the vesicles and renders them more elastic. Ethanol-containing liposomal preparations (Ethasomes[®]) were shown to improve the permeation of drugs through animal skin [530, 534]. Single chain surfactants (*e.g.* C₁₂EO₇) can also be incorporated into liquid-state liposomes to obtain more deformable bilayers [527, 533].

Cevc and Blume [510] have designed ultradeformable material carriers, which they called Transfersomes[®], that can spontaneously overcome the skin transport barrier due to the natural transepidermal water activity gradient. Transfersomes[®] are elastic vesicles prepared from lipids and an edge activator, such as a single-chain lipid or surfactant [510]. Only at the optimal balance between the amount of edge activator and the amount of bilayer forming lipid are the vesicles elastic. If the edge activator level in the vesicles is too low, the vesicles are rigid and if it is too high, the system micellizes.

It has been suggested that these vehicles can penetrate into the skin as a result of the hydration force. The difference in the concentration of water between the surface and the interior of the skin creates an osmotic gradient, which was reported to be sufficiently strong to push at least 0.5 mg of lipids per h and cm² through the skin barrier in the region of the SC [510]. When applied topically, Transfersomes[®] lose water and start to dry out. Given their high degree of hydrophilicity, they are attracted to the areas of higher water content in the narrow gaps between neighboring cells in the skin [510]. Initially, the diameter of

Transfersomes® is approximately 150 nm but they were shown to elongate and pass through the weakest intercellular junctions in the skin (transcutaneous channels of 20-30 nm) without disruption [512, 535] (Figure 2.19). This promising technology is currently undergoing phase I-III clinical trials for the topical delivery of drugs for treatment of inflammatory skin diseases and peripheral pain (www.idea-ag.de).

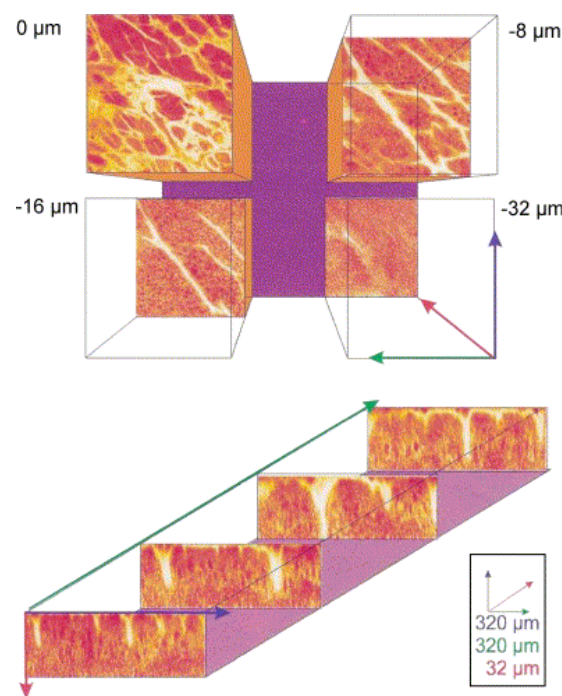


Figure 2.19. Top (upper panel) and side (lower panel) view of murine stratum corneum, visualised with the CLSM, after an epicutaneous application of a fluorescent lipophilic label in ultradeformable vesicles. The plethora of penetration pathways is seen. Less deformable colloids only penetrate into/along the widest such pathways. In this example, the SC is ~6 μm and the epidermis is approximately 15 μm wide. Reprinted with permission from Ref. [509], G. Cevc, Adv Drug Del Rev 56, 675 (2004). Copyright @ Elsevier.

2.8.5.2. Treatment of skin disease

Liposomal carriers have been successful in enhancing the clinical efficacy of a number of compounds, including tretinoin (acne) [536], corticoids (eczema) [537, 538], lidocaine (anesthetics) [539] and antipsoriatic drugs such as cyclosporin A, dithranol (1,8-dihydroxy-9-anthrone), vitamin D analogues, dypphyline, and MTX [519, 540, 541]. The first therapeutic formulation using lipid vesicles on the skin was commercialized shortly before 1990, and contained the antimycotic agent econazole. Since then, a number of liposome-based therapeutic products for localized drug delivery have been marketed (Table 2.7). In general, these products induce enhanced penetration of the encapsulated drug.

Recently, promising clinical data has been obtained in the treatment of psoriasis, which is characterized by cellular hyperproliferation, hyperparakeratosis, epidermal accumulation of polymorphonuclear leukocytes and dermal inflammation [542]. Dithranol is one of the oldest and most efficacious topical drugs for the treatment of stable plaque psoriasis. However, troublesome adverse reactions (*i.e.* irritating, burning, staining and necrotizing effects) limit patient compliance, and the highly unstable nature of the drug has dampened the enthusiasm of physicians and drug manufacturers. By encapsulating dithranol into liposomes, many of these side effects can be abolished. Agarwal *et al.* [540] studied a dithranol-loaded liposomal gel formulation in a washable aqueous base to treat patients with stable plaque psoriasis. The drug was entrapped into 500-700 nm MLV composed of PC derived from soy lecithin (Phospholipon 90H). A clinical trial was conducted on nine patients who applied this liposomal dithranol formulation for six weeks or until lesion clearance. Liposomal dithranol was found effective and almost free of adverse effects. Seven patients showed significant improvement and, among them, five had total clearance of lesions. The improved efficacy was attributed to the prolonged release of the drug through the psoriatic epidermis.

The parathyroid hormone related peptide (PTH) is a potent inhibitor of epidermal cell growth. When administered parenterally, it induces serious adverse events such as hypercalcaemia, hypercalciuria, and biochemical changes in liver or renal function. To date, no topical formulation of this peptide has been successfully developed. Holick *et al.* [543] have formulated PTH using liposomal Novasome A® cream. Novasome A® is a non-ionic stable liposomal preparation (65.5% water, 25% ethoxydiglycol, 8% glycerol dilaurate, 4% propylene glycol dicaprylate/dicaprate, 1.5% Chol, and 1% cetearyl alcohol and cetearyl glucoside; IGI Inc.) that has previously been shown to enhance percutaneous absorption of polypeptides in rodent skin [544]. A clinical trial was conducted to determine the safety and efficacy of topical PTH for treating plaque psoriasis on 15 patients who topically applied either PTH formulated in Novasome A® or the cream alone for 2 months. Patients that received the drug showed marked improvement in scaling (73%), erythema (51%) and induration (74%). Sixty per cent of patients had complete clearing of their lesions, and 85% experienced at least partial improvement. The Novasome A® placebo-treated lesions resulted in significantly less improvement. Besides, no serious adverse events, allergic reactions or dermatitis were reported following the administration of the liposomal formulation for up to one year. These results confirmed that liposomal PTH was safe and effective. Moreover, the cost of this peptide is similar to that of active vitamin D compounds or other conventional treatments used for this affliction.

2.8.5.3. Transdermal drug delivery

By virtue of their extreme and self-optimizing deformability, Transfersomes® have the ability to penetrate the skin and reach the systemic circulation [512, 538]. As mentioned before, the osmotic gradient theory was proposed to explain the transport of such vesicles through the skin.

To date, close to 50 different drugs (*e.g.* lidocaine, cyclosporin A, dexamethasone, tamoxifen, calcitonin) and polypeptides (*e.g.* calcitonin, insulin, SOD, interferons- α , β , and γ) have been successfully incorporated into Transfersomes® [545, 546]. Macromolecules such as insulin have been also associated with these utradeformable carriers (Transfersulin®) with promising therapeutic activity [545, 547]. After each Transfersulin® application on the intact skin, the first signs of systemic hypoglycemia are observed following 90 to 180 min, depending on the specific carrier composition. This result, which is nearly the same in mice, pigs, or humans implies a delay of 45 to 145 min relative to the onset of the subcutaneous insulin action [545-547]. It was reported that the epicutaneous administration (a dose 4 times that of Ultralente® insulin injection) of the Transfersulin® to patients suffering from type 1 diabetes mellitus was able to maintain the glycemia in the desirable range (<10 mmol/L) for more than 16 h after a single dosing [545]. Moreover, the blood glucose level was normalized (<5.6 mmol/L). It is noteworthy that the interexperimental standard deviation (~10%) was typically smaller than that associated with subcutaneous insulin injections (~50%). These preliminary results were very encouraging and certainly confirmed that highly deformable liposomes are superior to conventional phospholipid vesicles for the systemic delivery of drugs in a non-invasive manner.

Despite their long history of application onto the skin, the use of liposomes as transdermal delivery systems still remains controversial. Researchers disagree about the mechanism and extent of action. Even if it has been demonstrated that liposomes can enhance the skin bioavailability of drugs by several orders of magnitude, the total dose administered may largely exceed that given by the parenteral route [545]. This would make such an approach viable only for compounds that are not too expensive and that exhibit a high therapeutic index. Indeed, for drugs with a low safety margin, fluctuations in the barrier function of the skin may bring dramatic changes in the plasma levels which in turn may jeopardize the patient's health [548].

2.8.6. Ophthalmic disorders

Poor bioavailability of drugs from ocular dosage forms is mainly due to tear production, non-productive absorption, transient residence time, and impermeability of corneal epithelium. Though topical and localized application of drugs are still an acceptable and preferred way to achieve therapeutic levels, the primitive ophthalmic solution, suspension, and ointment dosage forms are no longer sufficient to combat various ocular diseases [549]. Intravitreal drug injection is the current therapy for disorders in the posterior segment. This procedure is associated with a high risk of complications, particularly when frequent, repeated injections are required. Thus, sustained-release technologies are being proposed, and the benefits of using colloidal carriers in intravitreal injections are currently under investigation for posterior drug delivery. These include the development of ocular colloidal drug delivery systems, such as liposomes, niosomes, nanoparticles, and microemulsions [550].

Liposomes have been found to both promote and reduce ocular drug absorption, indicating that a definite need exists for further studies to evaluate the interplay of drug, liposomes, and the corneal surface in determining the effectiveness of liposomes as vehicles for topically applied ophthalmic drugs [551].

Upon all ocular pathologies affecting the vision, macular degeneration, often called AMD or age-related macular degeneration, is the leading cause of vision loss and blindness in Americans age 65 and older. Macular degeneration is caused by choroidal neovascularisation, a growth of abnormal blood vessels under the central part of the retina (the macula). It is diagnosed as either dry (atrophic) or wet (exudative). The dry form is more common than the wet, with about 90% of AMD patients diagnosed with dry AMD. Although dry AMD is responsible for only 10% of the AMD condition, it does however

predispose a person to developing the wet, more severe form of AMD. Approved in 2000, Visudyne[®], is the first-ever drug therapy for the wet form of the disease. This liposomal product utilizes the lipophilic BPD-MA (verteporfine) to occlude abnormal blood vessels found in the eye while sparing overlying retinal tissue. Visudyne[®] is composed of DMPC/egg PG/BPD-MA. It is supplied in single-use 15 mg vials as a sterile, lipid-based, freeze-dried cake that requires reconstitution with sterile dextrose prior to i.v. administration.

Since the liposomal membrane is quite fluid, it is believed that BPD-MA in Visudyne[®] is easily transferred to lipoproteins and delivered to ocular tissue by the lipoproteins after injection into the bloodstream [552]. The drug is then activated by non-thermal light, which when applied in the presence of oxygen, results in the creation of highly reactive, short-lived singlet oxygen and oxygen free radicals [553]. These molecules in turn cause selective damage to the neovascular endothelium, resulting in vessel occlusion (Figure 2.20).

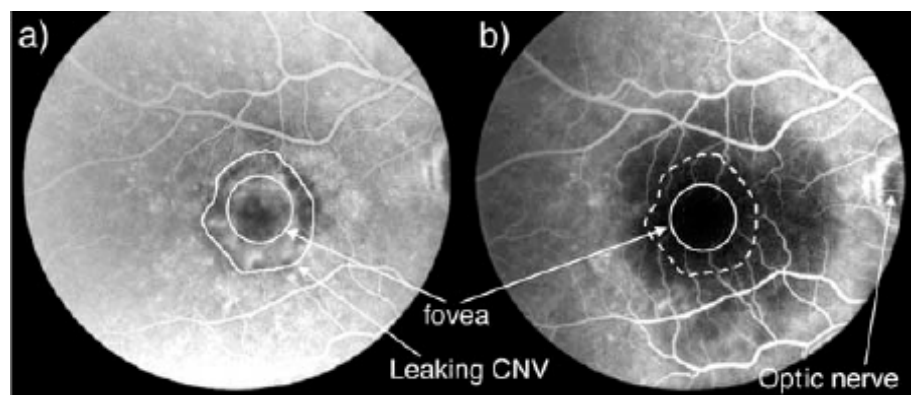


Figure 2.20. (A) Early frame of a fluorescein angiogram of the retina of a patient with predominantly classic choroidal neovascularization (CNV) in AMD before PDT, as demonstrated by the strong, well-demarcated hyperfluorescent region near the center of the macula. (B) The same eye after PDT with 12mg/m² of liposomal verteporfin and 100 J/cm²

of light at 689 nm, given at 600 mW/cm² approximately 15 min after the start of the slow i.v. injection. One week after PDT, the early phase of the fluorescein angiogram shows that the dark hypofluorescent spot has a diameter somewhat greater than that of the optic nerve (on the right), demonstrating that both the CNV and choriocapillaries remain closed, on this timescale. The dark spot also demonstrates that the retinal capillaries near the macula are still patent. Reprinted with permission from Ref. [554], H. van den Bergh, Semin Ophthalmol 16, 181 (2001). Copyright @ Routledge/Taylor & Francis Group, LLC.

This straightforward and simple treatment is performed as an outpatient procedure and usually takes no longer than 30 minutes. This therapy strategy is only for those whose new blood vessels are characterized as "predominantly classic": about 40% to 60% of new wet AMD patients, according to the Visudyne® maker Novartis. Visudyne is developed and commercialized through an alliance between QLT Inc (Canada) and Novartis Ophthalmics.

2.8.7. Other administration routes

2.8.7.1. Oral and buccal delivery

To date the delivery of macromolecular drugs such as peptides, proteins and DNA by the oral route remains a challenge. The hepatic first-pass metabolism, instability in the GI environment and poor permeability across the intestinal cell barrier contribute to poor oral bioavailability [555]. As early as the 1970s liposomes were investigated as a means to increase the absorption of macromolecular compounds [556, 557]. The first attempts failed given that the liposomes were rapidly destabilized by the harsh environment within the GI tract (low pH of the stomach, bile salts and lipases) [558, 559]. Hence, several strategies

have been proposed to increase the stability of liposomes. These include the addition of sterols [560], cross-linking of the liposomal membrane [561, 562], and incorporation of the vesicles into alginate-chitosan capsules [563]. Stabilized liposomes were shown to improve the oral absorption of several drugs such as insulin [560, 563, 564], heparin [565], SOD [566], erythropoietin [567], calcitonin and parathyroid hormone [568] with more or less success [569]. In most cases the amount of drug delivered systemically *via* this mode of administration remains low, making this approach more interesting for vaccination purposes where small doses are required.

The limitations associated with the oral route can be partly circumvented by delivering fragile drugs through the highly permeable and extensively vascularized buccal mucosa. The environment in the buccal cavity is less extreme than that in the stomach or large intestine. In terms of drug and peptide permeability, the buccal mucosa is generally less efficient than, for instance, the nasal mucosa [570]. Phospholipids with permeation enhancing properties (*e.g.* lysophosphatidylcholine and didecanoylphosphatidylcholine) [571] have been shown to increase absorption. Furthermore, bioadhesion and penetration in the buccal mucosa can be improved using lectinized liposomes [572] and deformable vesicles [573].

2.8.7.2. Nasal delivery

Due to the rich vasculature and high permeability of the nasal mucosa, rapid absorption rates can be achieved when drugs are administered nasally [574]. Contrary to the oral route, there is no hepatic first-pass metabolism or gastric acid-induced degradation associated with the nasal route. Nonetheless the nasal route is associated with a few limitations, including the restricted volume that can be placed in the nasal cavity, and the possible irritation of some drugs to the nasal mucosa [574]. Features such as mucociliary clearance, enzymatic barriers, and pathological conditions may also affect the absorption of

drugs. Liposomes offer attractive characteristics for intranasal drug delivery. They can sustain drug release [575], provide some protection against enzymatic degradation [576], temporarily disrupt the mucosa [577] and interact with the negatively charged mucus (provided they bear cationic lipids) [578]. Until now, drugs that have been successfully delivered nasally with liposomes include insulin [576, 577, 579], calcitonin [580], propanolol [581], nicotine [575], and desmopressin [578].

2.8.7.3. Vaginal delivery

For many years, the vagina was primarily used as a site for delivering contraceptive and antimicrobial agents. The vagina offers some exploitable properties that can be used to achieve effective local and systemic drug therapy [582]. However, an obvious limitation to vaginal applications is that this route is gender specific. Also, the state of the vaginal lumen is greatly influenced by the physiological changes brought about by the menstrual cycle, pregnancy, and postmenopausal conditions [583]. The drug efficacy is often limited by a poor retention at the site of action due to the self-cleansing action of the vaginal tract [582]. Due to their ability to provide prolonged release of incorporated material, liposomes have shown promise for hormonal contraception [584] and for treating infections [585] by the vaginal route. However, the major disadvantage in using liposomes vaginally is the liquid nature of the preparation that can limit their retention at the site of action. To overcome this limitation, bioadhesive gels containing liposomes have been developed [584, 586, 587].

As outlined above, liposomes have been administered by a number of alternative routes, mainly to increase the systemic absorption of drugs that have poor oral bioavailability. Despite a few reports demonstrating their efficacy, additional fundamental studies are required to better understand the mechanisms of drug absorption by these routes in order to develop more efficient vectors.

2.9. Other medical applications

2.9.1. Diagnostics

Liposomal agents have long been and are still considered as adequate imaging tools for nuclear medicine, computed tomography (CT), magnetic resonance, and ultrasound [588]. Liposomal contrast agents have been described for imaging of liver, spleen, lymph, and tumors as well as for the visualization of cardio-vascular pathologies, inflammation and infection sites, and long-circulating liposomes have been developed for blood pool imaging. CT has become a widely used technique to detect hepatosplenic metastasis due to the high water content and enlarged interstitial volumes associated with this condition that in turn result in a lower attenuation for the diseased site when compared to the surrounding parenchyma [589]. Unfortunately, certain tumors show similar attenuation to surrounding parenchyma. The use of contrast media or paramagnetic contrast media that consist of small molecular weight radio-opaque water-soluble material therefore becomes necessary. However, upon i.v. administration of low molecular weight contrast agents, tumors with similar blood flow to surrounding tissue can be obscured because of rapid equilibration of these agents with the extracellular space. One strategy to avoid this drawback is to target such agents to either the tumor or to healthy tissues by using liposomes.

The application of liposomes in medical imaging provides a targeting tool to achieve the desired distribution of contrast material. The distribution of liposomal contrast or radiolabeled molecules in the body will depend on the size and surface properties of the liposomes as well as the dose of lipid administered. Liposomal formulations with properties that favor MPS uptake including low lipid dose, large vesicle size and negative surface charge will serve for imaging the liver, spleen, lung, and bone marrow. By contrast, liposomal preparations having reduced MPS uptake, due to use of high lipid dose, small

vesicle size, pre-saturation of MPS, and surface coating with hydrophilic polymers will serve as blood and vascular pool agents [590].

For example, ^{111}In -labeled liposomes can be detected with 85% sensitivity in breast, kidney, pancreatic, and ovarian tumors in humans. These tumors are often visualized with difficulty using conventional scanning agents [591]. Biodistribution and pharmacokinetics of ^{111}In -DTPA-labeled PEGylated liposomes were studied in 17 patients with different types of locally advanced cancers. Gamma camera images showed that liposomal accumulation in tumor tissues was high, intermediate and relatively low for head and neck, lung, and breast cancer, respectively [277]. Liposomes administered i.v. also accumulate in phagocyte-rich synovium of inflamed arthritic joints [592]. Finally, Awasthi *et al.* demonstrated a remarkable tendency for liposomes to localize in the inflamed colon (colitis) of rats [593] and rabbits [594, 595], as shown by gamma camera imaging ($^{99\text{m}}\text{Tc}$ -labelling). More generally, all passive and active targeting strategies developed for liposomal drugs may be potentially applied to liposomal imaging agents. The development of tumor-targeted long circulating liposomes for radiolabelled molecules has recently been reviewed [596].

Liposomal contrast agents used in magnetic resonance imaging act by shortening T_1 spin-lattice and T_2 spin-spin relaxation times of surrounding water protons resulting in the increase or decrease of the intensity of the tissue signal. For optimal signal, all reporter metal atoms of contrast agents should be freely exposed for interaction with water. This requirement makes metal encapsulation into liposomes less attractive than the coupling of metals to the outer surface of the vesicles using polymeric chelators. Therefore, one of the strategies that has been employed includes the conjugation of groups that chelate metals to the polymeric segment of a polymer-lipid derivative in order to provide optimized agent-water interactions [597]. Although the proof of concept was successfully established, medical application of such liposomes remains limited due to the complexity and high cost

of the chemistry involved in the synthesis of polymer-lipid derivatives. Another approach consists of using gadolinium-diethylene-triamine-pentaacetic-acid-bis-methylamide (Gd-DTPA-BMA) encapsulated in PEGylated liposomes having their membrane in a fluid state at 37°C. Using this strategy, successful non-invasive NMR imaging of solid tumors was made possible in an osteosarcoma model in rats [598]. Liposomes as well as other polymeric contrast agents have been reported and reviewed by V.P. Torchilin [599].

2.9.2. Vaccine

Although live, replicating vaccines provide a strong humoral response owing to antibody production and cell-mediated immunity due to the activation of cytotoxic T lymphocytes, there is an increasing concern regarding their strong adverse effects. Killed non-replicative vaccines can be used as alternatives to live vaccines, however they can only induce a humoral response leading to a less efficient vaccination [600].

Liposomes display a number of advantages as carriers for immunoadjuvants and antigens. They can overcome the adverse effects observed with biological vaccines. Moreover, antigens can be encapsulated into the inner volume of liposomes or attached at their outer surface. Amphiphilic immunomodulating drugs such as lipid A, the lipid anchor portion of lipopolysaccharide (LPS or endotoxin) in the gram-negative bacterial outer membrane or hexadecylphosphocholine can be incorporated into the liposomal membrane [601, 602].

A large number of liposomal formulations of antigens have been evaluated and shown to lead to a systemic antibody response. Among them, the immune response caused by liposomal tetanus toxoid, influenza subunits, measles virus, polio virus peptides, and cholera toxins have been investigated [603-605].

Liposomes provide the enormous advantage of being able to combine several antigens, antigen helpers, and immunomodulators together in the same entity. Each of them can either be entrapped inside the liposomal inner volume or exposed at their surface. Although they possess these attractive qualities, potential drawbacks due to the possibility of antigenic competition may occur. Liposomes may therefore provide a sustained presentation of antigens to the immune system. As liposomes are avidly phagocytosed by macrophages at the site of injection, stimulation of a humoral response may also occur *via* the presentation of antigenic peptides to T cells by macrophages in the context of MHC class II molecules. It is however unclear how at least some liposomal antigens may enter the MHC class I pathway such as in the case of acid-sensitive liposome containing ovalbumin that were able to sensitize target cells for recognition by class I MHC-restricted ovalbumin-specific cytolytic T lymphocyte [606].

To date, all commercial vaccines are administered by i.v., s.c., intramuscular or oral routes. Regardless of the route used for liposomal vaccines, liposomes would act, at least partly, through a depot effect at the site of injection. Since interaction between liposomes and inflammatory cells is favourable to an effective immune response, conventional liposomes are preferred candidates over the so-called “stealth” liposomes. Epaxal®, a vaccine against hepatitis A, is the first approved liposomal-based vaccine and is based on the virosome technology developed and patented by Berna Biotech.

2.10. Nonmedical applications

Although liposomes have been mostly investigated as drug carriers in the pharmaceutical field, they display versatile properties that make them attractive systems for several other bio-related applications, which are briefly discussed below.

2.10.1. Biomembranes and membrane proteins

Because of their similarity in lipid composition and structure, liposomes have served as models for cell membranes in biological and medical research. They have been used to study biological events such as membrane fusion and cell interactions, the mode of action of certain substances and the conformation and function of membrane proteins, including ion pumps (sodium-potassium-, calcium-ATPases) [607, 608] and glucose transport proteins [609, 610]. Actually, liposomes have played a considerable role in understanding protein and cell function.

Liposomes have proven a convenient tool to study the PGP multidrug transporter (see Section 2.8.1.2) [611]. Reconstitution of this membrane transport protein into phospholipid vesicles, and measurement of kinetic characteristics of substrate transport, may help to understand its mechanism in cancerous cells. PGP purified from MDR cells and reconstituted into proteoliposomes, formed from defined phospholipids using a gel filtration technique, was shown to retain both ATPase activity and transport function.

2.10.2. Cosmetics

It is the cosmetic industry that first brought the attention of the general public to the value of liposomes as delivery systems. Several liposomal products have been marketed since Capture® (Christian Dior®) was introduced in 1987 (Table 2.11). They range from simple liposome pastes that are used as a replacement for creams, gels, and ointments to formulations containing various extracts, moisturizers, and to complex products containing recombinant proteins for wound or sunburn healing. In general, regulations for cosmetic active ingredients and excipients are less stringent than for pharmaceuticals making the

approval process more straightforward. Liposomal characteristics such as size, shape and lamellarity are indeed not so relevant when cosmetic applications are sought. Furthermore, it is often difficult to ascertain that the vesicular structure of liposomes in a gel phase or a creamy matrix is preserved upon conservation. Also, the presence of excipients, such as solvent (*e.g.* ethyl alcohol), high levels of salts (>0.5%), and preservatives in the final formulation can affect the stability of liposomes [612]. To circumvent this limitation, vesicles made of non-ionic surfactants (*i.e.* niosomes) such as polyglyceryl alkyl ethers can be used. Indeed, they are inexpensive, more stable chemically than phospholipids, and can be produced easily in large quantities by mixing and homogenizing aqueous solutions with molten surfactant [613, 614].

Table 2.11. Some liposomal cosmetic formulations that are currently on the market.

Product	Manufacturer	Formulation / Application claimed
Capture®	Christian Dior	Liposomal cream for the firmness of the face
Younger Looking Hair Conditioner®	Nexxus Y Serum	Liposomes encapsulating restorative and anti-aging nutrients for hair
Nactosomes®	Lancôme (L'Oréal)	Liposomes containing vitamins
Cure de Vitalité®	Payot Paris	Liposomal cream for the firmness of the face
Lait De Confort®	Guinot	Moisturising body lotion containing liposomes
Soothing After Shave Balm®	Pevonia	Celandine liposomes for soothing and calming the skin
Flawless Finish®	Elizabeth Arden	Liquid make-up containing liposomes
Eye Perfector®	Avon	Soothing cream to reduce eye irritation
Advanced Stop Signs®	Clinique	Anti-aging liposomal cream
Effet du Soleil®	L'Oréal	Liposomes encapsulating tanning agents
Hylagen Nutrients®	Marilyn Miglin	Liposomal cream for the firmness of the face
Aquasome LA®	Nikko Chemical Co.	Cream to retain skin moisture and protect the skin

Even in the absence of active ingredients, liposomes are valuable as raw materials for generation of the skin by replenishing lipid molecules and moisture [615]. They slow down water loss by forming an occlusive film on the surface of the epidermis. Often this is enough to improve skin elasticity and barrier function, which are the main causes of aging of the skin. Unsaturated PCs are the preferred ingredients to support the regeneration of the skin, and to the prevention of acne. They also help active agents like vitamins to diffuse into the skin [616]. Alternatively, hydrogenated phospholipids, known to penetrate the skin with difficulty, are mainly used for sun protection of the skin [612, 617].

Most of the commercialized liposomal cosmetic products are anti-aging skin creams. Liposome-based products generally display a series of positive effects, such as improvement of cutaneous hydration and skin texture, increase in skin glow, decrease in the depth of wrinkles, decrease in eye puffiness, and decrease in the number of aging spots [613]. Liposomal skin creams already share more than 10% of the over \$10 billion market. However, unrinsable sunscreens, long lasting perfumes, hair conditioners, aftershaves and similar products, are also taking significant fractions of the market (Table 2.11).

2.10.3. Food Industry

Lipid molecules, from fats to polar lipids, are one of the fundamental ingredients in almost any food. Lecithin and some other polar lipids are routinely extracted from nutrients, such as egg yolks or soy beans. Traditionally, polar lipids were used to stabilize water-in-oil and oil-in-water emulsions and creams, or to improve the dispersion of various instant powders in water. With the advent of microencapsulation technology, liposomes have become effective carriers for nutritionally valuable ingredients because they are formed entirely from food acceptable compounds.

Aspartame is a heat-labile sweetening agent that has been incorporated into liposomes to protect it from degradation during cooking. Nabisco Brands® patented an extrusion method to produce cookies containing REV-encapsulated aspartame [618]. The vesicles are formulated from phospholipids having a high phase T_c so that they retain their integrity in the leavened cookie. By encapsulating the aspartame in the liposome, one can maintain the aspartame in its stable form for a longer period of time and produce sustained release during storage prior to consumption. The encapsulant may be released when the cookie is baked or consumed. The sustained release properties of liposomes have also been exploited in various fermentation processes in which the encapsulated enzymes can greatly shorten fermentation times and improve the quality of the product. A classical example is cheesemaking, where liposomes reduce the cheese ripening times by 30–50%, and improve the fermentation and preservation of cheese [619, 620].

Interestingly, liposomes are also present naturally in human milk. Although the composition of breast-milk and the relationship to infant nutrition and development have been investigated in depth, the physical structure of human milk and the relationship of its “micro-structure” to nutritional and immunologic activity are still not completely understood. Milk is an elaborate suspension that contains more than 200 fat-soluble and water-soluble ingredients. It predominately consists of emulsion droplets and casein micelles. However, freeze fracture micrographs have revealed the presence of LUV with a diameter of about 500 nm [621]. Keller and co-workers (Biozone Laboratories Inc.) are investigating whether the occurrence of liposomes in human milk is a result of the complex colloidal equilibrium or has a specific role, for instance in antigen presentation and nutrient absorption. Due to these potential benefits in human nutrition, the supplementation of artificial milk with liposomes may be envisaged in the future.

2.11. Concluding remarks and perspectives

Liposomes have come a long way to become the successful partners of drugs that alone display a poor therapeutic index. The growing number of liposomal products now available on the market and currently under evaluation in clinical trials is proof of the vast potential of these lipid-based carriers. This success is largely attributed to the efforts of numerous laboratories worldwide whose synergistic input allowed for the realization of various liposomal-based medicines.

Following the initial importance of liposome discovery for membrane modeling, liposomes have long been restricted by the poor technology available in their early days where brilliant concepts such as active targeting by grafting specific ligands to the liposome surface were already introduced. Although no actively targeted liposomal products have yet been approved, the ongoing development of several of such candidates should soon offer a significant therapeutic improvement in oncology.

Despite all of the liposomal technology and manufacturing difficulties encountered throughout the years, the increasing basic scientific knowledge of the physicochemical and biological properties of liposomes has allowed the approval of the first pharmaceutical liposome products approximately 10 years ago. Among all the progress that has been achieved so far in this field, the most crucial accomplishments that can be cited are the control of liposome size by extrusion, the control of liposome permeability by using appropriate lipid compositions, the remote loading method allowing efficient drug encapsulation, the steric stabilization of vesicles by surface grafted hydrophilic polymers providing both long circulating properties and enabling ligand attachment to liposomes.

Many studies have already shown that the versatility of liposomes may result in future multifunctional drug carriers displaying innate properties, high specificity, and programmable destabilization upon diverse stimuli including light, pH or temperature changes. Although the technology is ready to create such theoretically ideal lipid-based vehicles, their medical application and pharmaceutical manufacturing remain to become feasible. The development of multifunctional carriers should be influenced by both the unmet clinical needs and the cost of such systems. Liposomologists may have considered a few decades ago that the technology was not progressing as fast as it should to build adequate liposomal products; yet, now it seems the situation is completely reversed. The disappointing failure of artificial virus-like particles for gene therapy applications is an example of a concept that was likely too sophisticated to become a medical and pharmaceutical reality.

At this stage, it is clear that liposomes have proven their medical utility in providing old drugs with a second life by significantly increasing their therapeutic index. The discovery of new drugs will further increase the application of liposome technology. The continuing progress in the manipulation of the properties of liposomal lipids and associated polymers will reinforce the success already achieved by liposomes in both medical and non-medical applications.

2.12. Acknowledgments

The authors acknowledge financial support from the Canadian Institutes of Health Research (CIHR).

2.13. References

- [1] A. D. Bangham and R. W. Horne, *J Mol Biol* 12, 660-68 (1964).
- [2] A. D. Bangham, M. M. Standish, J. C. Watkins and G. Weissmann, *Protoplasma* 63, 183-87 (1967).
- [3] A. D. Bangham, M. M. Standish and J. C. Watkins, *J Mol Biol* 13, 238-52 (1965).
- [4] A. D. Bangham, *Prog Biophys Mol Biol* 18, 29-95 (1968).
- [5] G. Gregoriadis and B. E. Ryman, *Eur J Biochem* 24, 485-91 (1972).
- [6] R. L. Juliano and D. Stamp, *Biochem Biophys Res Commun* 63, 651-58 (1975).
- [7] R. L. Juliano, *Prog Clin Biol Res* 9, 21-32 (1976).
- [8] X. Gao and L. Huang, *Gene Ther* 2, 710-22 (1995).
- [9] I. F. Uchegbu, *Pharm J* 263, 309-18 (1999).
- [10] E. Fattal, P. Couvreur and F. Puisieux, in *Les liposomes: aspects technologiques, biologiques et pharmacologiques*, edited J. Delattre, P. Couvreur, F. Puisieux, J. Philipot and F. Schuber, Tec & Doc-Lavoisier, Paris (1993), p.43-62.
- [11] I. V. Zhigaltsev, N. Maurer, Q. F. Akhong, R. Leone, E. Leng, J. Wang, S. C. Semple and P. R. Cullis, *J Controlled Release* 104, 103-11 (2005).
- [12] S. C. Semple, R. Leone, J. Wang, E. C. Leng, S. K. Klimuk, M. L. Eisenhardt, Z. N. Yuan, K. Edwards, N. Maurer, M. J. Hope, P. R. Cullis and Q. F. Ahkong, *J Pharm Sci* 94, 1024-38 (2005).
- [13] T. M. Allen and A. Chonn, *FEBS Lett* 223, 42-46 (1987).
- [14] T. M. Allen, C. Hansen and J. Rutledge, *Biochim Biophys Acta* 981, 27-35 (1989).
- [15] G. Blume and G. Cevc, *Biochim Biophys Acta* 1029, 91-97 (1990).
- [16] D. D. Lasic, F. J. Martin, A. Gabizon, S. K. Huang and D. Papahadjopoulos, *Biochim Biophys Acta* 1070, 187-92 (1991).
- [17] D. Papahadjopoulos, T. M. Allen, A. Gabizon, E. Mayhew, K. Matthay, S. K. Huang, K. D. Lee, M. C. Woodle, D. D. Lasic, C. Redemann and F. J. Martin, *Proc Natl Acad Sci USA* 88, 11460-64 (1991).
- [18] H. Takeuchi, H. Kojima, H. Yamamoto and Y. Kawashima, *Biol Pharm Bull* 24, 795-99 (2001).
- [19] V. P. Torchilin, T. S. Levchenko, K. R. Wihtman, A. A. Yaroslavov, A. M. Tsatsakis, A. K. Rizos, E. V. Michailova and M. I. Shtilman, *Biomaterials* 22, 3035-44 (2001).
- [20] C. Dufes, A. G. Schatzlein, L. Tetley, A. I. W. Gray, D.G., J. C. Olivier, W. Couet and I. F. Uchegbu, *Pharm Res* 17, 1250-58 (2000).
- [21] D. McPhail, L. Tetley, C. Dufes and I. F. Uchegbu, *Int J Pharm* 200, 73-86 (2000).
- [22] K. T. Al-Jamal, T. Sakthivel and A. T. Florence, *J Pharm Sci* 94, 102-13 (2005).
- [23] R. Fraley, S. Subramani, P. Berg and D. Papahadjopoulos, *J Biol Chem* 255, 10431-35 (1980).

- [24] P. L. Felgner, T. R. Gadek, M. Holm, R. Roman, H. W. Chan, M. Wenz, J. P. Northrop, G. M. Ringold and M. Danielsen, *Proc Natl Acad Sci USA* 84, 7413-17 (1987).
- [25] P. L. Felgner and G. M. Ringold, *Nature* 337, 387-88 (1989).
- [26] R. R. C. New, *Liposomes as Tools in Basic Research and Industry*. CRC Press, Boca Raton, FL (1995).
- [27] C. J. Chu, J. Dijkstra, M. Z. Lai, M. Z. Hong and F. C. Szoka, *Pharm Res* 7, 824-34 (1990).
- [28] R. M. Straubinger, N. Düzgünes and D. Papahadjopoulos, *FEBS Lett* 179, 148-54 (1985).
- [29] G. Storm and D. J. A. Crommelin, *Pharm Sci Technol Today* 1, 19-31 (1998).
- [30] D. D. Lasic, N. Weiner, M. Riaz and F. Martin, in *Pharmaceutical Dosage Forms: Disperse systems*, edited H.A. Liberman, M.M. Rieger and G.S. Bunker, Marcel Dekker, New York (1998), Vol. 3, p.43-86.
- [31] D. M. Small, *The Physical Chemistry of Lipids, from Alkanes to Phospholipids. Handbook of Lipid Research Series*. Plenum Press, New York (1986).
- [32] Y. Barenholz and D. J. Crommelin, in *Encyclopedia of Pharmaceutical Technology*, edited J. Swarbrick and J. C. Boylan, Marcel Dekker, New York (1994), Vol. 9, p.1-39.
- [33] F. Olson, C. A. Hunt, F. C. Szoka, W. J. Vail and D. Papahadjopoulos, *Biochim Biophys Acta* 557, 9-23 (1979).
- [34] L. Saunders, J. Perrin and D. B. Gammack, *J Pharm Pharmacol* 14, 567-72 (1962).
- [35] Y. Barenholz, D. Gibbes, B. J. Litman, J. Goll, T. E. Thompson and F. D. Carlson, *Biochemistry* 16, 2806-10 (1977).
- [36] O. Diat, D. Roux and F. Nallet, *J Phys II France* 3, 1427-52 (1993).
- [37] O. Diat and D. Roux, *J Phys II France* 3, 9-14 (1993).
- [38] N. Mignet, A. Brun, C. Degert, B. Delord, D. Roux, C. Hélène, R. Laversanne and J.-C. François, *Nucleic Acids Res* 28, 3134-42 (2000).
- [39] P. Simard, D. Hoarau, M. N. Khalid, E. Roux and J. C. Leroux, *Biochim Biophys Acta* 1715, 37-48 (2005).
- [40] O. Freund, J. Amédée, D. Roux and R. Laversanne, *Life Sci* 67, 411-19 (2000).
- [41] F. Gauffre and D. Roux, *Langmuir* 15, 3738-47 (1999).
- [42] P. Chenevier, B. Delord, J. Amédée, R. Bareille, F. Ichas and D. Roux, *Biochim Biophys Acta* 1593, 17-27 (2002).
- [43] A. Bernheim-Grosswasser, S. Ugazio, F. Gauffre, O. Viratelle, P. Mahy and D. Roux, *J Chem Phys* 112, 3424-30 (2000).
- [44] O. Freund, P. Mahy, J. Amedee, D. Roux and R. Laversanne, *J Microencapsulation* 17, 157-68 (2000).
- [45] M. J. Hope, M. B. Bally, G. Webb and P. R. Cullis, *Biochim Biophys Acta* 812, 55-65 (1985).
- [46] M. J. Hope, M. B. Bally, L. D. Mayer, A.S. Janoff and P.R. Cullis, *Chem Phys Lipids* 40, 89-107 (1986).

- [47] J. M. H. Kremer, M. W. J. van de Esker, C. Pathmamanoharan and P. H. Wiersema, *Biochemistry* 16, 3932-35 (1977).
- [48] S. Batzri and E. D. Korn, *Biochim Biophys Acta* 298, 1015-19 (1973).
- [49] J. R. Nordlund, C. F. Schmidt, S. N. Dicken and T. E. Thompson, *Biochemistry* 20, 3237-41 (1981).
- [50] F. J. Szoka and D. Papahadjopoulos, *Proc Natl Acad Sci USA* 75, 4194-98 (1978).
- [51] F. Szoka, F. Olson, T. Heath, W. Vail, E. Mayhew and D. Papahadjopoulos, *Biochim Biophys Acta* 601, 559-71 (1980).
- [52] C. Pidgeon, A. H. Hunt and K. Dittrich, *Pharm Res* 3, 23-34 (1986).
- [53] S. M. Gruner, R. P. Lenk, A. S. Janoff and M. J. Ostro, *Biochemistry* 24, 2833-42 (1985).
- [54] H. Talsma, A. Y. Ozer, L. VanBloois and D. J. Crommelin, *Drug Dev Ind Pharm* 15, 197-207 (1989).
- [55] C. Kirby and G. Gregoriadis, *Biotechnology* 2, 979-84 (1984).
- [56] D. Davis and A. G. Davies, *G. Immunol Lett* 14, 341-48 (1987).
- [57] C. Li and Y. Deng, *J Pharm Sci* 93, 1403-14 (2004).
- [58] Y. Kagawa and E. Racker, *J Biol Chem* 246, 5477-87 (1971).
- [59] H. G. Enoch and P. Strittmatter, *Proc Natl Acad Sci USA* 76, 145-49 (1979).
- [60] W. J. Gerritsen, A. J. Verkley, R. F. Zwaal and L. L. Van Deenen, *Eur J Biochem* 85, 255-61 (1978).
- [61] D. C. Drummond, O. Meyer, K. Hong, D. Kirpotin and D. Papahadjopoulos, *Pharmacol Rev* 51, 691-743 (1999).
- [62] S. Ugwu, A. Zhang, M. Parmar, B. Miller, T. Sardone, V. Peikov and I. Ahmad, *Drug Dev Ind Pharm* 31, 223-29 (2005).
- [63] M. Glavas-Dodov, E. Fredro-Kumbaradzi, K. Goracinova, M. Simonoska, S. Calis, S. Trajkovic-Jolevska and A. A. Hincal, *Int J Pharm* 291, 79-86 (2005).
- [64] N. J. Zuidam, R. de Vruet and D. J. A. Crommelin, in *Liposomes*, edited V.P. Torchilin and V. Weissig, Oxford University Press, New York (2003), p.31-77.
- [65] J. X. Zhang, S. Zalipsky, N. Mullah, M. Pechar and T. M. Allen, *Pharmacol Res* 49, 185-98 (2004).
- [66] K. Takeuchi, M. Ishihara, C. Kawaura, M. Noji, T. Furuno and M. Nakanishi, *FEBS Lett* 397, 207-09 (1996).
- [67] C. Matos, B. de Castro, P. Gameiro, J. L. Lima and S. Reis, *Langmuir* 20, 369-77 (2004).
- [68] M. Ollivon, A. Walter and R. Blumenthal, *Anal Biochem* 152, 262-74 (1986).
- [69] S. Lesieur, C. Grabielle-Madelmont, M. T. Paternostre and M. Ollivon, *Anal Biochem* 192, 334-43 (1991).
- [70] M. Vidal, in *Les liposomes: aspects technologiques, biologiques et pharmacologiques*, edited J. Delattre, P. Couvreur, F. Puisieux, J. Philipot and F. Schuber, Tec & Doc-Lavoisier, Paris (1993), p.69-86.
- [71] B. Ruozzi, G. Tosi, F. Forni, M. Fresta and M. A. Vandelli, *Eur J Pharm Sci* 25, 81-89 (2005).

- [72] A. R. Mohammed, N. Weston, A. G. Coombes, M. Fitzgerald and Y. Perrie, *Int J Pharm* 285, 23-34 (2004).
- [73] J. R. Lakowicz, *Principles of Fluorescence Spectroscopy*. Plenum Publishing Corp, New York (1983).
- [74] M. Ollivon, O. Eidelman, R. Blumenthal and A. Walter, *Biochemistry* 27, 1695-703 (1988).
- [75] R. Homan and H. J. Pownall, *Biochim Biophys Acta* 938, 155-66 (1988).
- [76] J. N. Weinstein, S. Yoshikami, P. Henkart, R. Blumenthal and W. A. Hagins, *Science* 195, 489-92 (1977).
- [77] E. J. Dufourc, C. Mayer, J. Stohrer, G. Althoff and G. Kothe, *Biophys J* 61, 42-57 (1992).
- [78] E. E. Burnell, P. R. Cullis and B. de Kruijff, *Biochim Biophys Acta* 603, 63-69 (1980).
- [79] P. B. Fenske, *Chem Phys Lipids* 64, 143-62 (1993).
- [80] T. Peleg-Shulmana, D. Gibson, R. Cohen, R. Abra and Y. Barenholz, *Biochim Biophys Acta* 1510, 278-91 (2001).
- [81] E. Roux, M. Lafleur, E. Lataste, P. Moreau and J.-C. Leroux, *Biomacromolecules* 4, 240-48 (2003).
- [82] J. H. Davis, *Biophys J* 27, 339-58 (1979).
- [83] M. Lafleur, P. R. Cullis and M. Bloom, *Eur Biophys J* 19, 55-62 (1990).
- [84] Y. P. Zhang, R. N. Lewis and R. N. McElhaney, *Biophys J* 72, 779-93 (1997).
- [85] F. Severcan, I. Sahin and N. Kazanci, *Biochim Biophys Acta* 1668, 215-22 (2005).
- [86] H. Egawa and K. Furusawa, *Langmuir* 15, 1660-66 (1999).
- [87] F. Severcan, S. Bayari and D. Karahan, *J Mol Struct* 480-481, 413-16 (1999).
- [88] F. Severcan, U. Baykal and S. Suzer, *Fresenius J Anal Chem* 355, 415-17 (1996).
- [89] Y. Maeda, H. Yamamoto and I. Ikeda, *Langmuir* 17, 6855-59 (2001).
- [90] A. Percot, X. X. Zhu and M. Lafleur, *J Polym Sci Part B: Polym Phys* 38, 907-15 (2000).
- [91] Y. Maeda, T. Higuchi and I. Ikeda, *Langmuir* 17, 7535-39 (2001).
- [92] J. F. Nagle and S. Tristam-Nagle, *Biochim Biophys Acta* 1469, 159-95 (2000).
- [93] N. Kucerka, D. Uhríková, J. Teixeira and P. Balgavý, *Physica B* 350, e639-e42 (2004).
- [94] P. Balgavý, M. Dubnickova, N. Kucerka, M. A. Kiselev, S. P. Yaradaikin and D. Uhríková, *Biochim Biophys Acta* 1512, 40-52 (2001).
- [95] J. Lemmich, K. Mortensen, J. H. Ipsen, T. Hønger, R. Bauer and O. G. Mouritsen, *Phys Rev E* 53, 5169-80 (1996).
- [96] J. Gallová, D. Uhríková, M. Hanulová, J. Teixeira and P. Balgavý, *Colloids Surf B Biointerfaces* 38, 11-14 (2004).
- [97] H. Chen, V. Torchilin and R. Langer, *Pharm Res* 13, 1378-83 (1996).
- [98] K. P. Moll, R. Stosser, W. Herrmann, H. H. Borchert and H. Utsumi, *Pharm Res* 21, 2017-24 (2004).

- [99] A. Frostell-Karlsson, H. Widegren, C. E. Green, M. D. Hamalainen, L. Westerlund, R. Karlsson, K. Fenner and H. van de Waterbeemd, *J Pharm Sci* 94, 25-37 (2005).
- [100] F. Petriat, E. Roux, J. C. Leroux and S. Giasson, *Langmuir* 20, 1393-400 (2004).
- [101] E. Roux, R. Stomp, S. Giasson, M. Pézolet, P. Moreau and J.-C. Leroux, *J Pharm Sci* 91, 1795-802 (2002).
- [102] L. L. Schramm, *Dictionary of Colloid and Interface Science*. Wiley-Interscience, New York (2001).
- [103] A. M. Samuni, A. Lipman and Y. Barenholz, *Chem Phys Lipids* 105, 121-34 (2000).
- [104] H. Girao, C. Mota and P. Pereira, *Curr Eye Res* 18, 448-54 (1999).
- [105] N. J. Zuidam, H. K. Gouw, Y. Barenholz and D. J. Crommelin, *Biochim Biophys Acta* 1240, 101-10 (1995).
- [106] A. S. Janoff, *Liposomes rational design*. Marcel Dekker Inc., New York (1999).
- [107] J. J. Liu, R. L. Hong, W. F. Cheng, K. Hong, F. H. Chang and Y. L. Tseng, *Anticancer Drugs* 13, 709-17 (2002).
- [108] S. H. Hwang, Y. Maitani, X. R. Qi, K. Takayama and T. Nagai, *Int J Pharm* 179, 85-95 (1999).
- [109] S. Clerc and Y. Barenholz, *Biochim Biophys Acta* 1240, 257-65 (1995).
- [110] E. C. A. van Winden and D. J. A. Crommelin, *Eur J Pharm Biopharm* 43, 295-307 (1997).
- [111] T. M. Allen, *Adv Drug Deliv Rev* 13, 285-309 (1994).
- [112] A. Gabizon and D. Papahadjopoulos, *Proc Natl Acad Sci USA* 85, 6949-53 (1988).
- [113] T. Ishida, H. Harashima and H. Kiwada, *Biosci Rep* 22, 197-224 (2002).
- [114] K. R. Whiteman, V. Subr, K. Ulbrich and V. P. Torchilin, *J Liposome Res* 11, 153-64 (2001).
- [115] H. Takeuchi, H. Kojima, H. Yamamoto and Y. Kawashima, *J Controlled Release* 75, 83-91. (2001).
- [116] J. H. L. Lee, H.B. and J. D. Andrade, *Prog Polym Sci* 20, 1043-79 (1995).
- [117] J. Brandrup, E. H. Immergut and E. A. Grulke, *Polymer Handbook* 4th Edition. Wiley Interscience, New York (1999).
- [118] C. Allen, N. Dos Santos, R. Gallagher, G. N. Chiu, Y. Shu, W. M. Li, S. A. Johnstone, A. S. Janoff, L. D. Mayer, M. S. Webb and M. B. Bally, *Biosci Rep* 22, 225-50 (2002).
- [119] M. A. Carignano and I. I. Szleifer, *Colloids Surf B Biointerfaces* 18, 169-82 (2000).
- [120] P. G. de Gennes, *Macromolecules* 13, 1069-75 (1980).
- [121] D. Marsh, R. Bartucci and L. Sportelli, *Biochim Biophys Acta* 1615, 33-59 (2003).
- [122] K. Hristova and D. Needham, *Macromolecules* 28, 991-1002 (1995).
- [123] P. Vermette and L. Meagher, *Colloids Surf B Biointerfaces* 28, 153-98 (2003).
- [124] A. K. Kenworthy, K. Hristova, D. Needham and T. J. McIntosh, *Biophys J* 68, 1921-36 (1995).
- [125] P. L. Ahl, S. K. Bhatia, P. Meers, P. Roberts, R. Stevens, R. Dause, W. R. Perkins and A. S. Janoff, *Biochim Biophys Acta* 1329, 370-82 (1997).

- [126] D.-Z. Liu, Y.-L. Hsieh, S.-Y. Chang and W.-Y. Chen, *Colloids Surf A Physicochem Eng Aspects* 212, 227-34 (2003).
- [127] O. Garбуzenko, S. Zalipsky, M. Qazen and Y. Barenholz, *Langmuir* 21, 2560-68 (2005).
- [128] T. M. Allen, C. B. Hansen and D. Lopes de Menezes, *Adv Drug Deliv Rev* 16, 267-84 (1995).
- [129] P. Laverman, M. G. Carstens, O. C. Boerman, E. T. Dams, W. J. Oyen, N. van Rooijen, F. H. Corstens and G. Storm, *J Pharmacol Exp Ther* 298, 607-12 (2001).
- [130] E. T. Dams, P. Laverman, W. J. Oyen, G. Storm, G. L. Scherphof, J. W. van Der Meer, F. H. Corstens and O. C. Boerman, *J Pharmacol Exp Ther* 292, 1071-79 (2000).
- [131] X. Y. Wang, T. Ishida, M. Ichihara and H. Kiwada, *J Controlled Release* 104, 91-102 (2005).
- [132] T. Ishida, T. Ichikawa, M. Ichihara, Y. Sadzuka and H. Kiwada, *J Controlled Release* 95, 403-12 (2004).
- [133] T. Ishida, M. Harada, X. Y. Wang, M. I. Ichihara, K. and H. Kiwada, *J Controlled Release* 105, 305-17 (2005).
- [134] T. L. Cheng, P. Y. Wu, M. F. Wu, J. W. Chern and S. R. Roffler, *Bioconjug Chem* 10, 520-28 (1999).
- [135] G. M. El Maghraby, A. C. Williams and B. W. Barry, *Int J Pharm* 292, 179-85 (2005).
- [136] T. L. Andresen, S. S. Jensen and K. Jorgensen, *Prog Lipid Res* 44, 68-97 (2005).
- [137] P. Crosasso, M. Ceruti, P. Brusa, S. Arpicco and F. C. Dosio, L., *J Controlled Release* 63, 19-30 (2000).
- [138] J. A. Zhang, G. Anyarambhatla, L. Ma, S. Ugwu, T. Xuan, T. Sardone and I. Ahmad, *Eur J Pharm Biopharm* 59, 177-87 (2005).
- [139] E. Maurer-Spurej, K. F. Wong, N. Maurer, D. B. Fenske and P. R. Cullis, *Biochim Biophys Acta* 1416, 1-10 (1999).
- [140] K. J. Schaper, H. B. Zhang and O. A. Raevsky, *Quant Struct-Act Relat* 20, 46-54 (2001).
- [141] S. Raffy and J. Teissie, *Biophys J* 76, 2072-80 (1999).
- [142] G. J. Charrois and T. M. Allen, *Biochim Biophys Acta* 1663, 167-77 (2004).
- [143] K. Hashizaki, H. Taguchi, C. Itoh, H. Sakai, M. Abe, Y. Saito and N. Ogawa, *Chem Pharm Bull* 53, 27-31 (2005).
- [144] H. Hayashi, K. Kono and T. Takagishi, *Biochim Biophys Acta* 1280, 127-34 (1996).
- [145] M. H. Gaber, K. Hong, S. K. Huang and D. Papahadjopoulos, *Pharm Res* 12, 1407-16 (1995).
- [146] H. Lamparski, U. Liman, J. A. Barry, D. A. Frankel, V. Ramaswami, M. F. Brown and D. F. O'Brien, *Biochemistry* 31, 685-94 (1992).
- [147] Z.-Y. Zhang, P. Shum, M. Yates, P. B. Messersmith and D. H. Thompson, *Bioconjug Chem* 13, 640-46 (2002).

- [148] M. J. Hope, D. C. Walker and P. R. Cullis, *Biochem Biophys Res Commun* 110, 15-22 (1983).
- [149] H. Ellens, J. Bentz and F. C. Szoka, *Biochemistry* 23, 1532-38 (1984).
- [150] S. C. Davis and F. C. Szoka, *Bioconjug Chem* 9, 783-92 (1998).
- [151] P. Meers, *Adv Drug Deliv Rev* 53, 265-72. (2001).
- [152] D. Needham and R. M. Hochmuth, *Biophys J* 55, 1001-09 (1988).
- [153] A. V. Titomirov, S. Sukharev and E. Kistanova, *Biochim Biophys Acta* 1088, 131-34 (1991).
- [154] P. F. Kiser, G. Wilson and D. Needham, *J Controlled Release* 68, 9-22 (2000).
- [155] P. Shum, J. M. Kim and D. H. Thompson, *Adv Drug Deliv Rev* 53, 273-84 (2001).
- [156] D. H. Thompson, O. V. Gerasimov, J. J. Wheeler, Y. Rui and V. C. Anderson, *Biochim Biophys Acta* 1279, 25-34 (1996).
- [157] A. Mueller, B. Bondurant and D. F. O'Brien, *Macromolecules* 33, 4799-804 (2000).
- [158] Z. Y. Zhang and B. D. Smith, *Bioconjug Chem* 10, 1150-52 (1999).
- [159] O. V. Gerasimov, A. Schwan and D. H. Thompson, *Biochim Biophys Acta* 1324, 200-14 (1997).
- [160] G. Kong and M. W. Dewhirst, *Int J Hyperthermia* 15, 345-70 (1999).
- [161] R. A. Demel and B. De Kruyff, *Biochim Biophys Acta* 457, 109-32 (1976).
- [162] B. Chowdhry, G. Lipka, A. Dalziel and J. Sturtevant, *Biophys J* 45, 633-35 (1984).
- [163] M. H. Gaber, N. Z. Wu, K. Hong, S. K. Huang, M. W. Dewhirst and D. Papahadjopoulos, *Int J Radiat Oncol Biol Phys* 36, 1177-87 (1996).
- [164] G. Arturson, *Acta Physiol Scand Suppl* 463, 111-22 (1979).
- [165] L. E. Gerlowski and R. K. Jain, *Int J Microcirc Clin Exp* 4, 363-72 (1985).
- [166] C. W. Song, M. S. Kang, J. G. Rhee and S. H. Levitt, *Ann NY Acad Sci* 335, 35-47 (1980).
- [167] G. Kong, G. Anyarambhatla, W. P. Petros, R. D. Braun, O. M. Colvin, D. Needham and M. W. Dewhirst, *Cancer Res* 60, 6950-57 (2000).
- [168] D. Needham and M. W. Dewhirst, *Adv Drug Deliv Rev* 53, 285-305 (2001).
- [169] D. Needham, G. Anyarambhatla, G. Kong and M. W. Dewhirst, *Cancer Res* 60, 1197-201 (2000).
- [170] A. J. Fenn, *Drug Deliv Technol* 2, 74-79 (2002).
- [171] K. Kono, *Adv Drug Deliv Rev* 53, 307-19 (2001).
- [172] H. Feil, Y. H. Bae, J. Feijen and S. W. Kim, *Macromolecules* 26, 2496-500 (1993).
- [173] K. Kono, H. Hayashi and T. Takagishi, *J Controlled Release* 30, 69-75 (1994).
- [174] J. C. Kim, S. K. Bae and J. D. Kim, *J Biochem* 121, 15-19 (1997).
- [175] H. Hayashi, K. Kono and T. Takagishi, *Bioconjug Chem* 10, 412-18 (1999).
- [176] J.-C. Kim and J.-D. Kim, *Colloids Surf B Biointerfaces* 24, 45-52 (2002).
- [177] M. B. Yatvin, W. Kreutz, B. A. Horwitz and M. Shinitzky, *Science* 210, 1253-55 (1980).
- [178] D. C. Drummond, M. Zignani and J.-C. Leroux, *Prog Lipid Res* 39, 409-60 (2000).
- [179] P. Venugopalan, S. Jain, S. Sankar, P. Singh, A. Rawat and S. P. Vyas, *Pharmazie* 56, 659-71 (2002).

- [180] V. P. Torchilin, F. Zhou and L. Huang, *J Liposome Res* 3, 201-55 (1993).
- [181] R. Cazzola, P. Viani, G. Cighetti and B. Cestaro, *Biochim Biophys Acta* 1329, 291-301 (1997).
- [182] M.-A. Yessine, M. Lafleur, C. Meier, H.-U. Petereit and J.-C. Leroux, *Biochim Biophys Acta* 1613, 28-38 (2003).
- [183] N. Skalko-Basnet, M. Tohda and H. Watanabe, *Biol Pharm Bull* 25, 1583-87 (2002).
- [184] C. Turner, N. Weir, C. Catterall, T. S. Baker, B. Carrington and M. N. Jones, *J Liposome Res* 12, 311-34 (2002).
- [185] A. Huang, S. J. Kennel and L. Huang, *J Biol Chem* 258, 14034-40 (1983).
- [186] S. Ohkuma and B. Poole, *Proc Natl Acad Sci USA* 75, 3327-31 (1978).
- [187] D. C. Litzinger and L. Huang, *Biochim Biophys Acta* 1113, 201-27 (1992).
- [188] O. V. Gerasimov, J. A. Boomer, M. M. Qualls and D. H. Thompson, *Adv Drug Deliv Rev* 38, 317-38 (1999).
- [189] N. Düzgünes, R. M. Straubinger, P. A. Baldwin, D. S. Friend and D. Papahadjopoulos, *Biochemistry* 24, 3091-98 (1985).
- [190] V. A. Slepushkin, S. Simoes, P. Dazin, M. S. Newman, L. K. Guo, M. C. Pedroso de Lima and N. Düzgünes, *J Biol Chem* 272, 2382-88 (1997).
- [191] R. Nayar, C. P. S. Tilcock, M. J. Hope, P. R. Cullis and A. J. Schroit, *Biochim Biophys Acta* 937, 31-41 (1988).
- [192] D. Collins, D. C. Litzinger and L. Huang, *Biochim Biophys Acta* 1025, 234-42 (1990).
- [193] J. M. Boggs, *Biochim Biophys Acta* 906, 353-404 (1987).
- [194] R. Nayar and A. J. Schroit, *Biochemistry* 24, 5967-71 (1985).
- [195] J. Connor and L. Huang, *Cancer Res* 46, 3431-35 (1986).
- [196] C. Cordeiro, D. J. Wiseman, P. Lutwyche, M. Uh, J. C. Evans, B. B. Finlay and M. S. Webb, *Antimicrob Agents Chemother* 44, 533-39 (2000).
- [197] S. Simoes, J. N. Moreira, C. Fonseca, N. Düzgünes and M. C. de Lima, *Adv Drug Deliv Rev* 56, 947-65 (2004).
- [198] D. Collins and L. Huang, *Cancer Res* 47, 735-39 (1987).
- [199] E. M. Stier, M. Mandal and K. D. Lee, *Mol Pharm* 2, 74-82 (2005).
- [200] G. Shi, W. Guo, S. M. Stephenson and R. J. Lee, *J Controlled Release* 80, 309-19 (2002).
- [201] S. Spagnou, A. D. Miller and M. Keller, *Biochemistry* 43, 13348-56 (2004).
- [202] D. C. Litzinger and L. Huang, *Biochim Biophys Acta* 1104, 179-87 (1992).
- [203] C. Y. Wang and L. Huang, *Proc Natl Acad Sci USA* 84, 7851-55 (1987).
- [204] J. Connor, N. Norley and L. Huang, *Biochim Biophys Acta* 884, 474-81 (1986).
- [205] D. Liu and L. Huang, *Biochim Biophys Acta* 1022, 348-54 (1990).
- [206] M.-S. Hong, S.-J. Lim, Y.-K. Oh and C.-K. Kim, *J Pharm Pharmacol* 54, 51-58 (2002).
- [207] Y. Rui, S. Wang, P. S. Low and D. H. Thompson, *J Am Chem Soc* 120, 11213-18 (1998).

- [208] J. Shin, P. Shum and D. Thompson, *J Controlled Release* 91, 187-200 (2003).
- [209] X. Guo and F. C. Szoka Jr., *Bioconjug Chem* 12, 291-300 (2001).
- [210] X. Guo, J. A. Mackay and F. C. Szoka, *Biophys J* 84, 1784-95 (2003).
- [211] M. C. de Lima, S. Simoes, P. Pires, R. Gaspar, V. Slepushkin and N. Düzgünes, *Mol Membr Biol* 16, 103-09 (1999).
- [212] K.-D. Lee, Y.-K. Oh, D. A. Portnoy and J. A. Swanson, *J Biol Chem* 271, 7249-52 (1996).
- [213] D. A. Portnoy, V. Auerbuch and I. J. Glomski, *J Cell Biol* 158, 409-14 (2002).
- [214] C. J. Provoda, E. M. Stier and K.-D. Lee, *J Biol Chem* 278, 35102-08 (2003).
- [215] E. Mathew, G. E. Hardee, C. F. Bennett and K. D. Lee, *Gene Ther* 10, 1105-15 (2003).
- [216] G. L. Lorenzi and K. D. Lee, *J Gene Med* 7, 1077-85 (2005).
- [217] F. Nicol, S. Nir and F. C. Szoka, *Biophys J* 78, 818-29 (2000).
- [218] N. K. Subbarao, R. A. Parente, F. C. Szoka, L. Nadasdi and K. Pongracz, *Biochemistry* 26, 2964-72 (1987).
- [219] R. A. Parente, S. Nir and F. C. Szoka, Jr., *Biochemistry* 29, 8720-28 (1990).
- [220] E. Fattal, S. Nir, R. A. Parente and F. C. Szoka, *Biochemistry* 33, 6721-31 (1994).
- [221] T. Kakudo, S. Chaki, S. Futaki, I. Nakase, K. Akaji, T. Kawakami, K. Maruyama, H. Kamiya and H. Harashima, *Biochemistry* 43, 5618-28 (2004).
- [222] S. Simoes, V. Slepushkin, E. Pretzer, P. Dazin, R. Gaspar, M. C. Pedroso de Lima and N. Düzgünes, *J Leukoc Biol* 65, 270-79 (1999).
- [223] S. Simoes, V. Slepushkin, P. Pires, R. Gaspar, M. P. de Lima and N. Düzgünes, *Gene Ther* 6, 1798-807 (1999).
- [224] W. Li, F. Nicol and F. C. Szoka Jr, *Adv Drug Deliv Rev* 56, 967-85 (2004).
- [225] M. J. Turk, J. A. Reddy, J. A. Chmielewski and P. S. Low, *Biochim Biophys Acta* 1559, 56-68 (2002).
- [226] H.-M. Lee and J. Chmielewski, *J Peptide Res* 65, 355-63 (2005).
- [227] K. Mechtler and E. Wagner, *New J Chem* 71, 3288-301 (1997).
- [228] A. Kichler, K. Mechtler, J. P. Behr and E. Wagner, *Bioconjug Chem* 8, 213-21 (1997).
- [229] S. Gottschalk, J. T. Sparrow, J. Hauer, M. P. Mims, F. E. Leland, S. L. Woo and L. C. Smith, *Gene Ther* 3, 48-57 (1996).
- [230] J. G. Duguid, C. Li, M. Shi, M. J. Logan, H. Alila, A. Rolland, E. Tomlinson, J. T. Sparrow and L. C. Smith, *Biophys J* 74, 2802-14 (1998).
- [231] S. M. Van Rossenberg, K. M. Slidregt-Bol, N. J. Meeuwenoord, T. J. Van Berkel, J. H. Van Boom, G. A. Van Der Marel and E. A. Biessen, *J Biol Chem* 277, 45803-10 (2002).
- [232] S. Takahashi, *Biochemistry* 29, 6257-64 (1990).
- [233] F. Nomura, T. Inaba, S. Ishikawa, M. Nagata, S. Takahashi, H. Hotani and K. Takiguchi, *Proc Natl Acad Sci USA* 101, 3420-25 (2004).
- [234] R. Ishiguro, M. Matsumoto and S. Takahashi, *Biochemistry* 35, 4976-83 (1996).

- [235] A. L. Bailey, M. A. Monck and P. R. Cullis, *Biochim Biophys Acta* 1324, 232-44 (1997).
- [236] J. L. Thomas, B. P. Devlin and D. A. Tirrell, *Biochim Biophys Acta* 1278, 73-78 (1996).
- [237] T. R. Kyriakides, C. Y. Cheung, N. Murthy, P. Bornstein, P. S. Stayton and A. S. Hoffman, *J Controlled Release* 78, 295-303 (2002).
- [238] K. Kono, K. I. Zenitani and T. Takagishi, *Biochim Biophys Acta* 1193, 1-9 (1994).
- [239] T. Mizoue, T. Horibe, K. Maruyama, T. Takizawa, M. Iwatsuru, K. Kono, H. Yanagie and F. Moriyasu, *Int J Pharm* 237, 129-37 (2002).
- [240] J.-C. Leroux, E. Roux, D. Le Garrec, K. Hong and D. C. Drummond, *J Controlled Release* 72, 71-84 (2001).
- [241] O. Meyer, D. Papahadjopoulos and J. C. Leroux, *FEBS Lett* 42, 61-64 (1998).
- [242] A. Huckriede, L. Bungener, T. Daemen and J. Wilschut, *Methods Enzymol* 373, 74-91 (2003).
- [243] M. Zignani, D. C. Drummond, O. Meyer, K. Hong and J.-C. Leroux, *Biochim Biophys Acta* 1463, 383-94 (2000).
- [244] E. Roux, M. Francis, F. M. Winnik and J.-C. Leroux, *Int J Pharm* 242, 25-36 (2002).
- [245] E. Roux, C. Passirani, S. Scheffold, J. P. Benoit and J.-C. Leroux, *J Controlled Release* 94, 447-51 (2004).
- [246] C. C. Pak, S. Ali, A. S. Janoff and P. Meers, *Biochim Biophys Acta* 1372, 13-27 (1998).
- [247] C. C. Pak, R. K. Erkulla, P. L. Ahl, A. S. Janoff and P. Meers, *Biochim Biophys Acta* 1419, 111-26 (1999).
- [248] F. M. Goni and A. Alonso, *Biosci Rep* 6, 443-63 (2000).
- [249] A. V. Villar, F. M. Goñi and A. Alonso, *FEBS Lett* 494, 117-20 (2001).
- [250] S. S. Jensen, T. L. Andresen, J. Davidsen, P. Hoyrup, S. D. Shnyder, M. C. Bibby, J. H. Gill and K. Jorgensen, *Mol Cancer Ther* 3, 1451-58 (2004).
- [251] T. L. Andresen, J. Davidsen, M. Begtrup, O. G. Mouritsen and K. Jorgensen, *J Med Chem* 47, 1694-703 (2004).
- [252] M. Murakami and I. Kudo, *J Biochem* 131, 285-92 (2002).
- [253] C. Lagorce-Pages, F. Paraf, D. Wendum, A. Martin and J. F. Flejou, *Virchows Arch* 444, 426-35 (2004).
- [254] J. Davidsen, K. Jorgensen, T. L. Andresen and O. G. Mouritsen, *Biochim Biophys Acta* 1609, 95-101 (2003).
- [255] C. Vermehren, T. Kiebler, I. Hylander, T. H. Callisen and K. Jorgensen, *Biochim Biophys Acta* 1373, 27-36 (1998).
- [256] K. Jørgensen, C. Vermehren and O. G. Mouritsen, *Pharm Res* 16, 1493-95 (1999).
- [257] D. Lasic, *Am Sci* 80, 20-31 (1992).
- [258] T. M. Allen and P. R. Cullis, *Science* 303, 1818-22 (2004).
- [259] G. Gregoriadis, *Trends Biotechnol* 13, 527-37 (1995).
- [260] R. K. Jain, *Science* 307, 58-62 (2005).

- [261] R. K. Jain, *Adv Drug Deliv Rev* 26, 71-90 (1997).
- [262] J. Folkman, *Curr Mol Med* 3, 643-51 (2003).
- [263] H. Maeda, J. Wu, T. Sawa, Y. Matsumura and K. Hori, *J Controlled Release* 65, 271-84 (2000).
- [264] R. V. J. Chari, *Adv Drug Deliv Rev* 31, 89-104 (1998).
- [265] S. K. Hobbs, W. L. Monsky, F. Yuan, W. G. Roberts, L. Griffith, V. P. Torchilin and R. K. Jain, *Proc Natl Acad Sci USA* 95, 4607-12 (1998).
- [266] F. Yuan, M. Dellian, D. Fukumura, M. Leunig, D. A. Berk, V. P. Torchilin and R. K. Jain, *Cancer Res* 55, 3752-56. (1995).
- [267] T. M. Allen and C. Hansen, *Biochim Biophys Acta* 1068, 133-44 (1991).
- [268] M. R. Mauk and R. C. Gamble, *Proc Natl Acad Sci USA* 76, 765-69 (1979).
- [269] H. Ellens, H. W. Morselt, B. H. Dontje, D. Kalicharan, C. E. Hulstaert and G. L. Scherphof, *Cancer Res* 43, 2927-34 (1983).
- [270] H. Ellens, E. Mayhew and Y. M. Rustum, *Biochim Biophys Acta* 714, 479-85 (1982).
- [271] S. C. Semple and A. Chonn, *J Liposome Res* 6, 33-60 (1996).
- [272] H. Harashima, K. Sakata and H. Kiwada, *Pharm Res* 10, 606-10 (1993).
- [273] T. Daemen, G. Hofstete, M. T. Ten-Kate, I. Bakker-Woudenberg and G. L. Scherphof, *Int J Cancer* 61, 716-21 (1995).
- [274] A. W. Segal, G. Gregoriadis, J. P. Lavender, D. Tarin and T. J. Peters, *Clin Sci Mol Med* 51, 421-25 (1976).
- [275] V. J. Richardson, B. E. Ryman, R. F. Jewkes, M. H. Tattersall and E. S. Newlands, *Int J Nucl Med Biol* 5, 118, 21-23. (1978).
- [276] G. Poste and R. Kirsh, *Biotechnology* 1, 869-78 (1983).
- [277] K. J. Harrington, S. Mohammadtaghi and P. S. Uster, *Clin Cancer Res* 7, 243-54 (2001).
- [278] P. K. Working, M. S. Newman, S. K. Huang, E. Mayhew, J. Vaage and D. D. Lasic, *J Liposome Res* 4, 667-87 (1994).
- [279] N. Z. Wu, D. Da, T. L. Rudoll, D. Needham, A. R. Whorton and M. W. Dewhirst, *Cancer Res* 53, 3765-70 (1993).
- [280] M. J. Parr, D. Masin, P. R. Cullis and M. B. Bally, *J Pharmacol Exp Ther* 280, 1319-27 (1997).
- [281] L. D. Mayer, G. Dougherty, T. O. Harasym and M. B. Bally, *J Pharmacol Exp Ther* 280, 1406-14 (1997).
- [282] R. L. Hong, C. J. Huang, Y. L. Tseng, V. F. Pang, S. T. Chen, J. J. Liu and F. H. Chang, *Clin Cancer Res* 5, 3645-52 (1999).
- [283] S. K. Huang, E. Mayhew, S. Gilani, D. D. Lasic, F. J. Martin and D. Papahadjopoulos, *Cancer Res* 52, 6774-81 (1992).
- [284] F. Yuan, M. Leunig, S. K. Huang, D. A. Berk, D. Papahadjopoulos and R. K. Jain, *Cancer Res* 54, 3352-56. (1994).
- [285] R. K. Jain, *Cancer Res* 50, 814s-19s (1990).
- [286] Y. Boucher and R. K. Jain, *Cancer Res* 52, 5110-14 (1992).

- [287] R. K. Jain, *Annu Rev Biomed Eng* 1, 241-63 (1999).
- [288] D. Papahadjopoulos, D. B. Kirpotin, J. W. Park, K. Hong, Y. Shao, R. Shalaby, G. Colbern and C. C. Benz, *J Liposome Res* 8, 425-42 (1999).
- [289] S. K. Huang, P. R. Stauffer, K. Hong, J. W. H. Guo, T. L. Phillips, A. Huang and D. Papahadjopoulos, *Cancer Res* 54, 2186-91 (1994).
- [290] G. Batist, G. Ramakrishnan, C. S. Rao, A. Chandrasekharan, J. Gutheil, T. Guthrie, P. Shah, A. Khojasteh, M. K. Nair, K. Hoelzer, K. Tkaczuk, Y. C. Park and L. W. Lee, *J Clin Oncol* 19, 1444-54 (2001).
- [291] S. S. Williams, T. R. Alosco, E. Mayhew, D. D. Lasic, F. J. Martin and R. B. Bankert, *Cancer Res* 53, 3964-67 (1993).
- [292] J. Vaage, D. Donovan, E. Mayhew, R. Abra and A. Huang, *Cancer* 72, 3671-75 (1993).
- [293] T. Siegal, A. Horowitz and A. Gabizon, *J Neurosurg* 83, 1029-37 (1995).
- [294] J. Vaage, E. Mayhew, D. D. Lasic and F. J. Martin, *Int J Cancer* 51, 942-48 (1992).
- [295] J. W. Park, K. Hong, D. B. Kirpotin, D. Papahadjopoulos and C. C. Benz, *Adv Pharmacol* 40, 399-435 (1997).
- [296] A. Gabizon, M. Chemla, D. Tzemach, A. T. Horowitz and D. Goren, *J Drug Target* 3, 391-98 (1996).
- [297] T. M. Allen and F. J. Martin, *Semin Oncol* 31, 5-15 (2004).
- [298] G. Batist, J. Barton, P. Chaikin, C. Swenson and L. Welles, *Expert Opin Pharmacother* 3, 1739-51 (2002).
- [299] G. Williams, P. Cortazar and R. Pazdur, *J Clin Oncol* 19, 3439-41 (2001).
- [300] D. W. Northfelt, B. J. Dezube, J. A. Thommes, B. J. Miller, M. A. Fischl, A. Friedman-Kien, L. D. Kaplan, C. Du Mond, R. D. Mamelok and D. Henry, *J Clin Oncol* 16, 2445-51 (1998).
- [301] F. Muggia and A. Hamilton, *Eur J Cancer* 37, S15-18 (2001).
- [302] Z. Symon, A. Peyser, D. Tzemach, O. Lyass, E. Sucher, E. Shezen and A. Gabizon, *Cancer* 86, 72-78 (1999).
- [303] G. Haran, R. Cohen and L. K. Bar, *Biochim Biophys Acta* 1151, 201-15 (1993).
- [304] T. L. Kuhl, D. E. Leckband, D. D. Lasic and J. N. Israelachvili, *Biophys J* 66, 1479-88 (1994).
- [305] D. D. Lasic, *Nature* 380, 561-62 (1996).
- [306] D. D. Lasic and D. Needham, *Chem Rev* 95, 2601-28 (1995).
- [307] A. Gabizon, H. Shmeeda and Y. Barenholz, *Clin Pharmacokinet* 42, 419-36 (2003).
- [308] B. Uziely, S. Jeffers, R. Isacson, K. Kutsch, D. Wei-Tsao, Z. Yehoshua, E. Libson, F. M. Muggia and A. Gabizon, *J Clin Oncol* 13, 1777-85 (1995).
- [309] M. E. O'Brien, N. Wigler, M. Inbar, R. Rosso, E. Grischke, A. Santoro, R. Catane, D. G. Kieback, P. Tomczak, S. P. Ackland, F. Orlandi, L. Mellars, L. Alland and C. Tendler, *Ann Oncol* 15, 440-49 (2004).
- [310] P. S. Gill, B. M. Espina, F. Muggia, S. Cabriales, A. Tulpule, J. A. Esplin, H. A. Liebman, E. Forssen, M. E. Ross and A. M. Levine, *J Clin Oncol* 13, 996-1003 (1995).

- [311] S. E. Krown, D. W. Northfelt, D. Osoba and J. S. Stewart, *Semin Oncol* 31, 36-52 (2004).
- [312] C. L. Bennett and E. A. Calhoun, *Semin Oncol* 31: 191-95 (2004).
- [313] S. M. Sieber, J. A. R. Mead and R. H. Adamson, *Cancer Treat Rep* 60, 1127-39 (1976).
- [314] N. L. Boman, M. B. Bally, P. R. Cullis, L. D. Mayer and M. S. Webb, *J Liposome Res* 5, 523-41 (1995).
- [315] M. S. Webb, T. O. Harasym, D. Masin, M. B. Bally and L. D. Mayer, *Br J Cancer* 72, 896-904 (1995).
- [316] D. N. Waterhouse, T. D. Madden, P. R. Cullis, M. B. Bally, L. D. Mayer and M. S. Webb, *Methods Enzymol* 391, 40-57 (2005).
- [317] J. P. Slotte, *Chem Phys Lipids* 102, 13-27 (1999).
- [318] A. H. Sarris, F. Hagemeister, J. Romaguera, M. A. Rodriguez, P. McLaughlin, A. M. Tsimberidou, L. J. Medeiros, B. Samuels, O. Pate, M. Ohlendorf, H. Kantarjian, C. Burge and F. Cabanillas, *Ann Oncol* 11, 69-72 (2000).
- [319] A. Hamada, T. Kawaguchi and M. Nakano, *Clin Pharmacokinet* 41, 705-18 (2002).
- [320] J. Borsa, G. R. Whitmore, F. A. Valeriote, D. Collins and W. R. Bruce, *J Natl Cancer Inst* 42, 235-42 (1969).
- [321] B. C. Baguley and E. M. Falkenhaug, *Cancer Chemother Rep* 55, 291-98 (1971).
- [322] R. Ganapathi, A. Krishan, I. Wodinsky, C. G. Zubrod and L. J. Lesko, *Cancer Res* 40, 630-33 (1980).
- [323] T. M. Allen, T. Mehra, C. Hansen and Y. C. Chin, *Cancer Res* 52, 2431-39 (1992).
- [324] Y. E. Rahman, K. R. Patel, E. A. Cerny and M. Maccoss, *Eur J Cancer Clin Oncol* 20, 1105-12 (1984).
- [325] T. Kobayashi, T. Kataoka, S. Tsukagoshi and Y. Sakurai, *Int J Cancer* 20, 581-87 (1977).
- [326] F. J. Giles, M. S. Tallman, G. Garcia-Manero, J. E. Cortes, D. A. Thomas, W. G. Wierda, S. Verstovsek, M. Hamilton, E. Barrett, M. Albitar and H. M. Kantarjian, *Cancer* 100, 1449-58 (2004).
- [327] M. V. Seiden, F. Muggia, A. Astrow, U. Matulonis, S. Campos, M. Roche, J. Sivret, J. Rusk and E. Barrett, *Gynecol Oncol* 93, 229-32 (2004).
- [328] D. L. Emerson, R. Bendele and E. Brown, *Clin Cancer Res* 6, 2903-12 (2000).
- [329] D. F. Kehrer, A. M. Bos and J. Verweij, *J Clin Oncol* 20, 1222-31 (2002).
- [330] G. Gregoriadis, E. J. Wills, C. P. Swain and A. S. Tavill, *Lancet* 1, 1313-16 (1974).
- [331] S. B. Kaye and V. J. Richardson, *Cancer Chemother Pharmacol* 3, 81-85 (1979).
- [332] G. Bradley and V. Ling, *Cancer Metastasis Rev* 13, 223-33 (1994).
- [333] C. Mamot, D. C. Drummond, K. Hong, D. B. Kirpotin and J. W. Park, *Drug Resist Updat* 6, 271-79 (2003).
- [334] C. A. Seid, I. J. Fidler, R. K. Clyne, L. E. Earnest and D. Fan, *Selective Cancer Ther* 7, 103-12 (1991).
- [335] A. Rahman, S. R. Husain, J. Siddiqui, M. Verma, M. Agresti, M. Center, A. R. Safa and R. I. Glazer, *J Natl Cancer Inst* 84, 1909-13 (1992).

- [336] A. R. Thierry, A. Rahman and A. Dritschilo, *Cancer Chemother Pharmacol* 35, 84-93 (1994).
- [337] A. R. Thierry, A. Dritschilo and A. Rahman, *Biochem Biophys Res Commun* 187, 1098-105 (1992).
- [338] J. H. Senior, *Crit Rev Ther Drug Carrier Syst* 3, 123-93 (1987).
- [339] M. Castaing, P. Brouant, A. Loiseau, C. Santelli-Rouvier, M. Santelli, S. Alibert-Franco, A. Mahamoud and J. Barbe, *J Pharm Pharmacol* 52, 289-96 (2000).
- [340] E. Choice, D. Masin, M. B. Bally, M. Meloche and T. D. Maden, *Transplantation* 60, 1006-12 (1995).
- [341] B. L. Lum and M. P. Gosland, *Hematol Oncol Clin North Am* 9, 319-36 (1995).
- [342] R. Krishna, M. St-Louis and L. D. Mayer, *Int J Cancer* 85, 131-41 (2000).
- [343] G. Kohler and C. Milstein, *Nature* 74, 381-94 (1975).
- [344] R. Abou-Jawde, T. Choueiri, C. Alemany and T. Mekhail, *Clin Ther* 25, 2121-37 (2003).
- [345] G. Blume, G. Cevc, M. D. J. A. Crommelin, I. A. J. M. Bakker-Wondenberg, C. Kluft and G. Storm, *Biochim Biophys Acta* 1149, 180-84 (1993).
- [346] K. Maruyama, O. Ishida, T. Takizawa and K. Moribe, *Adv Drug Deliv Rev* 40, 89-102 (1999).
- [347] T. M. Allen, E. Brandeis, C. B. Hansen, G. Y. Kao and S. Zalipsky, *Biochim Biophys Acta* 1237, 99-108 (1995).
- [348] C. B. Hansen, G. Y. Kao, E. H. Moase, S. Zalipsky and T. M. Allen, *Biochim Biophys Acta* 1239, 133-44 (1995).
- [349] S. Zalipsky, N. Mullah, J. A. Harding, J. Gittelman, L. Guo and S. A. Defrees, *Bioconjug Chem* 8, 111-18 (1997).
- [350] V. P. Torchilin, T. S. Levchenko, A. N. Lukyanov, B. A. Khaw, A. L. Klibanov, R. Rammohan, G. P. Samokhin and K. R. Whiteman, *Biochim Biophys Acta* 1511, 397-411 (2001).
- [351] L. Nobs, F. Buchegger, R. Gurny and E. Allémann, *J Pharm Sci* 93, 1980-92 (2004).
- [352] V. Torchilin, *Nat Rev Drug Discov* 4, 145-60 (2005).
- [353] J. W. Park, K. Hong, D. B. Kirpotin, G. Colbern, R. Shalaby, J. Baselga, Y. Shao, U. B. Nielsen, J. D. Marks, D. Moore, D. Papahadjopoulos and C. C. Benz, *Clin Cancer Res* 8, 1172-81 (2002).
- [354] K. Maruyama, T. Takizawa, T. Yuda, S. J. Kennel, L. Huang and M. Iwatsuru, *Biochim Biophys Acta* 1234, 74-80 (1995).
- [355] D. E. Lopes de Menezes, M. J. Kirchmeier, J. F. Gagne, L. M. Pilarski and M. T. Allen, *J Liposome Res* 9, 199-228 (1999).
- [356] D. E. Lopes de Menezes, L. M. Pilarski, A. R. Belch and T. M. Allen, *Biochim Biophys Acta* 1466, 205-20 (2000).
- [357] T. Ishida, M. J. Kirchmeier, E. H. Moase, S. Zalipsky and T. M. Allen, *Biochim Biophys Acta* 1515, 144-58 (2001).

- [358] T. M. Allen, D. R. Mumbengegwi and G. J. Charrois, *Clin Cancer Res* 11, 3567-73 (2005).
- [359] P. Sapra and T. M. Allen, *Clin Cancer Res* 10, 2530-37 (2004).
- [360] J. W. Park, K. Hong, P. Carter, H. Asgari, L. Y. Guo, A. Keller, C. Wirth, R. Shalaby, C. Kotts, W. I. Wood, D. Papahadjopoulos and C. C. Benz, *Proc Natl Acad Sci USA* 92, 1327-31 (1995).
- [361] D. Kirpotin, J. W. Park, K. Hong, S. Zalipsky, W. L. Li, P. Carter, C. Benz and D. Papahadjopoulos, *Biochemistry* 36, 66-75 (1997).
- [362] J. W. Park, K. Hong, D. Kirpotin, O. Meyer, D. Papahadjopoulos and C. C. Benz, *Cancer Lett* 118, 153-60 (1997).
- [363] U. B. Nielsen, D. B. Kirpotin, E. M. Pickering, K. Hong, J. W. Park, M. Refaat Shalaby, Y. Shao, C. C. Benz and J. D. Marks, *Biochim Biophys Acta* 1591, 109-18 (2002).
- [364] M. Mercadal, J. C. Domingo, J. Petriz, J. Garcia and M. A. de Madariaga, *Biochim Biophys Acta* 1418, 232-38 (1999).
- [365] C. Carrion, M. A. de Madariaga and J. C. Domingo, *Life Sci* 75, 313-28 (2004).
- [366] M. Singh, A. J. Ferdous, N. Kanikkannan and G. Faulkner, *Eur J Pharm Biopharm* 52, 13-20 (2001).
- [367] M. Sudhan Shaik, N. Kanikkannan and M. Singh, *J Controlled Release* 76, 285-95 (2001).
- [368] P. J. Konigsberg, R. Godtel, T. Kissel and L. L. Richer, *Biochim Biophys Acta* 1370, 243-51 (1998).
- [369] T. Volk, P. Holig, T. Merdan, R. Muller and R. E. Kontermann, *Biochim Biophys Acta* 1663, 158-66 (2004).
- [370] H. Yanagie, T. Tomita, H. Kobayashi, Y. Fujii, Y. Nonaka, Y. Saegusa, K. Hasumi, M. Eriguchi, T. Kobayashi and K. Ono, *Br J Cancer* 75, 660-65 (1997).
- [371] K. Maruyama, *Biol Pharm Bull* 23, 791-99 (2000).
- [372] M. Sugano, N. K. Egilmez, S. J. Yokota, F. A. Chen, J. Harding, S. K. Huang and R. B. Bankert, *Cancer Res* 60, 6942-49 (2000).
- [373] R. M. Abra, R. B. Bankert, F. Chen, N. K. Egilmez, K. Huang, R. Saville, J. L. Slater, M. Sugano and S. J. Yokota, *J Liposome Res* 12, 1-3 (2002).
- [374] F. Pastorino, C. Brignole, D. Marimpietri, P. Sapra, E. H. Moase, T. M. Allen and M. Ponzoni, *Cancer Res* 63, 86-92 (2003).
- [375] C. Brignole, D. Marimpietri, C. Gambini, T. M. Allen, M. Ponzoni and F. Pastorino, *Cancer Lett* 197, 199-204 (2003).
- [376] E. H. Moase, W. Qi, T. Ishida, Z. Gabos, B. M. Longenecker, G. L. Zimmermann, L. Ding, M. Krantz and T. M. Allen, *Biochim Biophys Acta* 1510, 43-55 (2001).
- [377] O. W. Press, A. G. Farr, K. I. Borroz, S. K. Anderson and P. J. Martin, *Cancer Res* 49, 4906-12 (1989).
- [378] D. Kirpotin, K. Hong, N. Mullah, D. Papahadjopoulos and S. Zalipsky, *FEBS Lett* 388, 115-18 (1996).

- [379] J. G. Molland, B. H. Barraclough, V. Gebski, J. Milliken and M. Bilous, *Aust N Z J Surg* 66, 64-70 (1996).
- [380] M. A. Cobleigh, C. L. Vogel, D. Tripathy, N. J. Robert, S. Scholl, L. Fehrenbacher, J. M. Wolter, V. Paton, S. Shak, G. Lieberman and D. J. Slamon, *J Clin Oncol* 17, 2639-48 (1999).
- [381] D. J. Slamon, B. S. Leyland-Jones, S., H. Fuchs, V. Paton, A. Bajamonde, T. Fleming, W. Eiermann, J. Wolter, M. Pegram, J. Baselga and L. Norton, *N Engl J Med* 344, 783-92 (2001).
- [382] D. Aragnol and L. D. Leserman, *Proc Natl Acad Sci USA* 83, 2699-703 (1986).
- [383] R. J. Debs, T. D. Heath and D. Papahadjopoulos, *Biochim Biophys Acta* 901, 183-90 (1987).
- [384] R. J. Lee and P. S. Low, *Biochim Biophys Acta* 1233, 134-44 (1995).
- [385] Y. Ogawa, H. Kawahara, N. Yagi, M. Kodaka, T. Tomohiro, T. Okada, T. Konakahara and H. Okuno, *Lipids* 34, 387-94 (1999).
- [386] T. Asai and N. Oku, *Methods Enzymol* 391, 163-76 (2005).
- [387] R. M. Schiffelers, G. A. Koning, T. L. ten Hagen, M. H. Fens, A. J. Schraa, A. P. Janssen, R. J. Kok, G. Molema and G. Storm, *J Controlled Release* 91, 115-22 (2003).
- [388] F. Pastorino, C. Brignole, D. Marimpietri, M. Cilli, C. Gambini, D. Ribatti, R. Longhi, T. M. Allen, A. Corti and M. Ponzoni, *Cancer Res* 63, 7400-09 (2003).
- [389] Y. Lu and P. S. Low, *Adv Drug Deliv Rev* 54, 675-93 (2002).
- [390] T. M. Allen, *Nat Rev Cancer* 2, 750-63 (2002).
- [391] S. Wang, R. J. Lee, G. Cauchon, D. G. Gorenstein and P. S. Low, *Proc Natl Acad Sci USA* 92, (1995).
- [392] M. M. Qualls and D. H. Thompson, *Int J Cancer* 93, 384-92 (2001).
- [393] X. Q. Pan, H. Wang and R. J. Lee, *Anticancer Res* 22, 1629-33 (2002).
- [394] X. Q. Pan, H. Wang, S. Shukla, M. Sekido, D. M. Adams, W. Tjarks, R. F. Barth and R. J. Lee, *Bioconjug Chem* 13, 435-42 (2002).
- [395] F. Curnis, G. Arrigoni, A. Sacchi, L. Fischetti, W. Arap, R. Pasqualini and A. Corti, *Cancer Res* 62, 867-74 (2002).
- [396] P. J. O'Connell, V. Gerakis and A. J. d'Apice, *J Biol Chem* 266, 4593-97 (1991).
- [397] W. Arap, R. Pasqualini and E. Ruoslahti, *Science* 279, 377-80 (1998).
- [398] R. Pasqualini, E. Koivunen, R. Kain, J. Lahdenranta, M. Sakamoto, A. Stryhn, R. A. Ashmun, L. H. Shapiro, W. Arap and E. Ruoslahti, *Cancer Res* 60, 722-27 (2000).
- [399] N. Maeda, Y. Takeuchi, M. Takada, Y. Namba and N. Oku, *Bioorg Med Chem Lett* 14, 1015-18 (2004).
- [400] N. Maeda, Y. Takeuchi, M. Takada, Y. Sadzuka, Y. Namba and N. Oku, *J Controlled Release* 100, 41-52 (2004).
- [401] K. Ichikawa, T. Hikita, N. Maeda, S. Yonezawa, Y. Takeuchi, T. Asai, Y. Namba and N. Oku, *Biochim Biophys Acta* 1669, 69-74 (2005).
- [402] B. L. Herwaldt, *Lancet* 354, 1191-99 (1999).
- [403] A. J. Coukell and R. N. Brogden, *Drugs* 55, 585-612 (1998).

- [404] I. I. Bekersky, R. M. Fielding, D. Buell and I. I. Lawrence, *Pharm Sci Technol Today* 2, 230-36 (1999).
- [405] A. W. Ng, K. M. Wasan and G. Lopez-Berestein, *Methods Enzymol* 391, 304-13 (2005).
- [406] F. Offner, V. Krcmery, M. Boogaerts, C. Doyen, D. Engelhard, P. Ribaud, C. Cordonnier, B. de Pauw, S. Durrant, J. P. Marie, P. Moreau, H. Guiot, G. Samonis, R. Sylvester, R. Herbrecht and EORTC Invasive Fungal Infections Group, *Antimicrob Agents Chemother* 48, 4808-12 (2004).
- [407] M. Moonis, I. Ahmad and B. K. Bachhawat, *J Antimicrob Chemother* 31, 569-79 (1993).
- [408] S. Arikan and J. H. Rex, *Curr Pharm Des* 7, 393-415 (2001).
- [409] A. De Logu, A. M. Fadda, C. Anchisi, A. M. Maccioni, C. Sinico, M. L. Schivo and F. Alhaique, *J Antimicrob Chemother* 40, 889-93 (1997).
- [410] R. R. New, M. L. Chance and S. Heath, *J Antimicrob Chemother* 8, 371-81 (1981).
- [411] R. D. Meyer, *Clin Infect Dis* 14, S154-S60 (1992).
- [412] G. Lopez-Berestein, V. Fainstein, R. Hopter, K. R. Mehta, M. Sullivan, M. Keating, M. Luna and E. M. Hersh, *J Infect Diseases* 151, 704-10 (1985).
- [413] G. Lopez-Berestein, M. G. Rosenblum and R. Mehta, *Cancer Drug Deliv* 1, 199-205 (1984).
- [414] J.-P. Sculier, A. Coune, F. Meunier, C. Brassinne, C. Laduron, C. Hollaert, N. Collette, C. Heymans and J. Klastersky, *Eur J Cancer Clin Oncol* 24, 527-38 (1988).
- [415] D. D. Lasic, *J Controlled Release* 48, 203-22 (1997).
- [416] J. P. Adler-Moore and R. T. Proffitt, *J Liposome Res* 3, 429-50 (1993).
- [417] R. Quiliz, *Cancer Control* 5, 439-49 (1998).
- [418] W. Mills, R. Chopra, D. C. Linch and A. H. Goldstone, *Br J Haematol* 86, 754-60 (1994).
- [419] F. Meunier, H. G. Prentice and O. Ringden, *J Antimicrob Chemother* 28B, 83-91 (1991).
- [420] O. Ringdén, F. Meunier, J. Tollemar, P. Ricci, S. Tura, E. Kuse, M. A. Viviani, N. C. Gorin, J. Klastersky and P. Fenaux, *J Antimicrob Chemother* 28B, 73-82 (1991).
- [421] T. J. Walsh, J. W. Hiemenz, N. L. Seibel, J. R. Perfect, G. Horwith, L. Lee, J. L. Silber, M. J. DiNubile, A. Reboli, E. Bow, J. Lister and E. J. Anaissie, *Clin Infect Dis* 26, 1383-96 (1998).
- [422] M. H. White, E. J. Anaissie, S. Kusne, J. R. Wingard, J. W. Hiemenz, A. Cantor, M. Gurwith, C. Du Mond, R. D. Mamelok and R. A. Bowden, *Clin Infect Dis* 24, 635-42 (1997).
- [423] R. T. Proffitt, A. Satorius, S. M. Chiang, L. Sullivan and J. P. Adler-Moore, *J Antimicrob Chemother* 28, 49-61 (1991).
- [424] G. W. Boswell, I. Bekersky, D. Buell, R. Hiles and T. J. Walsh, *Antimicrob Agents Chemother* 42, 263-68 (1998).

- [425] T. J. Walsh, V. Yeldandi, M. McEvoy, C. Gonzalez, S. Chanock, A. Freifeld, N. I. Seibel, P. O. Whitcomb, P. Jarosinski, G. Boswell, I. Bekersky, A. Alak, D. Buell, J. Barret and W. Wilson, *Antimicrob Agents Chemother* 42, 2391-98 (1998).
- [426] U. Persson, G. R. Tennvall, S. Andersson, G. Tyden and B. Wettermark, *Pharmacoeconomics* 2, 500-08 (1992).
- [427] M. A. Boogaerts, G. Tormans, E. Maes and B. Van Doorslaer, *Blood* 88, 501a (1996).
- [428] I. I. Salem, D. L. Flasher and N. Düzgünes, *Methods Enzymol* 391, 261-91 (2005).
- [429] R. M. Fielding, R. O. Lewis and L. Moon-McDermott, *Pharm Res* 15, 1775-81 (1998).
- [430] S. Sachetelli, H. Khalil, T. Chen, C. Beaulac, S. Senechal and J. Lagace, *Biochim Biophys Acta* 1463, 254-66 (2000).
- [431] J. A. Karlowsky and G. G. Zhanel, *Clin Infect Dis* 15, 654-67 (1992).
- [432] J. Dhillon, R. M. Fielding, J. P. Adler-Moore, R. Goodall and D. Mitchison, *J Antimicrob Chemother* 48, 869-76 (2001).
- [433] R. M. Fielding, L. Moon-McDermott, R. O. Lewis and M. J. Horner, *Antimicrob Agents Chemother* 43, 503-09 (1999).
- [434] T. C. Whitehead, A. M. Lovering, I. M. Cropley, P. Wade and R. N. Davidson, *Eur J Clin Microbiol Infect Dis* 17, 181-88 (1998).
- [435] E. A. Petersen, J. B. Grayson, E. M. Hersh, R. T. Dorr, S. M. Chiang, M. Oka and R. T. Proffitt, *J Antimicrob Chemother* 38, 819-28 (1996).
- [436] Y. Q. Xiong, L. I. Kupferwasser, P. M. Zack and A. S. Bayer, *Antimicrob Agents Chemother* 43, 1737-42 (1999).
- [437] M. S. Webb, N. L. Boman, D. J. Wiseman, D. Saxon, K. Sutton, K. F. Wong, P. Logan and M. J. Hope, *Antimicrob Agents Chemother* 42, 45-52 (1998).
- [438] J. Lagace, M. Dubreuil and S. Montplaisir, *J Microencapsul* 8, 53-61 (1991).
- [439] C. Beaulac, S. Clement-Major, J. Hawari and J. Lagace, *Antimicrob Agents Chemother* 40, 665-69 (1996).
- [440] C. Beaulac, S. Sachetelli and J. Lagacé, *J Antimicrob Chemother* 41, 35-41 (1998).
- [441] J. F. Gagne, A. Desormeaux, S. Perron, M. J. Tremblay and M. G. Bergeron, *Biochim Biophys Acta* 1558, 198-210 (2002).
- [442] A. Desormeaux and M. G. Bergeron, *Methods Enzymol* 391, 330-51 (2005).
- [443] M. Kende, C. R. Alving, W. L. Rill, G. M. J. Swartz and P. G. Canonico, *Antimicrob Agents Chemother* 27, 903-07 (1985).
- [444] N. Miyano-Kurosaki, J. S. Barnor, H. Takeuchi, T. Owada, H. Nakashima, N. Yamamoto, T. Matsuzaki, F. Shimada and H. Takaku, *Antivir Chem Chemother* 15, 93-100 (2004).
- [445] N. Düzgünes, S. Simoes, V. Slepushkin, E. Pretzer, D. Flasher, I. I. Salem, G. Steffan, K. Konopka and M. C. Pedroso de Lima, *Methods Enzymol* 391, 351-73 (2005).
- [446] P. Harvie, A. Desormeaux, N. Gagne, M. Tremblay, L. Poulin, D. Beauchamp and M. G. Bergeron, *AIDS* 9, 701-07 (1995).

- [447] A. Desormeaux, P. Harvie, S. Perron, B. Makabi-Panzu, D. Beauchamp, M. Tremblay, L. Poulin and M. G. Bergeron, AIDS 8, 1545-53 (1994).
- [448] P. Harvie, A. Desormeaux, M. C. Bergeron, M. Tremblay, D. Beauchamp, L. Poulin and M. G. Bergeron, Antimicrob Agents Chemother 40, 225-29 (1996).
- [449] S. T. Hirana, P. J. Moultona and J. T. Hancock, Free Rad Biol Med 23, 736-43 (1997).
- [450] M. Badger and J. C. Lee, Drug Discov Today 2, 427-35 (1997).
- [451] K. B. Bodman and I. M. Roitt, Fund Am Clin Immunol 2, 73-81 (1994).
- [452] P. K. Wong, C. Cuello, J. V. Bertouch, P. J. Roberts-Thomson, M. J. Ahern, M. D. Smith and P. P. Youssef, J Rheumatol 28, 2634-36 (2001).
- [453] E. S. Snell, Br J Dermatol 94, 15-23 (1976).
- [454] J. T. Dingle, J. L. Gordon, B. L. Hazleman, C. G. Knight, D. P. Page Thomas, N. C. Phillips and I. H. Shaw, Nature 271, 372-73 (1978).
- [455] J. M. Metselaar, M. H. Wauben, J. P. Wagenaar-Hilbers, O. C. Boerman and G. Storm, Arthritis Rheum 48, 2059-66 (2003).
- [456] J. M. Metselaar, W. B. van den Berg, A. E. M. Holthuysen, M. H. M. Wauben, G. Storm and P. L. E. M. van Lent, Ann Rheum Dis 63, 348-53 (2004).
- [457] E. S. Chan and B. N. Cronstein, Arthritis Res 4, 266-73 (2002).
- [458] E. S. El Desoky, Curr Ther Res 62, 92-112 (2001).
- [459] W. C. Foong and K. L. Green, J Pharm Pharmacol 45, 204-09 (1993).
- [460] A. S. Williams, J. P. Camilleri and B. D. Williams, Br J Rheumatol 33, 530-33 (1994).
- [461] A. S. Williams, J. P. Camilleri, R. M. Goodfellow and B. D. Williams, Br J Rheumatol 35, 719-24 (1996).
- [462] A. S. Williams, J. P. Camilleri, N. Amos and B. D. Williams, Clin Exp Immunol 102, 560-65 (1995).
- [463] M. J. Rogers, J. C. Frith, S. P. Luckman, F. P. Coxon, H. L. Benford, J. Monkkonen, S. Auriola, K. M. Chilton and R. G. Russell, Bone 24, 73S-79S (1999).
- [464] T. Osterman, K. Kippo, L. Lauren, I. Pasanen, R. Hannuniemi and R. Sellman, Inflamm Res 46, 79-85 (1997).
- [465] N. Giuliani, M. Pedrazzoni, G. Passeri and G. Girasole, Scand J Rheumatol 27, 38-41 (1998).
- [466] N. Pennanen, S. Lapinjoki, A. Urtti and J. Monkkonen, Pharm Res 12, 916-22 (1995).
- [467] J. Monkkonen, M. Taskinen, S. O. Auriola and A. Urtti, J Drug Target 2, 299-308 (1994).
- [468] P. Van Lent, A. Holthuysen, N. van Rooijen, L. van de Putte and W. van den Berg, Ann Rheum Dis 57, 408-13 (1998).
- [469] P. Van Lent, A. Holthuysen, N. van Rooijen, F. A. van de Loo, L. van de Putte and W. van den Berg, J Rheumatol 25, 1135-45 (1998).

- [470] P. Barrera, A. Blom, P. Van Lent, L. van Bloois, J. Beijnen, N. van Rooijen, M. C. de Waal Malefijt, L. B. van de Putte, G. Storm and W. B. van den Berg, *Arthritis Rheum* 43, 1951-59 (2000).
- [471] G. Jadot, A. Vaille, J. Maldonado and P. Vanelle, *Clin Pharmacokinet* 28, 17-25 (1995).
- [472] A. M. Michelson and K. Puget, *Acta Physiol Scand Suppl* 492, 67-80 (1980).
- [473] A. M. Michelson and K. Puget, *C R Seances Soc Biol Fil* 173, 380-93 (1979).
- [474] Y. Niwa, K. Somiya, A. M. Michelson and K. Puget, *Free Radic Res Commun* 1, 137-53 (1985).
- [475] M. L. Corvo, O. C. Boerman, W. J. Oyen, L. Van Bloois, M. E. Cruz, D. J. Crommelin and G. Storm, *Biochim Biophys Acta* 1419, 325-34 (1999).
- [476] M. L. Corvo, J. C. S. Jorge, R. van't Hof, M. E. M. Cruz, D. J. A. Crommelin and G. Storm, *Biochim Biophys Acta* 1564, 227-36 (2002).
- [477] M. L. Corvo, M. B. F. Martins, A. P. Francisco, J. G. Morais and M. E. M. Cruz, *J Controlled Release* 43, 1-8 (1997).
- [478] J. R. Levick, *Arthritis Rheum* 24, 1550-60 (1981).
- [479] S.-A. Cryan, *AAPS Journal* 7, E20-E41 (2005).
- [480] G. Taylor and I. Kellaway, in *Drug Delivery and Targeting: For Pharmacists and Pharmaceutical Scientists*, edited A.M. Hillery, A.W. Lloyd and J. Swarbrick, Taylor & Francis, New York (2001), p.269-300.
- [481] R. W. Niven, T. M. Carvajal and H. Schreier, *Pharm Res* 9, 515-20 (1992).
- [482] S. J. Farr, I. W. Kellaway, D. R. Parry-Jones and S. G. Woolfrey, *Int J Pharm* 26, 303-16 (1985).
- [483] R. W. Niven and H. Schreier, *Pharm Res* 7, 1127-33 (1990).
- [484] A. G. Bailey, *J Electrostastics* 42, 25-32 (1997).
- [485] J. C. Waldrep, B. E. Gilbert, C. M. Knight, M. B. Black, P. W. Scherer and V. Knight, *Chest* 111, 316-23 (1997).
- [486] M. Vidgren, J. C. Waldrep, J. Arppe, M. Black, J. A. Rodarte, W. Cole and V. Knight, *Int J Pharm* 115, 209-16 (1995).
- [487] J. S. Patton, *Adv Drug Deliv Rev* 19, 3-36 (1996).
- [488] J. R. Wright, *Am J Physiol* 259, L1-L12 (1990).
- [489] A. D. Bangham, *Lung* 165, 17-25 (1987).
- [490] M. Geiser, M. Baumann, L. M. Cruz-Orive, V. Im Hof, U. Waber and P. Gehr, *Am J Respir Cell Mol Biol* 10, 594-603 (1994).
- [491] S. A. Barker, K. M. G. Taylor and M. D. Short, *Int J Pharm* 102, 159-65 (1994).
- [492] C. Khanna, D. E. Hasz, J. S. Klausner and P. M. Anderson, *Clin Cancer Res* 2, 721-34 (1996).
- [493] M. P. Lambros, D. W. Bourne, S. A. Abbas and D. L. Johnson, *J Pharm Sci* 86, 1066-69 (1997).
- [494] E. W. Alton, P. G. Middleton, N. J. Caplen, S. N. Smith, D. M. Steel, F. M. Munkonge, P. K. Jeffery, D. M. Geddes, S. L. Hart, R. Williamson, K. I. Fasold, A.

- D. Miller, P. Dickinson, B. J. Stevenson, G. McLachlan, J. R. Dorin and D. J. Porteous, *Nat Genet* 5, 135-42 (1993).
- [495] K. S. Konduri, S. Nandedkar, D. A. Rickaby, N. Düzgünes and P. R. J. Gangadharam, *Methods Enzymol* 391, 413-27 (2005).
- [496] S. M. Saari, M. T. Vidgren, V. M. Turjanmaa, M. O. Koskinen and M. M. Nieminen, *Respir Med* 97, 152-58 (2003).
- [497] K. F. Chung and P. J. Barnes, *Thorax* 54, 825-57 (1999).
- [498] P. J. Barnes, *N Engl J Med* 332, 868-75 (1995).
- [499] P. J. Barnes, S. Pedersen and W. W. Busse, *Am J Respir Crit Care Med* 157, S1-S53 (1998).
- [500] B. J. Lipworth, *Arch Intern Med* 159, 941-55 (1999).
- [501] K. S. Konduri, S. Nandedkar, N. Düzgünes, V. Suzara, J. Artwohl, R. Bunte and P. R. J. Gangadharam, *J Allergy Clin Immunol* 111, 321-27 (2003).
- [502] D. A. Thomas, M. A. Myers, B. Wichert, H. Schreier and R. J. Gonzalez-Rothi, *Chest* 99, 1268-70 (1991).
- [503] S. M. Saari, M. T. Vidgren, M. O. Koskinen, V. M. Turjanmaa, J. C. Waldrep and M. M. Nieminen, *Chest* 113, 1573-79 (1998).
- [504] E. Kanaoka, S. Nagata and K. Hirano, *Int J Pharm* 188, 165-72 (1999).
- [505] F. Y. Liu, Z. Shao, D. O. Kildsig and A. K. Mitra, *Pharm Res* 10, 228-32 (1993).
- [506] Y. Li and A. K. Mitra, *Pharm Res* 13, 76-79 (1996).
- [507] S. Dokka, D. Toledo, X. Shi, V. Castranova and Y. Rojanasakul, *Pharm Res* 17, 521-25 (2000).
- [508] M. B. Delgado-Charro and R. H. Guy, in *Drug Delivery and Targeting: For Pharmacists and Pharmaceutical Scientists*, edited A.M. Hillery, A.W. Lloyd and J. Swarbrick, Taylor & Francis, New York (2001), p.207-35.
- [509] G. Cevc, *Adv Drug Del Rev* 56, 675-711 (2004).
- [510] G. Cevc and G. Blume, *Biochim Biophys Acta* 1104, 226-32 (1992).
- [511] V. Aguiella, K. Kontturi, L. Murtomäki and P. Ramírez, *J Controlled Release* 21, 249-57 (1994).
- [512] G. Cevc, A. Schätzlein and H. Richardsen, *Biochim Biophys Acta* 1564, 21-30 (2002).
- [513] D. Kobayashi, T. Matsuzawa, K. Sugibayashi, Y. Morimoto and M. Kimura, *Pharm Res* 11, 96-103 (1994).
- [514] B. W. Barry and S. L. Bennett, *J Pharm Pharmacol* 39, 535-46 (1987).
- [515] S. J. Moloney, *Arch Dermatol Res* 280, 67-70 (1988).
- [516] M. Mezei and V. Gulasekharam, *Life Sci* 26, 1473-77 (1980).
- [517] M. Mezei and V. Gulasekharam, *J Pharm Pharmacol* 34, 1473-77 (1980).
- [518] M. Mezei and V. Gulasekharam, *J Pharm Pharmacol* 34, 473-74 (1982).
- [519] K. Egbaria, C. Ramachandram and N. Weiner, *Skin Pharmacol* 4, 21-28 (1991).
- [520] J. A. Bouwstra, P. L. Honeywell-Nguyen, G. S. Gooris and M. Ponec, *Prog Lipid Res* 42, 1-36 (2003).

- [521] H. E. Hofland, J. A. Bouwstra, H. E. Bodde, F. Spies and H. E. Junginger, *Br J Dermatol* 132, 853-66 (1995).
- [522] K. Kriwet and C. C. Muller-Goymann, *Int J Pharm* 125, 231-42 (1995).
- [523] D. Yarosh, C. Bucana, P. Cox, L. Alas, J. Kibitel and M. Kripke, *J Invest Dermatol* 103, 461-68 (1994).
- [524] M. Kirjavainen, A. Urtti, I. Jaaskelainen, T. M. Suhonen, P. Paronen, R. Valjakka-Koskela, J. Kiesvaara and J. Mönkkönen, *Biochim Biophys Acta* 1304, 179-89 (1996).
- [525] S. Zellmer, W. Pfiel and J. Lasch, *Biochim Biophys Acta* 237, 176-82 (1995).
- [526] K. Vrhovnik, J. Kristl, M. Sentjurc and J. Smid-Korbar, *Pharm Res* 15, 525-30 (1998).
- [527] M. E. M. J. Van Kuijk-Meuwissen, H. E. Junginger and J. A. Bouwstra, *Biochim Biophys Acta* 1371, 31-39 (1998).
- [528] R. Krishna, G. Ghiu and L. D. Mayer, *Histol Histopathol* 16, 693-99 (2001).
- [529] M. E. Meuwissen, J. Janssen, C. Cullander, H. E. Junginger and J. A. Bouwstra, *Pharm Res* 15, 352-56 (1998).
- [530] E. Touitou, N. Dayan, L. Bergelson, B. Godin and M. Eliaz, *J Controlled Release* 65, 403-18 (2000).
- [531] J. Du Plessis, C. Ramachandran, N. Weiner and D. G. Muller, *Int J Pharm* 103, 277-82 (1994).
- [532] M. Foldvari, A. Gesztes and M. Mezei, *J Microencapsul* 7, 479-89 (1990).
- [533] M. E. M. J. van Kuijk-Meuwissen, L. Mougin, H. E. Junginger and J. A. Bouwstra, *J Controlled Release* 56, 189-96 (1998).
- [534] N. Dayan and E. Touitou, *Biomaterials* 21, 1879 (2000).
- [535] A. Schatzlein and G. Cevc, *Br J Dermatol* 38, 583-92 (1998).
- [536] M. Schafer-Korting, H. C. Korting and E. Ponce-Poschl, *Clin Investig* 72, 1086-91 (1994).
- [537] H. C. Korting, H. Zienicke, M. Schafer-Korting and O. Braun-Falco, *Eur J Clin Pharmacol* 39, 349-51 (1990).
- [538] G. Cevc and G. Blume, *Biochim Biophys Acta* 1663, 61-73 (2004).
- [539] M. E. Planas, P. Gonzalez, L. Rodriguez, S. Sanchez and G. Cevc, *Anesth Analg* 75, 615-21 (1992).
- [540] R. Agarwal, A. Saraswat, I. Kaur, O. P. Katare and B. Kumar, *J Dermatol* 29, 529-32 (2002).
- [541] E. Touitou, N. Shaco-Ezra, N. Dayan, M. Jushynski, F. Rafaeloff and R. Azoury, *J Pharm Sci* 81, 131-34 (1992).
- [542] D. M. Ashcroft, A. Li Wan Po and C. E. Griffiths, *J Clin Pharm Ther* 25, 1-10 (2000).
- [543] M. F. Holick, F. N. Chimeh and S. Ray, *Br J Dermatol* 149, 370-76 (2003).
- [544] D. Fleisher, S. M. Niemiec, C. K. Oh, Z. Hu, C. Ramachandran and N. Weiner, *Life Sci* 57, 1293-97 (1995).
- [545] G. Cevc, *Clin Pharmacokinet* 42, 461-74 (2003).

- [546] G. Cevc, Crit Rev Ther Drug Carrier Syst 13, 257-388 (1996).
- [547] G. Cevc, D. Gebauer, J. Stieber, A. Schatzlein and G. Blume, Biochim Biophys Acta 1368, 201-15 (1998).
- [548] V. V. Ranade, J Clin Pharmacol 31, 401-18 (1991).
- [549] I. P. Kaur, A. Garg, A. K. Singla and D. Aggarwal, Int J Pharm 269, 1-14 (2004).
- [550] R. M. Mainardes, M. C. Urban, P. O. Cinto, N. M. Khalil, M. V. Chaud, R. C. Evangelista and M. P. Gremiao, Curr Drug Targets 6, 363-71 (2005).
- [551] V. H. Lee, P. T. Urrea, R. E. Smith and D. J. Schanzlin, Surv Ophthalmol 29, 335-48 (1985).
- [552] U. Schmidt-Erfurth, T. Hasan, K. Schomacker, T. Flotte and R. Birngruber, Lasers Surg Med 17, 178-88 (1995).
- [553] R. Z. Renno and J. W. Miller, Adv Drug Deliv Rev 52, 63-78 (2001).
- [554] H. van den Bergh, Semin Ophthalmol 16, 181-200 (2001).
- [555] V. H. L. Lee and J. J. Yang, in Drug Delivery and Targeting: For Pharmacists and Pharmaceutical Scientists, edited A.M. Hillery, A.W. Lloyd and J. Swarbrick, Taylor & Francis, New York (2001), p.145-83.
- [556] H. M. Patel and B. E. Ryman, FEBS Lett 62, 60-63 (1976).
- [557] H. M. Patel and B. E. Ryman, Biochem Soc Trans 5, 1739-41 (1977).
- [558] M. H. Richards and C. R. Gardner, Biochim Biophys Acta 543, 508-22 (1978).
- [559] D. S. Deshmukh, W. D. Bear and H. Brockhoff, Life Sci 28, 239-42 (1981).
- [560] K. Muramatsu, Y. Maitani and T. Nagai, Biol Pharm Bull 19, 1055-58 (1996).
- [561] H. Chen, V. Torchilin and R. Langer, J Controlled Release 42, 263-72 (1996).
- [562] S. Alonso-Romanowski, N. S. Chiaramoni, V. S. Lioy, R. A. Gargini, L. I. Viera and M. C. Taira, Chem Phys Lipids 122, 191-203 (2003).
- [563] M. Ramadas, W. Paul, K. J. Dileep, Y. Anitha and C. P. Sharma, J Microencapsul 17, 405-11 (2000).
- [564] K. Katayama, Y. Kato, H. Onishi, T. Nagai and Y. Machida, Drug Dev Ind Pharm 29, 725-31 (2003).
- [565] M. Ueno, T. Nakasaki, I. Horikoshi and N. Sakuragawa, Chem Pharm Bull 30, 2245-47 (1982).
- [566] C. Regnault, M. Soursac, M. Roch-Arveiller, E. Postaire and G. Hazebroucq, Biopharm Drug Dispos 17, 165-74 (1996).
- [567] Y. Maitani, M. Hazama, Y. Tojo, N. Shimoda and T. Nagai, J Pharm Sci 85, 440-45 (1996).
- [568] M. Fukunaga, M. M. Miller and L. J. Deftos, Horm Metab Res 23, 166-67 (1991).
- [569] J. A. Roger and K. E. Anderson, Crit Rev Ther Drug Carr Syst 15, 421-80 (1998).
- [570] J. C. Verhoef, H. E. Bodde, A. G. de Boer, J. A. Bouwstra, H. E. Junginger, F. W. Merkus and D. D. Breimer, Eur J Drug Metab Pharmacokinet 15, 83-93 (1990).
- [571] J. Lee and Y. W. Choi, Arch Pharm Res 26, 421-25 (2003).
- [572] S. P. Vyas, V. Sihorkar and P. K. Dubey, Pharmazie 56, 554-60 (2001).
- [573] T. Z. Yang, X. T. Wang, X. Y. Yan and Q. Zhang, Chem Pharm Bull 50, 749-53 (2002).

- [574] A. B. Lansley and G. P. Martin, in *Drug Delivery and Targeting: For Pharmacists and Pharmaceutical Scientists*, edited A.M. Hillery, A.W. Lloyd and J. Swarbrick, Taylor & Francis, New York (2001), p.238-68.
- [575] B. H. Jung, B. C. Chung, S. J. Chung, M. H. Lee and C. K. Shim, *J Controlled Release* 66, 73-39 (2000).
- [576] K. Muramatsu, Y. Maitani, K. Takayama and T. Nagai, *Drug Dev Ind Pharm* 25, 1099-105 (1999).
- [577] V. H. Lee, A. Yamamoto and U. B. Kompella, *Crit Rev Ther Drug Carrier Syst* 8, 91-192 (1991).
- [578] S. L. Law, K. J. Huang and H. Y. Chou, *J Controlled Release* 70, 375-82 (2001).
- [579] Y. Maitani, S. Asano, S. Takahashi, M. Nakagaki and T. Nagai, *Chem Pharm Bull* 40, 1569-72 (1992).
- [580] S. L. Law, K. J. Huang, V. H. Y. Chou and J. Y. Cherng, *J Liposome Res* 11, 165 - 74 (2001).
- [581] B. N. Ahn, S. K. Kim and C. K. Shim, *J Controlled Release* 34, 203-10 (1995).
- [582] K. Vermani and S. Garg, *Pharm Sci Technol Today* 3, 359-64 (2000).
- [583] Y. Song, Y. Wang, R. Thakur, V. M. Meidan and B. Michniak, *Crit Rev Ther Drug Carrier Syst* 21, 195-256 (2004).
- [584] S. K. Jain, R. Singh and B. Sahu, *Drug Dev Ind Pharm* 23, 827-30 (1997).
- [585] Z. Pavelic, N. Skalko-Basnet and I. Jalsenjak, *Eur J Pharm Sci* 8, 345-51 (1999).
- [586] Z. Pavelic, N. Skalko-Basnet and R. Schubert, *Int J Pharm* 219, 139-49 (2001).
- [587] Z. Pavelic, N. Skalko-Basnet and I. Jalsenjak, *Acta Pharm* 54, 319-30 (2004).
- [588] C. Tilcock, *Liposomes as Tools in Basic Research and Industry*. CRC Press, Boca Raton (1995).
- [589] A. A. Moss, J. Schrumpf, P. Schnyder, M. Korobkin and R. R. Shimshak, *Radiology* 131, 427-30 (1979).
- [590] C. Tilcock, M. Yap, M. Szucs and D. Utkhede, *Nucl Med Biol* 21, 165-70 (1994).
- [591] A. F. Turner, C. A. Presant, R. T. Proffitt, L. E. Williams, D. W. Winsor and J. L. Werner, *Radiology* 166, 761-65 (1988).
- [592] B. D. Williams, M. M. O'Sullivan, G. S. Sagg, K. E. Williams, L. A. Williams and J. R. Morgan, *Ann Rheum Dis* 46, 314-18 (1987).
- [593] V. D. Awasthi, B. Goins, R. Klipper and W. T. Phillips, *J Drug Target* 10, 419-27 (2002).
- [594] V. Awasthi, B. Goins, L. McManus, R. Klipper and W. T. Phillipsa, *Nucl Med Biol* 30, 159-68 (2003).
- [595] V. D. Awasthi, D. Garcia, B. A. Goins and W. T. Phillips, *Int J Pharm* 253, 121-32 (2003).
- [596] K. J. Harrington, M. Mubashar and A. M. Peters, *Q J Nucl Med* 46, 171-80 (2002).
- [597] V. P. Torchilin, in *Medical Applications of Liposomes*, edited D.D. Lasic and D. Papahadjopoulos, Elsevier Science B.V., Amsterdam (1998), p.515-43.
- [598] P. Lang, O. Meyer, M. F. Wendland and M. Saeed, US Patent 6,468,505 (2002).
- [599] V. P. Torchilin, *Curr Pharm Biotechnol* 1, 183-215 (2000).

- [600] T. Daemen, A. De Haan, A. Arkema and J. Wilschut, in *Medical Applications of Liposomes*, edited D. Lasic and D. Papahadjopoulos, Elsevier Science B.V., Amsterdam (1998), p.117-43.
- [601] R. Zeisig, I. Eue, M. Kosch, I. Fichtner and D. Arndt, *Biochim Biophys Acta* 1283, 177-84 (1996).
- [602] N. Settelen, O. Roch, D. Bock, R. Rooke, S. Braun and O. Meyer, *J Controlled Release* 94, 237-44 (2004).
- [603] G. Gregoriadis, *Immunol Today* 11, 89-97 (1990).
- [604] C. R. Alving, *Biochim Biophys Acta* 1113, 307-22 (1992).
- [605] N. Van Rooijen, in *Vaccines: New-generation Immunological Adjuvants*, edited G. Gregoriadis, Plenum Press, New York (1995), p.15-24.
- [606] R. Reddy, F. Zhou, L. Huang, F. Carbone, M. Bevan and B. T. Rouse, *J Immunol Methods* 141, 157-63 (1991).
- [607] F. Cornelius, *Biochim Biophys Acta* 1071, 19-66 (1991).
- [608] H. de Lima Santos, M. Leone Lopes, B. Maggio and P. Ciancaglini, *Colloids Surfaces B: Biointerfaces* 41, 239-48 (2005).
- [609] M. Lachaal, A. L. Rampal, J. Ryu, W. Lee, J. Hah and C. Y. Jung, *Biochim Biophys Acta* 1466, 379-89 (2000).
- [610] T. J. Wheeler, D. Cole and M. A. Hauck, *Biochim Biophys Acta* 1414, 217-30 (1998).
- [611] P. Lu, R. Liu and F. Sharom, *Eur J Biochem* 268, 1687-97 (2001).
- [612] H. Lautenschläger, in *Hanbook of Cosmetic Science and Technology*, edited M. Paye and H.I. Maibach A.O. Barel, Marcel Dekker, New York (2001), p.201-09.
- [613] S. Benita, M.-C. Martini and M. Seiller, in *Microencapsulation - Methods and Industrial Applications*, edited S. Benita, Marcel Dekker, New York (1996), Vol. 73, p.587-632.
- [614] D. D. Lasic, in *Handbook of Biological Physics*, edited R. Lipowsky and E. Sackmann, Elsevier Science B.V., Amsterdam (1995), p.491-519.
- [615] G. Betz, A. Aeppli, N. Menshutina and H. Leuenberger, *Int J Pharm* 296, 44-54 (2005).
- [616] P. Lampen, W. Pittermann, H. M. Heise, M. Schmitt, H. Jungmann and M. Kietzmann, *J Cosmet Sci* 54, 119-31 (2003).
- [617] C. F. Rosen, *Dermatol Ther* 16, 8-15 (2003).
- [618] J. Finley, L. C. Haynes, B. V. Lengerich, H. Levine, P. Mathewson and M. S. Otterburn, US Patent No 4,999,208 (1991).
- [619] B. A. Law and J. S. King, *J Diary Res* 52, 183-88 (1991).
- [620] W. Alkhalfaf, J. C. Piard, M. el Soda, J. C. Gripon, M. Desmezeaud and L. Vassal, *J Food Sci* 53, 1674-79 (1988).
- [621] B. C. Keller, *Trends Food Sci Tech* 12, 25-31 (2001).

Chapitre 3. Objectifs et hypothèses de recherche

3.1. Hypothèses de recherche

Il a été démontré que les formulations de type liposomal pouvaient accroître l'activité de l'ara-C. Cependant, un des inconvénients majeurs des liposomes réside dans le faible rendement d'incorporation de principes actifs hydrophiles. Nous avons donc émis l'hypothèse que ce problème pouvait être surmonté par l'emploi de vésicules multilamellaires connues sous l'appellation Sphérolites®. De telles vésicules ne seraient toutefois efficaces que si elles parvenaient à retenir encapsulée l'ara-C suffisamment longtemps *in vivo* afin d'augmenter sa demi-vie plasmatique.

De plus, il est connu que l'encapsulation de l'ara-C dans des vésicules lipidiques possédant un ligand spécifique à leur surface (*e.g.* immunoliposomes) permet d'améliorer son efficacité thérapeutique en augmentant sa concentration à l'intérieur des cellules ciblées. Cependant, dans le cas de l'ara-C, les bénéfices associés à l'accumulation cellulaire par endocytose sont partiellement contrecarrés par l'inactivation du principe actif à l'intérieur des lysosomes. Un moyen de pallier à ce problème est d'utiliser des vésicules pouvant libérer leur contenu rapidement dans l'endosome suite à leur capture par la cellule. De telles vésicules peuvent être obtenues par greffage d'un polymère sensible au pH qui déstabilise les liposomes aux valeurs de pH rencontrées dans l'endosome. Bien que plusieurs formulations liposomales sensibles au pH aient été décrites jusqu'à présent, leur stabilité modérée et leur élimination rapide par le SPM après administration intraveineuse ont constitué des obstacles majeurs à leur utilisation *in vivo*.

3.2. Objectifs généraux

L'étude des forces de cisaillement sur des mélanges de molécules tensioactives et d'eau a donné naissance à un nouveau système particulaire nommé Sphérolites®. Depuis, ces vésicules sont principalement utilisées en cosmétologie étant donné leur fort rendement d'encapsulation et leur propriété stabilisante lors de la préparation d'émulsion. Très peu d'études ont été effectuées afin de démontrer leur utilité en tant que vecteurs pharmaceutiques pour l'encapsulation de principes actifs. Le premier objectif de la présente thèse consiste à optimiser la préparation de Sphérolites® pour l'encapsulation de l'ara-C et de démontrer leur utilisation comme vecteurs exploitables en sciences pharmaceutiques. Le deuxième objectif de la thèse porte sur la préparation et l'utilisation d'une formulation liposomale stable en milieu physiologique, capable de cibler la forme active de l'ara-C spécifiquement vers les cellules cancéreuses. Pour ce faire, le polymère DODA-P(NIPAM-*co*-MAA) est ajouté à la préparation de liposomes. En réponse à une baisse de pH, ce polymère change de conformation et déstabilise la bicouche lipidique, ce qui engendre la libération du principe actif. L'anticorps anti-CD33 a été sélectionné afin de cibler les liposomes sensibles au pH aux cellules leucémiques exprimant l'antigène de surface CD33. Cette nouvelle formulation, combinant à la fois un ciblage actif et un mécanisme de libération du médicament, possède toutes les propriétés nécessaires afin d'augmenter le ciblage de l'ara-C dans le cytoplasme des cellules cancéreuses et par conséquent son efficacité thérapeutique.

3.2.1. Objectifs spécifiques

Plus spécifiquement, la préparation des Sphérolites® est divisée en trois objectifs principaux :

- 1) Développer une/des formulation(s) de Sphérolites® employant des excipients déjà approuvés pour un usage parentéral et possédant des diamètres inférieurs à 300 nm afin d'éviter leur capture immédiate par le SPM.
- 2) Obtenir des vésicules capables de retenir suffisamment longtemps la molécule active encapsulée.
- 3) Évaluer les paramètres de pharmacocinétique et de biodistribution de ces vecteurs PEGylés suite à leur administration intraveineuse chez un animal sain.

En second lieu, plusieurs objectifs spécifiques doivent être atteints pour la mise au point d'une formulation liposomale permettant le ciblage de l'ara-C vers les cellules leucémiques et d'y libérer leur contenu dans les organelles cellulaires désirées. Ces objectifs sont les suivants :

- 1) Vérifier à l'aide d'essais de phagocytose *in vitro* que les liposomes sensibles au pH ont la capacité d'échapper au système immunitaire.
- 2) Modifier l'anticorps anti-CD33 afin de le fixer à la surface des liposomes en conservant son affinité pour le récepteur.
- 3) Démontrer *in vitro* que ces immunoliposomes sensibles au pH sont spécifiques envers les cellules leucémiques exprimant l'antigène de surface CD33.
- 4) Vérifier que la libération du contenu de la formulation liposomale n'est pas affectée par la présence de l'anticorps et démontrer l'efficacité de cette formulation *in vitro* par l'entremise d'essais de cytotoxicité.
- 5) Évaluer les paramètres de pharmacocinétique et de biodistribution de ces immunoliposomes sensibles au pH suite à leur administration intraveineuse chez des souris saines et immunodéprimées porteuses de cellules leucémiques.
- 6) Tester l'efficacité thérapeutique des immunoliposomes sensibles au pH et d'autres formulations contrôles chez les souris immunodéprimées porteuses de tumeurs.

Chapitre 4. Preparation and *in vivo* evaluation of PEGylated formulations

Pierre Simard¹, Didier Hoarau², Mohamed Nabil Khalid¹, Emmanuelle Roux¹,
and Jean-Christophe Leroux^{1*}

¹Canada Research Chair in Drug Delivery, Faculty of Pharmacy, University of Montreal,
C.P. 6128 Succ. Centre-ville, Montreal (Qc) Canada H3C 3J7

²Ethypharm Inc., 200 boul. Armand Frappier, Laval (Qc) Canada H7V 4A6

Published in: Biochim Biophys Acta 1715, 37-48 (2005).

4.1. Abstract

Spherulites are multilamellar vesicles obtained by shearing a lamellar phase of lipids and surfactants. They consist of concentric bilayers of amphiphiles alternating with layers of aqueous medium in which hydrophilic drugs can be sequestered with high yield. To be useful for drug targeting applications, spherulites should be small and long circulating. The objectives of this work were threefold. First, the spherulite size was optimized to obtain a mean diameter of less than 300 nm. Second, the vesicle composition was adjusted to minimize *in vitro* leakage of internal content. Third, the spherulites were coated with 1,2-distearoyl-*sn*-glycero-3-phosphatidylethanolamine-*N*-[methoxy

poly(ethylene glycol)] (DSPE-PEG) to impart them with a long half-life. Then, the PEGylated spherulites (Phospholipon 90G/Solutol HS15/cholesterol/DSPE-PEG 2000 or 5000) were loaded with 1- β -D-arabinofuranosylcytosine (ara-C) and injected intravenously to rats. They were compared to uncoated spherulites and to an ara-C solution. The surface-modified vesicles exhibited long circulation times with areas under the blood concentration vs time curve exceeding by 3.1-6.9 fold that of uncoated spherulites. Similarly, blood levels of ara-C encapsulated in PEGylated vesicles were higher than those of the controls, but they did not parallel the carrier pharmacokinetics. Two hours post-injection, most of the drug was cleared from the systemic circulation, reflecting rapid leakage of ara-C from the vesicles.

4.2. Introduction

Colloidal carriers have been investigated mainly for the delivery of anticancer agents to solid tumors after intravenous (IV) administration. Liposomes represent the most studied particulate drug carriers and are now considered to be a mainstream drug delivery technology. However, without appropriate surface modifications, these vehicles may not be suitable for passive accumulation of cytostatics into tumors, partly due to adsorption of plasma proteins (opsonins) onto the phospholipid membrane, triggering recognition and uptake of the liposomes by the mononuclear phagocytic system (MPS) [1]. Besides, a variety of blood proteins are known to adsorb onto the carrier *in vitro* and *in vivo* [2-4], some of which can cause membrane destabilization and early leakage of entrapped content [5-7].

A major advance in liposome technology came with the advent of Stealth® carriers, a technology which relies on surface coating with a flexible, hydrophilic polymer, usually a lipid derivative of poly(ethylene glycol) (PEG), to provide steric stabilization of the vesicle.

The highly hydrated PEG corona on the liposome surface can reduce interactions between cells and lipid head groups, act as a barrier to the binding of opsonins [3, 8, 9] and/or hinder the association of liposome-bound opsonins with macrophage receptors [10]. In return, the zone of steric hindrance created by the hydrophilicity and the chain flexibility of PEG slows down liposomal clearance by the MPS, and consequently increases their localization in solid tumors [11, 12]. The restricted binding of serum opsonins promoted by PEG chains, also prevents early leakage of the encapsulated molecule [5, 6].

Liposomes rely on passive targeting to increase the localization of anticancer drugs in the vicinity of tumoral cells. Growing tumors possess vasculature with enhanced permeability as a result of the disease process [13, 14]. Pore diameters in tumor capillaries can range from approximately 100 to 400 nm [15, 16]. Therefore, drug-loaded liposomes must be small enough to extravasate from the blood into tumor interstitial space through these pores [17]. Furthermore, particle size was shown to be critical in achieving long circulation times; an inverse correlation exists between liposome size and uptake by macrophages [18] or circulation time *in vivo* [15].

One of the major drawbacks of liposomes remains their relatively low entrapment efficiency (EE) [19]. Successful approaches have been developed to increase the encapsulation yield of many antineoplastic drugs. Indeed, amphiphilic drugs that are weak bases or weak acids can be loaded into the liposome core using remote loading procedures like the ammonium sulphate and pH-gradient methods for doxorubicin [20] and vincristine [21], respectively. These approaches are generally associated with much higher EE. However, for drugs that are poorly or not at all ionisable or that exhibit a high molecular weight, remote loading methods may not be appropriate. Furthermore, most liposomal preparation methods require the use of organic solvents, which need to be removed from the formulation during the process [22].

Recently, a new solvent-free process to prepare well defined multilamellar vesicles (MLV) with high encapsulation efficiencies has been described [23, 24]. Diat *et al.* [23, 24] discovered that moderate shearing of a lyotropic lamellar phase of surfactants in the presence of a minimal amount of water could lead to the formation of MLV (Figure 4.1). Moreover, the overall polyhedral structure of these multilayered vesicles was conserved upon dilution [25]. The MLV so formed have been referred to as Spherulites[®]. The particle size can be controlled precisely by varying the shear rate [23, 24] and the components in the preparation [26]. Like liposomes, spherulites have rapidly found many applications as encapsulating systems [26-29]. Both are composed of phospholipids, except that the structure of spherulites is made of uniformly spaced concentric bilayers of amphiphiles alternating with layers of aqueous medium. The interlamellar distances between two constitutive layers and the bilayer thickness are always constant within a single vesicle as evidenced by X-ray diffraction analysis. However, the interlamellar distance may slightly increase upon the encapsulation of compounds such as short DNA fragments [30] and copper (II) ions [31]. This organized structure remains very stable in the dispersion medium [26, 28, 31] and confers high EE for a variety of compounds, such as copper salts [31], fluorescent dye [29], and macromolecules like proteins [27] and DNA [26, 32].

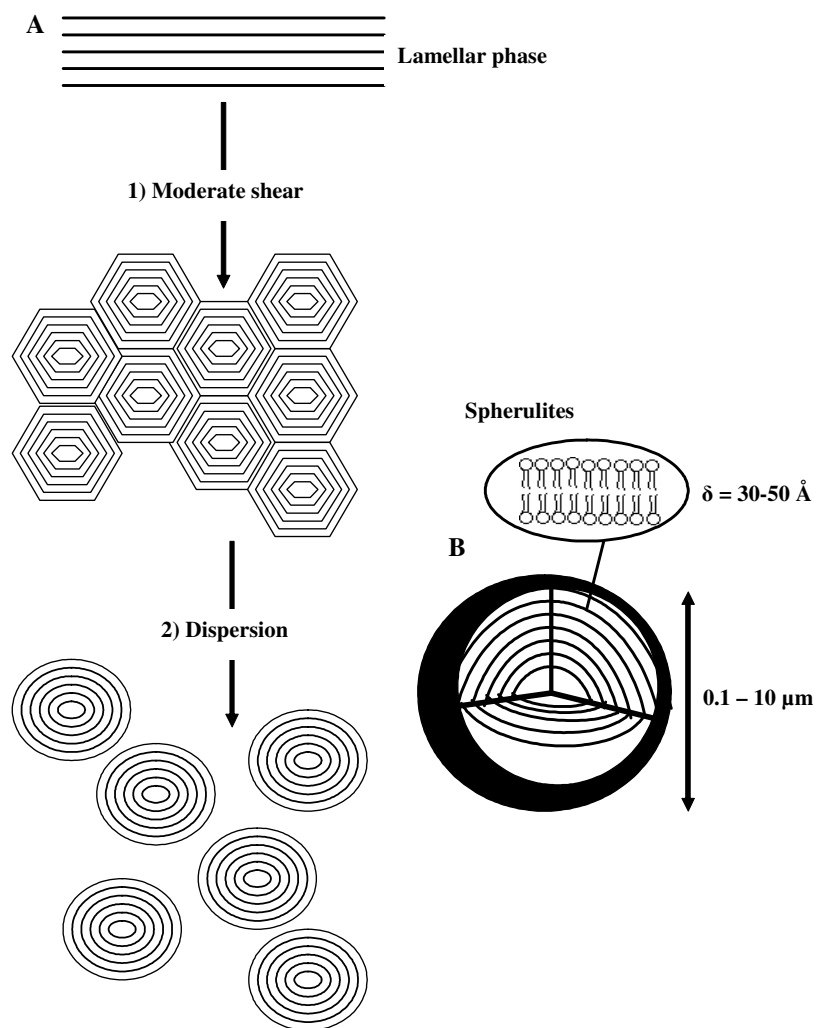


Figure 4.1. Process of preparation of spherulites in suspension (A) and a schematic representation of the spherulites structure (B). Spherulites are produced by applying a moderate shear to a lamellar phase of surfactant. The lamellar phase forms a close-packed organization of MLV in which regular stacking of surfactant bilayers ($n = 50\text{--}1000$ layers) are separated by aqueous layers. Compacted spherulites can be dispersed by adding an excess amount of solvent. The interlamellar distance between two constitutive layers and the bilayer thickness are typically between 50 and 200 Å. Reproduced from ref. [31] with permission.

Spherulites, as described in the literature, have diameters typically around 1 μm [25, 31] and are not suitable for drug targeting applications. Moreover, no pharmacokinetic study involving PEGylated spherulites has been published so far [33]. To be useful as drug delivery agents, these vesicles should exhibit a small size (<300 nm) and have a long circulating time. Accordingly, the objectives of this work were threefold. First, spherulites were prepared using amphiphiles approved for parenteral administration, and their size was optimized to obtain a diameter of less than 300 nm. Second, the vesicle composition was adjusted to minimize *in vitro* leakage of a model fluorescent dye. Third, the spherulites were coated with 1,2-distearoyl-*sn*-glycero-3-phosphatidylethanolamine-*N*-monomethoxy-PEG] (DSPE-PEG) to confer long circulation times to the vesicles after IV injection. In this study, we examined the effect of PEG chain length on the spherulite pharmacokinetic parameters and on the transport of a hydrophilic anticancer agent, *i.e.* 1- β -D-arabinofuranosylcytosine (ara-C). This drug, commonly used in the treatment of acute myelogenous leukaemias [34] represents an interesting model for delivery by sustained release systems due to its short biological half-life (16-20 min) [35, 36].

4.3. Material and methods

4.3.1. Material

Phospholipon® 90 G (P90) (94% of soybean phosphatidylcholine, PC) was a gift from Rhône-Poulenc Rörer (Köln, Germany). Lipoid® S75 (70% of soybean PC) was kindly provided by Lipoid GmbH (Ludwigshafen, Germany). Solutol® HS15 (PEG 660 12-hydroxystearate) was a gift from BASF (Ludwigshafen, Germany). DSPE-PEG 2000 and cholesterol (Chol, 99.5% pure) were obtained from Northern Lipids Inc. (Vancouver, BC, Canada). L- α -dioleoyl-phosphatidylethanolamine (DOPE) and DSPE-PEG 5000 were from Avanti Polar Lipids (Alabaster, AL). Tween® 20 (polyoxyethylene 20 sorbitan

monolaurate), Tween[®] 80 (polyoxyethylene 80 sorbitan monooleate), 2,4,6-trinitrobenzenesulfonic acid solution (TNBS) (1.7×10^{-1} M), Triton X-100, Sepharose[®] 2B, and ara-C were purchased from Sigma (St. Louis, MO). Trisodium 8-hydroxypyrene trisulfonate (HPTS) and *p*-xylene-bis-pyrimidium (DPX) were obtained from Molecular Probes (Eugene, OR). Sephadex[®] G-50 and G-100 were from Pharmacia Biotech (Uppsala, Sweden). [¹⁴C]-Cholesteryl oleate (52 mCi/mmol) and [³H]-ara-C (33 Ci/mmol) were purchased from Perkin Elmer (Boston, MA) and Amersham Pharmacia Biotech (Uppsala, Sweden), respectively. All products were used without further purification. Water was deionized with a MilliQ purification system (Millipore, Bedford, MA) before use.

4.3.2. Preparation of spherulites

Spherulites were prepared according to the procedure of Mignet *et al.* [26]. The lecithins and hydrophilic surfactants (Solutol HS15 or Tween) were precisely weighed and mixed. Then, a solution of NaCl 0.9% (*w/v*) was added and the mixture was hydrated overnight at room temperature. Spherulites were obtained through manual shearing of the lyotropic lamellar phase. Polarized light optical microscopy (Axiovert S100, Carl Zeiss Canada Ltée, Kirkland, Qc, Canada) was used to confirm the multilamellar properties of the vesicles. The lamellar phase presented a homogeneous birefringent texture characterized by Maltese crosses (Figure 4.2A) [23, 24]. Dilution of this preparation in saline led to the dispersion of vesicles without changing their structure, as ascertained by the presence of Maltese crosses. Formulations containing Chol were prepared using a similar method except that the lipid components were first dissolved in chloroform. The solvent was evaporated under reduced pressure, and the resulting film was further dried *in vacuo* (~ 0.1 mBar) for 30 min. The composition of all prepared formulations is listed in Table 4.1.

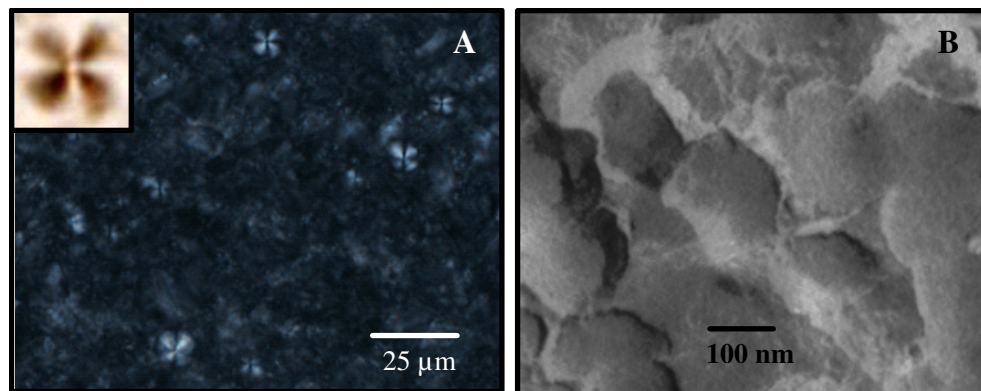


Figure 4.2. Polarization (**A**) and freeze-fracture electron micrograph (**B**) of a manually sheared spherulite sample (formulation 11). These non-diluted vesicles had a typical size about 200 nm and presented the birefringent texture.

4.3.3. Incorporation of DSPE-PEG

PEGylated spherulites were prepared by incubating preformed vesicles with DSPE-PEG (15 mg/mL) micelles for 1 h at 40°C, as described elsewhere for conventional liposomes [37]. This procedure allows PEG insertion in the outer leaflet only. The concentration of PEG represented 10 mol% of phospholipids exposed on the outside surface of spherulites (less than 1 mol% of total phospholipids). The amount of surface-exposed phospholipids was determined by the procedure of Barenholz *et al.* [38]. Spherulites (c.a. 280 nm) with 1% (*w/w*) DOPE were prepared and diluted with saline to a final volume of 0.6 mL (3.1 mg/mL total lipids/surfactant). Then, NaHCO₃ solution (0.2 mL, 0.8 M, pH 8.5) was mixed with the vesicle suspension. Twenty μL of 1.5% (*w/v*) TNBS were added and allowed to incubate in the dark for 30 min at ambient temperature. After the incubation

period, 0.4 mL of 2% (*v/v*) Triton X-100 in 1.5 N HCl was added to the sample to stop the reaction. The absorbance ($\lambda = 410$ nm) was measured on an Ultrospec 2000 spectrophotometer (Amersham Pharmacia Biotech, Uppsala, Sweden) within an hour after acidification. The total DOPE content was determined by the same procedure except that spherulites were first solubilized with 2.6% (*v/v*) of Triton X-100.

4.3.4. Freeze-fracture electron microscopy

The sheared lamellar phase was quenched using sandwich technique and liquid nitrogen-cooled propane. Using this technique, a cooling rate of 10,000°K/s is reached avoiding ice crystal formation and artefacts possibly caused by the cryofixation process. The cryo-fixed samples were stored in liquid nitrogen for less than 2 h before processing. The fracturing process was carried out in JEOL JED-9000 freeze-etching equipment and the exposed fracture planes were shadowed with Pt for 30 s in an angle of 25-35° and with carbon for 35 s (2kV/ 60-70mA, 0.13 nBar). The samples were cleaned with concentrated, fuming HNO₃ for 24 h followed by repeating agitation with fresh chloroform at least 5 times. The replicas cleaned this way were examined with a JEOL 100 CX electron microscope (Jeol USA, Peabody, MA).

4.3.5. Particle size analysis

Particle size was determined at ambient temperature by dynamic light scattering (DLS) at a 90° angle on a Coulter N4Plus (Coulter Electronics, Miami, FL) employing differential size distribution processor analysis. Measurements of the mean hydrodynamic diameter were performed in triplicate.

4.3.6. *In vitro* release of encapsulated compounds

4.3.6.1. Fluorescent dye (HPTS)

Spherulites were prepared as mentioned above except that the saline solution was replaced with a buffered solution of *N*-[2-hydroxyethyl]piperazine-*N'*-[2-ethanesulfonic acid] (HEPES) (20 mM, pH 7.4) containing the water-soluble fluorophore HPTS (35 mM) and the collisional quencher DPX (50 mM) [39]. Untrapped dye was removed by gel filtration over a Sephadex G-100 column (1 x 30 cm). The release of spherulite content was monitored at 37°C in HEPES buffer for 270 min at 37°C by a fluorescence dequenching assay on a Series 2 Aminco Bowman fluorimeter (Spectronics Instruments Inc, Rochester, NY). The extent of content release was calculated from HPTS fluorescence intensity ($\lambda_{\text{ex}} = 413$, $\lambda_{\text{em}} = 512$ nm) relative to measurement after vesicle disruption in 0.9% (v/v) Triton X-100, which gave complete release of encapsulated HPTS and DPX.

4.3.6.2. Ara-C

Lipids spiked with [¹⁴C]-cholesteryl oleate (57 pCi/mg total lipids/surfactant) were hydrated with a saline solution of ara-C (2% w/w of total lipids/surfactant) spiked with [³H]-ara-C (114 pCi/mg total lipids/surfactant) and the spherulites were prepared as described above. Drug loading was determined by radioactivity counting after separation of free ara-C from encapsulated ara-C by gel filtration over a Sephadex® G-50 (1.5 x 20 cm) column. Radioactivity was measured in a scintillation counter (Liquid Scintillation Analyser Tri-Carb 2100TR, Packard, Meriden, CT) after the addition of Hionic Fluor® scintillation cocktail. The EE was calculated using Equation 1:

$$\text{EE (\%)} = \frac{\text{AUC}_E}{\text{AUC}_T} \times 100 \quad \text{Eq. 1}$$

where AUC_E and AUC_T stand for area under the elution profile curve of the encapsulated and total drug in the feed, respectively.

The release of ara-C was assessed after incubation of radiolabeled spherulites in 50% (*v/v*) fresh rat serum at 37°C for 15 min. Released ara-C was separated from spherulites and excess serum components by gel filtration over a Sepharose® 2B column (1 x 30 cm) and assayed by radioactivity counting. The percentage of ara-C released was calculated with Equation 2.

$$\text{Ara-C released (\%)} = \frac{\text{AUC}_F}{\text{AUC}_T} \times 100 \quad \text{Eq. 2}$$

where AUC_F represents the area under the elution profile curve of the released drug. All experiments were conducted in triplicate.

4.3.7. *In vivo* pharmacokinetics and biodistribution

In vivo studies were carried out using male Sprague-Dawley rats (300-350 g) (Charles River, St-Constant, QC, Canada). The studies were approved by the Animal Welfare and Ethics Committee of the University of Montreal. The rats were surgically prepared for IV administration and arterial blood sampling, as previously described [40]. Briefly, polyethylene catheters were inserted into the femoral vein and artery, protected with a tethering system, and the rats were allowed to recover for at least 24 h. Ara-C-loaded spherulites labelled with [¹⁴C]-cholesteryl oleate and [³H]-ara-C were prepared as described in section 4.3.2.

The rats were subdivided into 4 groups (5 rats/group). The first group received only a saline solution of ara-C spiked with [³H]-ara-C, whereas the second, third and fourth groups were injected with ara-C loaded-spherulites that were respectively non-PEGylated or coated with 10 mol% of DSPE-PEG 2000 or 5000 (P90/Solutol HS15/Chol/DSPE-PEG, 57.4:14.8:27.2:0.6 mol%). The formulations (400 µL) were injected *via* the vein cannula with 0.33 µmol/kg of lipids, corresponding to 2.34 µg/kg ara-C, 6.2 µCi/kg of [³H]-ara-C and 5.7 µCi/kg of [¹⁴C]-cholesteryl oleate. Blood samples (400 µL) were collected at 5, 15, and 30 min, and 1, 2, 4, 8, 12 and 24 h post-injection. The rats were sacrificed after the last blood sampling point, weighed and perfused with saline, prior to harvesting liver, lungs, kidneys, spleen and heart. Blood and tissues were weighed and treated with Soluene 350® (Camberra Packard, Mississauga, ON, Canada). After digestion, blood samples were bleached by successive additions of hydrogen peroxide (H₂O₂, 30% v/v). The samples were left to stand in the dark overnight at 4°C following the addition of scintillation cocktail. Radioactivity was then measured using the scintillation counter in dual mode (³H/¹⁴C). Blood concentrations of spherulites and ara-C at the various time points were calculated on the assumption that blood represents 7.5% of rat body weight [41, 42]. The mean area under the blood concentrations *vs* time curve (AUC), the blood clearance (CL) and other pharmacokinetic parameters were determined using a non-compartmental model with PK Solutions 2.0 software (Summit Research Services, Montrose, CO, USA).

4.3.8. Statistical analysis

Differences in group means (multiple comparisons) were calculated by standard analysis of variance followed by the Kruskal-Wallis test to determine the significance of all paired combinations. The homogeneity of variances across groups was verified by Dunn's test (modified Nemenyi). A *P*-value ≤ 0.05 was considered significant

4.4. Results

4.4.1. Spherulite preparation characterization

Spherulite formulations with varying compositions were prepared and analyzed by DLS for size determination (Table 4.1). Figure 4.2B shows the freeze-fracture photomicrograph of a non-diluted sheared lamellar phase presenting the characteristic closely packed spherulite arrangement. Vesicles were obtained within a narrow range of surfactant (Tween or Solutol HS15), phospholipid (Lipoid S-75 or P90) and saline concentrations. Homogeneous multilamellar vesicles with average hydrodynamic diameters ranging between 180 and 340 nm were obtained when the proportion of surfactant and phospholipid comprised between 13-31% and 34-45% (*w/w*), respectively. As exemplified by formulations 5 to 8, size decreased with surfactant (Solutol HS15) concentration. It was not possible to formulate spherulites with diameters of less than 190 nm with the excipients listed in Table 4.1. Indeed, at very high surfactant concentrations (*i.e.* formulations 1 and 2), an isotropic effect was observed under polarized light microscopy. At the same concentration, Solutol HS 15 provided spherulite formulations with a slightly greater size than Tween 80 (compare formulations 4 and 6) and Tween 20 (compare formulations 10 and 11). The vesicles could withstand the addition of Chol up to 10% (*w/w*) (vs total lamellar phase components including the saline) or 27 mol% (vs lipid/surfactant). At 20% (*w/w*) (48 mol%) no spherulites were formed.

In order to avoid any interference with lamellar phase formation during the preparation process and to allow insertion of DSPE-PEG in the outer leaflet only, the lipid-PEG derivative was added to preformed spherulites after the dilution step. The proportion of PEG in the formulation corresponded to 10 mol% of surface-exposed phospholipids or 0.6 mol% of the total phospholipid content. The amount of PEG added was calculated on

the assumption that 14.4 ± 3.5 mol% of phospholipids were present on the external monolayer as determined by the TNBS assay. This value correlates well with that obtained by simple geometrical calculations for 200-nm spherulites (10% of the lipids) [29]. Decoration of the vesicles with PEG was not associated with a noticeable increase in diameter (data not shown), reflecting the difficulty to detect by DLS small size increments (5-7 nm) [37] for particles greater than 200 nm.

4.4.2. *In vitro* release of the fluorescent dye and ara-C

The release of HPTS was monitored over time for 3 different spherulite formulations (Figure 4.3). The release profile obtained for sample 4 (P90/Tween 80, 76:24 mol%) was characterized by a fast initial release and loss of 70% of the vesicle content within 7 min. The burst effect was significantly attenuated when Tween 80 was substituted for Solutol HS15 (formulation 9), and almost abolished after the incorporation of 27 mol% Chol (formulation 11). For these 2 systems, the release rate was almost constant and corresponded to 3.6 and 0.3 %/h, respectively. However, when incubated in 50% (v/v) plasma, the HPTS leakage from the formulation 11 increased significantly and reached approximately 50% after 3 h. Formulation 11, which exhibited the lowest leakage *in vitro*, was selected for further studies involving the anticancer drug, ara-C. Figure 4.4 shows the size exclusion chromatograms of both [³H]-ara-C and [¹⁴C]-labelled spherulites. The EE of ara-C was of 46 ± 1 % before the PEGylation step. After 15 min incubation in 50% (v/v) fresh rat serum at 37°C, uncoated, PEG 2000- and PEG 5000-coated spherulites released 57 ± 6 , 50 ± 2 and 43 ± 4 % of their cargo, respectively ($p \leq 0.05$ for PEG 5000 vs control). DLS analysis of the spherulite fraction revealed no change in vesicle mean size in the presence of serum (data not shown).

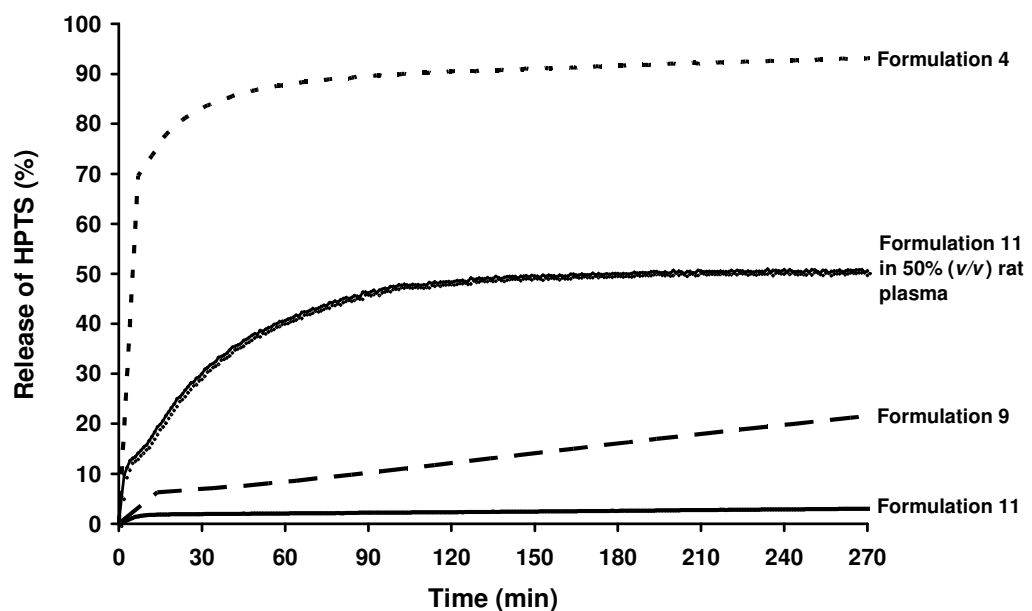


Figure 4.3. Release rate of encapsulated HPTS for formulations 4 (P90/Tween 80, 76:24 mol%, dotted line), 11 (P90/Solutol HS15/Chol, 58:15:27 mol%, solid line), and 9 (P90/Solutol HS15, 66:34 mol%, dashed line) in HEPES buffer at 37°C. The leakage of HPTS for the formulation 11 in 50% (v/v) rat plasma/HEPES buffer at 37°C is also presented as a function of time (bold dotted line). The extent of content release was calculated from HPTS fluorescence intensity ($\lambda_{\text{ex}} = 413$ nm, $\lambda_{\text{em}} = 512$ nm) relative to measurement after vesicle disruption in 0.9% (v/v) Triton X-100.

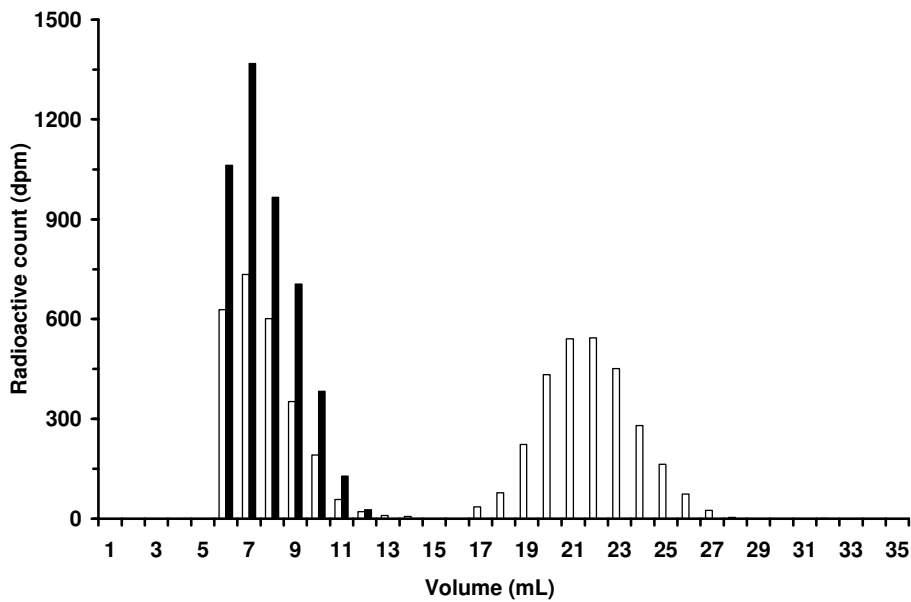
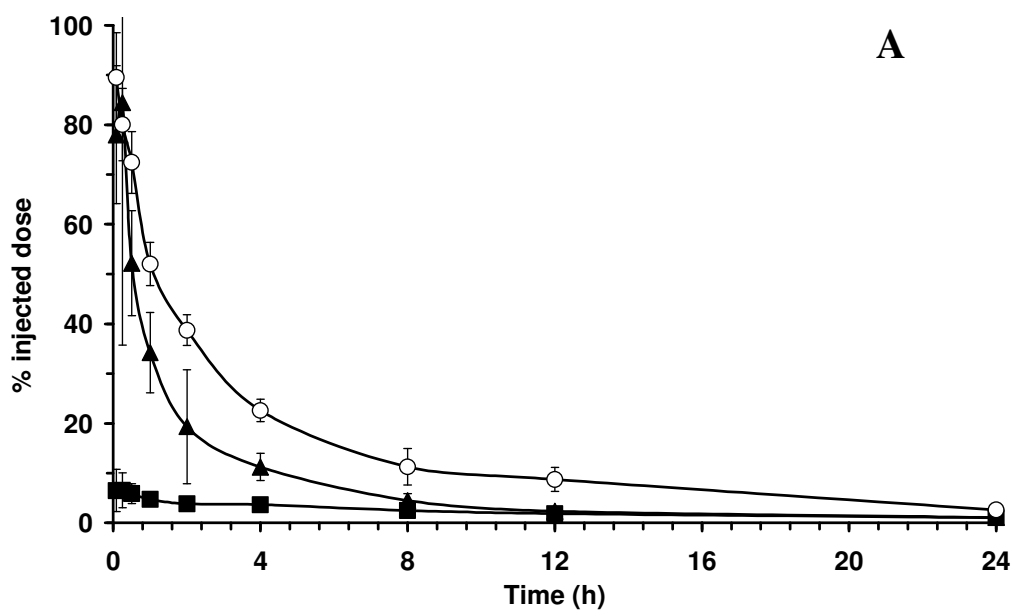


Figure 4.4. Elution profile of ara-C (open bars) and spherulites (P90/Solutol HS15/Chol, 58:15:27 mol%, closed bars) after passage over a Sephadex G50 column. The spherulites were labelled with 57 pCi/mg [^{14}C]-cholesteryl oleate and initially loaded with 2% drug (*w/w*) spiked with 114 pCi/mg [^3H]-ara-C. 46 ± 1% of ara-C was entrapped in the vesicles (*n* = 3).

4.4.3. Pharmacokinetic and Biodistribution

The pharmacokinetics and biodistribution of uncoated and PEGylated spherulites containing 0.9% (*w/w*) ara-C after purification, were assessed following IV administration to Sprague-Dawley rats (Figure 4.5A). Uncoated spherulites were rapidly cleared from the systemic circulation. Only 10% of the injected dose remained in the bloodstream 5 min after injection. As expected, the addition of PEG to the formulations significantly improved the circulation times. Indeed, it took 4 h and 12 h to eliminate 90% of the injected dose for

PEG 2000- and PEG 5000-coated vesicles, respectively. As shown in Table 4.2, PEGylation induced a 3.1 - 6.9 increase in AUC_{0-24h} vs the control formulation ($p \leq 0.05$). CL values also decreased accordingly. Figure 4.5B depicts the deposition of the carriers in various organs 24 h post-injection, a time point at which all formulations were eliminated from the bloodstream. Irrespective of their composition, the spherulites accumulated mainly in the organs of the MPS (liver and spleen), with the spleen demonstrating the highest vesicle concentration.



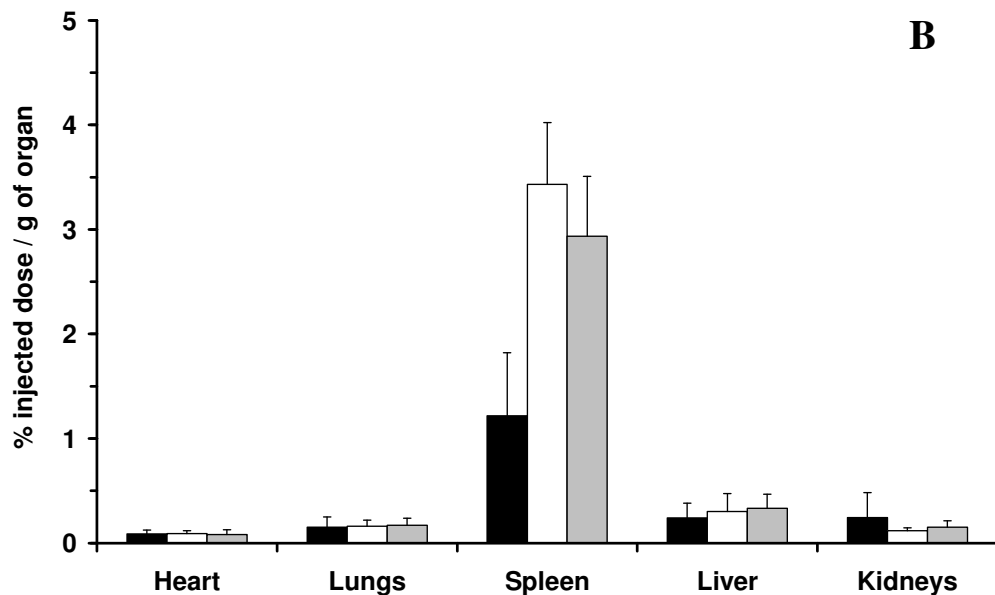
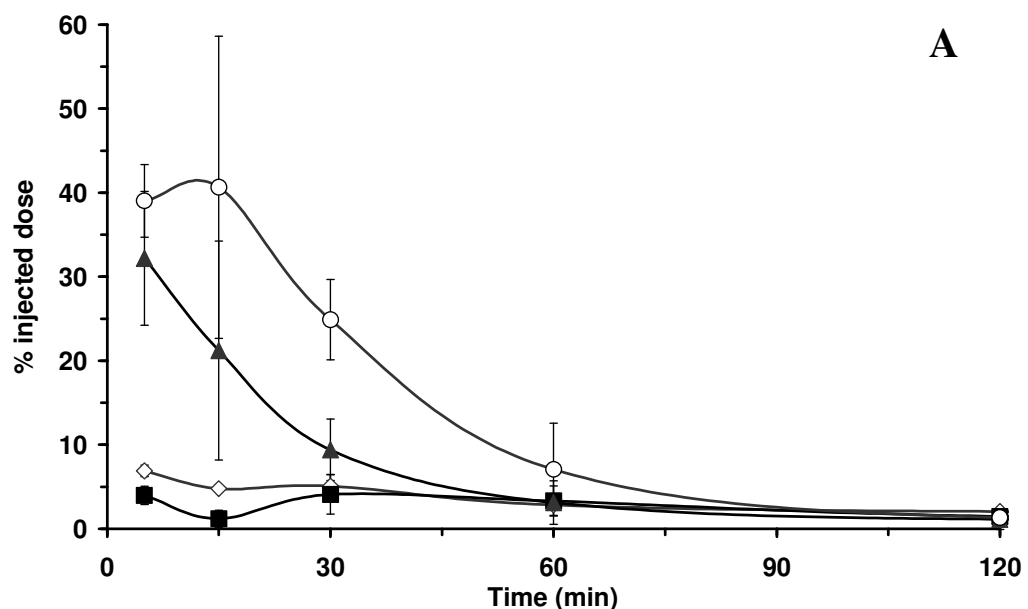


Figure 4.5. Blood concentration-time profiles (A) and tissue distribution 24 h post-administration (B) of uncoated (■, black bars), PEG 2000- (▲, white bars) and PEG 5000-coated spherulites (○, grey bars) (P90/Solutol HS15/Chol/DSPE-PEG, 57.4:14.8:27.2:0.6 mol%), after IV administration to rats. Spherulites were labelled with 0.25 µCi/mg [¹⁴C]-cholesteryl oleate. Each rat received 0.33 µmol/kg lipids/surfactant. Mean ± S.D (n = 5).

In parallel to the spherulite pharmacokinetics, the blood profiles of encapsulated ara-C were also monitored over time (Figure 4.5A). The formulations were compared to a solution of ara-C in saline. Both the free drug and ara-C entrapped in control spherulite formulation were rapidly eliminated, with approximately 5% of the injected dose remaining in the bloodstream 5 min after administration. As shown in Figure 4.6A and Table 4.2, the drug encapsulated in the PEGylated vesicles exhibited a 2.6 to 4.8-fold increase in AUC_{5-120min} ($p \leq 0.05$ for PEG 5000 vs control and free drug). However, 2 h

after injection, ara-C was completely cleared from the systemic circulation irrespective of the formulation. The encapsulated drug mainly accumulated in the liver (Figure 4.6B). As opposed to the spherulites, free ara-C was detected in the spleen (0.13 % injected dose/g of organ) at the end of the pharmacokinetic study. For all organs, drug accumulation remained low with less than 0.3% of the administered dose/g of organ found 24 h post injection.



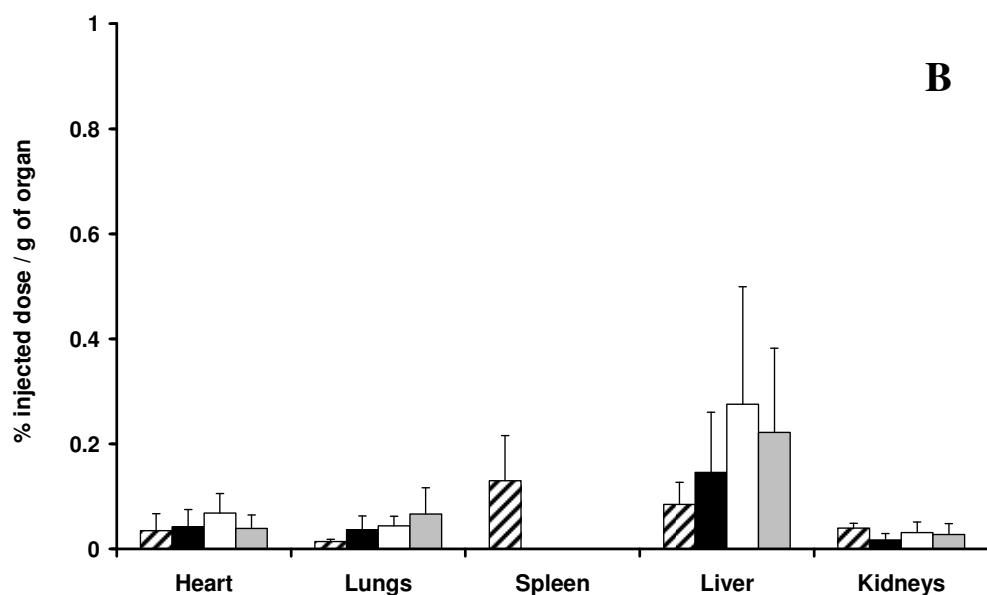


Figure 4.6. Blood concentration-time profiles (**A**) and tissue distribution 24 h post-administration (**B**) of free ara-C (right dashed bars) and ara-C loaded in uncoated (■, black bars), PEG 2000- (▲, white bars) and PEG 5000-coated spherulites (○, grey bars) (P90/Solutol HS15/Chol/DSPE-PEG, 57.4:14.8:27.2:0.6 mol%) after IV administration to rats. Spherulites were initially loaded with 2% (*w/w*) ara-C spiked with 100 μ Ci/mL [3 H]-ara-C. Free ara-C was removed by gel filtration over Sephadex G50. Each rat received 2.34 μ g/kg ara-C. Mean \pm S.D (n = 5).

4.5. Discussion

A simple method based on manual shearing of a lyotropic lamellar phase was used to prepare MLV composed of PC and surfactants. The first objective of this study was to optimize the spherulite size by modifying the formulation composition so as to obtain a

mean hydrodynamic diameter of less than 300 nm with monodisperse size distribution. The surfactants and phospholipids were selected based on their suitability for parenteral use. Spherulites were obtained following the application of an external shear force on well-defined lipid/surfactant/saline mixtures. Under moderate shear rate, the phospholipid/surfactant membranes are broken by the flow and wrapped around a spherical core forming the close-packed spherulite arrangement (Figures 4.1 and 4.2B). In this state, the orientation of the lamellar phase is not oriented with the membrane parallel to the flow direction velocity, as seen at very low and high shear rates [24, 27]. One characteristic of this intermediate state is that all spherulites formed under moderate shear rate have the same dimension. Moreover, the vesicle size can be correlated to the shear rate and amphiphile volume fraction [24, 43].

As shown in Table 4.1, the minimal size limit that could be reached was around 200 nm for a maximal surfactant concentration of approximately 30% (*w/w*). At higher surfactant concentrations, the organized lamellar arrangement was lost as revealed under polarized optical microscopy by the absence of Maltese crosses and the apparition of large aggregates upon dilution (data not shown). Although spherulites with diameters of 100 nm (polydisperse size) have been previously reported in the literature [44], such small vesicles were obtained with amphiphiles (*e.g.* macrogol oleate) that are not approved for parenteral use. The formulations could withstand the addition of 27 mol% Chol without affecting the structure of the sheared lamellar phase.

Table 4.1. Spherulite formulations and mean hydrodynamic diameters obtained by DLS.

Formulation	P90 (% w/w)	Lipoid S-75 (% w/w)	Solutol HS15 (% w/w)	Tween 20 (% w/w)	Tween 80 (% w/w)	Chol (% w/w)	NaCl(aq) (% w/w)	Mean Size ± S.D. (nm)
1		23			42		35	no spherulite
2		19	36				45	no spherulite
3		42			23		35	219 ± 38
4	42				23		35	190 ± 13
5	45		20				35	336 ± 42
6	42		23				35	238 ± 23
7	36		29				35	232 ± 31
8	34		31				35	183 ± 37
9	38		25				37	247 ± 65
10	42			13		10	35	216 ± 37
11	42		13			10	35	298 ± 26
12	34		11			20	35	no spherulite

The *in vitro* release kinetics of a model hydrophilic dye (*i.e.* HPTS) was investigated using three different spherulite formulations with mean diameters of ca. 250 nm. It has been previously reported that the long-term stability of spherulites is limited by the relatively high permeability of the surfactant/lipid bilayers [44]. However, it was found that the nature of surfactant greatly influenced leakage from the spherulites. Indeed, replacing Tween 80 by Solutol HS15 resulted in a strong reduction of the release rate (Figure 4.2). As both surfactants display the same hydrophilic–lipophilic balance value (HLB ≈ 15) [45] and same alkyl chain length (C₁₈), the change in permeability might be explained by a difference in membrane packing. The two surfactants have different polar head configurations, and the alkyl chain of Solutol HS 15 is saturated whereas that of Tween 80 is unsaturated. Indeed, it was reported that unsaturated alkyl chains produce a looser packing of liposomal membranes than saturated ones, which results in increased permeability for organic molecules [46-48]. Moreover, we showed that the addition of Chol (27 mol%) in the formulations further reduced dye leakage. This was expected since incorporation of Chol in lipidic vesicles has been shown to increase packing densities of phospholipid molecules [49], and thus reduce bilayer permeability to aqueous compounds

[48, 50]. From a pharmaceutical viewpoint, continuous leakage under storage conditions, even at a slow rate, is problematic as the spherulites would progressively empty their content. However, an interesting feature of the system is that the sheared lamellar phase can be stable for several months before the dilution step [31]. Therefore, in order to prevent excessive drug leakage during storage, the formulation could simply be diluted extemporaneously prior to its administration. In biological fluids, the spherulites were found to be relatively leaky, which is a concern when a long circulation time is sought.

As PEG was reported to protect the bilayer membrane from destabilization by lipoproteins [7, 51], its ability to reduce the diffusion of encapsulated molecules was examined both *in vitro* and *in vivo* for the spherulites composed of P90/Solutol HS15/Chol (58:15:27 mol%, formulation 11). The anticancer drug ara-C was entrapped in these spherulites with 46% efficiency. This entrapment yield compared advantageously to those reported for reverse-phase evaporation vesicles, MLV and small unilamellar vesicles, with EE of 15-20%, 5-7% and 1-2%, respectively [19]. Moreover, liposomes with the same composition (P90/Solutol HS15/Chol; 58:15:27 mol%) and size (270 nm) prepared by lipid hydration followed by extrusion yielded an EE of only 16% (data not shown). The relatively high EE obtained with spherulite technology can be explained by the preparation process. The latter allows the formation of a concentrated lamellar phase where the spherulites are in contact with each other and separated by only a thin aqueous layer at the vesicle junction [25] (Figure 4.2B). If a hydrophilic molecule is dissolved in the lamellar phase prior to applying the shear, it will be inserted in the water layers of the spherulites. However, the EE for ara-C was lower than expected, as yields greater than 80% were previously reported for macromolecules, such as proteins or DNA [26, 27]. Drug loss may occur by fragmentation of the most external layers during the dispersion process [52] and may be more important for smaller vesicles and molecules with low molecular weight.

Incubation of ara-C-loaded spherulites in 50% (*v/v*) rat serum was accompanied by a substantial loss of drug (almost 50% within 15 min), which was slightly lower for the PEGylated formulations. For the same incubation time and in the presence of blood proteins, the leakage of ara-C from uncoated spherulites was higher than for HPTS, probably due to the lower MW of the drug. Regarding the coated vehicles, it has been reported that PEG-lipid derivatives, when incorporated in appropriate concentrations, increase the lipid packing order and reducing the leakage of encapsulated hydrophilic substances [5, 6, 53]. The effect of PEG-5000 in diminishing drug leakage was significant compared to the control (43 vs 57%). Still, even PEGylated spherulites may readily interact with small amphiphiles (*e.g.* lysolecithins, peptides, and fatty acids) present in serum [51]. In contrast to larger proteins, these small molecules may exert their destabilizing effect despite the presence of the steric PEG-barrier.

Attachment of PEG to the liposomal surface was repeatedly shown to increase colloidal stability, as well as prolong the lifetime of the liposomes *in vivo* [54]. An interesting feature of this work, was that the amount of PEG added represented only 0.6 mol% of total spherulite components, which is far less than the 5-6 mol% PEG-lipid concentration commonly used in liposome formulations [9, 55]. However, as it was incorporated to preformed spherulites, its surface concentration amounted to 10 mol%. At this concentration, PEG provided spherulites and their encapsulated drug with longer circulation times *vs* the control formulations. Owing to its greater exclusion volume [56], PEG 5000 was more efficient than PEG 2000, in extending the spherulite half-life (128 *vs* 50 min). The PEGylated formulations were cleared more rapidly than stealth 100-nm liposomes composed of partially hydrogenated egg PC/Chol/DSPE-PEG 1900, which exhibit half-lives reaching 15.3 h in rats [11]. This could be partly attributed to the larger size of the spherulites [16] as well as to their composition, which may be more prone to opsonization. Twenty-four hours post-injection, spherulites were found in high proportions in the spleen, reflecting the splenic filtration of large sized (220-300 nm) long-circulating

colloids [57]. Likewise, ara-C was associated with a significantly higher blood AUC_{5-120min} when incorporated in PEGylated spherulites. However, 2 h after dosing, the drug was virtually eliminated (Figure 4.6A) from the bloodstream, whereas 19-39% of PEG-coated formulations was still circulating (Figure 4.5A). These results illustrate the rapid drug loss from the vesicles in biological fluids. This rapid leakage was previously reported for MLV-encapsulated [³H]-ara-C (PC/Chol/stearylamine), where only 0.86% of the injected dose remained in the bloodstream 3 h after IV administration [58]. However, Allen et al. [59] shown that prolonged circulation time and dose-independent pharmacokinetics have been observed for liposome-entrapped ara-C in mice bearing L1210 leukaemia. They demonstrated that the inclusion of free ara-C in a formulation presenting a slow leakage rate (HSPC/Chol/DSPE-PEG) resulted in a significant improvement in therapeutic effect.

Table 4.2. Mean pharmacokinetic parameters of spherulites and ara-C, free or encapsulated in uncoated and PEGylated spherulites (P90/Solutol HS15/Chol/DSPE-PEG, 57.4:14.8:27.2:0.6 mol%), after bolus IV administration to rats. Each data point is mean \pm S.D (n = 5 rats/group).

	AUC _{0-24h} spherulites ($\mu\text{g} \cdot \text{min}/\text{mL}$)	AUC _{∞} spherulites ($\mu\text{g} \cdot \text{min}/\text{mL}$)	T _{1/2} spherulites (min)	CL spherulites (mL/min)	AUC _{5-120min} ara-C* ($\mu\text{g} \cdot \text{min}/\text{mL}$)
Free ara-C	-	-	-	-	14.0 \pm 1.3
Uncoated spherulites	2 203 \pm 217	3 038 \pm 449	< 5	3.4 \pm 0.3	12.8 \pm 4.2
Spherulites-DSPE-PEG 2000	6 860 \pm 1 120	7 497 \pm 1 171	50 \pm 14	1.1 \pm 0.2	42.4 \pm 16.9
Spherulites-DSPE-PEG 5000	15 207 \pm 2 490	16 760 \pm 3 008	128 \pm 30	0.5 \pm 0.1	69.2 \pm 11.0

*The other pharmacokinetic parameters of ara-C could not be determined due to lack of data points within the first 2 h post-injection.

4.6. Conclusion

This work was the first attempt to apply spherulite technology to the encapsulation of an anticancer drug and presented the first pharmacokinetic study conducted with such PEGylated vesicles. Owing to their simple preparation process and high entrapment efficiency, these vesicles appear as attractive alternative drug delivery system to conventional liposomes. In addition, like liposomes, they can be coated with PEG-lipid derivatives to acquire long circulation times. Future work should now be aimed at minimizing content leakage in biological fluids and further downsizing the vesicles. This could be achieved by changing the phospholipid/surfactant composition (*e.g.* use of high phase transition lipids) and finely tuning the Chol content.

4.7. Acknowledgments

This project was partially funded by the Canada Research Chair Program. We extent our gratitude to Corrine Degert and René Laversanne (Ethypharm) for helpful discussions and their expertise on spherulites, and to Marie-Christine Jones and Thomas O'Hare for their critical reading of the manuscript.

4.8. References

- [1] J.H. Senior, Fate and behaviour of liposomes in vivo: a review of controlling factors, *Crit. Rev. Ther. Drug Carrier Syst.* 3 (1987) 123-193.
- [2] H.M. Patel, Serum opsonins and liposomes: their interaction and opsonophagocytosis, *Crit. Rev. Ther. Drug Carrier Syst.* 9 (1992) 39-90.

- [3] D.D. Lasic, F.J. Martin, A. Gabizon, S.K. Huang and D. Papahadjopoulos, Sterically stabilized liposomes: a hypothesis on the molecular origin of the extended circulation times, *Biochim. Biophys. Acta* 1070 (1991) 187-192.
- [4] S.C. Semple, A. Chonn and P.R. Cullis, Interactions of liposomes and lipid-based carrier systems with blood proteins: Relation to clearance behaviour *in vivo*, *Adv. Drug Deliv. Rev.* 32 (1998) 3-17.
- [5] M. Silvander, M. Johnsson and K. Edwards, Effects of PEG-lipids on permeability of phosphatidylcholine/cholesterol liposomes in buffer and in human serum, *Chem. Phys. Lipids* 97 (1998) 15-26.
- [6] A.N. Nikolova and M.N. Jones, Effect of grafted PEG-2000 on the size and permeability of vesicles, *Biochim. Biophys. Acta* 1304 (1996) 120-128.
- [7] T. Ishida, H. Harashima and H. Kiwada, Liposome clearance, *Biosci. Rep.* 22 (2002) 197-224.
- [8] A. Chonn and P.R. Cullis, Ganglioside GM1 and hydrophilic polymers increase liposome circulation times by inhibiting the association of blood proteins, *J. Liposome Res.* 2 (1992) 397-410.
- [9] G. Blume and G. Cevc, Molecular mechanism of the lipid vesicle longevity *in vivo*, *Biochim. Biophys. Acta* 1146 (1993) 157-168.
- [10] A. Klibanov, K. Maruyama, A.M. Beckerleg, V. Torchilin and L. Huang, Activity of amphiphatic poly(ethylene glycol) 5000 to prolong the circulation time of liposomes depends on the liposome size and is unfavorable for immunoliposomes binding to target, *Biochim. Biophys. Acta* 1062 (1991) 142-148.
- [11] D. Papahadjopoulos, T.M. Allen, A. Gabizon, E. Mayhew, K. Matthay, S.K. Huang, K.-D. Lee, M.C. Woodle, D.D. Lasic, C. Redemann and F.J. Martin, Sterically stabilized liposomes: Improvements in pharmacokinetics and antitumor therapeutic efficacy, *Proc. Natl. Acad. Sci. USA* 88 (1991) 11460-11464.
- [12] A. Gabizon and F. Martin, Polyethylene glycol-coated (pegylated) liposomal doxorubicin, *Drugs* 54 Suppl. 4 (1997) 15-21.
- [13] R.K. Jain, Transport of molecules across tumor vasculature, *Cancer Metastasis Rev.* 6 (1987) 559-593.
- [14] H.F. Dvorak, J.A. Nagy, J.T. Dvorak and A.M. Dvorak, Identification and characterization of the blood vessels of solid tumors that are leaky to circulating macromolecules, *Am. J. Pathol.* 133 (1988) 95-109.
- [15] O. Ishida, K. Maruyama, K. Sasaki and M. Iwatsuru, Size-dependent extravasation and interstitial localization of polyethyleneglycol liposomes in solid tumor-bearing mice, *Int. J. Pharm.* 190 (1999) 49-56.

- [16] D.C. Litzinger, A.M.J. Buiting, N. van Rooijen and L. Huang, Effect of liposome size on the circulation time and intraorgan distribution of amphipathic poly(ethylene glycol)-containing liposomes, *Biochim. Biophys. Acta* 1190 (1994) 99-107.
- [17] F. Yuan, M. Leunig, S.K. Huang, D.A. Berk, D. Papahadjopoulos and R.K. Jain, Microvascular permeability and interstitial penetration of sterically stabilized (stealth) liposomes in a human tumor xenograft, *Cancer Res.* 54 (1994) 3352-3356.
- [18] T.M. Allen, G.A. Austin, A. Chonn, L. Lin and K.C. Lee, Uptake of liposomes by cultured mouse bone marrow macrophages: influence of liposome composition and size, *Biochim. Biophys. Acta* 1061 (1991) 56-64.
- [19] F. Hong and E. Mayhew, Therapy of central nervous system leukemia in mice by liposome- entrapped 1-beta-D-arabinofuranosylcytosine, *Cancer Res.* 49 (1989) 5097-5102.
- [20] L.D. Mayer, M.B. Bally, M.J. Hope and P.R. Cullis, Techniques for encapsulating bioactive agents into liposomes, *Chem. Phys. Lipids* 40 (1986) 333-45.
- [21] N.L. Boman, D. Masin, L.D. Mayer, P.R. Cullis and M.B. Bally, Liposomal vincristine which exhibits increased drug retention and increased circulation longevity cures mice bearing P388 tumors, *Cancer Res.* 54 (1994) 2830-2833.
- [22] C. Witschi and E. Doelker, Residual solvents in pharmaceutical products: acceptable limits, influences on physicochemical properties, analytical methods and documented values, *Eur. J. Pharm. Biopharm.* 43 (1994) 215-242.
- [23] O. Diat and D. Roux, Preparation of monodisperse multilayer vesicles of controlled size and high encapsulation ratio, *J. Phys. II France* 3 (1993) 9-14.
- [24] O. Diat, D. Roux and F. Nallet, Effect of shear on a lyotropic lamellar phase, *J. Phys. II France* 3 (1993) 1427-1452.
- [25] T. Gulik-Krzywicki, J.C. Dedieu, D. Roux, C. Degert and R. Laversanne, Freeze-fracture electron microscopy of sheared lamellar phase, *Langmuir* 12 (1996) 4668-4671.
- [26] N. Mignet, A. Brun, C. Degert, B. Delord, D. Roux, C. Hélène, R. Laversanne and J.-C. François, The Spherulites: a promising carrier for oligonucleotide delivery, *Nucleic Acids Res.* 28 (2000) 3134-3142.
- [27] A. Bernheim-Grosswasser, S. Ugazio, F. Gauffre, O. Viratelle, P. Mahy and D. Roux, Spherulites: A new vesicular system with promising applications. An example: Enzyme microencapsulation, *J. Chem. Phys.* 112 (2000) 3424-3430.
- [28] O. Freund, J. Amédée, D. Roux and R. Laversanne, In vitro and in vivo stability of new multilamellar vesicles, *Life Sci.* 67 (2000) 411-419.

- [29] P. Chenevier, B. Delord, J. Amédée, R. Bareille, F. Ichas and D. Roux, RGD-functionalized Spherulites as targeted vectors captured by adherent cultured cells, *Biochim. Biophys. Acta* 1593 (2002) 17-27.
- [30] T. Pott and D. Roux, DNA intercalation in neutral multilamellar membranes, *FEBS Lett.* 511 (2002) 150-154.
- [31] F. Gauffre and D. Roux, Studying a new type of surfactant aggregate ("spherulites") as chemical microreactors. A first example: copper ion entrapping and particle synthesis, *Langmuir* 15 (1999) 3738-3747.
- [32] O. Freund, P. Mahy, J. Amedee, D. Roux and R. Laversanne, Encapsulation of DNA in new multilamellar vesicles prepared by shearing a lyotropic lamellar phase, *J. Microencapsulation* 17 (2000) 157-168.
- [33] O. Freund, Biodistribution and gastrointestinal drug delivery of new lipidic multilamellar vesicles, *Drug Deliv.* 8 (2001) 239-44.
- [34] M.J. Keating, K.B. McCredie, G.P. Bodey, T.L. Smith, E. Gehan and E.J. Freireich, Improved prospects for long term survival in adults with acute myelogenous leukemia, *J. Am. Med. Assoc.* 248 (1982) 2481-2486.
- [35] J. Borsa, G.R. Whitmore, F.A. Valeriote, D. Collins and W.R. Bruce, Studies on the persistence of methotrexate, cytosine arabinoside, and Leucovorin in the serum of mice, *J. Natl. Cancer Inst.* 42 (1969) 235-242.
- [36] B.C. Baguley and E.M. Falkenhaug, Plasma half-life of cytosine arabinoside (NSC-63878) in patients treated for acute myeloblastic leukaemia, *Cancer Chemother. Rep.* 55 (1971) 291-298.
- [37] P.S. Uster, T.M. Allen, B.E. Daniel, C.J. Mendez, M.S. Newman and G.Z. Zhu, Insertion of poly(ethylene glycol) derivatized phospholipid into pre-formed liposomes results in prolonged in vivo circulation time, *FEBS Lett.* 386 (1996) 243-246.
- [38] Y. Barenholz, D. Gibbes, B.J. Litman, J. Goll, T.E. Thompson and F.D. Carlson, A simple method for the preparation of homogenous phospholipid vesicles, *Biochemistry* 16 (1977) 2806-2810.
- [39] D.L. Daleke, K. Hong and D. Papahadjopoulos, Endocytosis of liposomes by macrophages: binding, acidification and leakage of liposomes monitored by a new fluorescence assay, *Biochim. Biophys. Acta* 1024 (1990) 352-366.
- [40] P. Moreau, L. Lamarche, A. K.-Laflamme, A. Calderone, N. Yamaguchi and J.d. Champlain, Chronic hyperinsulinaemia and hypertension: the role of the sympathetic nervous system, *J. Hypertension* 13 (1995) 333-340.
- [41] W.A. Ritschel, In vivo animal models for bioavailability assessment, *STP Pharma* 3 (1987) 125-141.

- [42] P. Calvo, B. Gouritin, H. Chacun, D. Desmaële, J. D'Angelo, J.P. Noel, D. Georghiou, E. Fattal, J.-P. Andreux and P. Couvreur, Long circulating PEGylated polycyanoacrylate nanoparticles as new drug carrier for brain delivery, *Pharm. Res.* 18 (2001) 1157-1166.
- [43] E. van der Linden and T. Hogervorst, Relation between the size of lamellar droplets in onion phases and their effective surface tension, *Langmuir* 12 (1996) 3127-3130.
- [44] M. Genty, G. Couarraze, R. Laversanne, C. Degert, J. Maccario and J.-L. Grossiord, Complex dispersions of multilamellar vesicles: a promising new carrier for controlled release and protection of encapsulated molecules, *J. Controlled Release* 90 (2003) 119-133.
- [45] A. Wade and P. Weller, *Handbook of Pharmaceutical Excipients*, American Pharmaceutical Association, Washington DC, 1994.
- [46] D. Rickwood and B.D. Hames, *Liposomes: A practical approach*, Editions R.R.C. New ed., IRL Press, Liverpool, 1990.
- [47] R. Urquhart, R.Y.S. Chan, Q.-T. Li, L. Tilley, F. Grieser and W.H. Sawyer, w-6 and w-3 fatty acids: monolayer packing and effects on bilayer permeability and cholesterol exchange, *Biochemistry Int.* 26 (1992) 831-841.
- [48] R.A. Demel, S.C. Kinsky, C.B. Kinsky and L.L.M. van Deesen, Effects of temperature and cholesterol on the glucose permeability of liposomes prepared with neutral and synthetic lecithins, *Biochim. Biophys. Acta* 150 (1968) 655-665.
- [49] R.A. Demel and B. De Kruyff, The function of sterols in membranes, *Biochim. Biophys. Acta* 457 (1976) 109-132.
- [50] D. Papahadjopoulos, M. Cowden and H. Kimelberg, Role of cholesterol in membranes. Effects on phospholipid-protein interactions, membrane permeability and enzymatic activity, *Biochim. Biophys. Acta* 330 (1973) 8-26.
- [51] H. Du, P. Chandaroy and S.W. Hui, Grafted poly-(ethylene glycol) on lipid surfaces inhibits protein adsorption and cell adhesion, *Biochim. Biophys. Acta* 1326 (1997) 236-248.
- [52] M. Genty, G. Couarraze, R. Laversanne, C. Degert, L. Navailles, T. Gulik-Krzywicki and J.-L. Grossiord, Characterization of a complex dispersion of multilamellar vesicles, *Colloid Polym. Sci.* 282 (2003) 32-40.
- [53] K. Hashizaki, H. Taguchi, C. Itoh, H. Sakai, M. Abe, Y. Saito and N. Ogawa, Effects of poly(ethylene glycol) (PEG) concentration on the permeability of PEG-grafted liposomes, *Chem. Pharm. Bull. (Tokyo)* 53 (2005) 27-31.
- [54] M.C. Woodle and D.D. Lasic, Sterically stabilized liposomes, *Biochim. Biophys. Acta* 1113 (1992) 171-199.

- [55] K. Maruyama, T. Takizawa, T. Yuda, S.J. Kennel, L. Huang and M. Iwatsuru, Targetability of novel immunoliposomes modified with amphipathic poly(ethylene glycol)s conjugated at their distal terminals to monoclonal antibodies, *Biochim. Biophys. Acta* 1234 (1995) 74-80.
- [56] D. Knoll and J. Hermans, Polymer-protein interactions: Comparison of experiment and excluded volume theory, *J. Biol. Chem.* 258 (1983) 5710-5715.
- [57] S.M. Moghimi, H. Hedeman, I.S. Muir, L. Illum and S.S. Davis, An investigation of the filtration capacity and the fate of large filtered sterically-stabilized microspheres in rat spleen, *Biochim. Biophys. Acta*. 1157 (1993) 233-240.
- [58] Y.E. Rahman, K.R. Patel, E.A. Cerny and M. MacCoss, The treatment of intravenously implanted Lewis lung carcinoma with two sustained release forms of 1-b-D-arabinofuranosylcytosine, *Eur. J. Cancer Clin. Oncol.* 20 (1984) 1105-1112.
- [59] T.M. Allen, T. Mehra, C. Hansen and Y.C. Chin, Stealth liposomes: an improved sustained release system for 1-beta-D-arabinofuranosylcytosine, *Cancer. Res.* 52 (1992) 2431-2439.

Chapitre 5. pH-sensitive immunoliposomes specific to the CD33 cell surface antigen of leukemic cells

Pierre Simard and Jean-Christophe Leroux*

Canada Research Chair in Drug Delivery, Faculty of Pharmacy, University of Montreal,
P.C. 6128 Downtown Station, Montreal (Qc), Canada, H3C 3J7

Published in: Int. J. Pharm. 381, 86-96 (2009)

5.1. Abstract

A promising avenue in cancer therapy using liposomal formulations is the combination of site-specific delivery with triggered drug release. The use of trigger mechanisms in liposomes could be relevant for drugs susceptible to lysosomal hydrolytic/enzymatic degradation. Here, we propose a polymeric pH-sensitive liposome system that is designed to release its content inside the endosomes through a polymer structural change following receptor-mediated internalization. Specifically, pH-sensitive immunoliposomes (ILs) were obtained by including a terminally-alkylated copolymer of *N*-isopropylacrylamide (NIPAM) in the liposome bilayer and by coupling the anti-CD33 monoclonal antibody to target leukemic cells. *In vitro* release of encapsulated fluorescent

probes and cytosine arabinoside (ara-C) revealed that pH-sensitivity of the vector was retained in the presence of the antibody upon incubation in plasma. Flow cytometry and confocal microscopy analyses demonstrated that the pH-sensitive ILs were efficiently internalized by various CD33⁺ leukemic cell lines while limited interaction was found for liposomes decorated with an isotype-matched control antibody. Finally, the pH-sensitive ILs-CD33 formulation exhibited the highest cytotoxicity against HL60 cells, confirming the role of the NIPAM copolymer in promoting the escape of intact ara-C in the endosomes. These results suggest that this pH-sensitive liposomal formulation could be beneficial in the treatment of acute myeloid leukemia.

5.2. Introduction

The advent of liposomal delivery systems for various ailments, such as cancer, has brought about significant therapeutic benefits over standard chemotherapy. They are now considered as a mainstream drug delivery technology. The growing number of liposomal formulations already on the market or currently under clinical evaluation is proof of the vast potential of these lipid-based carriers (Simard *et al.* 2007). The success of liposomes is mostly a consequence of their ability to reduce drug toxicity and prolong a drug's biological half-life. The long circulation times of these vectors are the combined effect of small particle size (<150 nm), adequate lipid composition, and PEGylation which limits recognition by the mononuclear phagocytes system (MPS) and enhances drug concentrations in tumors following intravenous (i.v.) administration (Gabizon & Papahadjopoulos 1988, Papahadjopoulos *et al.* 1991, Working *et al.* 1994). Solid tumors are characterized by a leaky vasculature and impaired lymphatic drainage, leading to the enhanced permeation and retention effect, which can be exploited to improve passive drug accumulation. Liposomes also offer benefits in the treatment of leukemia by providing

sustained drug levels in the bloodstream without being dependent on leaky blood vessels to access the neoplastic cells (Allen *et al.* 1992).

The newest generation of liposomes features direct molecular targeting of specific cells *via* ligand-mediated interactions. Blume *et al.* demonstrated that coupling plasminogen as a homing device to the end of the PEG chains combines long systemic vesicle circulation times with high target binding capability (Blume *et al.* 1993). The presence of targeting moieties such as antibodies can modify the biodistribution of the i.v. administered vesicles, increase the specificity of the interaction with target cells through receptors and bypass multidrug resistant transporters (Iden & Allen 2001, Mastrobattista *et al.* 1999). While internalization of liposomes by receptor-mediated endocytosis increases the intracellular drug levels, the endocytosed material may eventually be delivered to the acidic lysosomal compartment, where it can be hydrolyzed by various enzymes, resulting in diminished biological activity. This is particularly critical for drugs that are sensitive to degradation, such as nucleic acids, peptidic drugs, as well as biologically unstable anticancer drugs such as cytosine β -D arabinofuranoside (ara-C) (Connor & Huang 1986). For such fragile molecules, methods which can facilitate the release of the entrapped cargo in the cytosol are desirable.

Different triggered release mechanisms have been designed for liposomes in order to promote drug discharge in targeted tissues or cell compartments. These stimuli, including temperature (Weinstein *et al.* 1979), pH (Hope *et al.* 1983, Roux *et al.* 2002b), light (Zhang *et al.* 2002), enzymatic degradation (Davis & Szoka 1998), and ultrasounds (Kiser *et al.* 2000), have been efficiently used to initiate a breakdown of the bilayers. In particular, pH-sensitive liposomes were introduced in the early 1980's as a means of increasing drug delivery in tumors having a pH lower than the normal physiological value (Yatvin *et al.* 1980).

The most studied class of pH-sensitive liposomes consists of dioleoylphosphatidylethanolamine (DOPE) vesicles that are stabilized in the bilayer phase by mildly acidic amphiphiles such as oleic acid or cholesteryl-hemisuccinate (CHEMS) (Connor *et al.* 1984, Düzgünes *et al.* 1985). Upon acidification, the amphiphile headgroups are protonated, resulting in charge neutralization and destabilization of the vesicles due to the conversion of the DOPE component to the inverted hexagonal phase (Litzinger & Huang 1992). During this process, the liposomal structure is destroyed and the material encapsulated in the aqueous core is released. Although such liposomes have been shown to be efficient for cytoplasmic delivery in cultured cells, their moderate plasmatic stability and rapid clearance have hampered their use *in vivo* (Drummond *et al.* 2000). To increase the stability and prolong the circulation time of these DOPE-based formulations, different components have been added to the liposome membrane, such as PEG-derivatized lipids (Collins *et al.* 1990, Liu & Huang 1989, Woodle & Lasic 1992). As often reported for conventional liposomes, PEG-derivatives confer steric stability to the vesicles. However, they also hinder aggregation and dehydration of the membrane surface, thus reducing liposome fusion with cell membranes and the subsequent release of their contents (Holland *et al.* 1996, Kirpotin *et al.* 1996). To circumvent this drawback, Kirpotin *et al.* (1996) introduced approximately 10 years ago thiolytically cleavable PEG-lipid conjugates. This approach, which relies on the reduction of the disulfide linkage at the target site to form fusogenic DOPE/CHEMS vesicles, has shown little therapeutic benefit *in vivo*. Indeed, the system was found to be leaky in human plasma, and was rapidly eliminated from the circulation as the disulfide lipid derivative of PEG was cleaved in the bloodstream (Ishida *et al.* 2001). The groups of Thompson and Szoka investigated other strategies to prepare pH-sensitive liposomes (Gerasimov *et al.* 1999, Guo & Szoka 2003). The latter are based on the acid-catalyzed hydrolysis of bilayer-stabilizing lipids into surfactants or conical lipids. The encapsulated content is released over several hours under mildly acidic conditions. This may be too slow to target the release into the endosomal compartment which has a transit half-life toward the lysosomes of less than 40 min. Many other pH-

sensitive systems are based on pH-responsive peptides or proteins that can efficiently trigger membrane fusion/disruption at acidic pH. For example, the *N*-terminus of hemagglutinin (INF peptides from influenza) (Plank *et al.* 1994), GALA peptides (Simoes *et al.* 1998) and the listeriolysin O (Stier *et al.* 2005) have demonstrated reasonable enhancement of cytoplasmic delivery of biomacromolecules. Despite their interesting features, their clinical application may be limited due to potential immunogenicity (Huckriede *et al.* 2003).

Acid-triggered liposome destabilization/fusion can also be achieved by employing synthetic polyelectrolytes that undergo coil-to-globule phase transition upon protonation (Drummond *et al.* 2000, Roux *et al.* 2003, Yessine & Leroux 2004). Most polymers investigated so far for the design of pH-sensitive liposomes are based on poly(alkyl acrylic acid)s (Chen *et al.* 1999, Jones *et al.* 2003, Kyriakides *et al.* 2002), succinylated PEG (Kono *et al.* 1994, Mizoue *et al.* 2002), biodegradable polyphosphazenes (Couffin-Hoarau & Leroux 2004) and *N*-isopropylacrylamide (NIPAM) copolymers (Meyer *et al.* 1998, Roux *et al.* 2002a, Roux *et al.* 2003, Zignani *et al.* 2000). For example, poly(alkyl acrylate-*co*-methacrylic acid)s have been shown to express strong membrane destabilizing properties (Yessine *et al.* 2003) and have been used to construct pH-responsive lipoplexes (Yessine *et al.* 2006) and polyion complex micelles (Yessine *et al.* 2007) that were able to facilitate the transfer of oligonucleotides from the endosomes to the cytoplasm.

One of those polymers which have been shown to efficiently trigger the release of the content of liposomal formulations are NIPAM copolymers. The NIPAM homopolymer is characterized by a lower critical solution temperature (LCST), which is approximately 32°C in aqueous solution (Heskins & Guillet 1968). Below its LCST, the polymer is soluble, but precipitates when heated above this value. It is possible to increase the LCST above the physiological temperature and confer pH-sensitivity to the polymer by randomly copolymerizing a small proportion (< 10 mol%) of a titrable comonomer, such as

methacrylic acid (MAA) with NIPAM. Long alkyl chains can be introduced randomly or at one extremity of P(NIPAM-*co*-MAA) chains to allow anchoring of the polymer in the liposomal bilayer (Leroux *et al.* 2001). Upon acidification of the external medium, the polymer collapses, introducing a curvature in the bilayer plane, which induces membrane defects (Francis *et al.* 2001, Meyer *et al.* 1998, Petriat *et al.* 2004, Zignani *et al.* 2000) and triggers the release of the entrapped cargo inside acidic organelles (Francis *et al.* 2001, Roux *et al.* 2002a). Alternatively, it was shown that the terminally-alkylated NIPAM copolymer provided a steric barrier that enhanced, although marginally, the liposome circulation time *in vivo* (Roux *et al.* 2002b). The combination of both the terminally-alkylated NIPAM copolymer and a PEGylated lipid in the vesicle structure was found to provide liposomes with both strong pH-responsive properties and a long half-life (Bertrand *et al.* 2009, Roux *et al.* 2004). This manuscript reports the *in vitro* evaluation and characterization of pH-sensitive liposomes based on NIPAM copolymers for the delivery of ara-C.

The encapsulation of ara-C into pH-responsive liposomes was demonstrated beneficial as this drug can be destroyed or inactivated easily by hydrolases or peptidases (Connor & Huang 1986, Huang *et al.* 1983). Ara-C is a schedule-dependent antineoplastic drug used alone or in association with anthracycline agents in the treatment of acute myeloid leukemia (AML). When injected i.v. to animals or humans, the free drug is rapidly cleared, with most of it being deaminated to an inactive form in the first 20 min post-injection (Allen *et al.* 1992, Baguley & Falkenhaug 1971). The incorporation of ara-C into long-circulating PEGylated liposomes has been found to substantially increase its therapeutic effect on L1210/C2 leukemia (Allen *et al.* 1992). However, some studies have shown that when incorporated inside conventional liposomes, ara-C was localized within lysosomal organelles where it degraded into its inactive form (Connor & Huang 1986, Huang *et al.* 1983, Rustum *et al.* 1981).

The objective of the present work was to formulate pH-sensitive immunoliposomes (ILs) that would serve as effective chemotherapy agents against (AML). The ILs were designed to target CD33 (Gp67), a surface antigen expressed on over 80% of leukemia blasts from AML-suffering patients but not on healthy cells (Griffin *et al.* 1984). The murine anti-CD33 p67.6 monoclonal antibody (mAb) as targeting ligand binds the CD33 receptor with great avidity and is currently used in the clinic to treat AML. Indeed, the humanized p67.6 anti-CD33 conjugated with calicheamicin through an acid-labile linkage (gemtuzumab ozogamicin, Mylotarg[®]) has been approved in the United States in 2000 for the treatment of relapsed AML patients who are not candidates for conventional chemotherapy. Although this new treatment holds great promise, it is still associated with resistance to calicheamicin and serious side effects have been reported in a large proportion of treated patients (Giles *et al.* 2001). Thus, pH-sensitive ILs-CD33 with terminally-alkylated P(NIPAM-*co*-MAA) loaded with ara-C could be an interesting avenue to target specifically myeloid leukemic cells and increase the intracellular bioavailability of the active drug (Figure 5.1).

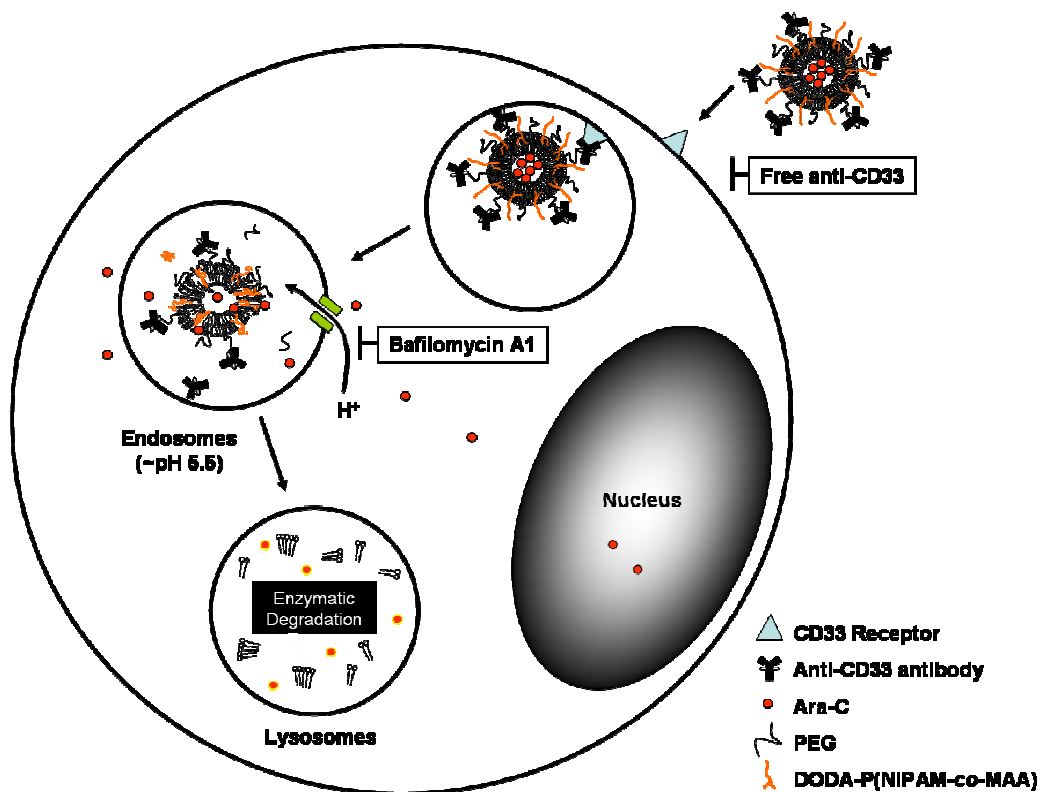


Figure 5.1. Schematic representation of the binding and the internalization of the pH-sensitive ILs-CD33 through receptor-mediated endocytosis. Upon acidification of the endosomes, DODA-P(NIPAM-co-MAA) destabilizes the liposomal bilayer, thereby triggering the rapid release of encapsulated ara-C. In competitive assays free anti-CD33 binds the CD33 receptor and impedes the binding and the internalization of the ILs-CD33. Once internalized, the release of the pH-sensitive liposomal content can be slowed down by the addition of baflomycin A1. The latter is a strong inhibitor of the vacuolar type H(+)ATPase, which inhibits the acidification of the endosomes/lysosomes (Yoshimori *et al.* 1991).

5.3. Material and Methods

5.3.1. Material

Egg phosphatidylcholine (EPC, 760 g/mol), 1,2-distearoyl-*sn*-glycero-3-phosphatidylethanolamine-*N*-monomethoxy-[poly(ethylene glycol)] (DSPE-PEG) 2000 and cholesterol (Chol, 99.5% pure) were obtained from Northern Lipids Inc. (Vancouver, BC, Canada). DSPE-PEG 3400-maleimide was purchased from Laysan Bio Inc. (Arab, AL). NIPAM, MAA, Triton X-100, formaldehyde 37% (*v/v*), Sodium dodecyl sulphate (SDS), Sepharose® CL-4B, Sephadex® G-50, dithiotreitol (DTT), sodium *meta*-periodate, Ellman's reagent, ara-C, calcein, mouse isotype control IgG1b MOPC21 and 3-(4,5-dimethylthiazol-2-yl)-2,5-diphenyl tetrazolium bromide (MTT) were purchased from Sigma-Aldrich (St. Louis, MO). Mowiol® was obtained from EMD Biosciences Inc (Darmstadt, Germany). Purified anti-CD33 antibodies were obtained from AbD Serotec (Raleigh, NC). 3-(2-pyridylthio)propionyl hydrazide (PDPH) and the BCA protein kit were purchased from Pierce (Rockford, IL). [³H]-Ara-C (15-30 Ci/mmol) was purchased from American Radiolabeled Chemicals (St-Louis, MO). The HL60 (human promyelocytic leukemia cells), KG-1 (human myeloid cells), A549 (human lung carcinoma cells) were purchased from American Type Tissue Collection (ATCC, Rockville, MD). The THP-1 (human acute monocytic leukemia) cell line was donated by professor Ong (University of Montreal, Qc, Canada). Cholesteryl 4,4-difluoro-5,7-dimethyl-4-bora-3a,4a-diaza-*s*-indacene-3-dodecanoate (cholesteryl-BODIPY FL C12), trisodium 8-hydroxypyrene trisulfonate (HPTS), *p*-xylene-bis-pyrimidium (DPX), Lysotracker Red®, DAPI, RPMI 1640, Dulbecco's modified Eagle's medium (DMEM), fetal bovine serum (FBS), penicillin G (100 U/mL) and streptomycin (100 µg/mL) solution, and trypan blue were obtained from Invitrogen (Burlington, ON, Canada). All products were used without further purification.

Water was deionized with a MilliQ purification system (Millipore, Bedford, MA) before use.

5.3.2. Preparation of copolymers

The terminally-alkylated polymer was synthesized by free radical polymerization of NIPAM and MAA employing 4,4'-azobis(4-cyano-*N,N*-dioctadecyl)pentanamide (DODA-501) as the lipophilic initiator (NIPAM/MAA/DODA 93:5:2 mol%) (Leroux *et al.* 2001). A fluorescently-labelled copolymer was also synthesized by adding methacryloxethyl thiocarbonyl rhodamine B during polymerization. The weight-average molecular weights (M_w) of the unlabelled and labelled copolymers were 11,000 (PI=2.1) and 8,600 (PI=1.9), respectively. At 37°C, these polymers undergo a coil-to-globule phase transition at pH 5.6, as ascertained by turbidimetry at 480 nm. The structure of the synthesized polymers was confirmed by H^1 -NMR spectroscopy, and the purity of the labelled copolymers was verified by thin layer chromatography on silica using a mixture of methanol and chloroform (49:1) as eluent. The rhodamine B content of the copolymer was assayed by spectrofluorimetry in PBS (pH 7.4) and was found to be 0.8 mol%.

5.3.3. Preparation of PEGylated pH-sensitive liposomes

Liposomes of EPC/Chol/DSPE-PEG2000/DSPE-PEG-maleimide (3:2:0.17:0.09 molar ratio) were prepared by the thin film hydration method. Briefly, lipids were dissolved in chloroform and mixed with 0.3 mol% of the fluorescent probe cholesteryl-BODIPY FL C12. This fluorescent marker is known to be a non-exchangeable lipidic probe (Dagar *et al.* 2001, Reaven *et al.* 1996). After solvent evaporation, the dried lipid film was placed in

vacuo (\sim 0.1 mBar) for at least 30 min to remove residual solvent. The film was then hydrated with a buffered solution of *N*-[2-hydroxyethyl]piperazine-*N'*-[2-ethanesulfonic acid] (HEPES) 20 mM (pH 7.2) and NaCl (144 mM), or the appropriate solution of dye/drug. The liposomes were then extruded several times through polycarbonate membranes (400, 200 and 100 nm) using a LiposoFast extruder (Avestin, Ottawa, ON, Canada) to yield vesicles with diameters of ca. 160 nm (polydispersity index of 0.05). DODA-P(NIPAM-*co*-MAA) was added to the lipid mixture at a ratio of 0.1-0.3 (*w/w*) prior to the hydration step and excess polymer was removed by size exclusion chromatography (SEC). The liposome concentration was determined by the phosphorus assay (Bartlett 1959).

5.3.4. Modification of the antibodies

The anti-CD33 (clone p67.6) and the isotype-matched control mouse IgG1 MOPC21 monoclonal antibodies (3-5 mg/mL) were oxidized at the carbohydrate sites with cold sodium *meta*-periodate (final concentration of 15 mM) at 4°C during 40 min in sodium acetate buffer (0.1 M, pH 5.5) (Morehead *et al.* 1991). Excess of *meta*-periodate was quenched by adding a solution of glycerol (\sim 15 mM) and removed by dialysis (cut-off 6-8000 g/mol) against acetate buffer (pH 5.5). After dialysis, the oxidized antibodies were reacted with PDPH (final concentration of 5 mM) (Ansell *et al.* 1996) during 5 h at room temperature under agitation. The PDPH-antibodies were dialyzed overnight against acetate buffer (0.1 M, pH 4.5). The following day, they were treated with DTT (25 mM) at room temperature for exactly 20 min. The reaction mixture was applied on Sephadex G-50 column and eluted with HBS (20 mM, pH 7.2) under a nitrogen flux. Twenty μ L of each of the collected fractions were treated with the Ellman's reagent (4 mg/mL in PBS) to verify the removal of excess DTT. The fractions containing the thiolated antibodies were pooled together under nitrogen atmosphere and the final protein concentration assayed with a BCA

kit. A gel electrophoresis (SDS-PAGE) under non-reducing conditions using 10% acrylamide was conducted to verify the integrity of the antibodies following the modification process.

Immediately after the antibody modification, the functionalized liposomes containing DSPE-PEG-maleimide were coupled to the thiolated antibodies at a ratio of 100 µg proteins per µmol of lipids under nitrogen atmosphere. The mixture was incubated for 30 min at room temperature, followed by an overnight incubation at 4°C on a rotating plate set at low speed. After the coupling period, all the formulations were incubated with β-mercaptoproethanol for 20 min at room temperature to quench free maleimide groups. The vesicles were then chromatographed over a Sepharose® CL-4B column equilibrated with isotonic HBS (pH 7.2), to separate the liposomes from the excess β-mercaptoproethanol and free antibodies. The amount of antibody conjugated was determined according to the modified-BCA protein assay method which included the use of 2% (*w/v*) SDS. With this coupling technique, it was estimated that 30-40 monoclonal antibody molecules were attached per individual liposome.

5.3.5. Particle Size

Particle size was determined at 25°C by dynamic light scattering (DLS) at a 173° angle on a Zetasizer Nanoseries (Malvern Instruments, Worcestershire, United Kingdom) using the Contin algorithm. The measurements of the mean hydrodynamic diameters (z-average) were performed in triplicate.

5.3.6. *In vitro* release of HPTS

ILs were prepared as mentioned above except that the lipid film was hydrated with a buffered solution of HEPES (20 mM, pH 7.4) containing the water-soluble fluorophore HPTS (35 mM) and the collisional quencher DPX (50 mM) (Daleke *et al.* 1990). After liposome formation, untrapped dye was removed by gel filtration over a Sephadex® G-50 column. The release of liposomal content was monitored during 30 min at 37°C in 2-N-(morpholino)ethanesulfonic acid (MES)-saline buffer (100 mM MES, 144 mM NaCl, pH 5.0 or 5.5) or in PBS (35 mM, pH 7.4) on a Series 2 Aminco Bowman fluorimeter (Spectronics Instruments Inc, Rochester, NY). Some formulations were incubated in 50% (v/v) preheated human plasma for 1 h at 37°C and then chromatographed onto CL-4B sepharose gel to remove the excess of plasma components before monitoring the release of HPTS. The extent of content release was calculated from HPTS fluorescence intensity ($\lambda_{\text{ex}} = 413$, $\lambda_{\text{em}} = 512$ nm) relative to measurement after vesicle disruption with Triton X-100 (10% w/v), which triggered complete release of encapsulated HPTS and DPX.

5.3.7. Encapsulation and *in vitro* release of ara-C

The araC-loaded liposomes were prepared by hydrating the lipid film with a solution of ara-C (230 mM, spiked with [³H]-ara-C, 5 µCi/mL) in HBS (5 mM, pH 7.4, 350 mOsm) for 5 h at 4°C. After the extrusion process, the non-encapsulated drug was removed by gel filtration (1.5 x 20 cm) on a Sepharose® CL-4B column. The ara-C loading was determined by measuring the radioactivity in the eluted fractions using a scintillation counter (Liquid Scintillation Analyser Tri-Carb 2100TR, Packard, Meriden, CT). The encapsulation efficiency (EE) was calculated using Equation 1:

$$\text{EE (\%)} = \frac{\text{AUC}_E}{\text{AUC}_T} \times 100 \quad \text{Eq. 1}$$

where AUC_E and AUC_T stand for area under the elution profile curve of the encapsulated and total drug in the feed, respectively.

The effect of plasma on pH-triggered release was assessed after incubation of the liposomes in 50% (*v/v*) human plasma at 37°C for 1 h. The excess of plasma components was removed by gel filtration, and the vesicles were incubated for 30 min at 37°C in PBS (pH 7.4) or isotonic MES buffer (pH 5.0). After incubation, the ara-C released was separated from the liposomes by ultrafiltration (5000 g x 15 min) using a Centricon® tubes (Millipore, cut-off 50 kDa). In a parallel experiment, the amount of drug directly released in 50% plasma was also measured. The extent of content released was calculated by radioactivity counting relative to measurement conducted after vesicle disruption with Triton X-100.

5.3.8. Cell culture

The human monocyte cell lines HL60, KG-1 and THP-1 were grown as suspension cultures in RPMI 1640, supplemented with 10% (*v/v*, KG-1 and THP-1) or 20% (*v/v*, HL60) heat-inactivated FBS, 2 mM glutamine, and 1% (*v/v*) penicillin G (100 units/mL) and streptomycin (100 µg/mL). The A549 cells were grown in monolayer in 75 cm²-flasks containing 15 mL of DMEM supplemented with 10% (*v/v*) heat-inactivated FBS, penicillin G, and streptomycin. Cells were maintained at 37 °C in a humidified atmosphere containing 5% CO₂. Cells were resuspended or scrapped, and counted using Trypan blue exclusion assay with a hemacytometer. All experiments were performed on mycoplasma-free cell lines. Only cells in the exponential phase of growth were used.

5.3.9. Binding and internalization assays

Leukemic HL60, KG-1, THP-1 (CD33⁺ expression) and lung carcinoma A549 (CD33⁻) cells (5×10^5 /tube) were incubated at 37°C for 2 h with 0.2 µmol of ILs labelled with the hydrophobic probe BODIPY FL C12. Competitive binding assays were performed in the presence of 20-fold excess free antibody. Unbound liposomes were removed by washing 3 times with cold PBS and the cells were fixed with 1% (v/v) formalin/PBS during 10 min at 4°C. Samples were analysed on a FACSCalibur flow cytometer (Becton Dickinson, San Jose, CA). Data were acquired and analysed with CellQuest software (Becton Dickinson). The mean fluorescence intensity (MFI) of single cells was recorded. Cell profiles were constructed according to parameters of side scatter (SSC) and forward scatter (FSC). This region was gated in order to exclude dead cells and cell debris. The excitation of cholesteryl-BODIPY FL C12 was obtained with an argon ion laser (488 nm) and the green fluorescence emission was recorded in the FL1 channel (530/30 nm). A total of 10,000 events were analysed for each sample. The upper limit of background fluorescence was set such that no more than 1% of the events with the autofluorescence controls (attributable to native cells) occurred in the positive region. The internalization of the ILs-CD33 formulations containing rhodamine-labelled DODA-P(NIPAM-*co*-MAA) was confirmed by confocal microscopy ($\lambda_{\text{ex}} = 543$, $\lambda_{\text{em}} = 560$ nm), following the same experimental conditions as mentioned above.

5.3.10. Evaluation of the binding affinity of ILs

To evaluate the affinity of the anti-CD33 ILs, a fixed number of HL60 cells (3×10^3) were incubated at 4°C with serial dilutions of the ILs during 3 h. Bound antibody was

then detected with a goat anti-mouse FITC-conjugated antibody by flow cytometry. The apparent dissociation constant (K_{Dapp}) was calculated from Equation 2:

$$\frac{1}{F} = \frac{1}{F_{max}} + \left(\frac{K_{Dapp}}{F_{max}} \right) \left[\frac{1}{C_{Ab}} \right] \quad \text{Eq. 2}$$

where C_{Ab} is the molar concentration of the antibody, F is the measured fluorescence value after subtracting the background fluorescence, and F_{max} is the fluorescence value obtained when the cells are incubated with saturating concentrations of antibody. When plotting the F_{max}/F ratio as a function of the inverse of C_{Ab} , a regression line, whose slope represents the K_{Dapp} , can be drawn (Benedict *et al.* 1997, Occhino *et al.* 2004).

5.3.11. Intracellular release of calcein

In order to determine the intracellular release of a fluorescent probe in acidic cell compartments, calcein was encapsulated in ILs at a self-quenched concentration (120 mM) (Francis *et al.* 2001). Leakage of calcein from the liposomes in the cells results in an increase in fluorescence. Ten μL of ILs or pH-sensitive ILs (2 $\mu\text{mol/mL}$ lipids) were incubated 30 min at 37°C with 5×10^5 HL60 cells in RPMI 1640 (10% *v/v* FBS, without red phenol). In some samples, 500 nM bafilomycin A1 was added to the cells 30 min before the liposome formulations to block the acidification of the endosomes (Yoshimori *et al.* 1991). In the case where Lysotracker Red® was used for the staining of acidic cell organelles (*i.e.* endosomes and lysosomes), the probe was incubated 30 min at a final concentration of 80 nM. After incubation, cells were washed 3 times with cold PBS (pH 7.4), and fixed with 4% (*w/v*) paraformaldehyde during 25 min. The cells were washed again with PBS, and the DAPI probe was added in each tube (300 μL , 0.1 μM , 20 min at room temperature) to counterstain the nucleus in blue. They were subsequently washed 3 times with PBS to remove excess dye. For fluorescence imaging, the cover slips were

mounted on glass slides containing a mixture of concentrated cells and Mowiol®. Cells were then analyzed on a Zeiss LSM 410 inverted confocal microscope (Zeiss, Jena, Germany) equipped with a high pressure mercury lamp (HBO 100) for excitation and a triple bandpass filter set. The cells were excited at 405, 488 and 543 nm, and fluorescence was collected by using emission windows set at 420, 505-530 and 560 nm, respectively.

5.3.12. Antiproliferative assay

Inhibition of cell proliferation was measured by MTT assay (Mosmann 1983). Briefly, HL60 in logarithmic phase of growth were synchronized in S-phase following exposure to 2 mM thymidine for 24 h. The synchronized cells were rinsed and resuspended in RPMI 1640 containing 10% (*v/v*) heat-inactivated FBS (thymidine-free) and were seeded in 96-well round bottom tissue culture plates (100 µL RPMI–FBS containing 3x10⁴ viable cells) at 37°C in a humid atmosphere containing 5% CO₂. The liposomal formulations encapsulating 300 mM of ara-C (spiked with [³H]-ara-C (16.7 µCi/mL)) were sterilized by filtration (0.45-µm pore size) and adjusted to the same ara-C concentration prior to their incubation with the cells. The encapsulated or free drug (20-40 µg/mL) were added to the cells 2 h after removing the thymidine, and incubated at 37°C for 2 h. Controls (100% cell survival) were prepared by adding sterile HBS (10 mM, pH 7.2) to the cells. After incubation, the cells were washed 3 times with non-complete RPMI by centrifugation (800 g x 2min), and resuspended in 100 µL complete medium. They were incubated for another 48 h, and MTT dissolved in PBS (10 µL of a 5 mg/mL solution) was added to each well. After 3 h, SDS (100 µL of a 10% (*w/v*) solution containing 0.01 N HCl) was added to each well to dissolve the reduced MTT. Absorbance was measured 24 h later at 570 nm using a Safire plate reader (Tecan, Medford, MA). Each experiment was undertaken at least in triplicate. To ascertain the significance of the differences observed between the liposomal formulations, statistical analysis of the data was performed using one-way analysis of

variance (ANOVA) followed by Fisher's least significant difference (LSD) test. Differences were considered significant at $p<0.05$.

5.4. Results and Discussion

5.4.1. Characterization of the pH-sensitive liposomes

In the past decade, we have extensively published on the synthesis, interaction with lipid bilayers and capacity of various pH-sensitive NIPAM copolymers to destabilize liposome membranes by introducing a curvature in the bilayer plane at acidic pH (Francis *et al.* 2001, Leroux *et al.* 2001, Meyer *et al.* 1998, Roux *et al.* 2002a, Roux *et al.* 2003, Roux *et al.* 2004, Zignani *et al.* 2000). We demonstrated that the interaction area between the phospholipids and the polymer increased at acidic pH while the copolymer was found to be partially dehydrated at neutral pH and physiological temperature. In this work, a terminally-alkylated copolymer was used in this study instead of a randomly-alkylated one, because it was shown to confer steric stability to the liposomes, while preserving its ability to destabilize liposomes at endosomal pH (Roux *et al.* 2004). When incorporated into PEGylated liposomes, the average particle size was ca. 160 nm, regardless of the initial ratio of polymer used (0.12-0.3 *w/w*). Experiments carried out with rhodamine-labelled DODA-P(NIPAM-*co*-MAA) revealed that $34 \pm 3\%$ of the polymer was incorporated into the liposomal formulation. This polymer incorporation efficiency was about half that previously reported with randomly-alkylated NIPAM copolymers incorporated by the same method (Zignani *et al.* 2000). Such a difference in the binding efficacy can be rationalized in terms of reduced anchoring points in the case of the terminally-alkylated polymer. The formulation was physically stable as no change in terms of size distribution was noted after storage of this unloaded pH-sensitive PEGylated formulation at 4°C over one year.

5.4.2. Modification of the antibodies

Different conjugation procedures have been reported for the coupling of targeting ligands to liposomes (Harasym *et al.* 1998, Nobs *et al.* 2004). The method chosen is important as it may modify the binding affinity of the antibody to its target. It may also affect its orientation at the vesicle surface and therefore its propensity to activate the complement system and be recognized by the MPS (Aragnol & Leserman 1986). The antibody modification method applied here relies on the use of carbohydrate sites located in the Fc portion of the antibody. The latter is therefore expected to adopt a spacial conformation whereby the Fc region is oriented toward the liposome surface and less accessible against undesirable recognition by the MPS, while the Fab' domains are oriented outward for optimal antibody-antigen interaction (Harasym *et al.* 1998). As mentioned in the methods section, the sugar site on the antibody was oxidized to create aldehyde functions which were then reacted with the hydrazide group of the spacer arm PDPH. The 2-pyridyldisulfide moiety of PDPH was reduced with DTT in order to introduce sulfhydryl groups in the protein without altering the native disulfide bonds (Ansell *et al.* 1996). Gel electrophoresis (SDS-PAGE) experiments and incubation of the antibodies at the different stages of modification with HL60 cell line ($CD33^+$) confirmed that the integrity and the antigen specificity were not affected during the process (data not shown). The PDPH-thiolated antibodies were coupled to the PEG termini of liposomes using a conventional DSPE-PEG-maleimide coupling method (Iden & Allen 2001, Kirpotin *et al.* 1997, Mastrobattista *et al.* 1999). A 10-15 nm increase in the vesicle diameter (z-average) was observed following grafting of the antibodies and a coupling efficiency of approximately 15-20% was obtained. Despite a large number of maleimide reactive groups available on the surface of liposomes, this value lies within the normal range for this coupling technique (Huwyler *et al.* 1996). Better coupling efficiencies can be obtained with other conjugation methods (Nobs *et al.* 2004), but the final orientation of the antibody at the vesicle surface is

not controlled. Furthermore, a ratio of ~20 µg antibody/µmol of lipids is generally sufficient to ensure efficient targeting (Ansell *et al.* 1996). The addition of DODA-P(NIPAM-*co*-MAA) to the liposome bilayer reduced the binding level of the CD33 antibody from 18 to 14 µg/µmol lipids, possibly through a steric hindrance effect. Indeed, the molecular weight of DODA-P(NIPAM-*co*-MAA) being greater than that of the PEG, the maleimide groups may be less accessible in the presence of the pH-sensitive polymer.

5.4.3. *In vitro* cellular association of ILs

In vitro cell association studies were performed to characterize the targeting efficiency of ILs to CD33⁺ leukemia cell lines. Figure 5.2A shows the binding of the pH-sensitive ILs labelled with the hydrophobic probe cholestryl-BODIPY FL C12 at 4°C (no endocytosis) and at 37°C (internalization). The ILs were recognized and internalized by the tumoral cells, corroborating previous data obtained with radiolabeled anti-CD33 antibodies (Caron *et al.* 1994, Press *et al.* 1996, Scheinberg *et al.* 1991). To determine the specificity of ILs-CD33 toward CD33⁺ cells, negative control binding experiments were performed using isotype-matched control ILs (ILs-MOPC21) or undecorated PEGylated liposomes (Figure 5.3). These negative controls resulted in significantly lower internalization values after 2 h incubation with HL60 cells compared to ILs-CD33. Confocal micrographs of the ILs-CD33 labelled with cholestryl-BODIPY FL C12 (data not shown) or rhodamine DODA-P(NIPAM-*co*-MAA) (Figure 5.2B, first 2 panels) confirmed the cytofluorometry analysis. The ILs-CD33 were taken up by the cells by a specific receptor-endocytosis process. The copolymer was distributed equally within the cells, and the intensity of the fluorescence was lower for the control ILs-MOPC21 formulation.

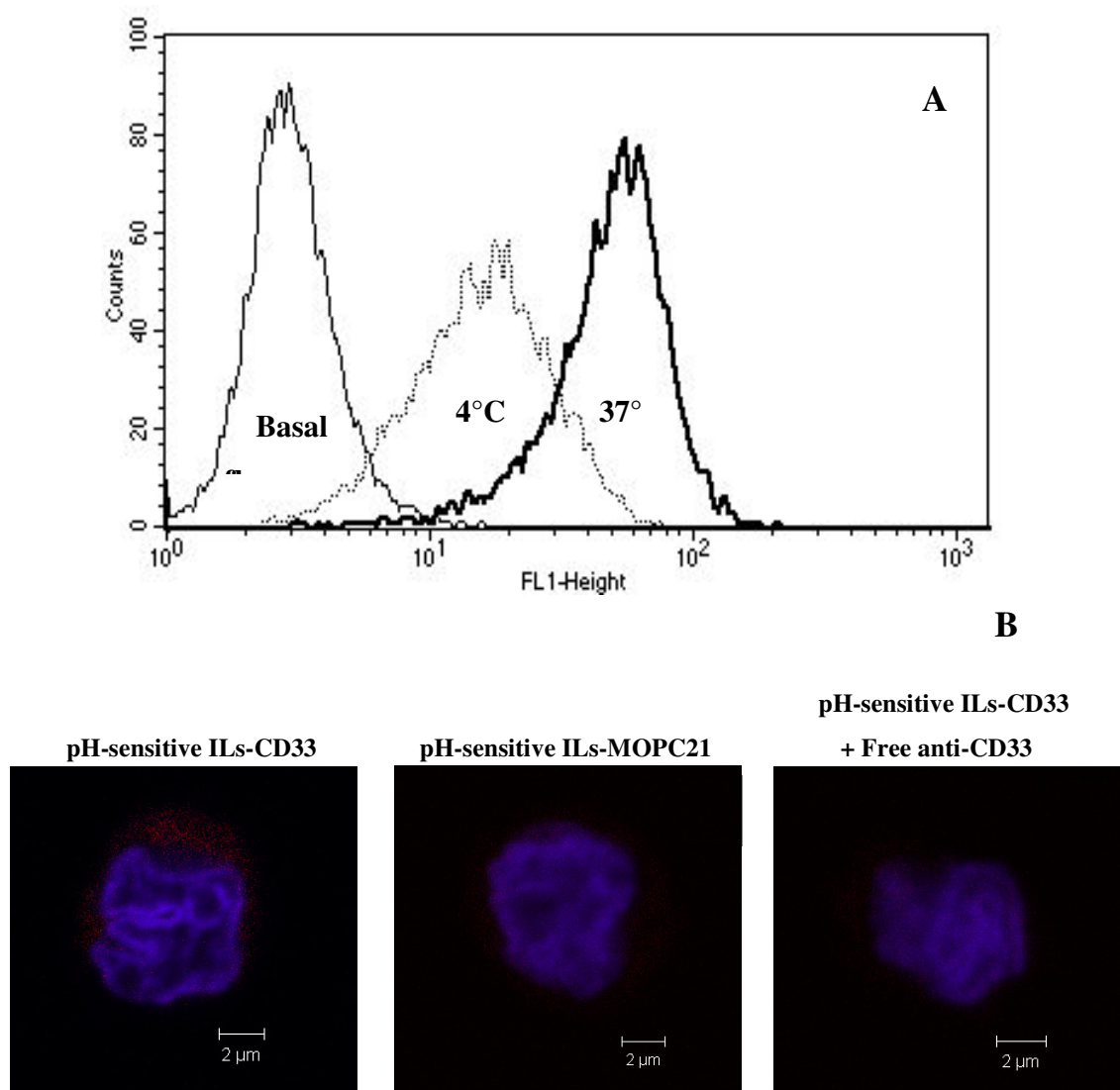


Figure 5.2. (A) Fluorescent labelling of HL60 ($CD33^+$) cells after 2 h incubation of pH-sensitive ILs-CD33 labelled with BODIPY FL C12 at 4°C (dotted light line) and 37°C (plain dark line) determined by flow cytometry. The x-axis represents the logarithm of green fluorescence signal, and the y-axis represents cell count. The first plain line represents basal cellular fluorescence (without any probe). (B) Confocal microscopy micrographs of an HL60 cell treated with ILs-CD33 (left panel), ILs-MOPC21 (middle panel), and pre-

incubated with free anti-CD33 during 30 min before the addition of the ILs-CD33 (right panel). All the formulations contain rhodamine-labelled DODA-P(NIPAM-*co*-MAA) (red). Nuclei were stained with DAPI (blue).

A slight reduction of cell-associated fluorescence was observed when comparing pH-sensitive ILs-CD33 to non-pH-sensitive ILs-CD33 (Figure 5.3A). A competitive binding assay was also conducted on HL60 cells by adding free anti-CD33 antibodies (20-fold) to the medium 30 min before adding the pH-sensitive ILs-CD33 formulation. The presence of free excess antibody produced a significant decrease in vesicle uptake, confirming the specificity of the interaction (Figures 5.2B last panel and Figure 5.3A). Finally, uptake experiments conducted with different CD33⁺ leukemia cells (HL60, KG1, THP-1) demonstrated that pH-sensitive ILs-CD33 were internalized by all cell lines expressing the receptor while limited interaction was found with the A549 (CD33⁻) cell line (Figure 5.3B).

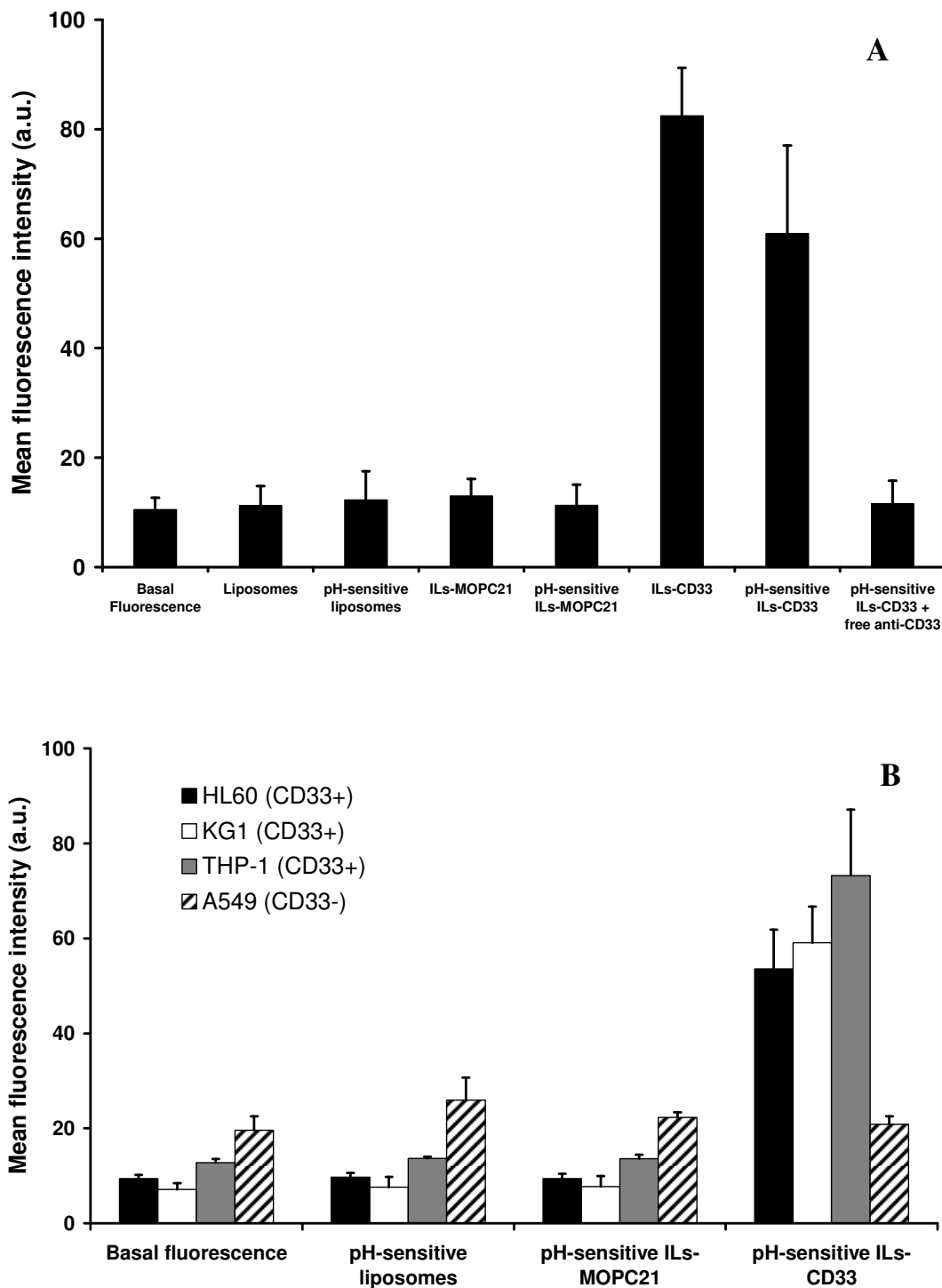


Figure 5.3. (A) Uptake of different liposome formulations by HL60 cells. The last bar represents competitive binding assays of pH-sensitive IL-CD33 performed in the presence of a 20-fold excess free anti-CD33 antibody. Mean \pm SD, n= 4. (B) Uptake of different pH-sensitive formulations by HL60 (black bars), KG1 (white bars), THP-1 (grey bars) and A549 (stripped bars) cells. Mean \pm SD, n = 3.

It was reported that the presence of a PEG corona may reduce the lateral mobility of the liposome-conjugated ligand and therefore limit the number of antibody molecules fully exposed at the surface of the liposome capable of interacting with the cell membrane receptor (Harasym *et al.* 1998, Mercadal *et al.* 1999). The repulsion between the cell surface and PEGylated liposomes may decrease the free energy gain of the ligand binding to its receptor, therefore reducing the apparent affinity constant. Kirpotin *et al.* (1997) demonstrated that by increasing the DSPE-PEG content (0 to 5.7 mol%) in anti-HER2 liposomes prepared with a short spacer, 4-(*N*-maleimidomethyl)cyclohexane-1-carboxylate (MMC), the liposome-cell binding affinity was decreased by 60-100 fold. However, when Fab' fragments were directly coupled to the extremity of the PEG chain (without a spacer), the surface grafted PEG did not affect the binding affinity. As lower internalization of the ILs-CD33 was obtained with the ILs decorated with DODA-P(NIPAM-*co*-MAA) compared to the control ILs-CD33 (Figure 5.3A), it was first hypothesized that the binding site on the antibodies may be hidden by the flexible chain of the pH-sensitive polymer, subsequently reducing the binding affinity for the receptor. Therefore the K_{Dapp} values were calculated for both formulations. The pH-sensitive and pH-insensitive ILs-CD33 were found to exhibit a comparable affinity for HL60 cells with K_{Dapp} of $7.7 \pm 1.1 \times 10^{-10}$ M and $7.9 \pm 1.7 \times 10^{-10}$ M, respectively. These data suggest that DODA-P(NIPAM-*co*-MAA) did not alter the affinity of ILs for the CD33 receptor and that the lower amount of antibody

grafted on the pH-sensitive vesicles (14 vs 18 µg antibody/µmol lipid) is probably accountable for the reduced internalization in HL60 cells.

5.4.4. *In vitro* release of HPTS and ara-C

A main concern for DOPE-based pH-sensitive liposomes, or any other polymer configuration such as randomly-alkylated NIPAM copolymer (Roux *et al.* 2003, Zignani *et al.* 2000) is the detrimental effect of PEGylation on the pH-sensitivity. Another issue regarding polymer-coated liposomes is their partial loss of pH-responsiveness (15-25%) following incubation in biological fluids (Roux *et al.* 2002a, Roux *et al.* 2003, Roux *et al.* 2002b). Protein adsorption onto pH-sensitive vehicles may stabilize the system and/or partially extract the copolymer from the lipid bilayers (Roux *et al.* 2002a). In a former study, it was demonstrated that pH-sensitivity of PEGylated liposomes could be largely preserved after incubation in human serum when DODA-P(NIPAM-*co*-MAA) was employed as the triggered release polymer (Roux *et al.* 2004). Therefore, using the fluorescent probe HPTS co-encapsulated with the collisional quencher DPX, we verified whether this polymer would also maintain its activity when complexed to PEGylated liposomes decorated with an antibody. Release kinetics performed in the absence of plasma proteins showed that the polymer efficiently triggered, within the first 10 min, the release of $80 \pm 1\%$ of liposomal content at pH 5.0 (data not shown). Figure 5.4 illustrates the percent of dye released from ILs bearing DODA-P(NIPAM-*co*-MAA) following 1 h incubation in 50% (*v/v*) human plasma. As expected, minimal dye leakage was observed at pH 7.4 (~5%, after 30 min). On the contrary, lowering the pH to 5.8 and 5.0 brought about a major increase in the release rate with 48 and 78% of HPTS released after 30 min, respectively. These data confirm that the pH-sensitive polymer fully preserved its ability to destabilize the liposomes at acidic pH after having been in contact with blood proteins, independently of the presence of the antibody at the liposome surface.

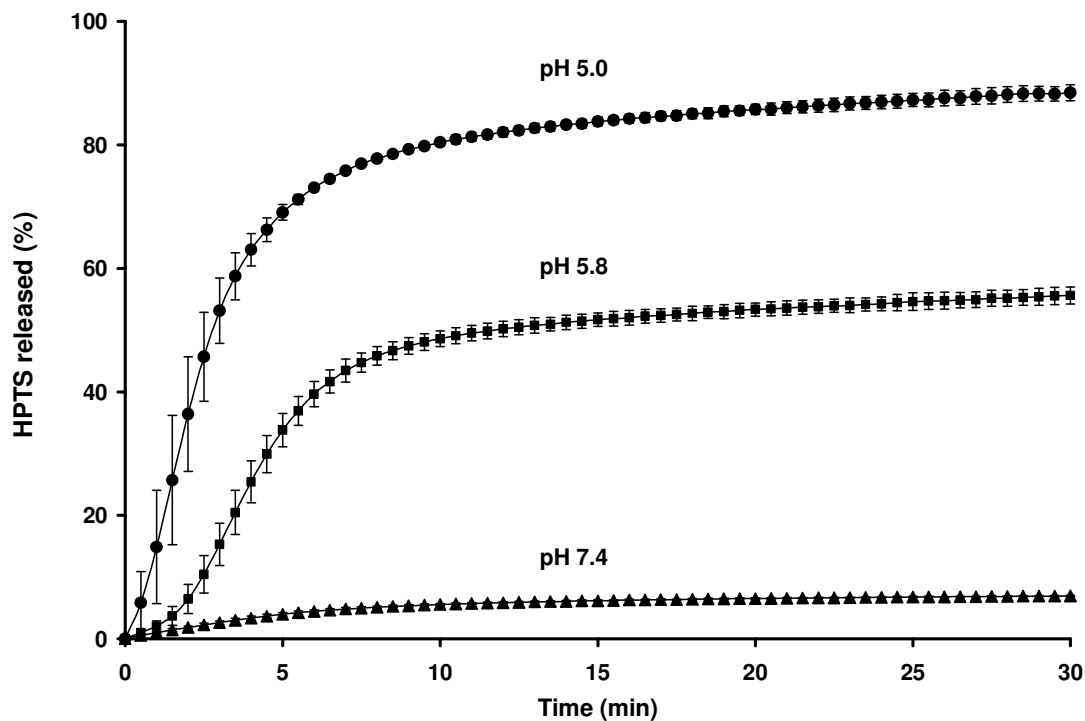


Figure 5.4. *In vitro* release of encapsulated HPTS at 37°C for pH-sensitive ILs at pH 5.0 (circle), 5.8 (square), and 7.4 (triangle) after 1 h incubation in 50% (v/v) human plasma. DODA-P(NIPAM-MAA) was incorporated during liposome preparation. The extent of content release was calculated from HPTS fluorescence intensity ($\lambda_{\text{ex}} = 413 \text{ nm}$, $\lambda_{\text{em}} = 512 \text{ nm}$) relative to the intensity obtained upon vesicle disruption with 10% (v/v) Triton X-100. Mean \pm SD, n = 3.

We then verified whether the anticancer drug ara-C could be released in a pH-dependent fashion from the ILs. For the pH-insensitive and pH-sensitive liposomes an entrapment efficiency of 10.7 ± 1.0 and $9.9 \pm 2.3\%$ was achieved, respectively. This indicated that DODA-P(NIPAM-*co*-MAA) did not affect the encapsulation of the drug. This entrapment efficiency is comparable to previously reported values which ranged from 1 to 20% (Hong & Mayhew 1989). Incubation of ara-C-loaded pH-insensitive or pH-sensitive ILs in 50% (*v/v*) human plasma during 1 h was accompanied by a small drug loss of $4.3 \pm 0.8\%$ and $5.6 \pm 0.9\%$ respectively, demonstrating that the stability of ILs in plasma was maintained in the presence of the pH-sensitive polymer. After removing the excess blood proteins, the ability of the pH-sensitive liposomes to release the encapsulated ara-C was also tested at pHs 5.0 and 7.4. As shown in Figure 5.5, after 30 min incubation at pH 5.0, the pH-sensitive formulations released ~90% of their content, whereas less than 6% leaked from the pH-insensitive liposomal formulations. At neutral pH, the DODA-P(NIPAM-*co*-MAA)-coated liposomes appeared slightly more permeable to ara-C than HPTS. The antibody had apparently no impact on the pH-triggered drug release. The data presented herein indicate that pH-sensitive ILs formulated with DODA-P(NIPAM-*co*-MAA) would be stable in the blood but would rapidly release ara-C under the mildly acidic conditions found in the endosomal compartment.

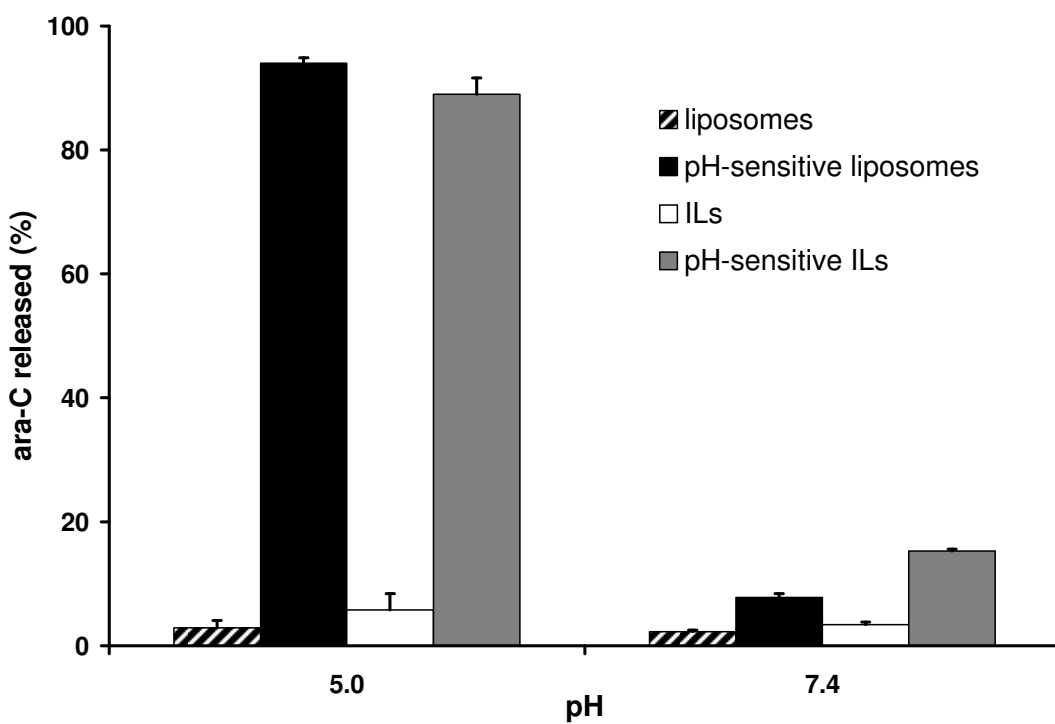


Figure 5.5. Percent of ara-C released from pH-insensitive liposomes (stripped bars), pH-sensitive liposomes (black bars), ILs (white bars), and pH-sensitive ILs (grey bars) after 30 min incubation at 37°C. The formulations were previously incubated in 50% (*v/v*) human plasma during 1 h at 37°C. Mean \pm SD, n = 3.

5.4.5. Intracellular release of quenched calcein

In order to verify that cargo release could be achieved in the endosomes, ILs containing calcein encapsulated at a self-quenched concentration were prepared and incubated 30 min with HL60 cells. Upon release of the dye from the liposomes into the endosomal/lysosomal lumen, the cellular fluorescence is expected to increase significantly.

Figure 5.6 shows confocal microscopy photographs of HL60 cells exposed to pH-insensitive ILs-CD33 (panel A) and pH-sensitive ILs-CD33 (panel B). It can be observed that after 30 min exposure, the calcein fluorescence remained largely quenched in the case of the pH-insensitive formulation, indicating minimal dye release. On the opposite, the pH-sensitive ILs rapidly released their content as revealed by the more intense and diffuse fluorescence signal. Similar findings were obtained using phagocytic RAW264.7 (unpublished data) or J774 cells (Francis *et al.* 2001) in the absence of an antibody. In order to confirm that the intracellular release of calcein was a consequence of the acidification of intracellular organelles, pH-sensitive ILs-CD33 were then incubated with HL60 previously exposed to bafilomycin A1, an inhibitor of endosome/lysosomes acidification (Yoshimori *et al.* 1991). As shown in Figure 5.6C, bafilomycin A1 suppressed the release of calcein, thereby confirming the pH-dependent release mechanisms of DODA-P(NIPAM-*co*-MAA)-coated ILs-CD33.

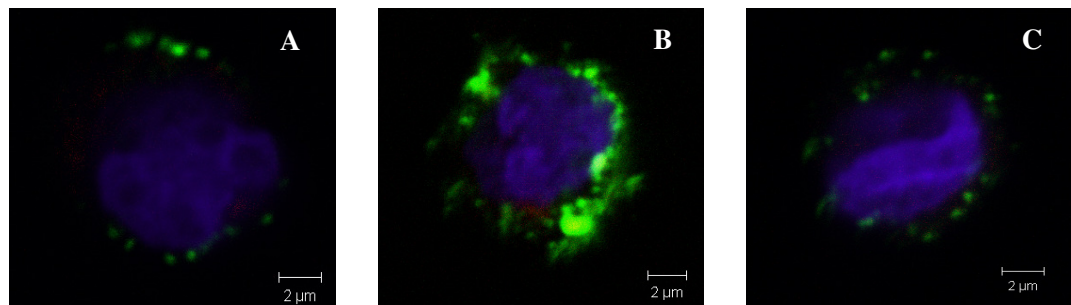


Figure 5.6. Confocal microscopy micrographs of HL60 cells treated with pH-insensitive ILs-CD33 (A) or pH-sensitive ILs-CD33 (B) containing self-quenched calcein (green). Panel C shows HL60 cells treated with bafilomycin A1 30 min before addition of pH-sensitive ILs-CD33. The Nuclei were stained with DAPI (blue), and the acidic compartments were stained with Lysotracker Red® (red).

5.4.6. Antiproliferative assay

The anticancer agent ara-C was encapsulated into different liposomal formulations and its cytotoxic activity monitored on HL60 cells. Ara-C is generally thought to act specifically on the process of DNA synthesis (S-phase) and, therefore, is regarded as cell-cycle-specific (Hamada *et al.* 2002). This drug was chosen because of its susceptibility to degradation of the *N*-glycosidic linkage upon exposure to lysosomal hydrolases. Indeed, with ara-C, the benefits associated to increased transport through internalizing epitopes are partly offset by drug inactivation within the lysosomal organelles (Huang *et al.* 1983). In theory, this problem can be circumvented by using vesicles that release ara-C upon pH-triggered destabilization in the endosomes (Brown & Silvius 1990, Connor & Huang 1986, Rui *et al.* 1998). The free drug is then translocated in the cytoplasm by nucleoside transporters located in the endosomal/lysosomal membranes (Brown & Silvius 1990, Pisoni & Thoene 1989).

To avoid prolonged incubation time, and reduce potential indirect cellular toxicity caused by the leakage of ara-C in the incubation medium, the cells were first exposed to thymidine. This procedure allowed to synchronize a maximum of HL60 cells in the S-phase, and subsequently increased the antiproliferative outcome of the drug. The cytotoxicity experiments were conducted 2 h after removing the thymidine, because free ara-C alone showed the highest level of toxicity at that time after synchronization (unpublished data). Figure 5.7 shows the percentage of surviving cells incubated with free ara-C or the following formulations: liposomes, ILs-MOPC21 and ILs-CD33 coated or not with DODA-P(NIPAM-*co*-MAA), at ara-C concentrations of 20 and 40 µg/mL. These concentrations were slightly above the IC₅₀ of free ara-C (5 µg/mL). Free ara-C was more toxic than the control non-targeted pH-insensitive formulations (liposomes and ILs-MOPC21). This phenomenon was also observed with other pH-sensitive systems, such as

non-targeted liposomes prepared with DOPE and oleic acid (8:2 molar ratio) where the liposomal formulations were found less cytotoxic than the free ara-C when incubated 3 h with the adherent L-929 cells (Connor & Huang 1986).

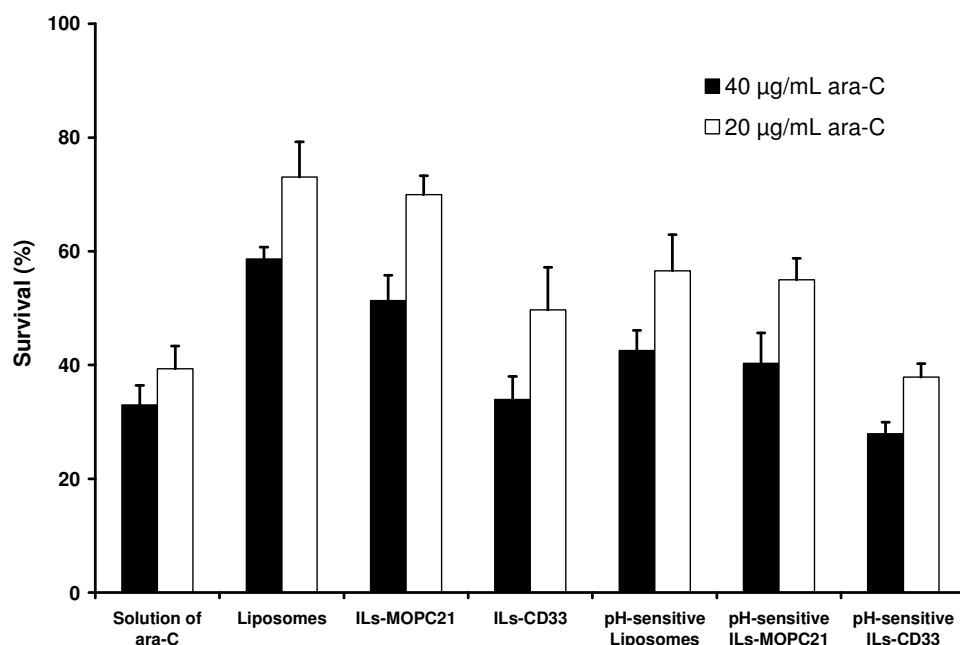


Figure 5.7. Toxicity of encapsulated and free ara-C at a final concentration of 20 (open bars) and 40 µg/mL (closed bars) on HL60 cells after an incubation time of 2 h. Mean ± SD, n = 3. At 20 µg/mL of ara-C, the cytotoxicity induced by pH-sensitive ILs-CD33 is statistically superior ($p<0.05$) to all the other liposomal formulations.

The decoration of the liposomes with the CD33 antibody produced a significant increase ($p<0.05$) in the cytotoxic activity of ara-C, reflecting the importance of receptor-mediated internalization for enhanced uptake of liposomal ara-C. Likewise, the addition of DODA-P(NIPAM-*co*-MAA) to the non-targeted liposomes improved significantly ($p<0.05$) their efficiency, possibly through facilitated release of ara-C from the endocytosed liposomes. Indeed, the higher cytotoxicity of the pH-insensitive *vs.* pH-sensitive liposomes cannot be attributed to differences in the concentration of unencapsulated ara-C in the cell culture medium as it was verified in a control experiment that the free ara-C levels in the culture medium were low and independent of the formulation (data not shown). It is important to mention that the polymer alone did not exert any cytotoxic activity even at concentrations largely exceeding those used in this experiment (data not shown).

The combination of both the CD33 antigen and pH-sensitive polymer resulted in the highest cytotoxic activity, although statistical significance *vs.* the ILs-CD33 formulation could be achieved only at 20 $\mu\text{g}/\text{mL}$. Similarly, the combination of site-specific and other types of pH-sensitive liposome formulations was reported as a promising system to increase the cytotoxicity of loaded ara-C against L-929 cells (Connor & Huang 1986), CV-1 cells (Brown & Silvius 1990) and KB cells (Rui *et al.* 1998, Sudimack *et al.* 2002) when compared to pH-insensitive formulations. For example, a DOPE-based pH-sensitive formulation targeting folate receptors showed a 16-fold decrease in ara-C IC₅₀ on adherent KB cells when compared to targeted pH-insensitive liposomes (Sudimack *et al.* 2002). It was hypothesized that this enhanced cytotoxicity of the DOPE-based formulation was conferred by the destabilization and/or fusion of the liposomes with the endosomal bilayer. Since NIPAM copolymers are devoid of membrane fusion activity (Zignani *et al.* 2000), it is possible that they are less efficient than DOPE-based liposomes in augmenting the intracellular bioavailability of ara-C. However, from a biological viewpoint, it may be difficult to compare different IL formulations, as the expression of target epitopes on cancer cells varies greatly, the turnover process is also divergent. Finally, these receptors may also

be up- or down-regulated depending on the cell cycle or the differentiation state of the cancer cells (Mastrobattista *et al.* 1999). Compared to DOPE-based liposomes, pH-sensitive liposomes prepared with NIPAM copolymers present clear advantages such as better plasma stability and long-circulating properties (Roux *et al.* 2004), which may eventually translate into better *in vivo* efficacy.

5.5. Conclusion

This study describes the preparation and *in vitro* evaluation of a targeted liposomal formulation containing pH-responsive properties that is selective toward leukemic cells expressing the CD33 antigen. The pH-sensitive copolymer DODA-P(NIPAM-*co*-MAA) was shown to destabilize the liposomal membrane of ILs under mildly acidic conditions and may play a beneficial role in the intracellular trafficking of encapsulated agents by facilitating the release of the encapsulated agent in the endosomes prior to its degradation in the lysosomes. However, at this stage the precise locus and extent of delivery of ara-C to the cytoplasm is still unknown. Future work will aim at evaluating the biodistribution and pharmacokinetic parameters of the pH-sensitive ILs-CD33 formulation in animal models and track the fate of the polymer under *in vivo* conditions. Considering these recent results and those previously published on pH-sensitive liposomes, the combination of site-specific and triggered drug release mechanisms may constitute a promising avenue in the treatment of AML.

5.6. Acknowledgements

Financial support from the Canadian Institutes of Health Research, the Canada Research Chair program and the Natural Sciences and Engineering Council of Canada

(Steacie fellowship to JCL) is acknowledged. P. Simard acknowledges a scholarship from the Fonds de la Recherche en Santé du Québec. We thank the Centre for Biorecognition and Biosensors (CBB) for access to their facilities.

5.7. References

- [1] Allen, T.M., Mehra, T., Hansen, C., Chin, Y.C., 1992. Stealth liposomes: an improved sustained release system for 1-beta-D-arabinofuranosylcytosine, *Cancer Res.*, 52, 2431-2439.
- [2] Ansell, S.M., Tardi, P.G., Buchkowsky, S.S., 1996. 3-(2-pyridyldithio)propionic acid hydrazide as a cross-linker in the formation of liposome-antibody conjugates, *Bioconjugate Chem.*, 7, 490-496.
- [3] Aragnol, D., Leserman, L.D., 1986. Immune clearance of liposomes inhibited by an anti-Fc receptor antibody in vivo, *Proc. Natl. Acad. Sci. U.S.A.*, 83, 2699-2703.
- [4] Baguley, B.C., Falkenhaug, E.M., 1971. Plasma half-life of cytosine arabinoside (NSC-63878) in patients treated for acute myeloblastic leukaemia, *Cancer Chemother. Rep.*, 55, 291-298.
- [5] Bartlett, G.R., 1959. Phosphorus assay in column chromatography, *J. Biol. Chem.*, 234, 466-468.
- [6] Benedict, C.A., MacKrell, A.J., Anderson, W.F., 1997. Determination of the binding affinity of an anti-CD34 single-chain antibody using a novel, flow cytometry based assay, *J. Immunol. Met.*, 201, 223-231.
- [7] Bertrand, N., Fleischer, J.G., Wasan, K.M., Leroux, J.-C., 2009. Pharmacokinetics and biodistribution of N-isopropylacrylamide copolymers for the design of pH-sensitive liposomes, *Biomaterials*, 30, 2598-2605.
- [8] Blume, G., Cevc, G., Crommelin, M.D.J.A., Bakker-Wondenberg, I.A.J.M., Kluft, C., Storm, G., 1993. Specific targeting with poly(ethylene glycol)-modified

- liposomes: coupling of homing devices to the ends of the polymeric chains combines effective target binding with long circulation times, *Biochim. Biophys. Acta*, 1149, 180-184.
- [9] Brown, P.M., Silvius, J.R., 1990. Mechanisms of delivery of liposome-encapsulated cytosine arabinoside to CV-1 cells in vitro. Fluorescence-microscopic and cytotoxicity studies, *Biochim. Biophys. Acta*, 1023, 341-355.
 - [10] Caron, P.C., Jurcic, J.G., Scott, A.M., Finn, R.D., Divgi, C.R., Graham, M.C., Jureidini, I.M., Sgouros, G., Tyson, D., Old, L.J., et al., 1994. A phase 1B trial of humanized monoclonal antibody M195 (anti-CD33) in myeloid leukemia: specific targeting without immunogenicity, *Blood*, 83, 1760-1768.
 - [11] Chen, T., Choi, L.S., Einstein, S., Klippenstein, M.A., Scherrer, P., Cullis, P.R., 1999. Proton-induced permeability and fusion of large unilamellar vesicles by covalently conjugated poly(2-ethylacrylic acid), *J. Liposome Res.*, 9, 387-405.
 - [12] Collins, D., Litzinger, D.C., Huang, L., 1990. Structural and functional comparisons of pH-sensitive liposomes composed of phosphatidylethanolamine and three different diacylsuccinylglycerols, *Biochim. Biophys. Acta*, 1025, 234-242.
 - [13] Connor, J., Huang, L., 1986. pH-sensitive immunoliposomes as an efficient and target-specific carrier for antitumor drugs, *Cancer Res.*, 46, 3431-3435.
 - [14] Connor, J., Yatvin, M.B., Huang, L., 1984. pH-sensitive liposomes: acid-induced liposome fusion, *Proc. Natl. Acad. Sci. USA*, 81, 1715-1718.
 - [15] Couffin-Hoarau, A.C., Leroux, J.C., 2004. Report on the use of poly(organophosphazenes) for the design of stimuli-responsive vesicles, *Biomacromolecules*, 5, 2082-2087.
 - [16] Dagar, S., Sekosan, M., Lee, B.S., Rubinstein, I., Önyüksel, H., 2001. VIP receptors as molecular targets of breast cancer: implications for targeted imaging and drug delivery, *J. Controlled Release*, 74, 129-134.

- [17] Daleke, D.L., Hong, K., Papahadjopoulos, D., 1990. Endocytosis of liposomes by macrophages: binding, acidification and leakage of liposomes monitored by a new fluorescence assay, *Biochim. Biophys. Acta*, 1024, 352-366.
- [18] Davis, S.C., Szoka, F.C., 1998. Cholesterol phosphate derivatives: synthesis and incorporation into a phosphatase and calcium-sensitive triggered release liposome, *Bioconjug. Chem.*, 9, 783-792.
- [19] Drummond, D.C., Zignani, M., Leroux, J.-C., 2000. Current status of pH-sensitive liposomes in drug delivery, *Prog. Lipid Res.*, 39, 409-460.
- [20] Düzgünes, N., Straubinger, R.M., Baldwin, P.A., Friend, D.S., Papahadjopoulos, D., 1985. Proton-induced fusion of oleic acid-phosphatidylethanolamine liposomes, *Biochemistry*, 24, 3091-3098.
- [21] Francis, M.F., Dhara, G., Winnik, F.M., Leroux, J.-C., 2001. *In vitro* evaluation of pH-sensitive polymer/niosome complexes, *Biomacromolecules*, 2, 741-749.
- [22] Gabizon, A., Papahadjopoulos, D., 1988. Liposome formulations with prolonged circulation time in blood and enhanced uptake by tumors, *Proc. Natl. Acad. Sci. U.S.A.*, 85, 6949-6953.
- [23] Gerasimov, O.V., Boomer, J.A., Qualls, M.M., Thompson, D.H., 1999. Cytosolic drug delivery using pH- and light-sensitive liposomes, *Adv. Drug Deliv. Rev.*, 38, 317-338.
- [24] Giles, F.J., Kantarjian, H.M., Kornblau, S.M., Thomas, D.A., Garcia-Manero, G., Wadelow, T.A., David, C.L., Phan, A.T., Colburn, D.E., Rashid, A., Estey, E.H., 2001. Mylotarg (gemtuzumab ozogamicin) therapy is associated with hepatic venoocclusive disease in patients who have not received stem cell transplantation, *Cancer*, 92, 406-413.
- [25] Griffin, J.D., Linch, D., Sabbath, K., Larcom, P., Schlossman, S.F., 1984. A monoclonal antibody reactive with normal and leukemic human myeloid progenitor cells, *Leuk. Res.*, 8, 521-534.

- [26] Guo, X., Szoka, J.F.C., 2003. Chemical approaches to triggerable lipid vesicles for drug and gene delivery, *Accc. Chem. Res.*, 36, 335-341.
- [27] Hamada, A., Kawaguchi, T., Nakano, M., 2002. Clinical pharmacokinetics of cytarabine formulations, *Clin. Pharmacokinet.*, 41, 705-718.
- [28] Harasym, T.O., Bally, M.B., Tardi, P., 1998. Clearance properties of liposomes involving conjugated proteins for targeting, *Adv. Drug Del. Rev.*, 32, 99-118.
- [29] Heskins, M., Guillet, J.E., 1968. Solution properties of poly(*N*-isopropylacrylamide), *J. Macromol. Sci. Chem.*, A2, 1441-1455.
- [30] Holland, J.W., Cullis, P.R., Madden, T.D., 1996. Poly(ethylene glycol)-lipid conjugates promote bilayer formation in mixtures of non-bilayer forming lipids, *Biochemistry*, 35, 2610-2617.
- [31] Hong, F., Mayhew, E., 1989. Therapy of central nervous system leukemia in mice by liposome-entrapped 1- β -D-arabinofuranosylcytosine, *Cancer Res.*, 49, 5097-5102.
- [32] Hope, M.J., Walker, D.C., Cullis, P.R., 1983. Ca²⁺ and pH induced fusion of small unilamellar vesicles consisting of phosphatidylethanolamine and negatively charged phospholipids: a freeze fracture study, *Biochem. Biophys. Res. Commun.*, 110, 15-22.
- [33] Huang, A., Kennel, S.J., Huang, L., 1983. Interactions of immunoliposomes with target cells, *J. Biol. Chem.*, 258, 14034-14040.
- [34] Huckriede, A., Bungener, L., Daemen, T., Wilschut, J., 2003. Influenza virosomes in vaccine development, *Methods Enzymol.*, 373, 74-91.
- [35] Huwyler, J., Wu, D., Pardridge, W.M., 1996. Brain drug delivery of small molecules using immunoliposomes, *Proc. Natl. Acad. Sci. USA*, 93, 14164-14169.
- [36] Iden, D.L., Allen, T.M., 2001. *In vitro* and *in vivo* comparison of immunoliposomes made by conventional coupling techniques with those made by a new post-insertion approach, *Biochim. Biophys. Acta*, 1513, 207-216.

- [37] Ishida, O., Maruyama, K., Tanahashi, H., Iwatsuru, M., Sasaki, K., Eriguchi, M., Yanagie, H., 2001. Liposomes bearing polyethyleneglycol-coupled transferrin with intracellular targeting property to the solid tumors *in vivo*, Pharm. Res., 18, 1042-1048.
- [38] Jones, R.A., Cheung, C.Y., Black, F.E., Zia, J.K., Stayton, P.S., Hoffman, A.S., Wilson, M.R., 2003. Poly(2-alkylacrylic acid) polymers deliver molecules to the cytosol by pH-sensitive disruption of endosomal vesicles, Biochem J., 372, 65-75.
- [39] Kirpotin, D., Hong, K., Mullah, N., Papahadjopoulos, D., Zalipsky, S., 1996. Liposomes with detachable polymer coating: destabilization and fusion of dioleoylphosphatidylethanolamine vesicles triggered by cleavage of surface-grafted poly(ethylene glycol), FEBS Lett., 388, 115-118.
- [40] Kirpotin, D., Park, J.W., Hong, K., Zalipsky, S., Li, W.L., Carter, P., Benz, C., Papahadjopoulos, D., 1997. Sterically stabilized anti-HER2 immunoliposomes: design and targeting to human breast cancer cells *in vitro*, Biochemistry, 36, 66-75.
- [41] Kiser, P.F., Wilson, G., Needham, D., 2000. Lipid-coated microgels for the triggered release of doxorubicin, J. Controlled Release, 68, 9-22.
- [42] Kono, K., Zenitani, K.I., Takagishi, T., 1994. Novel pH-sensitive liposomes: liposomes bearing a poly(ethylene glycol) derivative with carboxyl groups, Biochim. Biophys. Acta, 1193, 1-9.
- [43] Kyriakides, T.R., Cheung, C.Y., Murthy, N., Bornstein, P., Stayton, P.S., Hoffman, A.S., 2002. pH-sensitive polymers that enhance intracellular drug delivery *in vivo*, J. Controlled Release, 78, 295-303.
- [44] Leroux, J.-C., Roux, E., Le Garrec, D., Hong, K., Drummond, D.C., 2001. N-isopropylacrylamide copolymers for the preparation of pH-sensitive liposomes and polymeric micelles, J. Controlled Release, 72, 71-84.
- [45] Litzinger, D.C., Huang, L., 1992. Phosphatidylethanolamine liposomes: drug delivery, gene transfer and immunodiagnostic applications, Biochim. Biophys. Acta, 1113, 201-227.

- [46] Liu, D., Huang, L., 1989. Role of cholesterol in the stability of pH-sensitive, large unilamellar liposomes prepared by the detergent-dialysis method, *Biochim. Biophys. Acta*, 981, 254-260.
- [47] Mastrobattista, E., Koning, G.A., Storm, G., 1999. Immunoliposomes for the targeted delivery of antitumor drugs, *Adv. Drug Deliv. Rev.*, 40, 103-127.
- [48] Mercadal, M., Domingo, J.C., Petriz, J., Garcia, J., de Madariaga, M.A., 1999. A novel strategy affords high-yield coupling of antibody to extremities of liposomal surface-grafted PEG chains, *Biochim. Biophys. Acta*, 1418, 232-238.
- [49] Meyer, O., Papahadjopoulos, D., Leroux, J.C., 1998. Copolymers of N-isopropylacrylamide can trigger pH sensitivity to stable liposomes, *FEBS Lett.*, 42, 61-64.
- [50] Mizoue, T., Horibe, T., Maruyama, K., Takizawa, T., Iwatsuru, M., Kono, K., Yanagie, H., Moriyasu, F., 2002. Targetability and intracellular delivery of anti-BCG antibody-modified, pH-sensitive fusogenic immunoliposomes to tumor cells, *Int. J. Pharm.*, 237, 129-137.
- [51] Morehead, H.W., Talmadge, K.W., O'Shannessy, D.J., Siebert, C.J., 1991. Optimization of oxidation of glycoproteins: an assay for predicting coupling to hydrazide chromatographic supports, *J. Chromatogr. A*, 587, 171-176.
- [52] Mosmann, T., 1983. Rapid colorimetric assay for cellular growth and survival: application to proliferation and cytotoxicity assays, *J. Immunol. Met.*, 65, 55-63.
- [53] Nobs, L., Buchegger, F., Gurny, R., Allémann, E., 2004. Current methods for attaching targeting ligands to liposomes and nanoparticles, *J. Pharm. Sci.*, 93, 1980-1992.
- [54] Occhino, M., Raffaghello, L., Burrone, O., Gambini, C., Pistoia, V., Corrias, M.V., Bestagno, M., 2004. Generation and characterization of dimeric small immunoproteins specific for neuroblastoma associated antigen GD2, *Int. J. Mol. Med.*, 14, 383-388.

- [55] Papahadjopoulos, D., Allen, T.M., Gabizon, A., Mayhew, E., Matthay, K., Huang, S.K., Lee, K.-D., Woodle, M.C., Lasic, D.D., Redemann, C., Martin, F.J., 1991. Sterically stabilized liposomes: Improvements in pharmacokinetics and antitumor therapeutic efficacy, *Proc. Natl. Acad. Sci. USA*, 88, 11460-11464.
- [56] Petriat, F., Roux, E., Leroux, J.C., Giasson, S., 2004. Study of molecular interactions between a phospholipidic layer and a pH-sensitive polymer using the Langmuir balance technique, *Langmuir*, 20, 1393-1400.
- [57] Pétriat, F., Roux, E., Leroux, J.C., Giasson, S., 2004. Study of molecular interactions between a phospholipidic layer and a pH-sensitive polymer using the Langmuir balance technique, *Langmuir*, 20, 1393-1400.
- [58] Pisoni, R.L., Thoene, J.G., 1989. Detection and characterization of a nucleoside transport system in human fibroblast lysosomes, *J. Biol. Chem.*, 264, 4850-4856.
- [59] Plank, C., Oberhauser, B., Mechtler, K., Koch, C., Wagner, E., 1994. The influence of endosome-disruptive peptides on gene transfer using synthetic virus-like gene transfer systems, *J. Biol. Chem.*, 269, 12918-12924.
- [60] Press, O.W., Shan, D., Howell-Clark, J., Eary, J., Appelbaum, F.R., Matthews, D., King, D.J., Haines, A.M., Hamann, P., Hinman, L., Shochat, D., Bernstein, I.D., 1996. Comparative metabolism and retention of iodine-125, yttrium-90, and indium-111 radioimmunoconjugates by cancer cells, *Cancer. Res.*, 56, 2123-2129.
- [61] Reaven, E., Tsai, L., Azhar, S., 1996. Intracellular events in the "selective" transport of lipoprotein-derived cholestryl esters, *J. Biol. Chem.*, 271, 16208-16217.
- [62] Roux, E., Francis, M., Winnik, F.M., Leroux, J.-C., 2002a. Polymer-based pH-sensitive carriers as a means to improve the cytoplasmic delivery of drugs, *Int. J. Pharm.*, 242, 25-36.
- [63] Roux, E., Lafleur, M., Lataste, E., Moreau, P., Leroux, J.-C., 2003. On the characterization of pH-sensitive liposome/polymer complexes, *Biomacromolecules*, 4, 240-248.

- [64] Roux, E., Passirani, C., Scheffold, S., Benoit, J.P., Leroux, J.-C., 2004. Serum-stable and long-circulating, PEGylated, pH-sensitive liposomes, *J. Controlled Release*, 94, 447– 451.
- [65] Roux, E., Stomp, R., Giasson, S., Pézolet, M., Moreau, P., Leroux, J.-C., 2002b. Steric stabilization of liposomes by pH-responsive *N*-isopropylacrylamide copolymer, *J. Pharm. Sci.*, 91, 1795-1802.
- [66] Rui, Y., Wang, S., Low, P.S., Thompson, D.H., 1998. Dismenylcholine-folate liposomes: An efficient vehicle for intracellular drug delivery, *J. Am. Chem. Soc.*, 120, 11213-11218.
- [67] Rustum, Y.M., Mayhew, E., Szoka, F., J., C., 1981. Inability of liposome encapsulated 1-beta-D-arabinofuranosylcytosine nucleotides to overcome drug resistance in L1210 cells, *Eur. J. Cancer Clin. Oncol.* , 17, 809-817.
- [68] Scheinberg, D.A., Lovett, D., Divgi, C.R., Graham, M.C., Berman, E., Pentlow, K., Feirt, N., Finn, R.D., Clarkson, B.D., Gee, T.S., Larson, S.M., Oettgen, H.F., Old, L.J., 1991. A phase I trial of monoclonal antibody M195 in acute myelogenous leukemia: specific bone marrow targeting and internalization of radionuclide, *J. Clin. Oncol.*, 9, 478-490.
- [69] Simard, P., Leroux, J.C., Allen, C., Meyer, O., Liposomes for Drug Delivery, in: A.J. Domb, Y. Tabata, M.N.V. Kumar (Eds.), *Nanoparticles for Pharmaceuticals Applications*, American Scientific Publishers, Valencia, 2007, pp. 1-62.
- [70] Simoes, S., Slepushkin, V., Pedroso de Lima, M.C., Düzunges, N., 1998. Gene delivery by negatively charged ternary complexes of DNA, cationic liposomes and transferrin or fusogenic peptides, *Gene Ther.*, 5, 955-964.
- [71] Stier, E.M., Mandal, M., Lee, K.D., 2005. Differential cytosolic delivery and presentation of antigen by listeriolysin O-liposomes to macrophages and dendritic cells, *Mol. Pharm.*, 2, 74-82.

- [72] Sudimack, J.J., Guo, W., Tjarks, W., Lee, R.J., 2002. A novel pH-sensitive liposome formulation containing oleyl alcohol, *Biochim. Biophys. Acta*, 1564, 31-37.
- [73] Weinstein, J.N., Magin, R.L., Yatvin, M.B., Zaharko, D.S., 1979. Liposomes and local hyperthermia: selective delivery of methotrexate to heated tumors, *Science*, 204, 188-191.
- [74] Woodle, M.C., Lasic, D.D., 1992. Sterically stabilized liposomes, *Biochim. Biophys. Acta*, 1113, 171-199.
- [75] Working, P.K., Newman, M.S., Huang, S.K., Mayhew, E., Vaage, J., Lasic, D.D., 1994. Pharmacokinetics, biodistribution and therapeutic efficacy of doxorubicin encapsulated in stealth liposomes (Doxil), *J. Liposome Res.*, 4, 667-687.
- [76] Yatvin, M.B., Kreutz, W., Horwitz, B.A., Shinitzky, M., 1980. pH-sensitive liposomes: possible clinical implications, *Science*, 210, 1253-1255.
- [77] Yessine, M.-A., Lafleur, M., Meier, C., Petereit, H.-U., Leroux, J.-C., 2003. Characterization of the membrane-destabilizing properties of different pH-sensitive methacrylic acid copolymers, *Biochim. Biophys. Acta*, 1613, 28-38.
- [78] Yessine, M.A., Dufresne, M.H., Meier, C., Petereit, H.U., Leroux, J.C., 2007. Proton-actuated membrane-destabilizing polyion complex micelles, *Bioconjug. Chem.*, 18, 1010-1014.
- [79] Yessine, M.A., Leroux, J.C., 2004. Membrane-destabilizing polyanions: interaction with lipid bilayers and endosomal escape of biomacromolecules, *Adv. Drug Deliv. Rev.*, 56, 999-1021.
- [80] Yessine, M.A., Meier, C., Petereit, H.U., Leroux, J.C., 2006. On the role of methacrylic acid copolymers in the intracellular delivery of antisense oligonucleotides, *Eur. J. Pharm. Biopharm.*, 63, 1-10.
- [81] Yoshimori, T., Yamamoto, A., Moriyama, Y., Futai, M., Tashiro, Y., 1991. Bafilomycin A1, a specific inhibitor of vacuolar-type H(+)-ATPase, inhibits

- acidification and protein degradation in lysosomes of cultured cells, *J. Biol. Chem.*, 266, 17707-17712.
- [82] Zhang, Z.-Y., Shum, P., Yates, M., Messersmith, P.B., Thompson, D.H., 2002. Formation of fibrinogen-based hydrogels using phototriggerable diplasmalogen liposomes, *Bioconjug. Chem.*, 13, 640-646.
- [83] Zignani, M., Drummond, D.C., Meyer, O., Hong, K., Leroux, J.-C., 2000. *In vitro* characterization of a novel polymeric-based pH-sensitive liposome system, *Biochim. Biophys. Acta*, 1463, 383-394.

Chapitre 6. *In vivo* evaluation of pH-sensitive polymer-based immunoliposomes targeting the CD33 antigen

Pierre Simard¹ and Jean-Christophe Leroux^{1,2}

¹Canada Research Chair in Drug Delivery, Faculty of Pharmacy, University of Montreal, C.P. 6128 Succ. Centre-ville, Montreal (Qc) Canada H3C 3J7

²Institute of Pharmaceutical Sciences, ETH Zürich, Wolfgang-Pauli-Str. 10, 8093 Zürich, Switzerland.

Submitted to: *Molecular Pharmaceutics*

6.1. Abstract

The purpose of this study was to evaluate *in vivo* a targeted pH-sensitive liposomal formulation tailored to promote the efficient intracellular delivery of 1-beta-D-arabinofuranosylcytosine (ara-C) to human myeloid leukemia cells. Specifically, pH-sensitive immunoliposomes were obtained by anchoring a copolymer of dioctadecyl, *N*-isopropylacrylamide and methacrylic acid in bilayers of PEGylated liposomes (LP) and by coupling the whole anti-CD33 monoclonal antibody (MAb) or its Fab' fragments. Their pharmacokinetic and biodistribution profiles were assessed in Balb/c and leukemic HL60-

bearing immunodepressed (SCID) mice. In naive mice, non-targeted and pH-sensitive Fab'-LP had longer circulation times than LP with whole MAb. In SCID/HL60 (CD33⁺) mice, the pharmacokinetic and biodistribution profiles of LP and encapsulated ara-C were comparable between non-targeted and pH-sensitive Fab'-LP. In leukemic mice, only pH-insensitive, ara-C-loaded Fab' induced prolonged survival times. The apparent absence of pH-sensitive Fab'-LP effect could be related to lower exposure to ara-C in SCID mice.

6.2. Introduction

Acute myeloid leukemia (AML) is a disorder of hematopoietic stem cells where a disruption of the differentiation process allows uncontrolled growth of blasts clones in bone marrow. The accumulation of these abnormal cells eventually causes loss of normal hematopoietic function, eliciting neutropenia, anemia and thrombocytopenia¹. Unless treated, AML has been associated with a high mortality rate due to increased susceptibility to infections or bleeding, both of which can occur within weeks after onset of the disease.

1-β-D-arabinofuranosylcytosine (ara-C) remains the gold standard for first-line treatment of AML. It is part of current induction therapy, often in association with an anthracycline to improve the antitumoral response.² Ara-C is a pyrimidine analog pro-drug which penetrates cells by a carrier-mediated transporter used by other nucleosides.³ Once internalized, it needs to be metabolized intracellularly into its active triphosphate form (cytosine arabinoside triphosphate, ara-CTP) to exert its toxicity. Ara-CTP acts by inducing DNA breakdown through the inhibition of DNA synthesis and repair because of its effect on α- and β-DNA polymerases and its incorporation into DNA.^{4,5} *In vitro*, the efficiency of ara-C is dependent on its intracellular bioavailability and exposure time.⁶ In humans, the compound is rapidly converted to an inert metabolite, 1-β-D-arabinofuranosyluracil, by the ubiquitous enzyme cytidine deaminase, and eliminated by renal clearance within 7-20 min

after intravenous (i.v.) administration.⁷ As a consequence, repetitive dosing schedules or continuous i.v. infusion over 5-7 days and a high-dose regimen are required for optimal therapy.⁸ This intensive treatment is not always well tolerated, especially in the elderly. Furthermore, for about 10-50% of newly-diagnosed AML patients, treatment may not lead to remission, and the risk of developing resistance increases with each relapse. The chemoresistance of AML patients appears to be related to many different mechanisms, such as ara-C efflux by multi-drug resistance *P*-glycoprotein from malignant cells, the expression of cytoplasmic 5'-nucleotidase, an enzyme preventing ara-C phosphorylation of ara-C, and human equilibrative nucleoside transporter 1 deficiency involved in ara-C internalization.^{9,10} Therefore, efforts to facilitate ara-C delivery are expected to enhance the intracellular bioavailability of ara-CTP and improve the outcome of AML.

Previous studies have demonstrated the ability of liposomes (LP) to encapsulate ara-C, protect it from extracellular deamination and prolong its half-life.^{11, 12} Moreover, opportunities for new promising liposomal treatments have come from the identification of novel targets. Different targeting moieties have been investigated to facilitate the cellular uptake of ara-C-loaded LP. They include transferrin¹³, anti-D4.2 monoclonal antibody (MAb)¹⁴, anti-H-2K^k MAb¹⁵, and anti-CD33 MAb¹⁶. The latter binds the CD33 receptor, a 67-kDa glycoprotein expressed on the surface of leukemia cells, from more than 80-90% of patients with AML.¹⁷ This receptor is neither expressed on normal hematopoietic stem cells nor on non-myeloid tissue.¹⁸ Because CD33 is rapidly internalized after antibody binding, an antibody-cytotoxic agent conjugate or a targeted nanocarrier can effectively be taken up specifically by leukemia cells. The anticancer agent, calicheamicin, linked to recombinant, humanized anti-CD33 antibody called Mylotarg® (Gemtuzumab Ozogamicin), has demonstrated great clinical promises. Actually, Mylotarg® is approved by the US Food and Drug Administration since 2000 as a single-agent therapy for CD33-positive AML in first-relapse patients who are not considered candidates for standard cytotoxic therapy.¹⁹

Although liposomal ara-C can be specifically delivered to target cells with MAb, its degradation in lysosomes after receptor-mediated endocytosis limits its intracellular bioavailability.^{15, 20, 21} In this regard, pH-sensitive LP that are stable at physiological pH but undergo destabilization and release their content under acidic conditions constitute a hopeful approach. In our laboratory, promising *in vitro* results have been obtained with sterically-stabilized LP composed of egg phosphatidylcholine (EPC), cholesterol (Chol) and a pH-sensitive copolymer made of dioctadecyl (DODA), *N*-isopropylacrylamide (NIPAM) and methacrylic acid (MAA). Indeed, these polymeric pH-sensitive LP were found to be stable in the presence of plasma proteins^{16, 22, 23}, trigger the release of cargo entrapped cargo in acidic intracellular organelles,^{16, 24, 25} target specifically the CD33 cell surface antigen when decorated with a MAb,¹⁶ and induce cell death by delivering loaded active ara-C.^{16, 25} The present study is aimed at comparing immunoliposomes targeted *via* whole anti-CD33 MAb and its Fab' fragment to conventional poly(ethylene glycol) (PEG)ylated-LP in terms of their *in vivo* pharmacokinetic and biodistribution profiles in healthy and immunodeficient mice inoculated with HL60 leukemic (CD33⁺) cells. In a preliminary experiment, the anticancer efficacy of ara-C encapsulated in different pH-sensitive LP was also investigated.

6.3. Material and methods

6.3.1. Material

EPC (760 g/mol), 1,2-distearoyl-*sn*-glycero-3-phosphatidylethanolamine-*N*-monomethoxy (DSPE)-PEG 2000 and Chol (99.5% pure) were obtained from Northern Lipids Inc. (Vancouver, BC, Canada). DSPE-PEG 3400-maleimide was purchased from Laysan Bio Inc. (Arab, AL). NIPAM, MAA, Triton X-100, formaldehyde 37% (*v/v*), Sepharose[®] CL-4B, Sephadex[®] G-50, dithiotreitol (DTT), sodium *meta*-periodate, Ellman's

reagent, ara-C, and mouse isotype control IgG_{1b} MOPC21 were procured from Sigma-Aldrich (St. Louis, MO). Purified anti-CD33 antibodies were from AbD Serotec (Raleigh, NC). 3-(2-pyridylidithio)propionyl hydrazide (PDPH), bicinchoninic acid (BCATM) protein kit and Immunopure IgG₁ Fab' and F(ab)₂ preparation kit were bought from Pierce (Rockford, IL). Centricon-10 and -50 tubes were supplied by Millipore (Milford, MA). PD-10 desalting columns were from GE Healthcare Life Science (Uppsala, Sweden). [³H]-ara-C (15-30 Ci/mmol) was purchased from American Radiolabeled Chemicals (St Louis, MO). [¹⁴C]-Cholesteryl oleate (52 mCi/mmol) and [³H]-ara-C (33 Ci/mmol) were obtained from Perkin Elmer (Waltham, MA). HL60 (human promyelocytic leukemia cells) were from the American Type Culture Collection (Rockville, MD). Cholesteryl 4,4-difluoro-5,7-dimethyl-4-bora-3a,4a-diaza-s-indacene-3-dodecanoate (cholesteryl-BODIPY FL C12), RPMI 1640, Dulbecco's modified Eagle's medium, foetal bovine serum (FBS), penicillin G (100 U/mL), streptomycin (100 µg/mL) solution, and trypan blue were procured from Invitrogen (Burlington, ON, Canada). All products were used without further purification. Water was deionized with a MilliQ purification system (Millipore, Bedford, MA).

6.3.2. Preparation of copolymers

The terminally-alkylated polymer was synthesized by free radical polymerization of NIPAM and MAA employing 4,4'-azobis(4-cyano-*N,N*-dioctadecyl)pentanamide (DODA-501) as the lipophilic initiator (NIPAM/MAA/DODA 93:5:2 mol%), as described elsewhere.²⁶ The composition of the synthesized polymers was confirmed by H¹-NMR spectroscopy. The weight-average molecular weight (M_w) of the copolymer was 11,000 (polydispersity index (PI) = 2.1). This DODA-P(NIPAM-*co*-MAA) had coil-to-globule phase transition at pH 5.6 at 37°C.

6.3.3. Preparation of PEGylated pH-sensitive LP

LP of EPC/Chol/DSPE-PEG2000/DSPE-PEG-maleimide (3:2:0.17:0.09 molar ratio) were prepared by the thin film hydration method. Briefly, lipids and DODA-P(NIPAM-*co*-MAA) (0.12 w/w) were dissolved in chloroform and mixed with 0.3 mol% of the fluorescent probe cholesteryl-BODIPY FL C12. After solvent evaporation, the film was hydrated with a buffered solution of *N*-(2-hydroxyethyl)piperazine-*N'*-(2-ethanesulfonic acid) (HEPES) (HBS, 20 mM, pH 7.2) and NaCl (144 mM), or a solution of ara-C (230 mM, 5 mM HEPES, pH 7.4, 340 mOsm). The LP were then extruded several times through polycarbonate membranes (400, 200 and 100 nm) in a LiposoFast extruder (Avestin, Ottawa, ON, Canada) to yield vesicles with diameters of ca. 140 nm (PI of 0.03-0.05) as determined by dynamic light scattering (Zetasizer Nanoseries, Malvern Instruments, Worcestershire, UK). Excess polymer and unencapsulated ara-C were removed by gel filtration on a Sepharose® CL-4B column. LP concentration was quantified by phosphorous assay.²⁷

6.3.4. Modification of the antibodies

Anti-CD33 antibodies (clone p67.6) (5-10 mg/mL) were oxidized at carbohydrate sites with cold sodium *meta*-periodate (final concentration of 15 mM) at 4°C for 40 min in sodium acetate buffer (0.1 M, pH 5.5). After removing the excess by dialysis (cut off 6-8,000 g/mol), the oxidized antibodies were reacted with PDPH (final concentration of 5 mM) for 5 h at room temperature under agitation. PDPH-antibodies were purified overnight by dialysis against acetate buffer (0.1 M, pH 4.5). The following day, they were treated with DTT (25 mM) at room temperature for exactly 20 min. The reaction mixture was applied on a Sephadex G-50 column and eluted with HBS (20 mM, pH 7.2) under

nitrogen flux. Twenty μ L of each collected fraction were treated with Ellman's reagent (4 mg/mL in PBS) to verify the removal of excess DTT. Fractions containing thiolated antibodies were pooled together under nitrogen atmosphere, and the final protein concentration was assayed with a BCA kit.

6.3.5. Preparation of F(ab)₂ and Fab' fragments

F(ab)₂ fragments of antibody were produced with Immunopure IgG₁ Fab' and F(ab)₂ preparation kits. In brief, anti-CD33 antibody was concentrated in Centricon-50 tubes (5-10 mg/mL), resuspended in 0.5 mL of phosphate-buffered saline (PBS) and added to 0.5 mL of Immunopure IgG₁ mild elution buffer from kits containing 1 mM of cysteine. The solution was then incubated with an immobilized ficin column for 35-40 h at 37°C. It was eluted with 4 mL of Immunopure binding buffer, and fragments were separated on a protein A column, which retained Fc fragments and undigested IgG₁, whereas F(ab)₂ fragments were collected in 0.5-mL fractions. Fractions containing F(ab)₂ were analyzed from absorbance reading at 280 nm and pooled together. The F(ab)₂ fragments (110 kDa) were then concentrated in Centricon-50 tubes and resuspended in 1 mL PBS.

F(ab)₂ fragments were incubated with a final concentration of 0.05 M of 2-mercaptoethylamine-HCl (MEA, pH 6.0) for 90 min at 37°C under nitrogen atmosphere. MEA cleaves disulfide bridges between heavy chains but preserves disulfide linkages between heavy and light antibody chains. The solution (2.5 mL) was eluted on a PD-10 column (Sephadex® G-25 Medium gel, 5 cm), and Fab' fragments were collected in 0.5-mL fractions. Ellman's assay was performed to confirm the separation of MEA residue from the Fab' fragments. Fractions containing Fab' fragments (55 kDa) were determined from absorbance reading at 280 nm, pooled together and concentrated in Centricon-10 tubes under nitrogen atmosphere.

6.3.6. Coupling reaction

Immediately after antibody modification (whole antibodies or Fab' fragments), functionalized LP containing DSPE–PEG maleimide were coupled to thiolated antibodies or thiolated Fab' fragments under nitrogen atmosphere at a ratio of 100 and 35 µg proteins per µmol of lipids, respectively. The mixture was incubated for 30 min at room temperature, followed by overnight incubation at 4°C on a rotating plate set at low speed. After the coupling period, all the formulations were incubated with β-mercaptoproethanol for 20 min at room temperature to quench free maleimide groups. The vesicles were then chromatographed over a Sepharose® CL-4B column equilibrated with isotonic HBS (pH 7.2), to separate LP from excess β-mercaptoproethanol and free antibodies/fragments.

6.3.7. Liposomal lipid extraction procedure and ara-C assay

Lipids from the liposomal formulations were extracted before determining, by high performance liquid chromatography (HPLC), the ara-C concentration encapsulated into these vesicles. For lipid extraction, 200 µL of liposomal suspension was mixed with 250 µL of dichloromethane, followed by 500 µL of methanol. The mixture was then vortexed until a clear solution was obtained. Next, 250 µL of a 0.2-M NaOH solution and another 250 µL of dichloromethane were introduced and vortexed vigorously.²⁸ The sample, containing 2 phases, was centrifuged for 5 min (3,000 x g) in glass tubes. Lipids were located in the lower phase, and ara-C was found in the upper water-methanol phase. Ara-C concentration in the supernatant was assayed with a Waters HPLC system equipped with a 1,525 binary pump, a 2,487 dual wavelength absorbance detector, and Breeze chromatography software (Waters, Milford, MA). The mobile phase consisted of 100 mM sodium acetate (pH 5.5) plus 1% (v/v) acetonitrile.²⁹ The column was a Waters Nova-Pack C18, 60 Å, 4 µm (3.9 ×

300 mm). Flow rate, detection wavelength, temperature, and injection volume were set at 1 mL/min, 272 nm, 25°C, and 40 µL, respectively.

6.3.8. Cell culture and internalization assays

The human monocyte cell line HL60 (CD33⁺) was grown as cultures suspended in RPMI 1640, supplemented with 20% (*v/v*) heat-inactivated FBS, 2 mM glutamine, 1% (*v/v*) penicillin G (100 U/mL) and streptomycin (100 µg/mL). The cells were maintained at 37°C in a humidified atmosphere containing 5% CO₂. All experiments were performed on mycoplasma-free cell lines. Only cells in the exponential phase of growth were used.

Leukemic HL60 cells (5 x 10⁵/tube) were incubated at 37°C for 2 h with 0.2 µmol of different LP formulations labelled with the hydrophobic probe BODIPY FL C12. Competitive binding assays were conducted in the presence of 20-fold excess, free anti-CD33 antibody. At the end of the incubation period, LP that did not bind to the cells were removed by washing 3 times with cold, isotonic PBS. The cells were fixed with 1% (*v/v*) formalin/PBS for 10 min at 4°C, and the mean fluorescence intensity of single cells in each sample was recorded with a FACSCalibur flow cytometer (Becton Dickinson, San Jose, CA). Data were acquired and analyzed with CellQuest software (Becton Dickinson). Cell profiles were constructed according to parameters of side scatter and forward scatter. This region was gated in order to exclude dead cells and cell debris. Cholestryl-BODIPY FL C12 excitation was obtained with argon ion laser (488 nm) and green fluorescence emission were recorded in the FL1 channel (530/30 nm). A total of 10,000 events were analyzed for each sample. The upper limit of background fluorescence was set so that no more than 1% of events with autofluorescence controls (attributable to native cells) occurred in the positive region.

6.3.9. *In vivo pharmacokinetics and biodistribution*

In vivo studies were undertaken in naive female Balb/c mice (~20 g), and CB17 immunodepressed (SCID) mice 6-8 weeks old (Charles River, St-Constant, QC, Canada) inoculated with 1.2×10^7 leukemic HL60 cells *via* the tail vein. They were approved by the Animal Welfare and Ethics Committee of the University of Montreal in accordance with Canadian Council on Animal Care guidelines. Ara-C-loaded, pH-sensitive LP labelled with [^{14}C]-cholesteryl oleate and [^3H]-ara-C were prepared, as described in Section 2.3.

The Balb/c mice were divided into 4 groups (4 mice/group). The first group received a solution of ara-C spiked with [^3H]-ara-C, whereas the second, third and fourth groups were injected with ara-C-loaded, pH-sensitive LP, pH-sensitive MAb-LP and pH-sensitive Fab'-LP, respectively. The formulations (160 μL) were given *via* the tail vein with 40 $\mu\text{mol}/\text{kg}$ of lipids, corresponding to 3.4 mg/kg ara-C, 15 $\mu\text{Ci}/\text{kg}$ [^3H]-ara-C and 35 $\mu\text{Ci}/\text{kg}$ [^{14}C]-cholesteryl oleate. For experiments with SCID mice, ara-C-loaded, pH-sensitive LP and pH-sensitive Fab'-LP were injected 7 days post-inoculation of the HL60 cells, at the same dose as the Balb/c mice.

Blood samples (400 μL) and major organs (*i.e.* heart, lungs, spleen, liver, muscle, bone marrow, kidneys) were excised from individual euthanized animals at selected time points, *i.e.* 30 min, 1, 2, 4, 8, 12 and 24 h post-injection of the formulations. The mice were perfused with saline prior to harvesting the organs. Blood and tissues were weighed and treated with Solvable[®] (Perkin Elmer, Waltham, MA). After digestion, blood samples were bleached by successive additions of hydrogen peroxide (30% *v/v*). The samples were left to stand in the dark overnight at 4°C after the addition of Hionic Fluor[®] scintillation cocktail (Perkin Elmer). Radioactivity was measured by scintillation counter in dual mode (^3H / ^{14}C). The mean area under the blood concentrations *vs* time curve (AUC_{0-24h}), blood clearance

(CL) and volume of distribution (V_d) parameters were determined in a non-compartmental model. The apparent half-life of the β -elimination phase ($t_{1/2\beta}$) of all the formulations injected was calculated by linear regression of the 4 last time points of the pharmacokinetic data. The data were analyzed statistically by one-way analysis of variance followed by the Tukey test. Differences were considered significant at $p<0.05$.

6.3.10. *In vivo* survival experiment

SCID mice were inoculated with 1.2×10^7 HL60 cells *via* the tail vein. At 24 h post-inoculation, they were injected i.v. with saline (control) or a 8 mg/kg dose of free ara-C, ara-C-loaded Fab'-LP or pH-sensitive Fab'-LP. A second injection (8 mg/kg) of free and encapsulated ara-C was given to the mice 3 days after inoculation of the cells. They were monitored, weighed daily up to 79 days by Mispro Biotech Services Inc. (Montreal, Qc, Canada). The mice were euthanized when tumor size exceeded 1,500 mm³ or when they developed hind-leg paralysis. The significance of differences between the experimental groups ($n = 8$ mice/group) in the survival experiment was determined by Kaplan-Meier curves with the log-rank (Mantel-Cox) test using GraphPad Prism software version 5.0 (San Diego, CA). These findings were considered significant at $p<0.05$.

6.4. Results & Discussion

6.4.1. Preparation and characterization of pH-sensitive immunoliposomes

Ara-C, a potent inhibitor of DNA synthesis, has been employed clinically as an antitumor agent for the treatment of AML.^{2, 5} However, in plasma, tissues and cells, it is

easily deaminated by deoxycytidine deaminase into its uracil analogue, thereby losing its antitumor activity. The purpose of this study was to characterize the pharmacokinetics and biodistribution of ara-C encapsulated in pH-sensitive LP that target leukemia cells and rapidly release their cargo upon uptake. Drug release is triggered by destabilization of the bilayer membrane after the phase transition of membrane-anchored DODA-P(NIPAM-*co*-MAA). As opposed to most other pH-sensitive LP described in the literature³⁰, these liposomal formulations are relatively stable in the presence of blood proteins and exhibit long circulation times *in vivo*.^{16, 25, 31} To ensure better selectivity, such pH-sensitive LP can be further decorated with a targeting ligand. Recently, we reported the conjugation of anti-CD33 MAb to the surface of ara-C-loaded, pH-sensitive LP.¹⁶ These nanocarriers showed specific cellular uptake and improved ara-C cytotoxicity against HL60 leukemia cells. The whole MAb was attached to the LP surface after the oxidation of carbohydrate sites from the Fc fragment, derivatization with PDPH and conjugation with DSPE-PEG maleimide.¹⁶ As for Fab'-decorated LP (Figure 6.1), the fragments were prepared by first cleaving the whole MAb into F(ab)₂ on an immobilized ficin column in the presence of cysteine as activator.³² Fab' was then obtained from F(ab)₂ after incubation with MEA-HCl which cleaves disulfide bridges between the heavy chains (yield ca. 100%). Thiolated Fab' was reacted with DSPE-PEG maleimide, as described for the whole MAb.³³ Coupling efficiency for both proteins on the vesicles was in the 15-20% range (data not shown). This percentage lies within the normal range for this coupling technique.^{34, 35} To graft the same number of MAb and Fab' targeting moieties on the LP surface, the feed ratios of fresh thiolated proteins were fixed at 100 and 35 µg per µmol of lipids, respectively. Targeted vesicles, with a mean diameter of ~140 nm (PI = 0.03-0.05) were obtained.

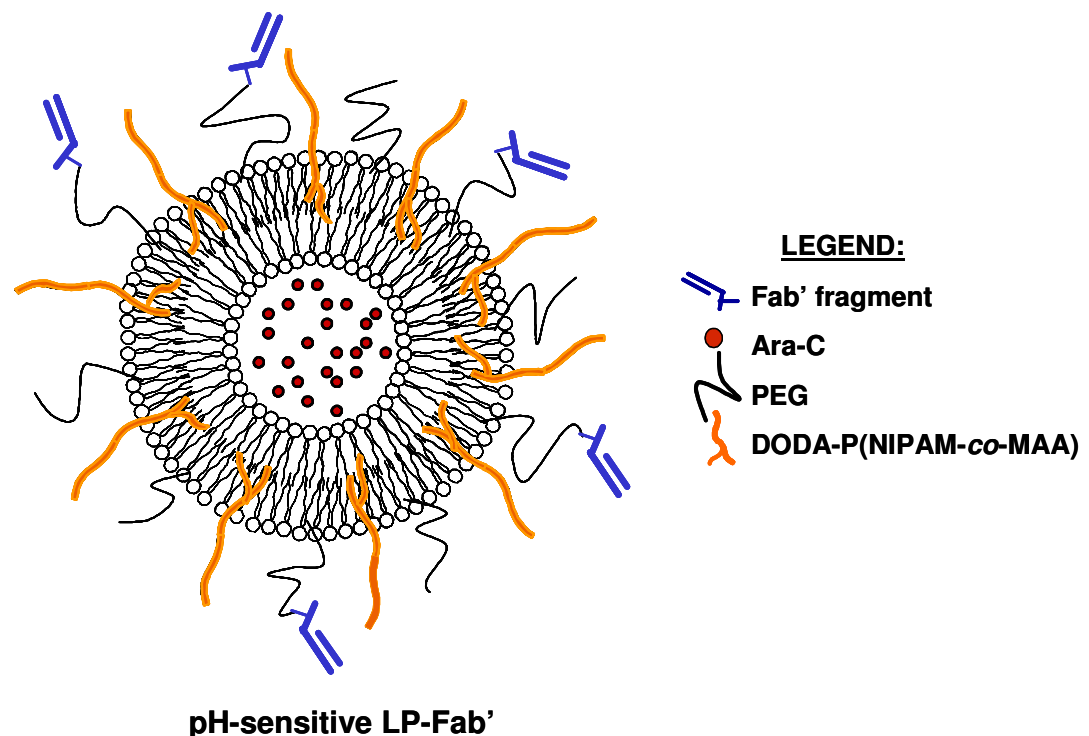


Figure 6.1. Schematic representation of pH-sensitive anti-CD33 Fab'-LP.

To determine whether attachment of anti-CD33 Fab' to pH-sensitive LP would target HL60 ($CD33^+$) cells *in vitro*, the formulations were fluorescently-labelled with cholestrylo-BODIPY FL C12, and cellular association (binding + internalization) was monitored by flow cytometry (Figure 6.2), as reported previously for LP decorated with the full MAb.¹⁶ As expected, a relatively low amount of non-targeted LP was taken up by HL60 cells after 2 h. Coating the LP with anti-CD33 Fab' resulted in a 4.5-fold increase in fluorescence intensity uptake, where 99% of the cells incubated with Fab'-LP were positively stained vs. only 5% for control LP. There was a slight difference between the uptake of pH-sensitive Fab'-LP and Fab'-LP devoid of DODA-P(NIPAM-*co*-MAA). This

phenomenon can be ascribed to the steric hindrance created by DODA-P(NIPAM-*co*-MAA) which possesses a M_w of 11,000 Da, largely superior to that of DSPE-PEG-maleimide (3400 Da). Similar results were obtained previously with the coupling of whole MAb.¹⁶ A competition experiment performed with 20-fold excess of free anti-CD33 MAb resulted in decreased cell association of the targeted Fab'-LP (Figure 6.2). These data confirmed the binding specificity of anti-CD33 Fab'-LP.

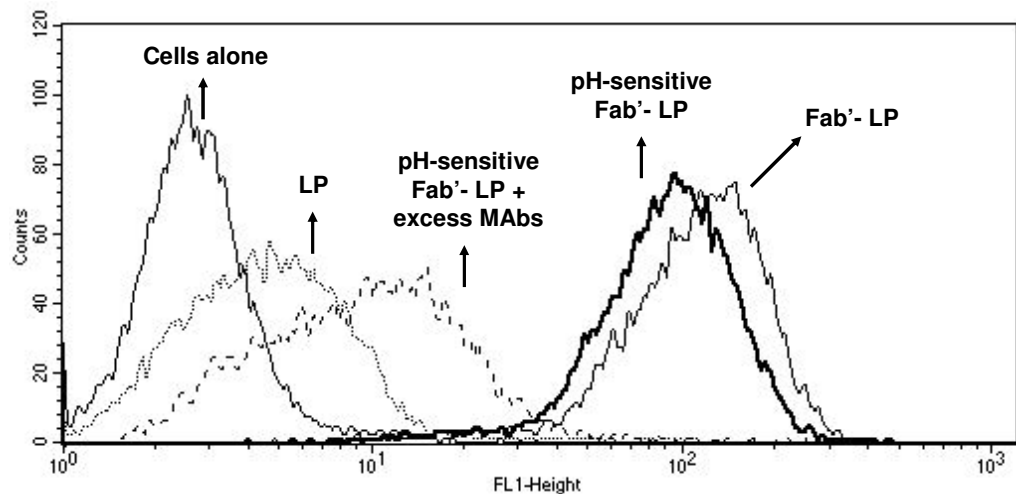
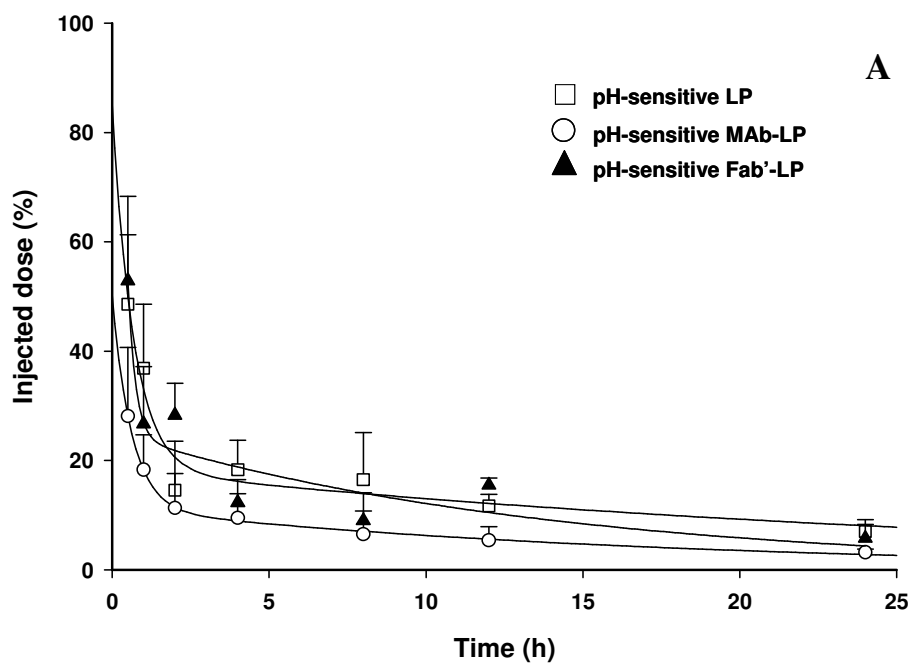


Figure 6.2. Fluorescent labelling of HL60 ($CD33^+$) cells after 2 h incubation of different LP formulations labelled with BODIPY FL C12 at 37°C, as determined by flow cytometry. The x-axis represents the logarithm of green fluorescence signal, and the y-axis is the cell count. The first plain line corresponds to basal cellular fluorescence (without any probe). The striped line represents competitive binding assays of pH-sensitive LP-Fab' performed in the presence of a 20-fold excess of free anti-CD33 antibody in the medium.

6.4.2. Pharmacokinetics and biodistribution in Balb/c mice

The pharmacokinetics and biodistribution profiles of non-targeted or targeted pH-sensitive LP loaded with ara-C were first examined in naive Balb/c mice, where distribution was not affected by the presence of tumor cells (Figures 6.3A, 6.5A and Supplementary Figure 6.7, Table 6.1). As reported previously by our group, non-targeted, PEGylated, pH-sensitive LP exhibited long circulation times.²³ In rats, we showed that biological half-life was comparable to that obtained with PEGylated LP in the absence of DODA-P(NIPAM-*co*-MAA).³¹ As illustrated in Figure 6.3A, in Balb/c mice, less than 16% of the total injected dose was still present in blood 12 h post-injection, which was approximately 2-fold lower than that observed in rat.²³ Compared to the non-targeted formulation, the decoration of pH-sensitive LP with whole anti-CD33 MAb resulted in a substantial decrease of liposomal blood levels. For example, 1 h after administration, 37% of injected pH-sensitive LP were still circulating *versus* only 18% of pH-sensitive MAb-LP. Overall, CL increased by more than 2-fold (Table 1). In contrast, the effect of anti-CD33 Fab' on the LP pharmacokinetic profile was relatively modest, with no noticeable impact on CL, the $t_{1/2\beta}$ and AUC_{0-24h} (1842 *vs.* 1743 nmol h/mL). The lower influence of antibody fragments on the circulation times of PEGylated LP was in accordance with the data published by other groups.³⁶⁻³⁸ The biodistribution profiles also reflected this difference between the MAb and Fab'-coated formulations (Figure 6.5). For example, at 1 h post-administration, 17% of MAb-LP was deposited in the liver compared to only 8 and 6% of LP and Fab'-LP, respectively ($p<0.05$ between MAb-LP and Fab'-LP). It has been shown that the Fc region of MAb can lead to enhanced removal of immunoliposomes by the mononuclear phagocyte system (MPS), mainly *via* Fc receptors on macrophages.³⁹ The coupling method employed in this work is supposed to position the Fc fragment towards the bilayer while exposing the Fab' domain on the surface.^{40, 41} However, some MAb may not be well orientated on the vesicles and present their Fc portion to macrophages. Although this procedure has

demonstrated superior circulation time *in vivo* compared to approaches relying on the random grafting of whole MAb, the CL of LP still remains rapid in the presence of the Fc fragment.⁴⁰ Another factor potentially at play is ligand density, with faster clearance observed at high MAb densities (>50 µg/µmol phospholipids).⁴² However, this should not be the case for our pH-sensitive MAb-LP considering the relatively low proportion of grafted MAb (<20 µg/µmol phospholipids).



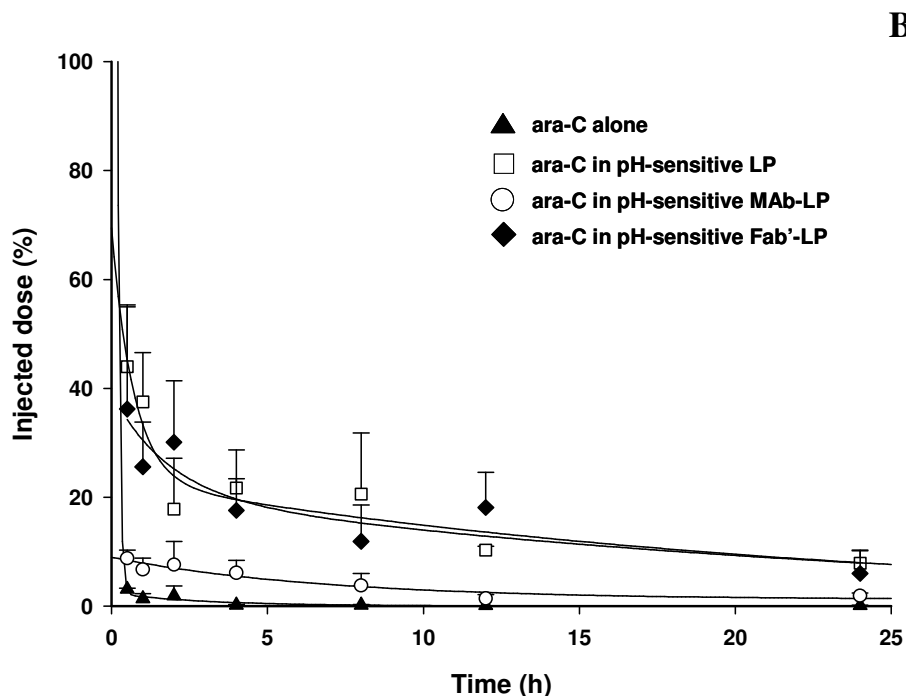


Figure 6.3. Blood concentration-time profiles of pH-sensitive LP and pH-sensitive LP bearing whole anti-CD33 MAb or the Fab' fragment (A) and of free and encapsulated ara-C (B) in naive Balb/c mice. Each mouse received i.v. 3.4 mg/kg ara-C and 40 μ mol/kg of lipids. Values represent the mean (\pm S.D.) obtained for $n = 4$ animals per group per time point.

The pharmacokinetic and biodistribution patterns of encapsulated ara-C followed a similar trend (Figures 6.3B, 6.5B and Supplementary Figure 6.7, Table 6.1). While free ara-C was cleared from the blood within minutes, its encapsulation resulted in an increase in circulation time. However, in the case of pH-sensitive MAb-LP, the gain was relatively modest compared to non-targeted and Fab'-LP (7 vs. 33-fold increase in the AUC,

respectively). Such an impact of MAb coating on ara-C blood levels could be explained by **i)** the greater clearance of pH-sensitive MAb-LP, as discussed above, and **ii)** a higher leakage rate from these LP compared to non-targeted or Fab'-LP. Although rapid ara-C release in plasma was not observed in our previous *in vitro* investigations¹⁶, increased permeability may occur *in vivo* upon activation of the innate immune system. Exposure of Fc fragments may lead to complement activation and subsequent destabilization of the LP membrane. In the case of pH-sensitive LP and pH-sensitive Fab'-LP formulations, the proportion of LP circulating in blood at different time points roughly corresponded to the percentage of circulating ara-C (compare Figures 6.3A & B). These data suggest that the drug remained mainly encapsulated in circulating LP during the time course of the study. Moreover, these 2 formulations exhibited similar V_d and CL values for encapsulated ara-C (Table 1). Liposomal ara-C accumulated mainly in the liver (Figure 6.5B) and spleen (Supplementary Figure 6.7). The higher concentration in the liver occurred with the pH-sensitive MAb LP formulation. Deposition into lungs, heart, kidneys, muscles, bone marrow and spleen was less than 3% of the injected dose for all formulations (data not shown).

Table 6.1. Comparison of the pharmacokinetic parameters of different pH-sensitive LP formulations and of encapsulated ara-C in naive Balb/c and SCID-HL60 mice

Formulations	Ara-C				Vectors			
	AUC (0? 24 h) ($\mu\text{g}\cdot\text{h}/\text{mL}$)	V_d (mL)	$t_{1/2\beta}$ (h)	CL (mL/h)	AUC (0? 24 h) (nmol \cdot h/mL)	V_d (mL)	$t_{1/2\beta}$ (h)	CL (mL/h)
NAIVE BALB/C MICE								
ara-C alone	5	31.1	1.5	14.3				
pH-sensitive LP	166	3.0	7.6	0.2	1842	2.5	6.1	0.2
pH-sensitive MAb-LP	36	13.8	7.8	0.9	913	4.0	4.3	0.5
pH-sensitive Fab'-LP	166	3.2	7.4	0.2	1743	1.9	5.3	0.2
SCID-HL60 MICE								
pH-sensitive LP	143	2.6	4.4	0.3	1983	2.0	3.4	0.3
pH-sensitive Fab'-LP	111	4.0	3.6	0.5	1563	3.0	3.5	0.4

It has been repeatedly demonstrated that ara-C encapsulation into LP can improve its AUC, mainly by slowing down its renal clearance and rapid deamination.^{11, 12, 43} Here, we show that adequate pharmacokinetic profiles can be maintained by using pH-sensitive LP decorated with Fab'. This is an important issue as improved efficacy of liposomal formulations in leukemia models has been correlated with increased circulation times.³⁶ In the next step, it was therefore important to verify whether the pharmacokinetic profile would be altered in SCID mice inoculated with leukemic HL60 cells.

6.4.3. Pharmacokinetics and biodistribution in SCID/HL60 mice

Since the first successful report of human cancer xenograft in SCID mice in 1987, they have become a popular host for growing human tumors and have been used to evaluate a variety of therapeutic strategies.^{36, 44} Most inoculated animals were found to have a survival rate of 7-10 weeks after the injection of HL60 cells when no treatment was given^{45, 46}. Surprisingly, it has been reported that CD33⁺ cells in bone marrow, spleen, and peripheral blood were detected at 10 weeks, although the presence of HL60 cells could be ascertained by chromosome analysis. The steady loss of cell surface markers over a 8-10-week period could make this model inadequate for the *in vivo* evaluation of anti-CD33 LP at later time points. Therefore, we decided to characterize the pharmacokinetics of ara-C-loaded LP, 7 days after the inoculation of HL60 cells.

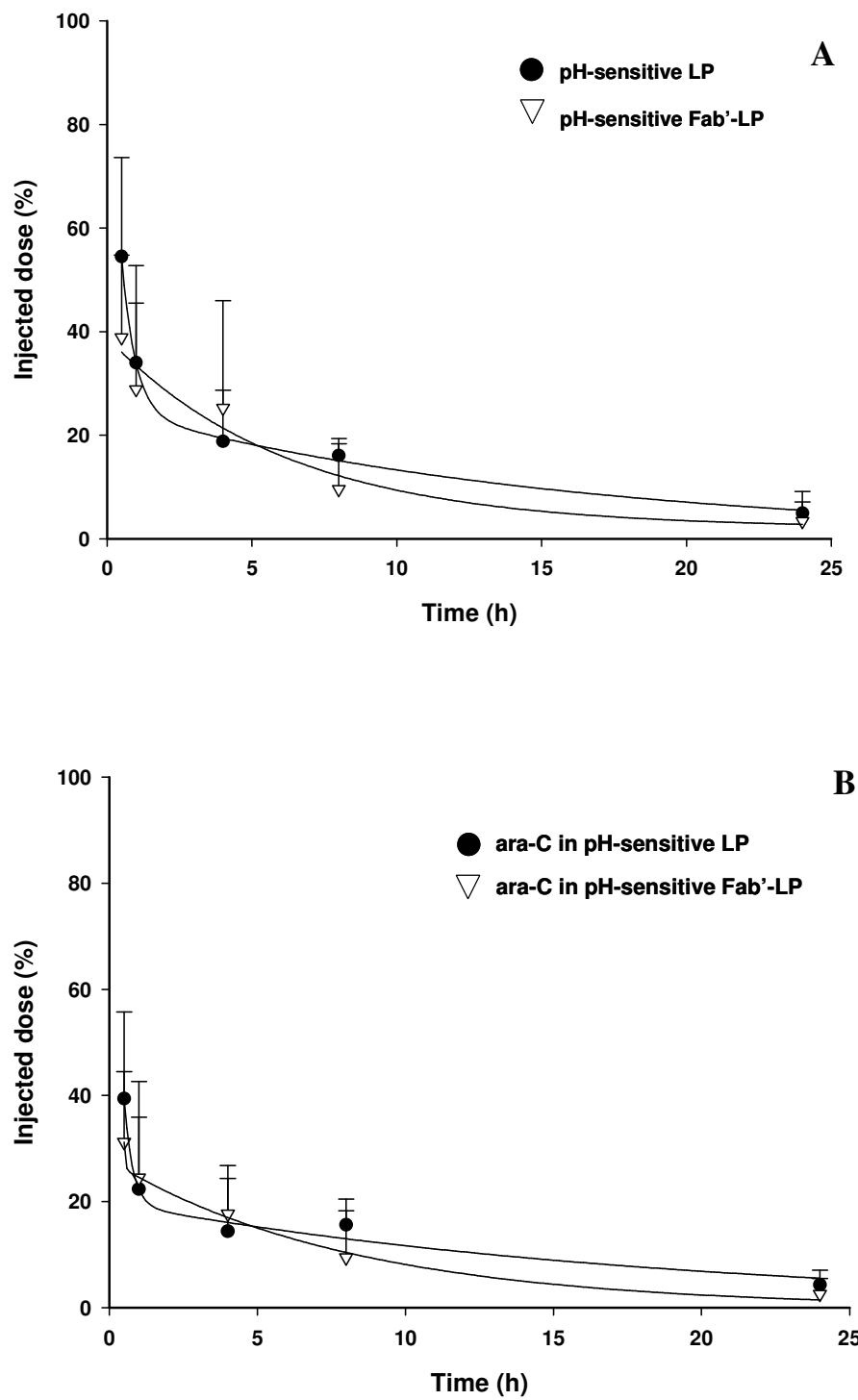


Figure 6.4. Blood concentration-time profiles of pH-sensitive LP and pH-sensitive anti-CD33 LP bearing the Fab' fragment (**A**) and of encapsulated ara-C (**B**) in SCID-HL60 mice. Each mouse received i.v. 3.4 mg/kg ara-C and 40 µmol/kg of lipids. Values represent the mean (\pm S.D.) obtained for n = 4 animals per group per time point.

HL60-bearing SCID mice were injected with pH-sensitive LP and pH-sensitive Fab'-LP. The MAb formulation was not retained due to its inadequate pharmacokinetic profile. As shown in Figures 6.4A & B, both formulations exhibited nearly superimposed blood profiles. The pharmacokinetic parameters of the non-targeted and Fab'-decorated LP were almost similar for LP and encapsulated ara-C (Table 1). Slightly faster clearance of Fab'-LP relative to LP was observed for the lipids and drugs. The overall AUC was about 20% lower for the Fab'-decorated formulation. Here again, the drug and carriers mostly localized in the liver, and no difference was noticeable between pH-sensitive LP and Fab'-LP formulations (Figure 6.5). Uptake into the lungs, heart, kidneys, muscle and bone marrow (data not shown) was similar for both formulations and was less than 2% of the injected dose. Compared to the Balb/c model, SCID/HL60 mice exhibited significantly less LP deposition in the spleen ($p<0.05$ for all time points) (Supplementary Figure 6.7). This could be explained by depleted immune cells in the SCID model.⁴⁷ Preferential accumulation of Fab'-LP in bone marrow was expected but, surprisingly, not observed. The lack of accumulation of the specific anti-CD33 formulation in bone marrow could be due to the low concentration of HL60 cells that may have reached the bone marrow 7 days after their inoculation. Indeed, Xu and Scheinberg⁴⁵ reported that only 17% of injected HL60 cells (3×10^7) reached the bone marrow after 6 weeks.

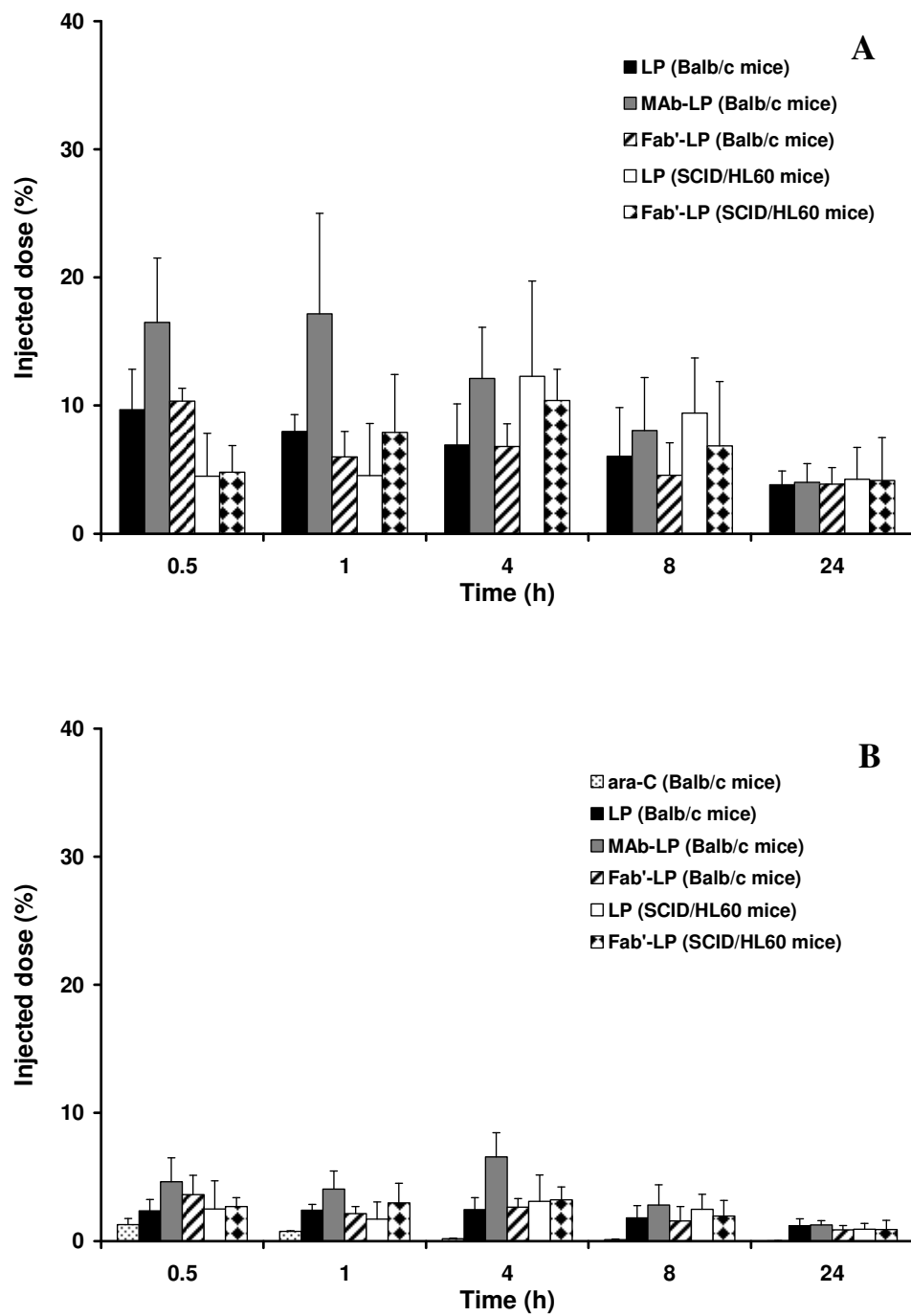


Figure 6.5. Liver distribution of different pH-sensitive LP formulations (**A**), and of free or encapsulated ara-C (**B**) in Balb/c and SCID/HL60 mice. Each mouse received i.v. 3.4 mg/kg ara-C and 40 μ mol/kg of lipids. Values represent the mean (\pm S.D.) obtained for $n = 4$ animals per group per time point.

6.4.4. Preliminary *in vivo* efficacy experiment

To examine the effects of treatment with different formulations of ara-C, a survival study was performed in HL60-bearing SCID mice at a dose of 8 mg of ara-C/kg injected twice (days 1 and 3 after cell injection) (Figure 6.6). The survival time of the leukemic mice treated with free ara-C was not significantly longer than that of untreated animals (*i.e.* injection of saline). The lack of antitumor activity of i.v.-administered free ara-C can be explained by its large V_d and fast CL (Table 1). Indeed, it has been shown previously that free ara-C could achieve extensive survival times only when the drug was given in a more intensive treatment schedule, as an infusion of 3 h on 4 consecutive days.^{48, 49} Ara-C encapsulation of ara-C into pH-insensitive Fab'-LP was found to improve its antitumor activity by significantly prolonging the lifespan of HL60/SCID mice by more than 10 days (mean survival time) compared to the controls (saline and free drug, $p < 0.05$). Ara-C encapsulation into nanocarriers such as liposomes can protect the drug against degradation in blood and prolong its circulation time, leading to improved antitumor efficacy.^{11, 21, 50, 51} Unfortunately, despite promising *in vitro* cytotoxicity data reported earlier by our group¹⁶, the mean survival time of leukemic mice treated with pH-sensitive Fab'-LP was shorter than that of animals treated with pH-insensitive formulations. The reason for the lack of antitumor efficacy of the pH-sensitive formulation is unknown, but it could be attributed to the lower AUC of this liposomal formulation in the SCID mouse model (Table 1). These preliminary results suggest that ara-C may not be the optimal drug to be delivered *via* these

pH-sensitive immunoliposomes and that circulation time may be a more important factor than rapid release in the endosomal compartment.

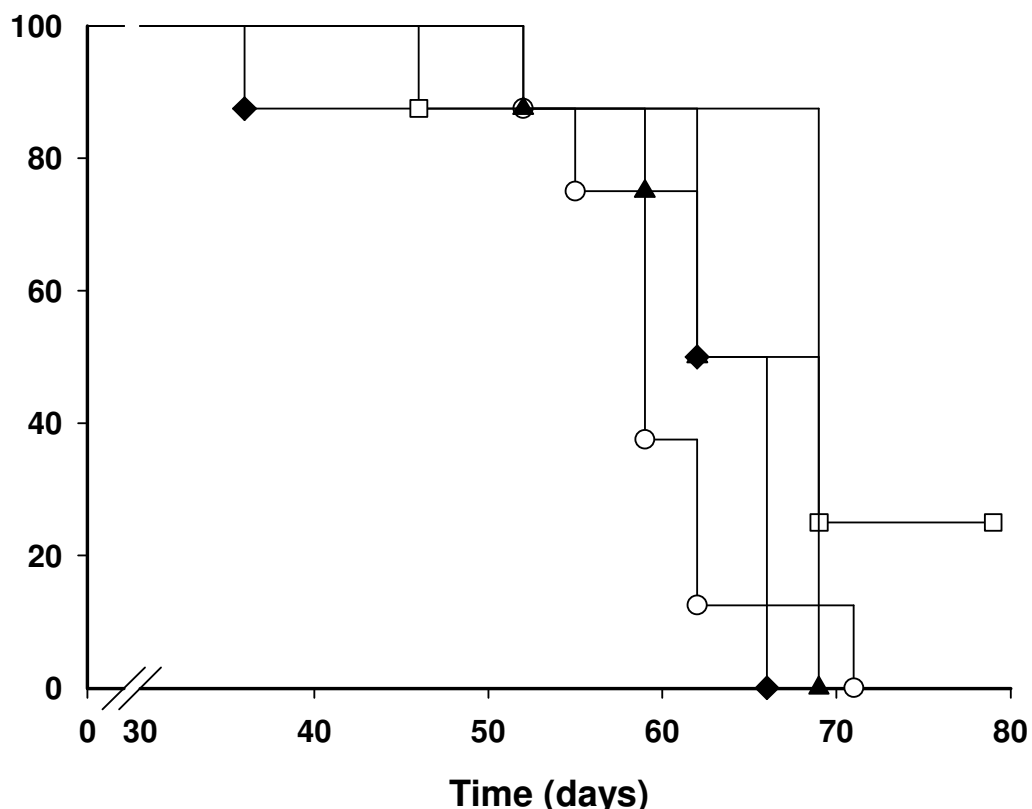


Figure 6.6. Kaplan-Meier plot for HL60-bearing SCID mice treated with various ara-C formulations. SCID mice ($n = 8$ mice/group) were injected with 1.2×10^7 HL60 cells (day 0) and were treated 24 h later with either saline (○), free ara-C (◆), ara-C-loaded Fab'-LP (□), and ara-C-loaded, pH-sensitive Fab'-LP loaded with ara-C (▲), at a dose of 8 mg ara-C/kg. A second injection of saline or ara-C formulations (8 mg ara-C/kg) was repeated at day 3. Mice were monitored daily and were euthanized when tumor size exceeded 1,500 mm³ or when hind-leg paralysis appeared.

6.5. Conclusion

This work showed that targeting pH-sensitive LP with an anti-CD33 Fab' fragment was at least as effective as whole MAb-LP in recognizing leukemia cells expressing CD33 receptors. However, Fab'-decorated LP exhibited longer circulation times *in vivo* in normal mice and provided higher ara-C blood levels. This could be explained by the lower uptake of Fab'-decorated pH-sensitive LP by the MPS compared to MAb-LP, but also by a lower leakage rate of the encapsulated drug. Moreover, the long-circulating properties of pH-sensitive Fab'-LP and encapsulated drugs were largely preserved in immunodeficient mice inoculated with leukemic cells. Unfortunately, although ara-C-loaded Fab'-LP were able to prolong the survival of leukemic mice compared to the free drug, the addition of pH-sensitive polymer did not add any benefit to the formulation. Further work is required to establish whether this pH-sensitive LP would be advantageous with other drugs or animal models.

6.6. Acknowledgements

Financial support from the Canadian Institutes of Health Research, the Canada Research Chair program and the Natural Sciences and Engineering Council of Canada (Steacie Fellowship to JCL) is acknowledged. P. Simard received scholarship support from Fonds de la recherche en santé du Québec. Thanks are due to François Plourde for his help with the *in vivo* work.

6.7. References

- (1) McCulloch, E. A. Stem cells in normal and leukemic hemopoiesis. *Blood* **1983**, *62*, 1-13.
- (2) Bishop, J. F. The treatment of adult acute myeloid leukemia. *Semin Oncol* **1997**, *24*, 57-69.
- (3) Plagemann, P. G.; Marz, R.; Wohlhueter, R. M. Transport and metabolism of deoxycytidine and 1-beta-D-arabinofuranosylcytosine into cultured Novikoff rat hepatoma cells, relationship to phosphorylation, and regulation of triphosphate synthesis. *Cancer Res* **1978**, *38*, 978-89.
- (4) Powis, G., Anticancer drugs: antimetabolite metabolism and natural anticancer agents. In *International encyclopedia of pharmacology and therapeutics*, Powis, G. Ed.; Pergamon Press: Oxford, **1994**; pp 71-94.
- (5) Kufe, D. W.; Munroe, D.; Herrick, D.; Egan, E.; Spriggs, D. Effects of 1-beta-D-arabinofuranosylcytosine incorporation on eukaryotic DNA template function. *Mol Pharmacol* **1984**, *26*, 128-34.
- (6) Muus, P.; Haanen, C.; Raijmakers, R.; de Witte, T.; Salden, M.; Wessels, J. Influence of dose and duration of exposure on the cytotoxic effect of cytarabine toward human hematopoietic clonogenic cells. *Semin Oncol* **1987**, *14*, 238-44.
- (7) Plunkett, W.; Liliemark, J. O.; Estey, E.; Keating, M. J. Saturation of ara-CTP accumulation during high-dose ara-C therapy: pharmacologic rationale for intermediate-dose ara-C. *Semin Oncol* **1987**, *14*, 159-66.
- (8) Estey, E. H. Therapeutic options for acute myelogenous leukemia. *Cancer* **2001**, *92*, 1059-73.
- (9) Galmarini, C. M.; Thomas, X.; Calvo, F.; Rousselot, P.; El Jafaari, A.; Cros, E.; Dumontet, C. Potential mechanisms of resistance to cytarabine in AML patients. *Leuk Res* **2002**, *26*, 621-9.

- (10) Leith, C. P.; Chen, I. M.; Kopecky, K. J.; Appelbaum, F. R.; Head, D. R.; Godwin, J. E.; Weick, J. K.; Willman, C. L. Correlation of multidrug resistance (MDR1) protein expression with functional dye/drug efflux in acute myeloid leukemia by multiparameter flow cytometry: identification of discordant MDR-/efflux+ and MDR1+/efflux- cases. *Blood* **1995**, 86, 2329-42.
- (11) Allen, T. M.; Mehra, T.; Hansen, C.; Chin, Y. C. Stealth liposomes: an improved sustained release system for 1-beta-D-arabinofuranosylcytosine. *Cancer Res* **1992**, 52, 2431-9.
- (12) Hamada, A.; Kawaguchi, T.; Nakano, M. Clinical pharmacokinetics of cytarabine formulations. *Clin Pharmacokinet* **2002**, 41, 705-18.
- (13) Brown, P. M.; Silvius, J. R. Mechanisms of delivery of liposome-encapsulated cytosine arabinoside to CV-1 cells in vitro. Fluorescence-microscopic and cytotoxicity studies. *Biochim Biophys Acta* **1990**, 1023, 341-51.
- (14) Ho, R. J.; Rouse, B. T.; Huang, L. Target-sensitive immunoliposomes as an efficient drug carrier for antiviral activity. *J Biol Chem* **1987**, 262, 13973-8.
- (15) Connor, J.; Huang, L. pH-sensitive immunoliposomes as an efficient and target-specific carrier for antitumor drugs. *Cancer Res* **1986**, 46, 3431-35.
- (16) Simard, P.; Leroux, J. C. pH-sensitive immunoliposomes specific to the CD33 cell surface antigen of leukemic cells. *Int J Pharm* **2009**, 381, 86-96.
- (17) Scheinberg, D. A.; Tanimoto, M.; McKenzie, S.; Strife, A.; Old, L. J.; Clarkson, B. D. Monoclonal antibody M195: a diagnostic marker for acute myelogenous leukemia. *Leukemia* **1989**, 3, 440-5.
- (18) Griffin, J. D.; Linch, D.; Sabbath, K.; Larcom, P.; Schlossman, S. F. A monoclonal antibody reactive with normal and leukemic human myeloid progenitor cells. *Leuk Res* **1984**, 8, 521-34.
- (19) Larson, R. A.; Sievers, E. L.; Stadtmauer, E. A.; Lowenberg, B.; Estey, E. H.; Dombret, H.; Theobald, M.; Voliotis, D.; Bennett, J. M.; Richie, M.; Leopold, L. H.; Berger, M. S.; Sherman, M. L.; Loken, M. R.; van Dongen, J. J.; Bernstein, I. D.;

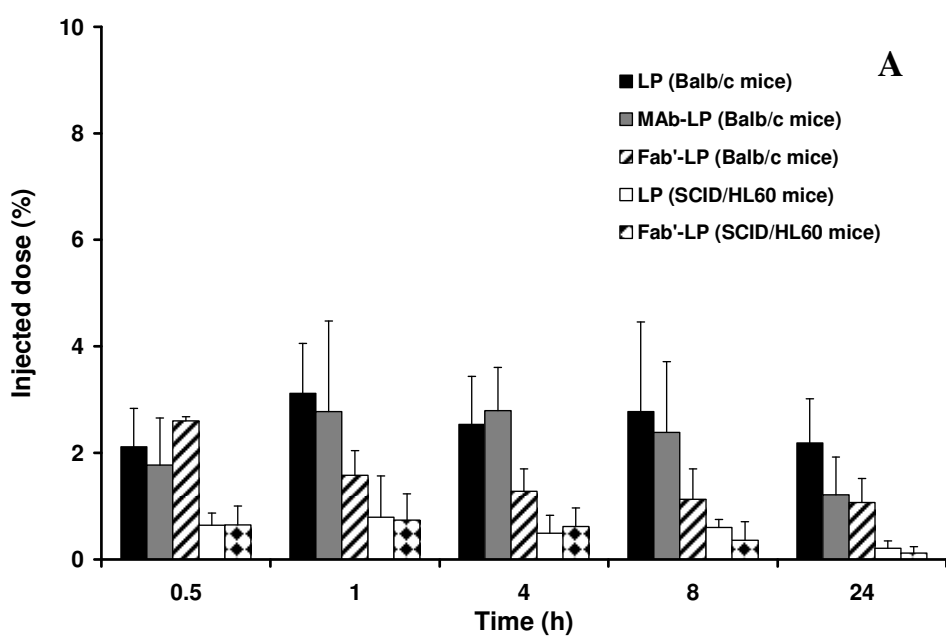
- Appelbaum, F. R. Final report of the efficacy and safety of gemtuzumab ozogamicin (Mylotarg) in patients with CD33-positive acute myeloid leukemia in first recurrence. *Cancer* **2005**, 104, 1442-52.
- (20) Huang, A.; Kennel, S. J.; Huang, L. Interactions of immunoliposomes with target cells. *J Biol Chem* **1983**, 258, 14034-40.
- (21) Rustum, Y. M.; Dave, C.; Mayhew, E.; Papahadjopoulos, D. Role of liposome type and route of administration in the antitumor activity of liposome-entrapped 1-beta-D-arabinofuranosylcytosine against mouse L1210 leukemia. *Cancer Res* **1979**, 39, 1390-95.
- (22) Roux, E.; Stomp, R.; Giasson, S.; Pézolet, M.; Moreau, P.; Leroux, J.-C. Steric stabilization of liposomes by pH-responsive N-isopropylacrylamide copolymer. *J Pharm Sci* **2002**, 91, 1795-802.
- (23) Bertrand, N.; Fleischer, J. G.; Wasan, K. M.; Leroux, J.-C. Pharmacokinetics and biodistribution of N-isopropylacrylamide copolymers for the design of pH-sensitive liposomes. *Biomaterials* **2009**, 30, 2598-605.
- (24) Francis, M. F.; Dhara, G.; Winnik, F. M.; Leroux, J.-C. *In vitro* evaluation of pH-sensitive polymer/niosome complexes. *Biomacromolecules* **2001**, 2, 741-9.
- (25) Roux, E.; Francis, M.; Winnik, F. M.; Leroux, J.-C. Polymer-based pH-sensitive carriers as a means to improve the cytoplasmic delivery of drugs. *Int J Pharm* **2002**, 242, 25-36.
- (26) Leroux, J.-C.; Roux, E.; Le Garrec, D.; Hong, K.; Drummond, D. C. N-isopropylacrylamide copolymers for the preparation of pH-sensitive liposomes and polymeric micelles. *J Controlled Release* **2001**, 72, 71-84.
- (27) Bartlett, G. R. Phosphorus assay in column chromatography. *J Biol Chem* **1959**, 234, 466-8.
- (28) Gubernator, J.; Drulis-Kawa, Z.; Kozubek, A. A simply and sensitive fluorometric method for determination of gentamicin in liposomal suspensions. *Int J Pharm* **2006**, 327, 104-9.

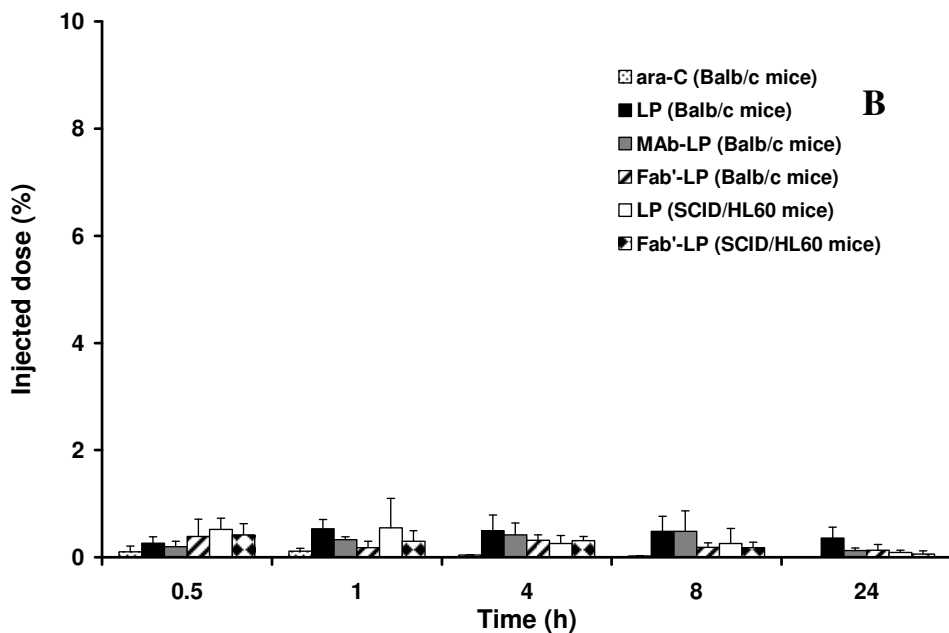
- (29) Esposito, E.; Pastesini, C.; Cortesi, R.; Gambari, R.; Menegatti, E.; Nastruzzi, C. Controlled release of 1-b-D-arabinofuranosylcytosine (ara-C) from hydrophilic gelatin microspheres: in vitro studies. *Int J Pharm* **1995**, *117*, 151-8.
- (30) Drummond, D. C.; Zignani, M.; Leroux, J.-C. Current status of pH-sensitive liposomes in drug delivery. *Prog Lipid Res* **2000**, *39*, 409-60.
- (31) Roux, E.; Passirani, C.; Scheffold, S.; Benoit, J. P.; Leroux, J.-C. Serum-stable and long-circulating, PEGylated, pH-sensitive liposomes. *J Controlled Release* **2004**, *94*, 447-51.
- (32) Mariani, M.; Camagna, M.; Tarditi, L.; Seccamani, E. A new enzymatic method to obtain high-yield F(ab)2 suitable for clinical use from mouse IgG1. *Mol Immunol* **1991**, *28*, 69-77.
- (33) Sapra, P.; Allen, T. M. Ligand-targeted liposomal anticancer drugs. *Prog Lipid Res* **2003**, *42*, 439-62.
- (34) Huwyler, J.; Wu, D.; Pardridge, W. M. Brain drug delivery of small molecules using immunoliposomes. *Proc Natl Acad Sci USA* **1996**, *93*, 14164-9.
- (35) Dufresne, I.; Desormeaux, A.; Bestman-Smith, J.; Gourde, P.; Tremblay, M. J.; Bergeron, M. G. Targeting lymph nodes with liposomes bearing anti-HLA-DR Fab' fragments. *Biochim Biophys Acta* **1999**, *1421*, 284-94.
- (36) Sapra, P.; Moase, E. H.; Ma, J.; Allen, T. M. Improved therapeutic responses in a xenograft model of human B lymphoma (Namalwa) for liposomal vincristine versus liposomal doxorubicin targeted via anti-CD19 IgG2a or Fab' fragments. *Clin Cancer Res* **2004**, *10*, 1100-11.
- (37) Maruyama, K.; Takahashi, N.; Tagawa, T.; Nagaike, K.; Iwatsuru, M. Immunoliposomes bearing polyethyleneglycol-coupled Fab' fragment show prolonged circulation time and high extravasation into targeted solid tumors in vivo. *FEBS Lett* **1997**, *413*, 177-80.

- (38) Cheng, W. W.; Allen, T. M. Targeted delivery of anti-CD19 liposomal doxorubicin in B-cell lymphoma: a comparison of whole monoclonal antibody, Fab' fragments and single chain Fv. *J Controlled Release* **2008**, 126, 50-8.
- (39) Aragnol, D.; Leserman, L. D. Immune clearance of liposomes inhibited by an anti-Fc receptor antibody *in vivo*. *Proc Natl Acad Sci USA* **1986**, 83, 2699-703.
- (40) Ansell, S. M.; Tardi, P. G.; Buchkowsky, S. S. 3-(2-pyridylidithio)propionic acid hydrazide as a cross-linker in the formation of liposome-antibody conjugates. *Bioconjugate Chem* **1996**, 7, 490-6.
- (41) Harasym, T. O.; Bally, M. B.; Tardi, P. Clearance properties of liposomes involving conjugated proteins for targeting. *Adv Drug Deliv Rev* **1998**, 32, 99-118.
- (42) Allen, T. M.; Brandeis, E.; Hansen, C. B.; Kao, G. Y.; Zalipsky, S. A new strategy for attachment of antibodies to sterically stabilized liposomes resulting in efficient targeting to cancer cells. *Biochim Biophys Acta* **1995**, 1237, 99-108.
- (43) Juliano, R. L.; Stamp, D. Pharmacokinetics of liposome-encapsulated anti-tumor drugs. Studies with vinblastine, actinomycin D, cytosine arabinoside, and daunomycin. *Biochem Pharmacol* **1978**, 27, 21-7.
- (44) Williams, S. S.; Alosco, T. R.; Mayhew, E.; Lasic, D. D.; Martin, F. J.; Bankert, R. B. Arrest of human lung tumor xenograft growth in severe combined immunodeficient mice using doxorubicin encapsulated in sterically stabilized liposomes. *Cancer Res* **1993**, 53, 3964-7.
- (45) Xu, Y.; Scheinberg, D. A. Elimination of human leukemia by monoclonal antibodies in an athymic nude mouse leukemia model. *Clin Cancer Res* **1995**, 1, 1179-87.
- (46) Terpstra, W.; Prins, A.; Visser, T.; Wognum, B.; Wagemaker, G.; Lowenberg, B.; Wielenga, J. Conditions for engraftment of human acute myeloid leukemia (AML) in SCID mice. *Leukemia* **1995**, 9, 1573-7.
- (47) Custer, R. P.; Bosma, G. C.; Bosma, M. J. Severe combined immunodeficiency (SCID) in the mouse. Pathology, reconstitution, neoplasms. *Am J Pathol* **1985**, 120, 464-77.

- (48) Skipper, H. E.; Schabel, F. M., Jr.; Wilcox, W. S. Experimental evaluation of potential anticancer agents. XXI. Scheduling of arabinosylcytosine to take advantage of its S-phase specificity against leukemia cells. *Cancer Chemother Rep* **1967**, *51*, 125-65.
- (49) Skipper, H. E.; Schabel, F. M., Jr.; Mellett, L. B.; Montgomery, J. A.; Wilkoff, L. J.; Lloyd, H. H.; Brockman, R. W. Implications of biochemical, cytokinetic, pharmacologic, and toxicologic relationships in the design of optimal therapeutic schedules. *Cancer Chemother Rep* **1970**, *54*, 431-50.
- (50) Hong, F.; Mayhew, E. Therapy of central nervous system leukemia in mice by liposome-entrapped 1- β -D-arabinofuranosylcytosine. *Cancer Res* **1989**, *49*, 5097-102.
- (51) Kobayashi, T.; Kataoka, T.; Tsukagoshi, S.; Sakurai, Y. Enhancement of anti-tumor activity of 1-beta-D-arabinofuranosylcytosine by encapsulation in liposomes. *Int J Cancer* **1977**, *20*, 581-7.

6.8. Supplementary Figure





Supplementary Figure 6.7. Spleen distribution of different pH-sensitive LP formulations (A) and of free or encapsulated ara-C (B) in Balb/c and SCID/HL60 mice. Each mouse received i.v. 3.4 mg/kg ara-C and 40 μ mol/kg of lipids. Values represent the mean (\pm S.D.) obtained for $n = 4$ animals per group per time point.

Chapitre 7. Discussion générale

Les travaux effectués dans le cadre de ce projet de doctorat avaient pour but de mettre au point des systèmes vésiculaires lipidiques pour vectoriser l'ara-C. Deux vecteurs pharmaceutiques ont été évalués : (i) une nouvelle forme de vésicules multilamellaires apparentées à la structure des liposomes (Sphérolites[®]) et (ii) une formulation liposomale sensible au pH ciblant les cellules leucémiques. Cette dernière avait la particularité de posséder un polymère sensible au pH capable de libérer rapidement le principe actif suite à l'endocytose du vecteur. Ces deux formes pharmaceutiques ont été caractérisées *in vitro* et *in vivo* quant à leur stabilité, cinétique de libération, pharmacocinétique et biodistribution.

7.1. Vésicules lipidiques testées

7.1.1. Sphérolites[®]

Les Sphérolites[®] sont des vésicules plurilamellaires constituées de plusieurs couches de tensioactifs disposées de façon concentrique (Diat & Roux 1993, Roux & Gauffre 1999). On entend par phase lamellaire, une phase solide hydratée dans lequel plusieurs bicouches sont disposées en un réseau parallèle, séparées par des couches d'eau ou d'une solution aqueuse. Les dimensions de ces vésicules sont généralement de l'ordre de 1 à 50 µm de diamètre. Les Sphérolites[®] ont d'abord été décrites par Diat *et al.* (1993). Elles sont obtenues par cisaillement modéré d'un mélange de tensioactifs et d'eau suivie d'une étape de dilution avec une solution aqueuse (Diat & Roux 1993, Diat *et al.* 1993). De structure très comparable aux liposomes MLV, les Sphérolites[®] possèdent leurs propres caractéristiques: (i) une méthode de préparation ne nécessitant pas de solvant organique; (ii) un taux d'encapsulation élevé (iii) un arrangement lamellaire concentré dans laquelle les

bicouches de tensioactifs sont séparées par une distance bien précise; (iv) et une capacité à réfléchir la lumière polarisée de façon à produire une croix de malte lorsque observées sous microscope. Il a été démontré que les Sphérolites® permettaient d'encapsuler avec un excellent rendement des métaux (Gauffre & Roux 1999) et des sels inorganiques (Kim *et al.* 2000) afin de créer des microréacteurs chimiques. Ce n'est que récemment que les Sphérolites® ont été appliquées dans le domaine pharmaceutique. De l'ADN (Mignet *et al.* 2000) et des protéines (Bernheim-Grosswasser *et al.* 2000) ont été encapsulées avec succès. Cependant, toutes les vésicules décrites dans la littérature avaient un diamètre supérieur à 1 µm et étaient donc peu adaptées pour des applications en vectorisation des médicaments.

La nouveauté de notre projet de recherche consistait à utiliser cette technologie de fabrication des Sphérolites® afin de produire des vésicules de diamètre inférieur à 300 nm, dans laquelle un agent anticancéreux serait encapsulé. Étant donné la très courte demi-vie de l'ara-C lorsque administrée par la voie i.v. et son utilisation fréquente dans le traitement de la LMA, nous avons considéré que cette molécule était un modèle approprié pour évaluer les Sphérolites® comme nouveau vecteur pharmaceutique. Tel que consigné dans le Tableau 4.1 (Chapitre 4), plusieurs excipients couramment employés dans le domaine pharmaceutique ont été testés afin de préparer des Sphérolites®. L'objectif était d'obtenir des vésicules de moins de 300 nm capables de retenir le principe actif dans le plasma. En effet, un diamètre de 100-300 nm est essentiel afin de concevoir un système injectable par la voie i.v. et capable de circuler longtemps au niveau systémique.

7.1.2. Liposomes sensibles au pH

Plusieurs types de liposomes répondant à un stimulus, tels que des variations de température, de lumière et de pH ont été développés dans le but d'augmenter la biodisponibilité du contenu liposomal au site visé (Chapitre 2). Pour ce projet de recherche,

nous avons conféré une sensibilité au pH aux liposomes en complexant le DODA-P(NIPAM-*co*-MAA). Ce dernier a largement été caractérisé au sein du laboratoire au cours des 10 dernières années, tant au niveau de sa structure (Roux *et al.* 2003), de son interaction avec des bicouches lipidiques (Roux *et al.* 2003), de sa capacité à libérer diverses molécules encapsulées (Francis *et al.* 2001, Roux *et al.* 2002a, Roux *et al.* 2003), que de son effet sur les temps de circulation des liposomes *in vivo* (Bertrand *et al.* 2009, Roux *et al.* 2004, Roux *et al.* 2002b). Les principaux avantages de ce polymère reposent sur (i) une précipitation ou un changement de conformation à pH 5-6 à 37°C (idéal pour cibler la libération dans les endosomes), (ii) un ancrage efficace dans les bicouches lipidiques dû à sa partie terminale hydrophobe résultant en une formulation stable dans le sang (iii) un agencement efficace entre celui-ci et le PEG conférant furtivité *in vivo* et sensibilité au pH. Ces avantages ne se retrouvent généralement pas dans les formulations liposomales à base de DOPE ou de copolymères de différentes structures ou conformations chimiques (Drummond *et al.* 2000, Roux *et al.* 2002a).

7.2. Caractérisation *in vitro*

7.2.1. Caractérisation des Sphérolites®

Suite aux essais de formulations, nous avons sélectionné quelques formulations pour caractériser leurs cinétiques de libération au moyen d'un marqueur fluorescent. Le principe de ces libérations est simple : un marqueur fluorescent (HPTS) est co-encapsulé avec un « quencher » (DPX) qui absorbe la lumière émise par le marqueur. Lorsque le HPTS est libéré et se retrouve dilué dans un milieu externe, donc éloigné du DPX, la fluorescence émise par le HPTS peut être détectée. Ces essais ont permis d'identifier la formulation qui a été retenue pour encapsuler efficacement l'ara-C. La préparation choisie pour les essais *in*

vivo était constituée de Phospholipon 90, de Solutol HS15, de cholestérol, de DSPE-PEG à un ratio molaire de 57,4:14,8:27,2:0,6 mol%. La saturation des chaînes alkyl du Solutol HS15 contenant 18 carbones et l'ajout de cholestérol ont grandement aidé à stabiliser les membranes lipidiques et conséquemment, à réduire la perméabilité des Sphérulites® formés. Le cholestérol est d'ailleurs connu pour améliorer l'étanchéité des membranes liposomales (Demel *et al.* 1968). Cependant, l'ajout de 20% *p/p* de cholestérol dans la préparation des Sphérulites® s'est démontré nuisible pour leur formation (Chapitre 4, Table 4.1). Tel qu'espéré, une encapsulation très élevée de l'ara-C (46%) fut obtenue avec cette formulation. Ce taux est largement supérieur à celui généralement réalisé avec les liposomes uni- et multilamellaires (de l'ordre de 1 à 10%) (Hong & Mayhew 1989). Une formulation liposomale constituée des mêmes excipients utilisés dans la préparation des Sphérulites® a démontré un rendement d'encapsulation de l'ara-C de 16%. Le pouvoir élevé d'encapsulation des Sphérulites® est dû à la méthode de préparation reposant sur l'utilisation complète de la phase aqueuse (contenant le principe actif) afin de séparer les bicouches lipidiques formant les vésicules. Quant aux liposomes extrudés, ces derniers se déforment et se rassemblent sous forme de vésicules sphériques lors de leur passage au travers de membranes de polycarbonates, induisant ainsi une perte du principe actif dans le milieu de dispersion et conséquemment, un faible rendement d'encapsulation est observé. Un taux élevé d'encapsulation était désiré pour les Sphérulites® afin de réduire au maximum le volume d'injection pour d'éventuels essais précliniques.

7.2.2. Incorporation du PEG et propriétés *in vitro*

Tel que mentionné précédemment (Chapitre 2), l'ajout d'un polymère flexible, hydrophile et inerte, tel que le PEG, fut un avancement majeur dans le développement de vecteurs de médicaments. Qu'il soit ajouté lors de la préparation des vecteurs, ou post-

incorporé, le PEG a démontré à maintes reprises sa capacité à: (i) réduire les interactions des vecteurs avec les phagocytes (Lasic *et al.* 1991), (ii) diminuer l'adsorption d'opsonines endogènes (Figure 7.1) (Chonn & Cullis 1992), (iii) diminuer les probabilités d'activation du système du complément (Bradley *et al.* 1998), (iv) diminuer la fuite prématuée du principe actif encapsulé (Silvander *et al.* 1998), (v) prolonger le temps de circulation systémique (Chonn & Cullis 1992, Maruyama *et al.* 1995) et (vi) finalement, permettre l'attachement d'une molécule de reconnaissance à l'extrémité de sa chaîne et ainsi former des systèmes de vectorisation ciblés (Maruyama *et al.* 1995).

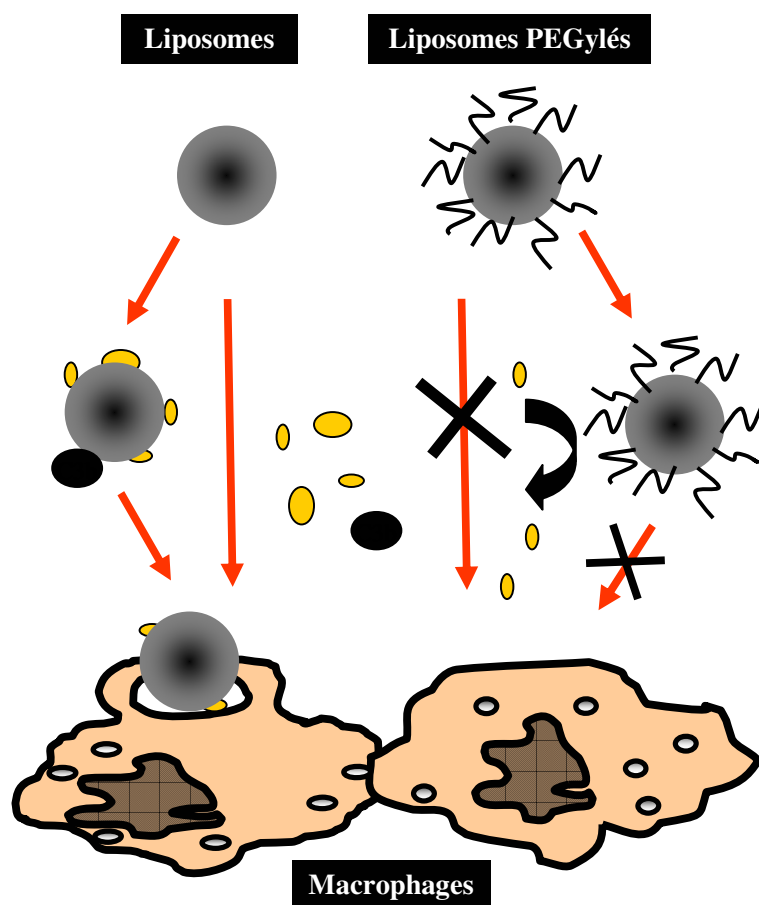


Figure 7.1. Effet du PEG sur la diminution de l'opsonisation et la reconnaissance des liposomes par les macrophages.

7.2.2.1. Sphérolites[®] PEGylées

Le DSPE-PEG a été employé afin d'augmenter la demi-vie biologique des Sphérolites[®]. Il a été incorporé par une incubation des vésicules déjà formées avec des micelles de DSPE-PEG (15 mg/mL) pendant 1 h à 40 °C. Cette technique, couramment employée lors de la préparation de liposomes furtifs (Iden & Allen 2001), a été privilégiée afin de ne pas déstabiliser la structure concentrique des Sphérolites[®]. Ainsi, le PEG se retrouve seulement exposé à la surface des vésicules suite à sa post-insertion. L'ajout de 0,6 mol% de DSPE-PEG était une nouveauté pour les Sphérolites[®]. L'addition de ce dernier n'a entraîné aucun changement de la taille des vecteurs et n'a pas provoqué de libération prématurée de leur contenu. Un essai colorimétrique a été développé afin de s'assurer que le PEG était réellement fixé sur les Sphérolites[®] (Chapitre 4; Section 4.3.3). De plus, les observations de microscopie sous verres polarisées ont démontré que la structure caractéristique des Sphérolites[®] était toujours conservée. L'influence bénéfique de l'insertion du DSPE-PEG de différentes longueurs de chaînes sur les Sphérolites[®] a été démontrée suite à leur administration chez l'animal (Chapitre 4; Section 4.4.3).

7.2.2.2. Liposomes PEGylés sensibles au pH

Les travaux antérieurs réalisés au laboratoire avaient montré que le PEG pouvait être combiné au DODA-P(NIPAM-*co*-MAA) au sein de liposomes composés de phosphatidylcholine d'œuf et de cholestérol afin d'obtenir une formulation liposomale sensible au pH stable en présence de protéines plasmatiques à pH 7,4 mais très labile dans

un milieu modérément acide (endosomes) (Francis *et al.* 2001, Roux *et al.* 2002a, Roux *et al.* 2004). De plus, il avait été observé que ces liposomes sensibles au pH en association avec le DSPE-PEG possédaient une barrière stérique à leur surface permettant d'augmenter significativement leur temps de demi-vie après une administration intraveineuse chez le rat (Roux *et al.* 2003, Roux *et al.* 2002b). Cependant, aucune étude exhaustive de phagocytose n'avait été effectuée avec ce vecteur auparavant.

Les macrophages, principalement ceux de la rate et les cellules de Kupffer du foie, sont responsables de l'élimination rapide des vecteurs pharmaceutiques lors de leur administration parentérale. La phagocytose par le SPM joue un rôle clé dans l'initiation d'une réponse immunitaire, elle peut résulter d'un contact direct entre les vecteurs et les cellules ou par l'intermédiaire des protéines plasmatiques (*i.e.* opsonines). Nous avons donc incorporé un dérivé du cholestérol fluorescent, le cholestéryl-BODIPY FL C12, au sein de différentes formulations liposomales afin de mesurer l'influence du PEG et du polymère sensible au pH sur la phagocytose des liposomes par les macrophages. Ces liposomes ont été incubés pendant 1, 2 et 3 h avec des macrophages de souris RAW264.7 et la fluorescence associée aux vecteurs internalisés a été mesurée en cytométrie de flux (Figure 7.2) (résultats non publiés, Méthodes en annexe). La Figure 7.2 montre que le polymère sensible au pH permet à lui seul de créer une diminution de l'internalisation des liposomes par des macrophages comparé à des liposomes conventionnels. Le DODA-P(NIPAM-*co*-MAA), ancré dans la bicouche lipidique du liposome, possède une extrémité bien hydratée et flexible en milieu aqueux (Roux *et al.* 2003) procurant une certaine stabilisation stérique. Lorsqu'il est co-incorporé avec du DSPE-PEG5000, l'effet protecteur contre l'internalisation des liposomes est amélioré (Figure 7.2). Ces résultats *in vitro* confirment les résultats obtenus antérieurement chez l'animal (Roux *et al.* 2002b).

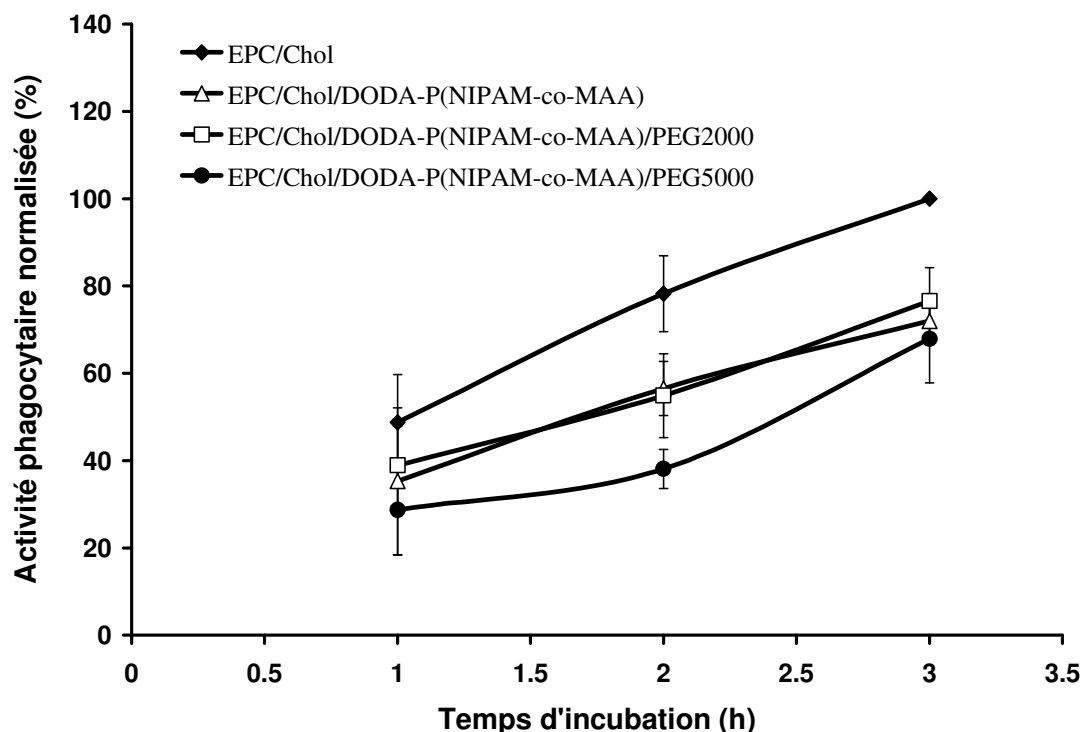


Figure 7.2. Internalisation des liposomes par les macrophages RAW264.7 en fonction du temps. La capacité phagocytaire normalisée (% cellules fluorescentes multipliée par l'intensité moyenne de fluorescence) a été obtenue par cytométrie de flux. Les liposomes ont été préparés tel que décrit par Roux *et al.* (Roux *et al.* 2002b). Moyenne ± écart-type ($n=3$).

7.2.3. Modification de l'anticorps

La présence de PEG dans la formulation de liposomes servait non seulement à créer un effet furtif vis-à-vis du système immunitaire mais permettait également la fixation d'une

molécule de reconnaissance à la surface des vecteurs. Effectivement, l'un des principaux objectifs du projet de recherche était de diriger les liposomes sensibles au pH vers leur site d'action, c'est-à-dire, les cellules cancéreuses circulantes. Le principal avantage de cette spécificité repose sur le fait que les tissus sains peuvent davantage être évités, diminuant ainsi la toxicité associée au principe actif encapsulé. Il existe différents procédés pour coupler un anticorps ou une molécule de reconnaissance à la surface d'un vecteur. La liaison aux liposomes peut être covalente (Mastrobattista *et al.* 1999, Sapra & Allen 2003) ou physique par l'intermédiaire d'une autre molécule ayant une affinité pour le ligand (Gray *et al.* 1988, Longman *et al.* 1995). Les approches utilisant une conjugaison covalente sont privilégiées car l'emploi d'une molécule intermédiaire peut augmenter le diamètre hydrodynamique du vecteur et son antigénicité (Park *et al.* 1997).

Deux stratégies peuvent être employées afin de coupler un anticorps à la surface d'un liposome de façon covalente. La première méthode consiste à fixer l'anticorps directement sur un phospholipide. Cependant, la molécule peut se retrouver positionnée aléatoirement dans la bicoche lipidique et potentiellement à l'intérieur du vecteur (Huang *et al.* 1980). De plus, certaines conditions de préparation de liposomes seront à éviter afin de ne pas modifier l'intégrité du ligand (Allen *et al.* 1980). Si l'anticorps est conjugué à la surface de liposomes préformés, un lipide possédant une fonction réactive doit être incorporé aux vésicules pour permettre le couplage avec le ligand, lui-même préalablement modifié chimiquement. Une seconde méthode très commune consiste à coupler l'anticorps à l'extrémité d'un polymère tel que le PEG. Étant donné les nombreux groupements amines primaires (NH_2) présents dans les anticorps, il est possible de faire réagir ces amines avec un agent de condensation, tel que le 1-éthyl-3-(3-diméthylaminopropyl)carbodiimide (EDC) afin de créer un lien amide avec un acide carboxylique présent sur un lipide ou un polymère (Endoh *et al.* 1981). La méthode que nous avons choisie repose sur l'utilisation d'une molécule supplémentaire qui agira en tant que bras espaceur entre l'anticorps et le PEG. La majorité des bras espaces décrits dans la littérature reposent également sur

l'utilisation des amines de l'anticorps. Parmi ceux couramment employés, on retrouve principalement le 4-(*p*-maléimidophényl)butyrate de *N*-succinimidyle (SMPB) et le 3-(2-pyridyldithio)propionate de *N*-succinimidyle (SPDP) qui possèdent une fonction thiol (-SH) capable de réagir avec le PEG-maléimide (Boeckler *et al.* 1996). Bien que ces composés soient largement utilisés et que des résultats très prometteurs aient été obtenus, plusieurs inconvénients ont été rapportés, tels que (i) le risque d'affecter le site de liaison de l'anticorps pour son récepteur, (ii) la présentation aléatoire de l'anticorps sur les liposomes empêchant ainsi une exposition adéquate de la partie Fab' reconnaissant le récepteur et (iii) le risque de présenter la portion Fc de l'anticorps et ainsi augmenter la reconnaissance des immunoliposomes par le système immunitaire et diminuer ses temps de circulation *in vivo*.

Tel que mentionné aux Chapitres 5 et 6, nous avons choisi de coupler l'anticorps sur les liposomes sensibles au pH suite à l'introduction de groupements aldéhydes (-CHO) par oxydation des sucres présents sur la partie Fc de l'anticorps. Suite à l'oxydation par le periodate de sodium, le bras espaceur hétéro-bifonctionnel, l'acide 3-(2-pyridyldihio)propionique d'hydrazide (PDPH), est fixé sur l'anticorps en formant un lien hydrazone. Par la suite, le PDPH est déprotégé par le dithiothreitol (DTT) afin de permettre la génération d'un thiol qui sera couplé au PEG-maléimide préalablement inséré dans la membrane des liposomes. Les différentes étapes de couplage sont résumées à la Figure 7.3. Une efficacité de couplage de l'ordre de 15 à 20% ainsi qu'une augmentation de la taille du diamètre de l'ordre de 10-15 nm ont été observées.

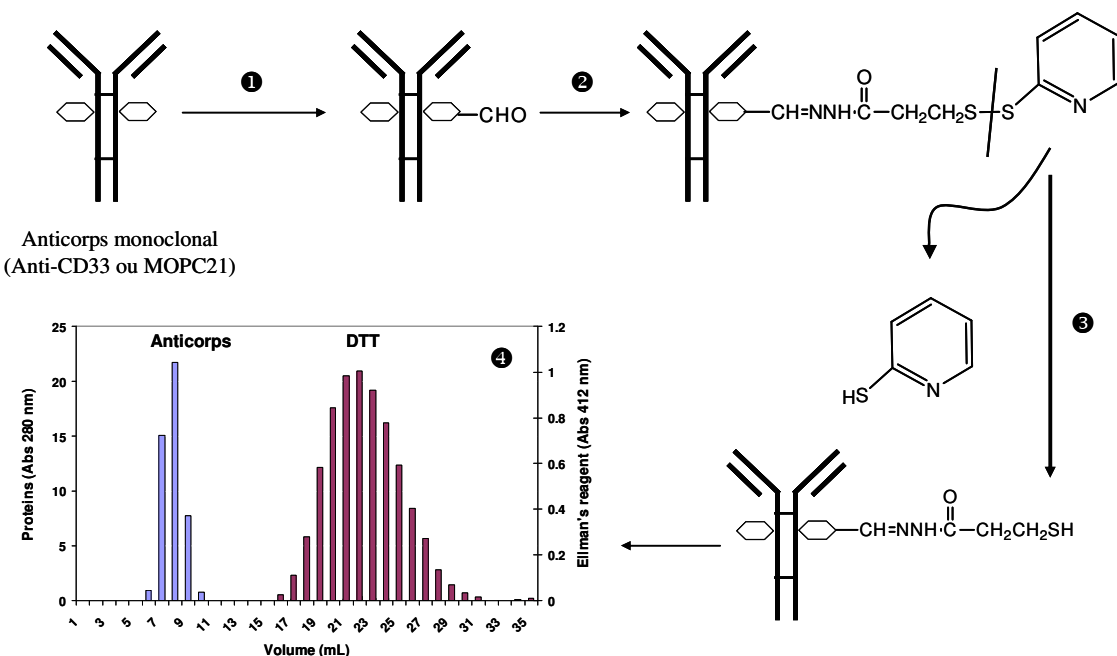


Figure 7.3. Principales étapes de modifications de l'anticorps effectuées avant leur couplage aux liposomes : 1) Oxydation de la partie sucre des IgGs par le periodate de sodium (40 min, 4°C). 2) Fixation du PDPH (5 h, 25°C). 3) Clivage des ponts disulfure par le DTT (20 min, 25°C). 4) Purification de l'anticorps modifié par chromatographie d'exclusion de taille (Sephadex® G50).

Le fragment Fab' de l'anticorps anti-CD33 a également été employé afin de cibler les liposomes sensibles au pH envers les cellules leucémiques. Celui-ci a été obtenu en clivant l'anticorps complet en deux fractions : la partie Fc et le fragment F(ab)₂. L'enzyme ficine, immobilisée sur une colonne de billes d'agarose, en présence de cystéine, permet de séparer les deux parties de l'anticorps sans altérer son affinité pour le récepteur (Mariani *et*

al. 1991). Le fragment Fab' est ensuite obtenu à partir d'une incubation de 90 min du F(ab)₂ en présence de mercaptoéthylamine permettant de cliver les ponts hydrogènes dans les chaînes lourdes de l'anticorps. Un rendement quantitatif de modification de l'anticorps d'environ 100% fut obtenu avec cette technique. Le fragment Fab' présentant alors une fonction thiol peut réagir avec le DSPE-PEG maléimide dans les mêmes conditions expérimentales que celles utilisées dans le couplage de l'anticorps complet. Afin de fixer des quantités similaires de ligands, *i.e.* d'anticorps complet ou de fragment Fab' à la surface des liposomes, des ratios initiaux de couplage de 100 et 35 µg de protéines par µmol de lipides ont été respectés, respectivement. Des immunoliposomes-Fab' de taille d'environ 140 nm (indice de polydispersité de 0.03 à 0.05) de diamètre ont été ainsi obtenus.

7.2.4. Spécificité des formulations liposomales

Afin de s'assurer de la spécificité des formulations des immunoliposomes anti-CD33, nous avons incorporé le marqueur fluorescent cholestéryl-BODIPY FL C12 dans la membrane liposomale. Par la suite, les différentes formulations ont été incubées avec plusieurs lignées cellulaires exprimant ou non le récepteur CD33. Tel que présenté dans la Figure 5.3 (Chapitre 5), les immunoliposomes se sont avérés spécifiques aux récepteurs CD33 présents sur les cellules leucémiques HL60, KG1, et THP-1 (CD33⁺). D'ailleurs, cette spécificité a été confirmée par des expériences de compétition réalisées en présence de l'anticorps anti-CD33 libre (Chapitre 5; Figure 5.3). De plus, la faible affinité des liposomes modifiés avec un anticorps contrôle non spécifique (MOPC21) pour les cellules CD33⁺ et la capture limitée d'immunoliposomes-CD33 par des cellules CD33⁻ (A549) ont clairement établi l'affinité spécifique de nos formulations pour le récepteur CD33. Des résultats similaires ont été observés pour les formulations dotées du fragment Fab' de l'anticorps. En effet, une internalisation spécifique et supérieure de 4,5 fois a été obtenue pour les liposomes-Fab' comparativement aux liposomes sans ligand (Chapitre 6; Figure

6.2). Ceci se reflète également par le nombre de cellules devenues fluorescentes suite à l'internalisation des ces vecteurs, c'est-à-dire 99% des cellules HL60 ont démontré une fluorescence associée aux liposomes-Fab', contrairement à seulement 5% pour les cellules incubées avec les formulations contrôles. Il faut cependant noter que la présence du DODA-P(NIPAM-*co*-MAA) à la surface des liposomes diminue l'efficacité de greffage de l'anticorps (complet et fragment Fab'), probablement par effet stérique.

7.2.5. Rôle du DODA-P(NIPAM-*co*-MAA)

7.2.5.1. Stabilité des immunoliposomes et libération *in vitro*

Suite à l'ajout d'un anticorps à la surface de ces liposomes, il fallait s'assurer que toutes les propriétés du DODA-P(NIPAM-*co*-MAA) étaient conservées. Nous avons co-encapsulé le HPTS et son « quencher », le DPX, dans les immunoliposomes sensibles au pH et avons démontré que la présence de l'anticorps n'affectait pas la libération de la sonde fluorescente lors d'une incubation à pH acide (Figure 7.4). Une cinétique de libération *in vitro* a également été effectuée après une pré-incubation de 1 h dans du plasma humain (Chapitre 5; Figure 5.4). Après 30 min d'incubation à 37°C et à un pH neutre, seulement 5% du contenu était libéré contre 78% à pH 5.0. L'ara-C a été encapsulée dans ces liposomes avec un rendement d'environ 10% de la dose initiale ajoutée. La présence du DODA-P(NIPAM-*co*-MAA) n'a pas affecté l'encapsulation de cette molécule. Cependant, nous avons noté un effet de ce dernier sur la fuite de l'ara-C à 4°C. Lors de leur conservation à 4°C, la concentration de polymère dans la formulation avait un impact important sur l'étanchéité de la membrane et donc de la stabilité de la formulation. Il s'est avéré qu'en diminuant la quantité initiale de polymère de 0,3 à 0,1 (*p/p*) la stabilité, en terme de fuite du principe actif, passait de 4 à 18 jours. Cette perte prématurée de la molécule encapsulée n'avait pas été observée avec l'HPTS. Dans le plasma, les

immunoliposomes sensibles au pH se sont avérés relativement stables, avec seulement 5,6% d'ara-C libérée après 1 h d'incubation. Par contre, à pH 5,0, ceux-ci ont libéré 90% de leur contenu en ara-C après 30 min, contrairement à 6% seulement de libération pour les immunoliposomes contrôles sans DODA-P(NIPAM-*co*-MAA) (Chapitre 5; Figure 5.5).

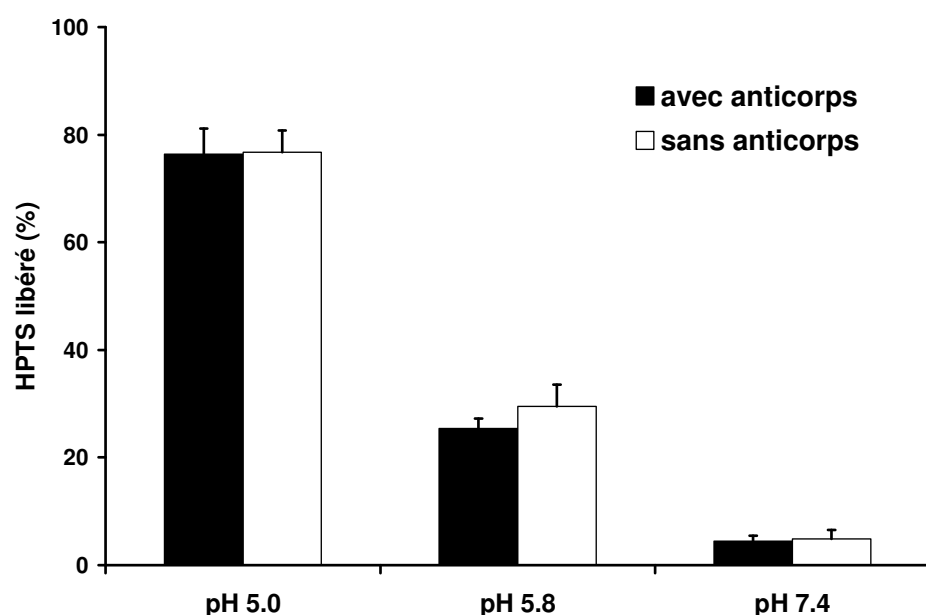


Figure 7.4. Pourcentage de HPTS libéré des liposomes sensibles au pH en présence ou non de l'anticorps anti-CD33 à leur surface. La libération du marqueur fluorescent à pH acide indique que la capacité du copolymère à déstabiliser la bicoche lipidique est retenue malgré la présence d'un anticorps.

7.2.5.2. Libération intracellulaire du contenu des immunoliposomes

La libération intracellulaire du contenu des formulations sensibles au pH a également été mesurée dans deux types cellulaires, des macrophages et des monocytes, au moyen de deux techniques: l'observation de la libération intracellulaire de la calcéine par microscopie à fluorescence et des essais de cytotoxicité avec l'ara-C. Lorsque la calcéine se retrouve encapsulée à très forte concentration à l'intérieur des vésicules, sa fluorescence est «quenchée». Cependant, lorsque celle-ci fuit du liposome et se retrouve diluée, une forte intensité de fluorescence peut être observée par microscopie à fluorescence. Suite à une incubation de différentes formulations avec des cellules HL60 ($CD33^+$), une intensité de fluorescence beaucoup plus forte et diffuse a été notée pour les immunoliposomes sensibles au pH par rapport aux immunoliposomes sans DODA-P(NIPAM-*co*-MAA). Cette différence de libération avait également déjà été mise en évidence chez les macrophages de souris RAW264.7 et J774 avec des liposomes sensibles au pH ne comportant pas de ligand (Francis *et al.* 2001). La libération du contenu liposomal provoqué par le DODA-P(NIPAM-*co*-MAA) a été réduite suite à une pré-incubation des cellules avec la bafilomycine A1, un inhibiteur de l'acidification des endosomes/lysosomes (Chapitre 5; Figure 5.6), démontrant ainsi la nécessité de l'acidification pour la libération dépendante du pH des formulations renfermant le DODA-P(NIPAM-*co*-MAA). Des observations similaires ont également été rapportées dans la littérature pour d'autres polymères sensibles au pH utilisés dans la préparation de liposomes tels que le poly(acide éthylacrylique) (Chen *et al.* 2004).

Finalement, la libération cytoplasmique de l'ara-C a été vérifiée suite à une étude d'efficacité de plusieurs formulations sur les cellules HL60 exprimant le récepteur CD33 (Simard & Leroux 2009). Une toxicité plus importante de l'ara-C a été observée lorsqu'elle était chargée dans des liposomes sensibles au pH plutôt que dans une formulation contrôle. Cette différence avait aussi été démontrée suite à une post-insertion d'un autre copolymère

NIPAM et de MAA chez des cellules de J774 (Roux *et al.* 2002a). La présence de l'anticorps CD33 sur les liposomes a produit une différence significative de l'activité cytotoxique de l'ara-C, démontrant l'importance de l'internalisation médiée par les récepteurs pour l'ara-C liposomale. La combinaison d'un ciblage actif et d'un mécanisme de libération induit a provoqué une plus forte mortalité des cellules HL60 à une dose de 20 µg/mL comparée aux autres formulations testées (Chapitre 5; Figure 5.7). Aucune étude de cytotoxicité n'a été effectuée avec les formulations de Sphérulites® étant donnée l'importante fuite de l'ara-C (43-57 %) *in vitro* en présence de protéines plasmatiques (Chapitre 4; Section 4.4.2).

7.3. Caractérisation *in vivo*

7.3.1. Pharmacocinétique et biodistribution des Sphérulites®

Les Sphérulites® ont été injectées chez le rat afin d'établir leur profil pharmacocinétique, ainsi que ceux de l'ara-C encapsulée. Pour ce faire, un dérivé d'oléate de cholestérol marqué au ¹⁴C et l'ara-C-[H³] ont été utilisés dans les formulations. Suite à leur administration par voie intraveineuse chez le rat, les Sphérulites® PEGylées ont démontré des temps de demi-vie respectifs de 128 et 50 min lorsque des PEG de masse molaire 5000 et 2000 ont été incorporés dans la bicouche (Chapitre 4; Figure 4.6 et Tableau 4.2). En comparaison, les vecteurs nus avaient une demi-vie inférieure à 5 min. Malgré un effet bénéfique du PEG sur le temps de circulation des liposomes, la clairance de ces derniers demeurait toutefois assez élevée, ceci probablement en raison de leur taille (300 nm). En effet, les Sphérulites® PEGylées ont démontré un fort tropisme pour le foie et la rate. À titre de comparaison, une formulation liposomale de diamètre de 100 nm composée

de phosphatidylcholine d'oeuf, de cholestérol et DSPE-PEG1900 possède un temps de demi-vie de 15,3 h chez le rat (Papahadjopoulos *et al.* 1991).

Il a été rapporté dans la littérature que l'ara-C en solution est rapidement inactivée et éliminée de la circulation sanguine (< 20 min) après injection par voie intraveineuse (Allen *et al.* 1992b, Baguley & Falkenhaug 1971). L'encapsulation de l'ara-C dans les Sphérulites® PEGylées s'est traduite par une augmentation de sa demi-vie. Des aires sous la courbe ($ASC_{5-120\text{min}}$) de 3 à 5 fois supérieures ont été obtenues pour l'ara-C encapsulée dans les Sphérulites® comportant une chaîne de PEG de longueur 2000 et 5000, respectivement, par rapport à l'ara-C seule ou encapsulée dans des vésicules non-PEGylées (Chapitre 4, Tableau 4.2). Cette augmentation du temps de circulation demeure toutefois modeste et reflète une fuite rapide du contenu liposomal dans le sang. Ces résultats indiquent qu'il deumeure nécessaire de parfaire la composition des Sphérulites® afin de réduire davantage leur taille et leur perméabilité à l'ara-C.

7.3.2. Pharmacocinétique et biodistribution des immunoliposomes sensibles au pH

Contrairement aux Sphérulites®, les liposomes sensibles au pH ont démontré une stabilité accrue de la bicoche lipidique face aux protéines plasmatiques, puisque 21% de l'ara-C encapsulée se retrouvait encore en circulation 8 h après l'injection de la formulation chez la souris saine. Par contre, la présence de l'anticorps complet à la surface de ces liposomes a grandement diminué les temps de circulation de l'ara-C encapsulée. En effet, après 8 h, seulement 4% de la dose injectée se retrouvait dans le système sanguin. D'ailleurs, le suivi des lipides à l'aide du marqueur non-échangeable, l'oléate de [^{14}C]-cholestéryle, a permis de confirmer ces résultats. En effet, on a retrouvé 2,5 fois plus de

liposomes PEGylés circulant que la formulation portant l'anticorps anti-CD33 à sa surface 8 h après leur administration. Ceci confirme que la diminution des temps de circulation de l'ara-C encapsulée dans les immunoliposomes-CD33 est principalement due à une élimination plus rapide de la formulation ciblée. Ces résultats étaient prévisibles, puisqu'il a été reporté dans la littérature que la présence d'anticorps complet à la surface des vecteurs colloïdaux favorisait une reconnaissance par le système immunitaire (Aragnol & Leserman 1986). Plus précisément, la portion Fc de l'anticorps exogène (couplé sur les liposomes) serait à l'origine d'une activation rapide du système du complément, d'une reconnaissance non spécifique et d'une élimination et/ou une internalisation accentuée par les cellules et les organes du SPM. D'ailleurs, lorsque l'on regarde les résultats de l'accumulation des vecteurs dans les différents organes collectés, on constate très clairement une accumulation prononcée au niveau des organes du SPM. En effet, 1 h après l'administration des immunoliposomes-CD33, plus de 17% de la dose injectée se retrouve séquestrée au niveau du foie contre moins de 8% de la dose injectée pour les liposomes PEGylés.

Étant donné les faibles quantités circulantes d'ara-C encapsulée dans les immunoliposomes-CD33 sensibles au pH, l'emploi du fragment Fab' anti-CD33 en remplacement de l'anticorps complet a été envisagé. Celui-ci est de masse molaire inférieure à l'anticorps complet (50 vs 150 kDa), ne possède pas de portion Fc, par conséquent il est moins activateur du système complément et moins reconnaissable par le SPM (Cheng & Allen 2008, Maruyama *et al.* 1997). Le fragment Fab' a donc été couplé sur les liposomes PEGylés sensibles au pH (Chapitre 6, Figure 6.1) et ces derniers ont été administrés chez l'animal sain et porteur de tumeurs. Des résultats très encourageants ont été obtenus chez la souris Balb/c saine. En effet, le couplage du fragment Fab' de l'anticorps sur les liposomes a permis d'augmenter les temps de circulation comparables à ceux des liposomes PEGylés. Des ASC similaires ont été obtenues pour les liposomes-Fab' et les liposomes contrôles, 1743 et 1842 nmol/h/mL respectivement, correspondant à un ASC ~2 fois supérieure à celle des formulations renfermant l'anticorps complet (Chapitre

6, Figure 6.3 et Tableau 6.1). Étant donné que l'ara-C demeure encapsulée, ces observations sont également notables pour les profils de pharmacocinétique de l'ara-C. L'incorporation de l'ara-C dans les liposomes sensibles au pH nus, présentant l'anticorps complet ou le fragment Fab' anti-CD33 a permis de diminuer la clairance de celle-ci lorsqu'elle est comparée à l'ara-C injectée en solution (Chapitre 6; Tableau 6.1).

7.3.3. Le modèle murin de la leucémie myéloblastique aiguë

7.3.3.1. Pharmacocinétique et biodistribution des immunoliposomes sensibles au pH

Les souris SCID innoculées de cellules HL60 ($CD33^+$) sont un bon modèle *in vivo* pour étudier l'influence d'une molécule de reconnaissance à la surface des vecteurs. Ce modèle animal est couramment utilisé afin d'étudier les traitements de la LMA puisqu'étant immunodéprimées, les souris ne développent pas de réaction immunitaire envers les cellules humaines et donc le rejet de greffe n'est observé que dans de très rares exceptions (Terpstra *et al.* 1995). Les souris SCID ne possèdent pas de lymphocyte T, ni de lymphocyte B; par contre, elles possèdent les cellules NK et les macrophages. Il a été rapporté que suite à l'administration des cellules HL60, celles-ci circulent dans l'organisme de la souris et finissent par s'accumuler au niveau de la moelle osseuse et des ganglions lymphatiques après quelques jours (Xu & Scheinberg 1995). Les pharmacocinétiques des liposomes PEGylés avec et sans Fab' anti-CD33 et de l'ara-C encapsulée ont donc été caractérisées chez la souris SCID inoculée de cellules HL60. Nous avons mis en évidence que le fragment Fab' entraînait une légère diminution du temps de circulation des liposomes sensibles au pH chez la souris porteuse de tumeurs (ASC de 1563 *vs.* 1983 nmol h/mL, Chapitre 6; Figure 6.4 et Tableau 6.1). Ceci s'est traduit par une clairance légèrement plus rapide pour les liposomes couplés au Fab', tant pour les vecteurs que l'ara-C encapsulée. Aucune accumulation préférentielle n'a été observée dans la moelle osseuse

des souris SCID/HL60 ayant reçues la formulation liposomale spécifique au récepteur CD33. Une étude d'efficacité préliminaire de cette formulation liposomale sensible au pH spécifique envers les cellules leucémiques a également été effectuée chez la souris SCID/HL60 comme modèle de la LMA.

7.3.3.2. Étude préliminaire d'efficacité thérapeutique des immunoliposomes

Une étude préliminaire d'efficacité des différentes formes d'ara-C a également été effectuée chez la souris femelle immunodéprimée inoculée de cellules HL60. Brièvement, 1.2×10^7 cellules HL60 ont été injectées *via* la veine de la queue. 24h après l'implantation des cellules leucémiques, une dose de 8 mg/kg d'ara-C a été administrée sous forme : (i) libre (ii) encapsulée dans les liposomes, (iii) encapsulée dans les liposomes-Fab' anti-CD33 ou enfin (iv) encapsulée dans des liposomes Fab' anti-CD33 sensibles au pH, selon les groupes. Un groupe de souris ayant reçu seulement une injection de salin physiologique a également été utilisé comme groupe contrôle. Une deuxième injection d'ara-C à 8 mg/kg, formulée de la même façon que la première injection, a été administrée 3 jours après l'inoculation des cellules HL60. Afin de s'assurer de l'efficacité du traitement dans ces conditions expérimentales, les souris ont été surveillées de façon journalière, pesées et euthanasiées en cas de paralysie au niveau des pattes arrières ou du développement d'une masse tumorale supérieure à 1500 cm^2 . Il s'agit d'une étude préliminaire puisqu' aucune optimisation des quantités de cellules inoculées, des doses d'ara-C et/ou de liposomes n'a été évaluée préalablement. Les résultats sont les suivants : en premier lieu, l'ara-C seule n'a pas permis de prolonger la survie des souris leucémique comparativement aux souris non traitées (Chapitre 6, Figure 6.6). Ceci peut s'expliquer par son élimination rapide suivant une injection intraveineuse ainsi que par le grand volume de distribution de l'ara-C, qui réduit la biodisponibilité pour atteindre les monocytes cancéreux (Chapitre 6, Table 6.1). Une augmentation des temps de survie de ce groupe contrôle pourrait potentiellement être

obtenue par une infusion d'une durée de 3 à 4 h répétées sur plusieurs jours consécutifs (Skipper *et al.* 1967, 1970). En second lieu, l'encapsulation de l'ara-C à l'intérieur des liposomes-Fab' a permis de prolonger significativement le taux de survie moyen des souris SCID/HL60 de plus de 10 jours comparé aux souris des groupes contrôles ($p<0.05$ comparé aux groupes non-traitées et ara-C libre). Enfin, bien que l'encapsulation de l'ara-C dans les liposomes protège le principe actif contre sa dégradation prémature dans le sang, prolonge ses temps de circulation systémique et améliore son activité thérapeutique (Allen *et al.* 1992, Hong *et al.* 1989, Kobayashi *et al.* 1977), aucune amélioration supplémentaire du taux de survie moyen des souris leucémiques n'a été observée pour les immunoliposomes sensibles au pH. Une diminution de l'AUC de cette formulation chez le modèle de souris SCID pourrait être une cause possible de cette inefficacité thérapeutique (Cahpitre 6, Table 6.1 et Figure 6.4). Au final, cette étude préliminaire suggère que l'ara-C n'est probablement pas le principe actif le plus adapté pour ces immunoliposomes sensibles au pH. De plus, ces résultats soulèvent l'hypothèse que le temps de circulation systémique de ces vecteurs pourrait être un facteur plus important que la libération rapide et contrôlée du principe actif dans les endosomes après internalisation.

Conclusion

Malgré les progrès réalisés ces dernières années au niveau du traitement de la LMA, cette maladie demeure dévastatrice avec un pronostic défavorable, surtout chez les personnes âgées. Le traitement basé sur la combinaison de l'ara-C avec une anthracycline, et la transplantation de cellules souches demeurent les traitements les plus efficaces jusqu'à présent. Cependant, ces thérapies intensives sont limitées à un nombre très restreint de patients, tout comme leur guérison. La vectorisation de l'ara-C est une voie prometteuse pour le traitement de la LMA. Plusieurs études ont démontré qu'il était possible de prolonger la survie des animaux avec des formulations vectorisées d'ara-C. Afin d'être avantageuses pour l'humain, ces nouvelles formes pharmaceutiques doivent tenir compte d'une diminution de la toxicité causée par le traitement actuel, malgré une augmentation de la biodisponibilité de l'ara-C nécessaire pour combattre la résistance et à induire l'apoptose des cellules tumorales.

Les différents travaux effectués au cours de cette thèse ont montré qu'il était possible d'encapsuler de l'ara-C avec un bon rendement dans des Sphérolites® possédant un diamètre inférieur au micromètre et en utilisant des lipides et surfactifs biocompatibles. L'incorporation de PEG à la surface de ces vésicules a aussi permis d'augmenter le temps de circulation *in vivo*. Cependant, les Sphérolites® présentent toujours l'inconvénient de posséder des membranes très perméables aux petites molécules encapsulées. La fuite du principe actif pourrait éventuellement être réduite en augmentant la rigidité des membranes de ces formulations par l'utilisation de différents lipides hydrogénés (*e.g.* DPPC, DSPC, HSPC, etc.) ou par l'emploi d'une teneur plus élevée en cholestérol (10-20% *p/p*). De même que des diamètres d'environ 100 nm seraient souhaitables afin de conférer des temps

de circulation prolongés dans l'organisme et une réduction de la capture par les organes du SPM.

Les liposomes, un système nanoparticulaire très exploité et développé, a permis d'étudier l'effet *in vitro* et *in vivo* de l'incorporation d'un polymère sensible au pH, le DODA-P(NIPAM-*co*-MAA), ainsi que le couplage d'un ligand spécifique. Ces travaux ont démontré qu'une technique de modification d'anticorps efficace a été obtenue afin de permettre leur fixation à la surface des liposomes. Ces immunoliposomes, contenant à leur surface l'anti-CD33 complet ou son fragment Fab' démontrent des propriétés de sélectivité envers les cellules leucémiques (CD33⁺). L'incorporation du polymère sensible au pH s'est démontrée utile dans la déstabilisation de la bicouche lipidique afin de libérer le contenu des liposomes dans un environnement acide. Une biodisponibilité accrue de la molécule encapsulée peut être obtenue par l'emploi de ce polymère en évitant la dégradation de molécules fragiles, telle que l'ara-C, dans les lysosomes intracellulaires composées de plusieurs enzymes. Les études de pharmacocinétique et de biodistribution chez l'animal sain et porteur de tumeurs ont démontré que ce système demeure stable, que l'ara-C demeure encapsulée malgré les différentes contraintes physiologiques (*i.e.* présence de nombreuses protéines plasmatiques, système immunitaire actif, débit sanguin élevé, etc.) exercées sur les vecteurs. Une étude préliminaire d'efficacité a été effectuée pour évaluer ces immunoliposomes sensibles au pH dans le traitement de la LMA. Bien que l'encapsulation de l'ara-C dans les liposomes ciblés ait permis de prolonger le taux de survie moyen des souris leucémiques, aucune amélioration supplémentaire n'a été observée suite à l'incorporation DODA-P(NIPAM-*co*-MAA) dans les liposomes.

Les résultats de ce projet de recherche on montré que les immunoliposomes sensibles au pH pouvaient augmenter l'efficacité de l'ara-C liposomale *in vitro*. Bien que des données intéressantes aient été obtenues, certains aspects doivent être optimisés. Notamment, la rétention du médicament dans les liposomes pH-sensibles est insuffisante

pour permettre de conserver la formulation pendant plusieurs mois. Ce problème pourrait être réglé en modifiant les excipients utilisés et/ou en vérifiant si une post-incorporation du P(NIPAM-*co*-MAA) sur des liposomes déjà formés serait efficace. Une méthode d'encapsulation active pourrait être également développée afin de favoriser une plus grande encapsulation d'ara-C dans ces liposomes. Les données obtenues chez l'animal, bien que préliminaires, n'ont pu mettre en évidence l'avantage des immunoliposomes sensibles au pH. Divers protocoles/régimes d'administration des immunoliposomes pourraient être testés afin d'améliorer l'efficacité du traitement. Il est aussi possible que les modèles choisis ne soient pas adaptés à une telle formulation. Dans ce cas, des investigations additionnelles impliquant d'autres molécules actives, ainsi que des modèles animaux différents devraient être menées afin de confirmer le potentiel thérapeutique de ces formulations.

Bibliographie

- Allen, T.M., 1992. Stealth liposomes: Five years on, *J. Liposome Res.*, 2, 289-305.
- Allen, T.M., Mehra, T., Hansen, C., Chin, Y.C., 1992a. Stealth liposomes: an improved sustained release system for 1-beta-D- arabinofuranosylcytosine, *Cancer Res.*, 52, 2431-2439.
- Allen, T.M., Mehra, T., Hansen, C., Chin, Y.C., 1992b. Stealth liposomes: an improved sustained release system for 1-beta-D-arabinofuranosylcytosine, *Cancer. Res.*, 52, 2431-2439.
- Allen, T.M., Romans, A.Y., Kercet, H., Segrest, J.P., 1980. Detergent removal during membrane reconstitution, *Biochim. Biophys. Acta*, 601, 328-342.
- Andoljsek, D., Preloznik Zupan, I., Zontar, D., Cernelc, P., Mlakar, U., Modic, M., Pretnar, J., Zver, S., 2002. Cell markers in the recognition of acute myeloblastic leukaemia subtypes, *Cell Mol Biol Lett*, 7, 343-345.
- Aoshima, M., Tsukagoshi, S., Sakurai, Y., Ohishi, J., Ishida, T., 1976. Antitumor activities of newly synthesized N4-acyl-1-beta-D-arabinofuranosylcytosine, *Cancer Res*, 36, 2726-2732.
- Aragon, D., Leserman, L.D., 1986. Immune clearance of liposomes inhibited by an anti-Fc receptor antibody in vivo, *Proc. Natl. Acad. Sci. U.S.A.*, 83, 2699-2703.
- Arnaout, M.A., Todd, R.F., 3rd, Dana, N., Melamed, J., Schlossman, S.F., Colten, H.R., 1983. Inhibition of phagocytosis of complement C3- or immunoglobulin G-coated particles and of C3bi binding by monoclonal antibodies to a monocyte-granulocyte membrane glycoprotein (Mol), *J Clin Invest*, 72, 171-179.
- Baguley, B.C., Falkenhaug, E.M., 1971. Plasma half-life of cytosine arabinoside (NSC-63878) in patients treated for acute myeloblastic leukaemia, *Cancer Chemother. Rep.*, 55, 291-298.
- Balaian L., Ball, E.D., 2005. Anti-CD33 monoclonal antibodies enhance the cytotoxic effects of cytosine arabinoside and idarubicin on acute myeloid leukemia cells through similarities in their signaling pathways, *Exp Hematology*, 33, 199-211.

- Ball, E.D., Davis, R.B., Griffin, J.D., Mayer, R.J., Davey, F.R., Arthur, D.C., Wurster-Hill, D., Noll, W., Elghetany, M.T., Allen, S.L., et al., 1991. Prognostic value of lymphocyte surface markers in acute myeloid leukemia, *Blood*, 77, 2242-2250.
- Bennett, J.M., Catovsky, D., Daniel, M.T., Flandrin, G., Galton, D.A., Gralnick, H.R., Sultan, C., 1976. Proposals for the classification of the acute leukaemias. French-American-British (FAB) co-operative group, *Br J Haematol*, 33, 451-458.
- Benoy, C.J., Elson, L.A., Schneider, R., 1972. Multiple emulsions, a suitable vehicle to provide sustained release of cancer chemotherapeutic agents, *Br J Pharmacol*, 45, 135P-136P.
- Benoy, C.J., Schneider, R., Elson, L.A., Jones, M., 1974. Enhancement of the cancer chemotherapeutic effect of the cell cycle phase specific agents methotrexate and cytosine arabinoside when given as a water-oil-water emulsion, *Eur. J. Cancer*, 10, 27-33.
- Bernheim-Grosswasser, A., Ugazio, S., Gauffre, F., Viratelle, O., Mahy, P., Roux, D., 2000. Spherulites: A new vesicular system with promising applications. An example: Enzyme microencapsulation, *J. Chem. Phys.*, 112, 3424-3430.
- Bertrand, N., Fleischer, J.G., Wasan, K.M., Leroux, J.-C., 2009. Pharmacokinetics and biodistribution of N-isopropylacrylamide copolymers for the design of pH-sensitive liposomes, *Biomaterials*, 30, 2598-2605.
- Bishop, J.F., 1997. The treatment of adult acute myeloid leukemia, *Semin Oncol*, 24, 57-69.
- Boeckler, C., Frisch, B., Muller, S., Schuber, F., 1996. Immunogenicity of new heterobifunctional cross-linking reagents used in the conjugation of synthetic peptides to liposomes, *J Immunol Methods*, 191, 1-10.
- Bolwell, B.J., Cassileth, P.A., Gale, R.P., 1988. High dose cytarabine: a review, *Leukemia*, 2, 253-260.

- Bradley, A.J., Devine, D.V., Ansell, S.M., Janzen, J., Brooks, D.E., 1998. Inhibition of liposome-induced complement activation by incorporated poly(ethylene glycol)-lipids, *Arch. Biochem. Biophys.*, 357, 185-194.
- Burke, J.M., Jurcic, J.G., Scheinberg, D.A., 2002. Radioimmunotherapy for acute leukemia, *Cancer Control*, 9, 106-113.
- Canada, Statistiques canadiennes sur le cancer 2009, produit par la Société canadienne du cancer en collaboration avec Statistiques Canada, les Registres du cancer des provinces et des territoires et l'Agence de la santé publique du Canada, www.cancer.ca, vol. 1, Ottawa, 2009.
- Capranico, G., Butelli, E., Zunino, F., 1995. Change of the sequence specificity of daunorubicin-stimulated topoisomerase II DNA cleavage by epimerization of the amino group of the sugar moiety, *Cancer Res.*, 55, 312-317.
- Caron, P.C., Co, M.S., Bull, M.K., Avdalovic, N.M., Queen, C., Scheinberg, D.A., 1992. Biological and immunological features of humanized M195 (anti-CD33) monoclonal antibodies, *Cancer Res.*, 52, 6761-6767.
- Cattel, L., Ceruti, M., Dosio, F., 2003. From conventional to stealth liposomes: a new frontier in cancer chemotherapy, *Tumori*, 89, 237-249.
- Chabner, B.A., Hande, K.R., Drake, J.C., 1979. Ara-C metabolism: implications for drug resistance and drug interactions, *Bull Cancer*, 66, 89-92.
- Chames, P., Van Regenmortel, M., Weiss, E., Baty, D., 2009. Therapeutic antibodies: successes, limitations and hopes for the future, *Br J Pharmacol*, 157, 220-233.
- Chen, T., McIntosh, D., He, Y., Kim, J., Tirrell, D.A., Scherrer, P., Fenske, D.B., Sandhu, A.P., Cullis, P.R., 2004. Alkylated derivatives of poly(ethylacrylic acid) can be inserted into preformed liposomes and trigger pH-dependant intracellular delivery of liposomal contents, *Mol. Membr. Biol.*, 21, 385-393.
- Cheng, W.W., Allen, T.M., 2008. Targeted delivery of anti-CD19 liposomal doxorubicin in B-cell lymphoma: a comparison of whole monoclonal antibody, Fab' fragments and single chain Fv, *J Control Release*, 126, 50-58.

- Chonn, A., Cullis, P.R., 1992. Ganglioside GM1 and hydrophilic polymers increase liposome circulation times by inhibiting the association of blood proteins, *J. Liposome Res.*, 2, 397-410.
- Civin, C.I., Strauss, L.C., Brovall, C., Fackler, M.J., Schwartz, J.F., Shaper, J.H., 1984. Antigenic analysis of hematopoiesis. III. A hematopoietic progenitor cell surface antigen defined by a monoclonal antibody raised against KG-1a cells, *J Immunol*, 133, 157-165.
- Connor, J., Huang, L., 1986. pH-sensitive immunoliposomes as an efficient and target-specific carrier for antitumor drugs, *Cancer Res.*, 46, 3431-3435.
- Cortes, J., Estey, E., O'Brien, S., Giles, F., Shen, Y., Koller, C., Beran, M., Thomas, D., Keating, M., Kantarjian, H., 2001. High-dose liposomal daunorubicin and high-dose cytarabine combination in patients with refractory or relapsed acute myelogenous leukemia, *Cancer*, 92, 7-14.
- Damle, N.K., Frost, P., 2003. Antibody-targeted chemotherapy with immunoconjugates of calicheamicin, *Curr Opin Pharmacol*, 3, 386-390.
- Demel, R.A., Kinsky, S.C., Kinsky, C.B., van Deesen, L.L.M., 1968. Effects of temperature and cholesterol on the glucose permeability of liposomes prepared with neutral and synthetic lecithins, *Biochim. Biophys. Acta*, 150, 655-665.
- Diat, O., Roux, D., 1993. Preparation of monodisperse multilayer vesicles of controlled size and high encapsulation ratio, *J. Phys. II France*, 3, 9-14.
- Diat, O., Roux, D., Nallet, F., 1993. Effect of shear on a lyotropic lamellar phase, *J. Phys. II France*, 3, 1427-1452.
- Dijoseph, J.F., Dougher, M.M., Armellino, D.C., Evans, D.Y., Damle, N.K., 2007. Therapeutic potential of CD22-specific antibody-targeted chemotherapy using inotuzumab ozogamicin (CMC-544) for the treatment of acute lymphoblastic leukemia, *Leukemia*, 21, 2240-2245.
- Drummond, D.C., Zignani, M., Leroux, J.-C., 2000. Current status of pH-sensitive liposomes in drug delivery, *Prog. Lipid Res.*, 39, 409-460.

- Endoh, H., Suzuki, Y., Hashimoto, Y., 1981. Antibody coating of liposomes with 1-ethyl-3-(3-dimethyl-aminopropyl)carbodiimide and the effect on target specificity, *J. Immunol. Methods*, 44, 79-85.
- Estey, E.H., 2001. Therapeutic options for acute myelogenous leukemia, *Cancer*, 92, 1059-1073.
- Fassas, A., Anagnostopoulos, A., 2005. The use of liposomal daunorubicin (DaunoXome) in acute myeloid leukemia, *Leuk Lymphoma*, 46, 795-802.
- Fassas, A., Buffels, R., Anagnostopoulos, A., Gacos, E., Vadikolia, C., Haloudis, P., Kaloyannidis, P., 2002. Safety and early efficacy assessment of liposomal daunorubicin (DaunoXome) in adults with refractory or relapsed acute myeloblastic leukaemia: a phase I-II study, *Br J Haematol*, 116, 308-315.
- Feldman, E.J., Brandwein, J., Stone, R., Kalaycio, M., Moore, J., O'Connor, J., Wedel, N., Roboz, G.J., Miller, C., Chopra, R., Jurcic, J.C., Brown, R., Ehmann, W.C., Schulman, P., Frankel, S.R., De Angelo, D., Scheinberg, D., 2005. Phase III randomized multicenter study of a humanized anti-CD33 monoclonal antibody, lintuzumab, in combination with chemotherapy, versus chemotherapy alone in patients with refractory or first-relapsed acute myeloid leukemia, *J Clin Oncol*, 23, 4110-4116.
- Fram, R., Major, P., Egan, E., Beardsley, P., Rosenthal, D., Kufe, D., 1983. A phase I-II study of combination therapy with thymidine and cytosine arabinoside, *Cancer Chemother Pharmacol*, 11, 43-47.
- Francis, M.F., Dhara, G., Winnik, F.M., Leroux, J.-C., 2001. *In vitro* evaluation of pH-sensitive polymer/niosome complexes, *Biomacromolecules*, 2, 741-749.
- Freund, O., Amédée, J., Roux, D., Laversanne, R., 2000. In vitro and in vivo stability of new multilamellar vesicles, *Life Sci.*, 67, 411-419.
- Fukushima, S., Juni, K., Nakano, M., 1983. Preparation of and drug release from W/O/W type double emulsions containing anticancer agents, *Chem Pharm Bull (Tokyo)*, 31, 4048-4056.

- Ganong, W.F., Physiologie médicale, De Boeck Université, San Francisco, 2001.
- Gauffre, F., Roux, D., 1999. Evidence for a pH difference controlled by thermodynamics between the interior and the exterior of a new type of vesicles in suspension, *Langmuir*, 15, 3070-3077.
- Gilliland, D.G., Jordan, C.T., Felix, C.A., 2004. The molecular basis of leukemia, *Hematology Am Soc Hematol Educ Program*, 80-97.
- Glantz, M.J., Jaeckle, K.A., Chamberlain, M.C., Phuphanich, S., Recht, L., Swinnen, L.J., Maria, B., LaFollette, S., Schumann, G.B., Cole, B.F., Howell, S.B., 1999. A randomized controlled trial comparing intrathecal sustained-release cytarabine (DepoCyt) to intrathecal methotrexate in patients with neoplastic meningitis from solid tumors, *Clin Cancer Res*, 5, 3394-3402.
- Goldsby, R.A., Kindt, T.J., Osborne, B.A., Kuby, J., Immunologie : le cours de Janis Kuby : avec questions de révision Dunod, Paris, 2003.
- Gray, A.G., Morgan, J., Linch, D.C., Huehns, E.R., 1988. Uptake of antibody directed cytotoxic liposomes by CD3 on human T cells, *Clin. Exp. Immunol.*, 72, 168-173.
- Griffin, J.D., Linch, D., Sabbath, K., Larcom, P., Schlossman, S.F., 1984. A monoclonal antibody reactive with normal and leukemic human myeloid progenitor cells, *Leuk Res*, 8, 521-534.
- Griffin, J.D., Ritz, J., Nadler, L.M., Schlossman, S.F., 1981. Expression of myeloid differentiation antigens on normal and malignant myeloid cells, *J Clin Invest*, 68, 932-941.
- Harris, J.M., Chess, R.B., 2003. Effect of pegylation on pharmaceuticals, *Nat Rev Drug Discov*, 2, 214-221.
- Hong, F., Mayhew, E., 1989. Therapy of central nervous system leukemia in mice by liposome-entrapped 1- β -D-arabinofuranosylcytosine, *Cancer Res.*, 49, 5097-5102.
- Hori, K., Tsuruo, T., Naganuma, K., Tsukagoshi, S., Sakurai, Y., 1984. Antitumor effects and pharmacology of orally administered N4-palmitoyl-1-beta-D-arabinofuranosylcytosine in mice, *Cancer Res*, 44, 172-177.

- Huang, A., Huang, L., Kennel, S.J., 1980. Monoclonal antibody covalently coupled with fatty acid. A reagent for in vitro liposome targeting, *J. Biol. Chem.*, 255, 8015-8018.
- Ichikawa, H., Onishi, H., T., T., Machida, Y., Nagai, T., 1993. Evaluation of the conjugate between N4-(4-carboxybutyryl)-1-beta-D-arabinofuranosylcytosine and chitosan as a macromolecular prodrug of 1-beta-D-arabinofuranosylcytosine, *Drug Des. Discov.*, 10, 343-353.
- Iden, D.L., Allen, T.M., 2001. *In vitro* and *in vivo* comparison of immunoliposomes made by conventional coupling techniques with those made by a new post-insertion approach, *Biochim. Biophys. Acta*, 1513, 207-216.
- Kato, Y., Saito, M., Fukushima, H., Takeda, Y., Hara, T., 1984. Antitumor activity of 1-beta-D-arabinofuranosylcytosine conjugated with polyglutamic acid and its derivative, *Cancer Res.*, 44, 25-30.
- Kim, D.-W., Oh, S.-G., Yi, S.-C., Bae, S.-Y., Moon, S.-K., 2000. Preparation of indium-tin oxide particles in shear-induced multilamellar vesicles (spherulites) as chemical reactors, *Chem. Mater.*, 12, 996-1002.
- Kim, S., Kim, D.J., Geyer, M.A., Howell, S.B., 1987. Multivesicular liposomes containing 1-beta-D-arabinofuranosylcytosine for slow-release intrathecal therapy, *Cancer Res.*, 47, 3935-3937.
- Kobayashi, T., Kataoka, T., Tsukagoshi, S., Sakurai, Y., 1977. Enhancement of anti-tumor activity of 1-beta-D-arabinofuranosylcytosine by encapsulation in liposomes, *Int. J. Cancer*, 20, 581-587.
- Kobayashi, T., Tsukagoshi, S., Sakurai, Y., 1975. Enhancement of the cancer chemotherapeutic effect of cytosine arabinoside entrapped in liposomes on mouse leukemia L-1210, *Gann*, 66, 719-720.
- Kodama, K., Morozumi, M., Saitoh, K., Kuninaka, A., Yoshino, H., Saneyoshi, M., 1989. Antitumor activity and pharmacology of 1-beta-D-arabinofuranosylcytosine-5'-stearylphosphate: an orally active derivative of 1-beta-D-arabinofuranosylcytosine, *Jpn J Cancer Res.*, 80, 679-685.

- Koller-Lucae, S.K., Schott, H., Schwendener, R.A., 1997. Interactions with human blood in vitro and pharmacokinetic properties in mice of liposomal N4-octadecyl-1-beta-D-arabinofuranosylcytosine, a new anticancer drug, *J Pharmacol Exp Ther*, 282, 1572-1580.
- Lajaunias, F., Dayer, J.M., Chizzolini, C., 2005. Constitutive repressor activity of CD33 on human monocytes requires sialic acid recognition and phosphoinositide 3-kinase-mediated intracellular signaling, *Eur J Immunol*, 35, 243-251.
- Larson, R.A., Sievers, E.L., Stadtmauer, E.A., Lowenberg, B., Estey, E.H., Dombret, H., Theobald, M., Voliotis, D., Bennett, J.M., Richie, M., Leopold, L.H., Berger, M.S., Sherman, M.L., Loken, M.R., van Dongen, J.J., Bernstein, I.D., Appelbaum, F.R., 2005. Final report of the efficacy and safety of gemtuzumab ozogamicin (Mylotarg) in patients with CD33-positive acute myeloid leukemia in first recurrence, *Cancer*, 104, 1442-1452.
- Lasic, D.D., Applications of Liposomes, in: R.L.a.E. Sackmann (Ed.), *Handbook of Biological Physics*, vol. 1, Elsevier Science B.V., Amsterdam, 1995, pp. 491-519.
- Lasic, D.D., Martin, F.J., Gabizon, A., Huang, S.K., Papahadjopoulos, D., 1991. Sterically stabilized liposomes: a hypothesis on the molecular origin of the extended circulation times, *Biochim. Biophys. Acta*, 1070, 187-192.
- Le Hir, A., *Pharmacie galénique : bonnes pratiques de fabrication des médicaments*, 8e ed., Elsevier Masson S.A.S., Paris, 2006.
- Lee, M.D., Ellestad, G.A., Borders, D.B., 1991. Calicheamicins: discovery, structure, chemistery, and interaction with DNA, *Acc. Chem. Res.*, 24, 235-243.
- Leone, G., Rutella, S., Voso, M.T., Fianchi, L., Scardocci, A., Pagano, L., 2004. In vivo priming with granulocyte colony-stimulating factor possibly enhances the effect of gemtuzumab-ozogamicin in acute myeloid leukemia: results of a pilot study, *Haematologica*, 89, 634-636.

- Liu, B., Cui, C., Duan, W., Zhao, M., Peng, S., Wang, L., Liu, H., Cui, G., 2009. Synthesis and evaluation of anti-tumor activities of N(4) fatty acyl amino acid derivatives of 1-beta-arabinofuranosylcytosine, *Eur J Med Chem*, 44, 3596-3600.
- Longman, S.A., Cullis, P.R., Choi, L., de Jong, G., Bally, M.B., 1995. A two-step targeting approach for delivery of doxorubicin-loaded liposomes to tumour cells in vivo, *Cancer Chemother. Pharmacol.*, 36, 91-101.
- Mahlknecht, U., Dransfeld, C.L., Bulut, N., Kramer, M., Thiede, C., Ehninger, G., Schaich, M., 2009. SNP analyses in cytarabine metabolizing enzymes in AML patients and their impact on treatment response and patient survival: identification of CDA SNP C-451T as an independent prognostic parameter for survival, *Leukemia*, 23, 1929-1932.
- Major, P.P., Egan, E.M., Beardsley, G.P., Minden, M.D., Kufe, D.W., 1981. Lethality of human myeloblasts correlates with the incorporation of arabinofuranosylcytosine into DNA, *Proc Natl Acad Sci USA*, 78, 3235-3239.
- Mariani, M., Camagna, M., Tarditi, L., Seccamani, E., 1991. A new enzymatic method to obtain high-yield F(ab)2 suitable for clinical use from mouse IgG1, *Mol. Immunol.*, 28, 69-77.
- Marsh, J.H., Kreis, W., Barile, B., Akerman, S., Schulman, P., Allen, S.L., DeMarco, L.C., Schuster, M.W., Budman, D.R., 1993. Therapy of refractory/relapsed acute myeloid leukemia and blast crisis of chronic myeloid leukemia with the combination of cytosine arabinoside, tetrahydrouridine, and carboplatin, *Cancer Chemother Pharmacol*, 31, 481-484.
- Maruyama, K., Takahashi, N., Tagawa, T., Nagaike, K., Iwatsuru, M., 1997. Immunoliposomes bearing polyethyleneglycol-coupled Fab' fragment show prolonged circulation time and high extravasation into targeted solid tumors in vivo, *FEBS Lett.*, 413, 177-180.
- Maruyama, K., Takizawa, T., Yuda, T., Kennel, S.J., Huang, L., Iwatsuru, M., 1995. Targetability of novel immunoliposomes modified with amphipathic poly(ethylene

- glycol)s conjugated at their distal terminals to monoclonal antibodies, *Biochim. Biophys. Acta*, 1234, 74-80.
- Mastrobattista, E., Koning, G.A., Storm, G., 1999. Immunoliposomes for the targeted delivery of antitumor drugs, *Adv. Drug Deliv. Rev.*, 40, 103-127.
- Mignet, N., Brun, A., Degert, C., Delord, B., Roux, D., Hélène, C., Laversanne, R., François, J.-C., 2000. The Spherulites: a promising carrier for oligonucleotide delivery, *Nucleic Acids Res.*, 28, 3134-3142.
- Mitchell, T., Sariban, E., Kufe, D., 1986. Effects of 1-beta-D-arabinofuranosylcytosine on proto-oncogene expression in human U-937 cells, *Mol Pharmacol*, 30, 398-402.
- Murry, D.J., Blaney, S.M., 2000. Clinical pharmacology of encapsulated sustained-release cytarabine, *Ann Pharmacother*, 34, 1173-1178.
- Muus, P., Haanen, C., Raijmakers, R., de Witte, T., Salden, M., Wessels, J., 1987. Influence of dose and duration of exposure on the cytotoxic effect of cytarabine toward human hematopoietic clonogenic cells, *Semin Oncol*, 14, 238-244.
- Naito, K., Takeshita, A., Shigeno, K., Nakamura, S., Fujisawa, S., Shinjo, K., Yoshida, H., Ohnishi, K., Mori, M., Terakawa, S., Ohno, R., 2000. Calicheamicin-conjugated humanized anti-CD33 monoclonal antibody (gemtuzumab zogamicin, CMA-676) shows cytoidal effect on CD33-positive leukemia cell lines, but is inactive on P-glycoprotein-expressing sublines, *Leukemia*, 14, 1436-1443.
- Okochi, H., Nakano, M., 1997. Comparative study of two preparation methods of w/o/w emulsions:stirring and membrane emulsification, *Chem Pharm Bull (Tokyo)*, 45, 1323-1326.
- Pagano, L., Fianchi, L., Caira, M., Rutella, S., Leone, G., 2007. The role of Gemtuzumab Ozogamicin in the treatment of acute myeloid leukemia patients, *Oncogene*, 26, 3679-3690.
- Pal, R., 1996. Multiple O/W/O Emulsion Rheology, *Langmuir*, 12, 2220-2225.
- Papahadjopoulos, D., Allen, T.M., Gabizon, A., Mayhew, E., Matthay, K., Huang, S.K., Lee, K.D., Woodle, M.C., Lasic, D.D., Redemann, C., Martin, F.J., 1991. Sterically

- stabilized liposomes: improvement in pharmacokinetics and antitumor therapeutic efficacy, Proc. Natl. Acad. Sci. U.S.A., 88, 11460-11464.
- Park, J.W., Hong, K., Kirpotin, D.B., Papahadjopoulos, D., Benz, C.C., 1997. Immunoliposomes for cancer treatment, Adv. Pharmacol., 40, 399-435.
- Paul, S.P., Taylor, L.S., Stansbury, E.K., McVicar, D., 2000. Myeloid specific human CD33 is an inhibitory receptor with differential ITIM function in recruiting the phosphatases SHP-1 and SHP-2, Blood, 96, 483-490.
- Plunkett, W., Liliemark, J.O., Estey, E., Keating, M.J., 1987. Saturation of ara-CTP accumulation during high-dose ara-C therapy: pharmacologic rationale for intermediate-dose ara-C, Semin Oncol, 14, 159-166.
- Powis, G., Anticancer drugs: antimetabolite metabolism and natural anticancer agents, in: G. Powis (Ed.), International encyclopedia of pharmacology and therapeutics, vol. 1st ed., Pergamon Press, Oxford, 1994, p. 506.
- Prokop, A., Davidson, J.M., 2008. Nanovehicular intracellular delivery systems, J Pharm Sci, 97, 3518-3590.
- Rhoades, R., Pflanzer, R., 2003. Human Physiology, 4th Edition, Thomson Brooks/Cole, Pacific Grove, CA, 1120 pages.
- Richardson, V.J., Curt, G.A., Ryman, B.E., 1982. Liposomally trapped AraCTP to overcome AraC resistance in a murine lymphoma in vitro, Br J Cancer, 45, 559-564.
- Rosowsky, A., Kim, S.H., Ross, J., Wick, M.M., 1982. Lipophilic 5'-(alkyl phosphate) esters of 1-beta-D-arabinofuranosylcytosine and its N4-acyl and 2,2'-anhydro-3'-O-acyl derivatives as potential prodrugs, J Med Chem, 25, 171-178.
- Roux, D., Gauffre, F., 1999. The "onion" phase and its potential use in chemistry, Eur. Chem. Chronicle, 3, 17-24.
- Roux, E., Francis, M., Winnik, F.M., Leroux, J.-C., 2002a. Polymer-based pH-sensitive carriers as a means to improve the cytoplasmic delivery of drugs, Int. J. Pharm., 242, 25-36.

- Roux, E., Lafleur, M., Lataste, E., Moreau, P., Leroux, J.-C., 2003. On the characterization of pH-sensitive liposome/polymer complexes, *Biomacromolecules*, 4, 240-248.
- Roux, E., Passirani, C., Scheffold, S., Benoit, J.P., Leroux, J.-C., 2004. Serum-stable and long-circulating, PEGylated, pH-sensitive liposomes, *J. Controlled Release*, 94, 447-451.
- Roux, E., Stomp, R., Giasson, S., Pézolet, M., Moreau, P., Leroux, J.-C., 2002b. Steric stabilization of liposomes by pH-responsive *N*-isopropylacrylamide copolymer, *J. Pharm. Sci.*, 91, 1795-1802.
- Royer, B., Arock, M., 1998. Therapeutical uses of haematopoietic growth factors. I. Erythropoietin and thrombopoietin, *Ann Biol Clin*, 56, 143-152.
- Sapra, P., Allen, T.M., 2003. Ligand-targeted liposomal anticancer drugs, *Prog Lipid Res*, 42, 439-462.
- Scheinberg, D.A., Lovett, D., Divgi, C.R., Graham, M.C., Berman, E., Pentlow, K., Feirt, N., Finn, R.D., Clarkson, B.D., Gee, T.S., et al., 1991. A phase I trial of monoclonal antibody M195 in acute myelogenous leukemia: specific bone marrow targeting and internalization of radionuclide, *J Clin Oncol*, 9, 478-490.
- Schroder, J.K., Kirch, C., Seeber, S., Schutte, J., 1998. Structural and functional analysis of the cytidine deaminase gene in patients with acute myeloid leukaemia, *Br J Haematol*, 103, 1096-1103.
- Schwartz, M.A., Lovett, D.R., Redner, A., Finn, R.D., Graham, M.C., Divgi, C.R., Dantis, L., Gee, T.S., Andreeff, M., Old, L.J., et al., 1993. Dose-escalation trial of M195 labeled with iodine 131 for cytoreduction and marrow ablation in relapsed or refractory myeloid leukemias, *J Clin Oncol*, 11, 294-303.
- Schwendener, R.A., Horber, D.H., Odermatt, B., Schott, H., 1996. Oral antitumour activity in murine L1210 leukaemia and pharmacological properties of liposome formulations of N4-alkyl derivatives of 1-beta-D-arabinofuranosylcytosine, *J Cancer Res Clin Oncol*, 122, 102-108.

- Schwendener, R.A., Schott, H., 1992. Treatment of L1210 murine leukemia with liposome-incorporated N4-hexadecyl-1-beta-D-arabinofuranosyl cytosine, *Int J Cancer*, 51, 466-469.
- Shipley, J.L., Butera, J.N., 2009. Acute myelogenous leukemia, *Exp. Hematol.*, 37, 649-658.
- Sievers, E.L., Larson, R.A., Stadtmauer, E.A., Estey, E., Lowenberg, B., Dombret, H., Karanes, C., Theobald, M., Bennett, J.M., Sherman, M.L., Berger, M.S., Eten, C.B., Loken, M.R., van Dongen, J.J., Bernstein, I.D., Appelbaum, F.R., 2001. Efficacy and safety of gemtuzumab ozogamicin in patients with CD33-positive acute myeloid leukemia in first relapse, *J Clin Oncol*, 19, 3244-3254.
- Silvander, M., Johnsson, M., Edwards, K., 1998. Effects of PEG-lipids on permeability of phosphatidylcholine/cholesterol liposomes in buffer and in human serum, *Chem. Phys. Lipids*, 97, 15-26.
- Skipper, H.E., Schabel, F.M., Jr. Wilcox, W.S., 1967, Experimental evaluation of potential anticancer agents. XXI. Scheduling of arabinosylcytosine to take advantage of its S-phase specificity against leukemia cells. *Cancer Chemother Rep*, 51, 125-165.
- Skipper, H.E., Schabel, F.M., Jr. Mellett, L.B. Montgomery, J.A., Wilkoff, L.J., Lloyd, H.H., Brockman, R.W., 1970, Implications of biochemical, cytokinetic, pharmacologic, and toxicologic relationships in the design of optimal therapeutic schedules. *Cancer Chemother Rep*, 54, 431-450.
- Simard, P., Hoarau, D., Khalid, M.N., Roux, E., Leroux, J.C., 2005. Preparation and in vivo evaluation of PEGylated spherulite formulations, *Biochim. Biophys. Acta*, 1715, 37-48.
- Simard, P., Leroux, J.C., 2009. pH-sensitive immunoliposomes specific to the CD33 cell surface antigen of leukemic cells, *Int J Pharm*, 381, 86-96.
- Stone, R.M., 2002. Treatment of acute myeloid leukemia: state-of-the-art and future directions, *Semin Hematol*, 39, 4-10.

- Tallman, M.S., Gilliland, D.G., Rowe, J.M., 2005. Drug therapy for acute myeloid leukemia, *Blood*, 106, 1154-1163.
- Tattersall, M.H., Ganeshaguru, K., Hoffbrand, A.V., 1974. Mechanisms of resistance of human acute leukaemia cells to cytosine arabinoside, *Br J Haematol*, 27, 39-46.
- Taylor, V.C., Buckley, C.D., Douglas, M., Cody, A.J., Simmons, D.L., Freeman, S.D., 1999, The myeloid-specific sialic acid-binding receptor, CD33, associates with the protein-tyrosine phosphatases, SHP-1 and SHP-2, *J Biol Chem*, 274, 11505-11512.
- Terpstra, W., Prins, A., Visser, T., Wognum, B., Wagemaker, G., Lowenberg, B., Wielenga, J., 1995. Conditions for engraftment of human acute myeloid leukemia (AML) in SCID mice, *Leukemia*, 9, 1573-1577.
- Ulyanova, T., Blasioli, J., Woodford-Thomas, T.A., Thomas, M.L., 1999. The sialoadhesin CD33 is a myeloid-specific inhibitory receptor, *Eur J Immunol*, 29, 3440-3449.
- Walter, R.B., Gooley, T.A., van der Velden, V.H., Loken, M.R., van Dongen, J.J., Flowers, D.A., Bernstein, I.D., Appelbaum, F.R., 2007. CD33 expression and P-glycoprotein-mediated drug efflux inversely correlate and predict clinical outcome in patients with acute myeloid leukemia treated with gemtuzumab ozogamicin monotherapy, *Blood*, 109, 4168-4170.
- Walter, R.B., Raden, B.W., Zeng, R., Hausermann, P., Bernstein, I.D., Cooper, J.A., 2008. ITIM-dependant endocytosis of CD33-related Siglecs: role of intracellular domain, tyrosine phosphorylation, and the tyrosine phosphatases, Shp1 and Shp2, *J Leuc Biol*, 83, 200-211.
- Waugh, A., Grant, A., 2007. Anatomie et physiologie normales et pathologiques, Ross et Wilson; 2e édition française ed., Elsevier Masson, Issy-les-Moulineaux, 507 pages.
- Wellhausen, S.R., Peiper, S.C., 2002. CD33: biochemical and biological characterization and evaluation of clinical relevance, *J Biol Regul Homeost Agents*, 16, 139-143.
- Xu, Y., Scheinberg, D.A., 1995. Elimination of human leukemia by monoclonal antibodies in an athymic nude mouse leukemia model, *Clin. Cancer Res.*, 1, 1179-1187.

Zenhausern, R., Zwicky, C., Solenthaler, M., Fey, M.F., Tobler, A., 2003. Leucémies aigues de l'adulte, Forum Med. Suisse, 29/30, 684-692.

Matériel et méthode – Étude de la phagocytose *in vitro*

Les études de phagocytose des différentes formulations liposomales, contenant le marqueur lipophile cholestéryl-BODIPY FL C12, ont été effectuées à l'aide des macrophages de souris RAW264.7. Ces cellules ont été cultivées dans un incubateur à 37°C (5% CO₂) dans 15 mL de milieu de culture DMEM de forte teneur en glucose et contenant 10% (v/v) de sérum de bœuf fœtal, pénicilline G et streptomycine. 2,5 x 10⁵ cellules (1 mL) ont été déposées dans des plaques stériles de 24 trous. Après 24 h, le milieu de culture a été remplacé par du nouveau milieu de culture RPMI 1640 (sans rouge de phénol). Les cellules ont été mises en contact avec une concentration finale de 0,7 µmol de lipides/mL de formulations liposomales pendant 1, 2 et 3 h. Après les différents temps d'incubation, les cellules ont été nettoyées 3 fois à l'aide du tampon phosphate (PBS) froid (4°C, pH 7,4) afin d'arrêter l'internalisation. Par la suite, les cellules ont été fixées à 4°C à l'aide de la formaline 1% (v/v) pendant 10 min, décollées du fond des trous par grattage et resuspendues dans 600 µL de PBS pour l'analyse de la fluorescence. Des expériences effectuées à 4°C ont été effectuées en parallèle, pour déterminer la quantité de liposomes adsorbés non spécifiquement à la surface des membranes cellulaires. Toutes les expériences ont été effectuées en triplicata. La fluorescence associée aux cellules a été analysée par cytométrie de flux (Becton Dickinson Immunocytometry Systems, San Jose, Californie, États-Unis). Un total de 10 000 événements a été analysé dans chacun des tubes. Les résultats sont exprimés en terme de capacité phagocytaire (CP) tel que obtenue par l'équation 1 :

$$\text{CP} = \text{Intensité de fluorescence moyenne} \times \% \text{ de cellules fluorescentes détectées} \text{ (Eq. 1)}$$

Afin d'exclure les vésicules seulement adsorbées et non internalisées, la CP mesurée à 4°C a été soustraite de celle obtenue à 37 °C comme suit (équation 2) :

$$\text{CP} = \text{CP à } 37^\circ\text{C} - \text{CP à } 4^\circ\text{C} \text{ (Eq. 2)}$$

Les résultats obtenus sont présentés à la Figure 7.2.